

The following document is an incomplete copy of the MCNP Version 4A manual. The most pertinent sections for criticality calculations were chosen to be included here. The complete document is available.

LA-12625-M
Manual

UC 705
and
UC 700

Issued: November 1993

MCNPTM—A General Monte Carlo N-Particle Transport Code

Version 4A

Judith F. Briesmeister, Editor

An Affirmative Action/Equal Opportunity Employer

DISCLAIMER

This report was prepared as an account of work sponsored by an agency of the United States Government. Neither the United States Government nor any agency thereof, nor any of their employees, makes any warranty, express or implied, or assumes any legal liability or responsibility for the accuracy, completeness, or usefulness of any information, apparatus, product, or process disclosed, or represents that its use would not infringe privately owned rights. Reference herein to any specific commercial product, process, or service by trade name, trademark, manufacturer, or otherwise, does not necessarily constitute or imply its endorsement, recommendation, or favoring by the United States Government or any agency thereof. The views and opinions of authors expressed herein do not necessarily state or reflect those of the United States Government or any agency thereof.

FOREWORD

This manual is a practical guide for the use of our general-purpose Monte Carlo code MCNP. The first chapter is a primer for the novice user. The second chapter describes the mathematics, data, physics, and Monte Carlo simulation found in MCNP. This discussion is not meant to be exhaustive—details of the particular techniques and of the Monte Carlo method itself will have to be found elsewhere. The third chapter shows the user how to prepare input for the code. The fourth chapter contains several examples, and the fifth chapter explains the output. The appendices show how to use MCNP on various computer systems and also give details about some of the code internals.

The Monte Carlo method emerged from work done at Los Alamos during World War II. The invention is generally attributed to Fermi, von Neumann, Ulam, Metropolis, and Richtmyer. MCNP is the successor to their work and represents over 400 person-years of development.

Neither the code nor the manual is static. The code is changed as the need arises and the manual is changed to reflect the latest version of the code. This particular manual refers to Version 4A.

MCNP and this manual are the product of the combined effort of many people in the Radiation Transport Group (X-6) of the Applied Theoretical Physics Division (X Division) at the Los Alamos National Laboratory.

The code and manual can be obtained from the Radiation Shielding Information Center (RSIC), P. O. Box X, Oak Ridge, TN, 37831.

J. F. Briesmeister
Editor
505-667-7277
FAX: 505-665-5538
email: mcnp@lanl.gov

COPYRIGHT NOTICE FOR MCNP VERSION 4A

Copyright 1988, the Regents of the University of California. MCNP was produced under a U.S. Government contract (w-7405-eng-36) by the Los Alamos National Laboratory, which is operated by the University of California for the U.S. Department of Energy. The U.S. Government is licensed to use, reproduce, and distribute MCNP. Permission is granted to the public to copy MCNP without charge, provided that this notice is reproduced on all copies. Neither the government nor the University makes any warranty, express or implied, or assumes any liability or responsibility for the use of MCNP.

CONTENTS

| | |
|--|------|
| CHAPTER 1. PRIMER | 1-1 |
| I. PARTICLE TRANSPORT CALCULATIONS WITH MONTE CARLO | 1-2 |
| II. INTRODUCTION TO MCNP FEATURES | 1-4 |
| III. MCNP GEOMETRY | 1-13 |
| IV. MCNP INPUT FOR SAMPLE PROBLEM | 1-19 |
| V. HOW TO RUN MCNP | 1-29 |
| VI. TIPS FOR CORRECT AND EFFICIENT PROBLEMS | 1-31 |
| VII. REFERENCES | 1-33 |
| CHAPTER 2. GEOMETRY, DATA, PHYSICS, AND MATHEMATICS | 2-1 |
| I. INTRODUCTION | 2-1 |
| A. History | 2-2 |
| B. MCNP Structure | 2-5 |
| C. History Flow | 2-6 |
| II. GEOMETRY | 2-9 |
| A. Complement Operator | 2-9 |
| B. Repeated Structure Geometry | 2-10 |
| C. Surfaces | 2-11 |
| III. CROSS SECTIONS | 2-16 |
| A. Neutron Interaction Data | 2-17 |
| B. Photon Interaction Data | 2-21 |
| C. Electron Interaction Data | 2-22 |
| D. Neutron Dosimetry Cross Sections | 2-23 |
| E. Neutron Thermal $S(\alpha, \beta)$ Tables | 2-23 |
| F. Multigroup Tables | 2-24 |
| IV. PHYSICS | 2-24 |
| A. Particle Weight | 2-25 |
| B. Particle Tracks | 2-26 |
| C. Neutron Interactions | 2-26 |
| D. Photon Interactions | 2-50 |
| E. Electron Interactions | 2-57 |
| V. TALLIES | 2-66 |
| A. Surface Current Tally | 2-68 |

| | |
|---|------------|
| B. Flux Tallies | 2-68 |
| C. Track Length Cell Energy Deposition Tallies | 2-70 |
| D. Pulse Height Tallies | 2-72 |
| E. Flux at a Detector | 2-73 |
| F. Additional Tally Features | 2-83 |
| VI. ESTIMATION OF THE MONTE CARLO PRECISION | 2-86 |
| A. Monte Carlo Means, Variances, and Standard Deviations | 2-87 |
| B. Precision and Accuracy | 2-88 |
| C. The Central Limit Theorem | 2-90 |
| D. Estimated Relative Errors in MCNP | 2-91 |
| E. MCNP <i>FOM</i> | 2-94 |
| F. Separation of Relative Error into Two Components | 2-95 |
| G. Variance of the Variance | 2-97 |
| H. History Score Probability Density Function | 2-99 |
| I. Forming Statistically Valid Confidence Intervals | 2-105 |
| VII. VARIANCE REDUCTION | 2-112 |
| A. General Considerations | 2-112 |
| B. Variance Reduction Techniques | 2-117 |
| VIII. CRITICALITY CALCULATIONS | 2-141 |
| A. Criticality Program Flow | 2-141 |
| B. Estimation of k_{eff} Confidence Intervals and Prompt Neutron Lifetimes | 2-144 |
| IX. VOLUMES AND AREAS | 2-156 |
| A. Rotationally Symmetric Volumes and Areas | 2-157 |
| B. Polyhedron Volumes and Areas | 2-157 |
| C. Stochastic Volume and Area Calculation | 2-158 |
| X. PLOTTER | 2-159 |
| XI. PSEUDORANDOM NUMBERS | 2-161 |
| XII. REFERENCES | 2-164 |
| CHAPTER 3 DESCRIPTION OF MCNP INPUT | 3-1 |
| I. INP FILE | 3-1 |
| A. Message Block | 3-1 |
| B. Initiate-Run | 3-2 |
| C. Continue-Run | 3-2 |
| D. Card Format | 3-4 |
| E. Particle Designators | 3-7 |
| F. Default Values | 3-7 |

| | |
|---|------------|
| G. Input Error Messages | 3-8 |
| H. Geometry Errors | 3-8 |
| II. CELL CARDS | 3-9 |
| A. Shorthand Cell Specification | 3-12 |
| III. SURFACE CARDS | 3-12 |
| A. Surfaces Defined by Equations | 3-12 |
| B. Axisymmetric Surfaces Defined by Points | 3-16 |
| C. General Plane Defined by Three Points | 3-18 |
| IV. DATA CARDS | 3-18 |
| A. Problem Type (MODE) Card | 3-19 |
| B. Geometry Cards | 3-19 |
| C. Variance Reduction | 3-28 |
| D. Source Specification | 3-39 |
| E. Tally Specification | 3-59 |
| F. Material Specification Cards | 3-91 |
| G. Energy and Thermal Treatment Specification | 3-99 |
| H. Problem Cutoff Cards | 3-107 |
| I. User Data Arrays | 3-110 |
| J. Peripheral Cards | 3-110 |
| V. SUMMARY OF MCNP INPUT FILE | 3-123 |
| A. Input Cards | 3-123 |
| B. Storage Limitations | 3-126 |
| CHAPTER 4 EXAMPLES | 4-1 |
| I. GEOMETRY SPECIFICATION | 4-1 |
| II. COORDINATE TRANSFORMATIONS | 4-14 |
| III. REPEATED STRUCTURE AND LATTICE EXAMPLES | 4-19 |
| IV. TALLY EXAMPLES | 4-34 |
| A. FMn Examples (Simple Form) | 4-34 |
| B. FMn Examples (General Form) | 4-36 |
| C. FSn Examples | 4-37 |
| D. FTn Examples | 4-38 |
| E. Repeated Structure/Lattice Tally Example | 4-41 |
| F. TALLYX Subroutine Examples | 4-44 |
| V. SOURCE EXAMPLES | 4-47 |
| VI. SOURCE SUBROUTINE | 4-50 |
| VII. SRCDX SUBROUTINE | 4-51 |

| | |
|--|----------------|
| CHAPTER 5. OUTPUT | 5-1 |
| I. DEMO PROBLEM AND OUTPUT | 5-1 |
| II. TEST1 PROBLEM AND OUTPUT | 5-10 |
| III. CONC PROBLEM AND OUTPUT | 5-50 |
| IV. KCODE | 5-64 |
| V. EVENT LOG AND GEOMETRY ERRORS | 5-97 |
| A. Event Log | 5-97 |
| B. Debug Print | 5-99 |
| APPENDICES | A-1 |
| B. MCNP GEOMETRY AND TALLY PLOTTING | B-1 |
| C. INSTALLING MCNP ON VARIOUS SYSTEMS | C-1 |
| D. MODIFYING MCNP | D-1 |
| E. GLOBAL CONSTANTS, VARIABLES, AND ARRAYS | E-1 |
| F. DATA TABLE FORMATS | F-1 |
| G. NEUTRON CROSS-SECTION LIBRARIES | G-1 |
| H. FISSION SPECTRA CONSTANTS AND FLUX-TO-DOSE FACTORS | H-1 |
| I. PTRAC TABLES | I-1 |
| INDEX | INDEX-1 |

MCNP—A General Monte Carlo
N-Particle Transport Code
Version 4A

Radiation Transport Group
Los Alamos National Laboratory

ABSTRACT

MCNP is a general-purpose Monte Carlo N-Particle code that can be used for neutron, photon, electron, or coupled neutron/photon/electron transport, including the capability to calculate eigenvalues for critical systems. The code treats an arbitrary three-dimensional configuration of materials in geometric cells bounded by first- and second-degree surfaces and fourth-degree elliptical tori.

Pointwise cross-section data are used. For neutrons, all reactions given in a particular cross-section evaluation (such as ENDF/B-VI) are accounted for. Thermal neutrons are described by both the free gas and $S(\alpha, \beta)$ models. For photons, the code takes account of incoherent and coherent scattering, the possibility of fluorescent emission after photoelectric absorption, absorption in pair production with local emission of annihilation radiation, and bremsstrahlung. A continuous slowing down model is used for electron transport that includes positrons, k x-rays, and bremsstrahlung but does not include external or self-induced fields.

Important standard features that make MCNP very versatile and easy to use include a powerful general source, criticality source, and surface source; both geometry and output tally plotters; a rich collection of variance reduction techniques; a flexible tally structure; and an extensive collection of cross-section data.

NOTES:

CHAPTER 1 PRIMER

WHAT IS COVERED IN CHAPTER 1

- Brief explanation of the Monte Carlo method.
- Summary of MCNP features.
- Introduction to geometry.
- Description of MCNP data input illustrated by a sample problem.
- How to run MCNP.
- Tips on problem setup.

Chapter 1 will enable the novice to start using MCNP, assuming very little knowledge of the Monte Carlo method and no experience with MCNP. The primer begins with a short discussion of the Monte Carlo method. Five features of MCNP are introduced: (1) nuclear data and reactions, (2) source specifications, (3) tallies and output, (4) estimation of errors, and (5) variance reduction. The third section explains MCNP geometry setup, including the concept of cells and surfaces. A general description of an input deck is followed by a sample problem and a detailed description of the input cards used in the sample problem. Section V tells how to run MCNP, VI lists tips for setting up correct problems and running them efficiently, and VII is the references for Chapter 1. The word "card" is used throughout this document to describe a single line of input up to 80 characters.

MCNP is a general-purpose, continuous-energy, generalized-geometry, time-dependent, coupled neutron/photon/electron Monte Carlo transport code. It can be used in several transport modes: neutron only, photon only, electron only, combined neutron/photon transport where the photons are produced by neutron interactions, neutron/photon/electron, photon/electron, or electron/photon. The neutron energy regime is from 10^{-11} MeV to 20 MeV, and the photon and electron energy regimes are from 1 keV to 1000 MeV. The capability to calculate k_{eff} eigenvalues for fissile systems is also a standard feature.

The user creates an input file that is subsequently read by MCNP. This file contains information about the problem in areas such as:

- the geometry specification,
- the description of materials and selection of cross-section evaluations,
- the location and characteristics of the neutron, photon, or electron source,
- the type of answers or tallies desired, and
- any variance reduction techniques used to improve efficiency.

Each area will be discussed in the primer by use of a sample problem.

Remember five "rules" when running a Monte Carlo calculation. They will be more meaningful as you read this manual and gain experience with MCNP, but no matter how sophisticated a user you may become, never forget the following five points:

CHAPTER 1

Introduction

1. Define and sample the geometry and source well;
2. You cannot recover lost information;
3. Question the stability and reliability of results;
4. Be conservative and cautious with variance reduction biasing; and
5. The number of histories run is not indicative of the quality of the answer.

The following sections compare Monte Carlo and deterministic methods and provide a simple description of the Monte Carlo method.

A. Monte Carlo Method vs Deterministic Method

Monte Carlo methods are very different from deterministic transport methods. Deterministic methods, the most common of which is the discrete ordinates method, solve the transport equation for the average particle behavior. By contrast, Monte Carlo does not solve an explicit equation, but rather obtains answers by simulating individual particles and recording some aspects (tallies) of their average behavior. The average behavior of particles in the physical system is then inferred (using the central limit theorem) from the average behavior of the simulated particles. Not only are Monte Carlo and deterministic methods very different ways of solving a problem, even what constitutes a solution is different. Deterministic methods typically give fairly complete information (for example, flux) throughout the phase space of the problem. Monte Carlo supplies information only about specific tallies requested by the user.

When Monte Carlo and discrete ordinates methods are compared, it is often said that Monte Carlo solves the integral transport equation, whereas discrete ordinates solves the integro-differential transport equation. Two things are misleading about this statement. First, the integral and integro-differential transport equations are two different forms of the same equation; if one is solved, the other is solved. Second, Monte Carlo “solves” a transport problem by simulating particle histories rather than by solving an equation. No transport equation need ever be written to solve a transport problem by Monte Carlo. Nonetheless, one can derive an equation that describes the probability density of particles in phase space; this equation turns out to be the same as the integral transport equation.

Without deriving the integral transport equation, it is instructive to investigate why the discrete ordinates method is associated with the integro-differential equation and Monte Carlo with the integral equation. The discrete ordinates method visualizes the phase space to be divided into many small boxes, and the particles move from one box to another. In the limit as the boxes get progressively smaller, particles moving from box to box take a differential amount of time to move a differential distance in space. In the limit this approaches the integro-differential transport equation, which has derivatives in space and time. By contrast, Monte Carlo transports particles between events (for example, collisions) that are separated in space and time. Neither differential space nor time are inherent parameters of Monte Carlo transport. The integral equation does not have time or space derivatives.

Monte Carlo is well suited to solving complicated three-dimensional time-dependent problems. Because the Monte Carlo method does not use phase space boxes, there are no averaging approximations required in space, energy, and time. This is especially important in allowing detailed representation of all aspects of physical data.

B. The Monte Carlo Method

Monte Carlo can be used to duplicate theoretically a statistical process (such as the interaction of nuclear particles with materials) and is particularly useful for complex problems that cannot be modeled by computer codes that use deterministic methods. The individual probabilistic events that comprise a process are simulated sequentially. The probability distributions governing these events are statistically sampled to describe the total phenomenon. In general, the simulation is performed on a digital computer because the number of trials necessary to adequately describe the phenomenon is usually quite large. The statistical sampling process is based on the selection of random numbers—analogue to throwing dice in a gambling casino—hence the name “Monte Carlo.” In particle transport, the Monte Carlo technique is pre-eminently realistic (a theoretical experiment). It consists of actually following each of many particles from a source throughout its life to its death in some terminal category (absorption, escape, etc.). Probability distributions are randomly sampled using transport data to determine the outcome at each step of its life.

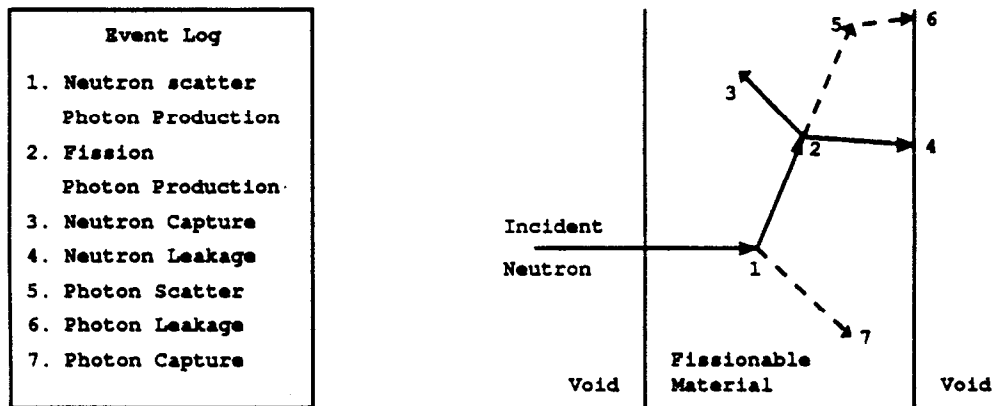


Figure 1.1

Figure 1.1 represents the random history of a neutron incident on a slab of material that can undergo fission. Numbers between 0 and 1 are selected randomly to determine what (if any) and where interaction takes place, based on the rules (physics) and probabilities (transport data) governing the processes and materials involved. In this particular example, a neutron collision occurs at event 1. The neutron is scattered in the direction shown, which is selected randomly from the physical scattering distribution. A photon is also produced and is temporarily stored, or banked, for later analysis. At event 2, fission occurs, resulting in the termination of the incoming neutron and the birth of two outgoing neutrons and one photon. One neutron and

CHAPTER 1

Features

the photon are banked for later analysis. The first fission neutron is captured at event 3 and terminated. The banked neutron is now retrieved and, by random sampling, leaks out of the slab at event 4. The fission-produced photon has a collision at event 5 and leaks out at event 6. The remaining photon generated at event 1 is now followed with a capture at event 7. Note that MCNP retrieves banked particles such that the last particle stored in the bank is the first particle taken out.

This neutron history is now complete. As more and more such histories are followed, the neutron and photon distributions become better known. The quantities of interest (whatever the user requests) are tallied, along with estimates of the statistical precision (uncertainty) of the results.

II. INTRODUCTION TO MCNP FEATURES

Various features, concepts, and capabilities of MCNP are summarized in this section. More detail concerning each topic is available in later chapters or appendices.

A. Nuclear Data and Reactions

MCNP uses continuous-energy nuclear and atomic data libraries. The primary sources of nuclear data are evaluations from the Evaluated Nuclear Data File (ENDF)¹ system, the Evaluated Nuclear Data Library (ENDL)² and the Activation Library (ACTL)³ compilations from Livermore, and evaluations from the Applied Nuclear Science (T-2) Group⁴⁻⁶ at Los Alamos. Evaluated data are processed into a format appropriate for MCNP by codes such as NJOY⁷. The processed nuclear data libraries retain as much detail from the original evaluations as is feasible to faithfully reproduce the evaluator's intent.

Nuclear data tables exist for neutron interactions, neutron-induced photons, photon interactions, neutron dosimetry or activation, and thermal particle scattering $S(\alpha, \beta)$. Photon and electron data are atomic rather than nuclear in nature. Each data table available to MCNP is listed on a directory file, XSDIR. Users may select specific data tables through unique identifiers for each table, called ZAIDs. These identifiers generally contain the atomic number Z, mass number A, and library specifier ID.

Over 500 neutron interaction tables are available for approximately 100 different isotopes and elements. Multiple tables for a single isotope are provided primarily because data have been derived from different evaluations, but also because of different temperature regimes and different processing tolerances. More neutron interaction tables are constantly being added as new and revised evaluations become available. Neutron-induced photon production data are given as part of the neutron interaction tables when such data are included in the evaluations.

Photon interaction tables exist for all elements from Z=1 through Z=94. The data in the photon interaction tables allow MCNP to account for coherent and incoherent scattering, photoelectric absorption with the possibility of fluorescent emission, and pair production. Scattering angular distributions are modified by atomic form factors and incoherent scattering functions.

Cross sections for nearly 2000 dosimetry or activation reactions involving over 400 target nuclei in ground and excited states are part of the MCNP data package. These cross sections can be used as energy-dependent response functions in MCNP to determine reaction rates but can not be used as transport cross sections.

Thermal data tables are appropriate for use with the $S(\alpha, \beta)$ scattering treatment in MCNP. The data include chemical (molecular) binding and crystalline effects that become important as the neutron's energy becomes sufficiently low. Data at various temperatures are available for light and heavy water, beryllium metal, beryllium oxide, benzene, graphite, polyethylene, and zirconium and hydrogen in zirconium hydride.

B. Source Specification

MCNP's generalized user-input source capability allows the user to specify a wide variety of source conditions without having to make a code modification. Independent probability distributions may be specified for the source variables of energy, time, position and direction, and for other parameters such as starting cell(s) or surface(s). Information about the geometrical extent of the source can also be given. In addition, source variables may depend on other source variables (for example, energy as a function of angle) thus extending the built-in source capabilities of the code. The user can bias all input distributions.

In addition to input probability distributions for source variables, certain built-in functions are available. These include various analytic functions for fission and fusion energy spectra such as Watt, Maxwellian and Gaussian spectra; Gaussian for time; and isotropic, cosine, and monodirectional for direction. Biasing may also be accomplished by special built-in functions.

A surface source allows particles crossing a surface in one problem to be used as the source for a subsequent problem. The decoupling of a calculation into several parts allows detailed design or analysis of certain geometrical regions without having to rerun the entire problem from the beginning each time. The surface source has a fission volume source option that starts particles from fission sites where they were written in a previous run.

MCNP provides the user three methods to define an initial criticality source to estimate k_{eff} , the ratio of neutrons produced in successive generations in fissile systems.

C. Tallies and Output

The user can instruct MCNP to make various tallies related to particle current, particle flux, and energy deposition. MCNP tallies are normalized to be per starting particle except for a few special cases with criticality sources. Currents can be tallied as a function of direction across any set of surfaces, surface segments, or sum of surfaces in the problem. Charge can be tallied for electrons and positrons. Fluxes across any set of surfaces, surface segments, sum of surfaces, and in cells, cell segments, or sum of cells are also available. Similarly, the fluxes at designated detectors (points or rings) are standard tallies. Heating and fission tallies give the energy deposition in specified

CHAPTER 1

Features

cells. A pulse height tally provides the energy distribution of pulses created in a detector by radiation. In addition, particles may be flagged when they cross specified surfaces or enter designated cells, and the contributions of these flagged particles to the tallies are listed separately. Tallies such as the number of fissions, the number of absorptions, the total helium production, or any product of the flux times the approximately 100 standard ENDF reactions plus several nonstandard ones may be calculated with any of the MCNP tallies. In fact, any quantity of the form

$$C \int \phi(\mathbf{E}) \mathbf{f}(\mathbf{E}) \, d\mathbf{E}$$

may be tallied, where $\phi(\mathbf{E})$ is the energy-dependent fluence, and $\mathbf{f}(\mathbf{E})$ is any product or summation of the quantities in the cross-section libraries or a response function provided by the user. The tallies may also be reduced by line-of-sight attenuation. Tallies may be made for segments of cells and surfaces without having to build the desired segments into the actual problem geometry. All tallies are functions of time and energy as specified by the user and are normalized to be per starting particle.

In addition to the tally information, the output file contains tables of standard summary information to give the user a better idea of how the problem ran. This information can give insight into the physics of the problem and the adequacy of the Monte Carlo simulation. If errors occur during the running of a problem, detailed diagnostic prints for debugging are given. Printed with each tally is also its statistical relative error corresponding to one standard deviation. Following the tally is a detailed analysis to aid in determining confidence in the results. Ten pass/no pass checks are made for the user-selectable tally fluctuation chart (TFC) bin of each tally. The quality of the confidence interval still cannot be guaranteed because portions of the problem phase space possibly still have not been sampled. Tally fluctuation charts, described in the following section, are also automatically printed to show how a tally mean, error, variance of the variance, and slope of the largest history scores fluctuate as a function of the number of histories run.

Tally results can be displayed graphically, either while the code is running or in a separate postprocessing mode.

D. Estimation of Monte Carlo Errors

MCNP tallies are normalized to be per starting particle and are printed in the output accompanied by a second number R , which is the estimated relative error defined to be one estimated standard deviation of the mean $S_{\bar{x}}$ divided by the estimated mean \bar{x} . In MCNP, the quantities required for this error estimate—the tally and its second moment—are computed after each complete Monte Carlo history, which accounts for the fact that the various contributions to a tally from the same history are correlated. For a well-behaved tally, R will be proportional to $1/\sqrt{N}$ where N is the number of histories. Thus, to halve R , we must increase the total number of histories fourfold. For a poorly behaved tally, R may increase as the number of histories increases.

The estimated relative error can be used to form confidence intervals about the estimated mean, allowing one to make a statement about what the true result is. The Central Limit Theorem states that as N approaches infinity there is a 68% chance that the true result will be in the range $\bar{x}(1 \pm R)$ and a 95% chance in the range $\bar{x}(1 \pm 2R)$. *It is extremely important to note that these confidence statements refer only to the precision of the Monte Carlo calculation itself and not to the accuracy of the result compared to the true physical value.* A statement regarding accuracy requires a detailed analysis of the uncertainties in the physical data, modeling, sampling techniques and approximations, etc., used in a calculation.

The guidelines for interpreting the quality of the confidence interval for various values of R are listed in Table 1.1.

Table 1.1
Guidelines for Interpreting the Relative Error R^*

| <u>Range of R</u> | <u>Quality of the Tally</u> |
|--------------------------------|--|
| 0.5 to 1.0 | Not meaningful |
| 0.2 to 0.5 | Factor of a few |
| 0.1 to 0.2 | Questionable |
| < 0.10 | Generally reliable |
| < 0.05 | Generally reliable for point detectors |

* $R = S_{\bar{x}}/\bar{x}$ and represents the estimated relative error at the 1σ level. These interpretations of R assume that all portions of the problem phase space are being sampled well by the Monte Carlo process.

For all tallies except next-event estimators, hereafter referred to as point detector tallies, the quantity R should be less than 0.10 to produce generally reliable confidence intervals. Point detector results tend to have larger third and fourth moments of the individual tally distributions, so a smaller value of R , < 0.05, is required to produce generally reliable confidence intervals. The estimated uncertainty in the Monte Carlo result must be presented with the tally so that all are aware of the estimated precision of the results.

Keep in mind the footnote to Table 1.1. For example, if an important but highly unlikely particle path in phase space has not been sampled in a problem, the Monte Carlo results will not have the correct expected values and the confidence interval statements may not be correct. The user can guard against this situation by setting up the problem so as not to exclude any regions of phase space and by trying to sample all regions of the problem adequately.

Despite one's best effort, an important path may not be sampled often enough, causing confidence interval statements to be incorrect. To try to inform the user about this behavior, MCNP calculates a figure of merit (FOM) for one tally bin of each tally as a function of the number of histories and prints the results in the tally fluctuation charts at the end of the output. The FOM is defined as

$$FOM \equiv 1/(R^2T),$$

CHAPTER 1

Features

where T is the computer time in minutes. The more efficient a Monte Carlo calculation is, the larger the FOM will be because less computer time is required to reach a given value of R .

The FOM should be approximately constant as N increases because R^2 is proportional to $1/N$ and T is proportional to N . *Always examine the tally fluctuation charts to be sure that the tally appears well behaved, as evidenced by a fairly constant FOM .* A sharp decrease in the FOM indicates that a seldom-sampled particle path has significantly affected the tally result and relative error estimate. In this case, the confidence intervals may not be correct the fraction of the time that statistical theory would indicate. Examine the problem to determine what path is causing the large scores and try to redefine the problem to sample that path much more frequently.

After each tally, an analysis is done and additional useful information is printed about the TFC tally bin result. The nonzero scoring efficiency, the zero and nonzero score components of the relative error, number and magnitude of negative history scores, if any, and the effect on the result if the largest observed history score in the TFC were to occur again on the very next history are given. A table just before the TFCs summarizes the results of these checks for all tallies in the problem. Ten statistical checks are made and summarized in table 160 after each tally, with a pass yes/no criterion. The empirical history score probability density function (PDF) for the TFC bin of each tally is calculated and displayed in printed plots.

The TFCs at the end of the problem include the variance of the variance (an estimate of the error of the relative error), and the slope (the estimated exponent of the PDF large score behavior) as a function of the number of particles started.

All this information provides the user with statistical information to aid in forming valid confidence intervals for Monte Carlo results. There is no GUARANTEE, however. The possibility always exists that some as yet unsampled portion of the problem may change the confidence interval if more histories were calculated. Chapter 2 contains more information about estimation of Monte Carlo precision.

E. Variance Reduction

As noted in the previous section, R (the estimated relative error) is proportional to $1/\sqrt{N}$, where N is the number of histories. For a given MCNP run, the computer time T consumed is proportional to N . Thus $R = C/\sqrt{T}$, where C is a positive constant. There are two ways to reduce R : (1) increase T and/or (2) decrease C . Computer budgets often limit the utility of the first approach. For example, if it has taken 2 hours to obtain $R = 0.10$, then 200 hours will be required to obtain $R = 0.01$. For this reason MCNP has special variance reduction techniques for decreasing C . (Variance is the square of the standard deviation.) The constant C depends on the tally choice and/or the sampling choices.

1. Tally Choice

As an example of the tally choice, note that the fluence in a cell can

be estimated either by a collision estimate or a track length estimate. The collision estimate is obtained by tallying $1/\Sigma_t$ (Σ_t =macroscopic total cross section) at each collision in the cell and the track length estimate is obtained by tallying the distance the particle moves while inside the cell. Note that as Σ_t gets very small, very few particles collide but give enormous tallies when they do, a high variance situation (see page 2-95). In contrast, the track length estimate gets a tally from every particle that enters the cell. For this reason MCNP has track length tallies as standard tallies, whereas the collision tally is not standard in MCNP, except for estimating k_{eff} .

2. Nonanalog Monte Carlo

Explaining how sampling affects C requires understanding of the nonanalog Monte Carlo model.

The simplest Monte Carlo model for particle transport problems is the analog model that uses the natural probabilities that various events occur (for example, collision, fission, capture, etc.). Particles are followed from event to event by a computer, and the next event is always sampled (using the random number generator) from a number of possible next events according to the natural event probabilities. This is called the analog Monte Carlo model because it is directly analogous to the naturally occurring transport.

The analog Monte Carlo model works well when a significant fraction of the particles contribute to the tally estimate and can be compared to detecting a significant fraction of the particles in the physical situation. There are many cases for which the fraction of particles detected is very small, less than 10^{-6} . For these problems analog Monte Carlo fails because few, if any, of the particles tally, and the statistical uncertainty in the answer is unacceptable.

Although the analog Monte Carlo model is the simplest conceptual probability model, there are other probability models for particle transport. They estimate the same average value as the analog Monte Carlo model, while often making the variance (uncertainty) of the estimate much smaller than the variance for the analog estimate. Practically, this means that problems that would be impossible to solve in days of computer time can be solved in minutes of computer time.

A nonanalog Monte Carlo model attempts to follow "interesting" particles more often than "uninteresting" ones. An "interesting" particle is one that contributes a large amount to the quantity (or quantities) that needs to be estimated. There are many nonanalog techniques, and they all are meant to increase the odds that a particle scores (contributes). To ensure that the average score is the same in the nonanalog model as in the analog model, the score is modified to remove the effect of biasing (changing) the natural odds. Thus, if a particle is artificially made q times as likely to execute a given random walk, then the particle's score is weighted by (multiplied by) $1/q$. The average score is thus preserved because the average score is the sum, over all random walks, of the probability of a random walk multiplied by the score resulting from that random walk.

A nonanalog Monte Carlo technique will have the same expected tallies as an analog technique if the expected weight executing any given random walk

CHAPTER 1

Features

is preserved. For example, a particle can be split into two identical pieces and the tallies of each piece are weighted by 1/2 of what the tallies would have been without the split. Such nonanalog, or variance reduction, techniques can often decrease the relative error by sampling naturally rare events with an unnaturally high frequency and weighting the tallies appropriately.

3. Variance Reduction Tools in MCNP

There are four classes of variance reduction techniques⁸ that range from the trivial to the esoteric.

Truncation Methods are the simplest of variance reduction methods. They speed up calculations by truncating parts of phase space that do not contribute significantly to the solution. The simplest example is geometry truncation in which unimportant parts of the geometry are simply not modeled. Specific truncation methods available in MCNP are energy cutoff and time cutoff.

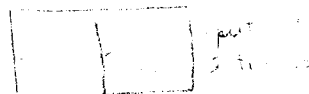
Population Control Methods use particle splitting and Russian roulette to control the number of samples taken in various regions of phase space. In important regions many samples of low weight are tracked, while in unimportant regions few samples of high weight are tracked. A weight adjustment is made to ensure that the problem solution remains unbiased. Specific population control methods available in MCNP are geometry splitting and Russian roulette, energy splitting/roulette, weight cutoff, and weight windows.

Modified Sampling Methods alter the statistical sampling of a problem to increase the number of tallies per particle. For any Monte Carlo event it is possible to sample from any arbitrary distribution rather than the physical probability as long as the particle weights are then adjusted to compensate. Thus with modified sampling methods, sampling is done from distributions that send particles in desired directions or into other desired regions of phase space such as time or energy, or change the location or type of collisions. Modified sampling methods in MCNP include the exponential transform, implicit capture, forced collisions, source biasing, and neutron-induced photon production biasing.

Partially-Deterministic Methods are the most complicated class of variance reduction methods. They circumvent the normal random walk process by using deterministic-like techniques, such as next event estimators, or by controlling of the random number sequence. In MCNP these methods include point detectors, DXTRAN, and correlated sampling.

Variance reduction techniques, used correctly, can greatly help the user to produce a more efficient calculation. Used poorly, they can result in a wrong answer with good statistics and few clues that anything is amiss. Some variance reduction methods have general application and are not easily misused. Others are more specialized and attempts to use them carry high risk. The use of weight windows tends to be more powerful than the use of importances but typically requires more input data and more insight into the problem. The exponential transform for thick shields is not recommended for the inexperienced user; rather, use many cells with increasing importances (or decreasing weight windows) through the shield. Forced collisions are used

particles are split into one
some unless optically
cause. Then particles
are split into tracks.



CHAPTER 1 Features

to increase the frequency of random walk collisions within optically thin cells but should be used only by an experienced user. The point detector estimator should be used with caution, as should DXTRAN.

For many problems, variance reduction is not just a way to speed up the problem but is absolutely necessary to get any answer at all. Deep penetration problems and pipe detector problems, for example, will run too slowly by factors of trillions without adequate variance reduction. Consequently, users have to become skilled in using the variance reduction techniques in MCNP. Most of the following techniques can not be used with the pulse height tally.

The following summarizes briefly the main MCNP variance reduction techniques. Detailed discussion is in Chapter 2, page 2-112.

- a. *Energy cutoff*: Particles whose energy is out of the range of interest are terminated so that computation time is not spent following them.
- b. *Time cutoff*: Like the energy cutoff but based on time.
- c. *Geometry splitting with Russian roulette*: Particles transported from a region of higher importance to a region of lower importance (where they will probably contribute little to the desired problem result) undergo Russian roulette; that is, some of those particles will be killed a certain fraction of the time, but survivors will be counted more by increasing their weight the remaining fraction of the time. In this way, unimportant particles are followed less often, yet the problem solution remains undistorted. On the other hand, if a particle is transported to a region of higher importance (where it will likely contribute to the desired problem result), it may be split into two or more particles (or tracks), each with less weight and therefore counting less. In this way, important particles are followed more often, yet the solution is undistorted because on average total weight is conserved.
- d. *Energy splitting/Russian roulette*: Particles can be split or rouletted upon entering various user-supplied energy ranges. Thus important energy ranges can be sampled more frequently by splitting the weight among several particles and less important energy ranges can be sampled less frequently by rouletting particles.
- e. *Weight cutoff/Russian roulette*: If a particle weight becomes so low that the particle becomes insignificant, it undergoes Russian roulette. Most particles are killed, and some particles survive with increased weight. The solution is unbiased because total weight is conserved, but computer time is not wasted on insignificant particles.
- f. *Weight window*: As a function of energy, geometrical location, or both, low-weighted particles are eliminated by Russian roulette and high-weighted particles are split. This technique helps keep the weight dispersion within reasonable bounds throughout the problem. An importance generator is available that estimates the optimal limits for a weight window.
- g. *Exponential transformation*: To transport particles long distances, the distance between collisions in a preferred direction is artificially increased and the weight is correspondingly artificially decreased. Because large

CHAPTER 1

Features

weight fluctuations often result, it is highly recommended that the weight window be used with the exponential transform.

- h. Implicit capture:* When a particle collides, there is a probability that it is captured by the nucleus. In analog capture, the particle is killed with that probability. In implicit capture, also known as survival biasing, the particle is never killed by capture; instead, its weight is reduced by the capture probability at each collision. Important particles are permitted to survive by not being lost to capture. On the other hand, if particles are no longer considered useful after undergoing a few collisions, analog capture efficiently gets rid of them.
- i. Forced collisions:* A particle can be forced to undergo a collision each time it enters a designated cell that is almost transparent to it. The particle and its weight are appropriately split into a collided and uncollided part. Forced collisions are often used to generate contributions to point detectors, ring detectors, or DXTRAN spheres.
- j. Source variable biasing:* Source particles with phase space variables of more importance are emitted with a higher frequency but with a compensating lower weight than are less important source particles. This technique can be used with pulse height tallies.
- k. Point and ring detectors:* When the user wishes to tally a flux-related quantity at a point in space, the probability of transporting a particle precisely to that point is vanishingly small. Therefore, pseudoparticles are directed to the point instead. Every time a particle history is born in the source or undergoes a collision, the user may require that a pseudoparticle be tallied at a specified point in space. In this way, many pseudoparticles of low weight reach the detector, which is the point of interest, even though no particle histories could ever reach the detector. For problems with rotational symmetry, the point may be represented by a ring to enhance the efficiency of the calculation.
- l. DXTRAN:* DXTRAN, which stands for deterministic transport, improves sampling in the vicinity of detectors or other tallies. It involves deterministically transporting particles on collision to some arbitrary, user-defined sphere in the neighborhood of a tally and then calculating contributions to the tally from these particles. Contributions to the detectors or to the DXTRAN spheres can be controlled as a function of geometric cell or as a function of the relative magnitude of the contribution to the detector or DXTRAN sphere.

The DXTRAN method is a way of obtaining large numbers of particles on user-specified "DXTRAN spheres." DXTRAN makes it possible to obtain many particles in a small region of interest that would otherwise be difficult to sample. Upon sampling a collision or source density function, DXTRAN estimates the correct weight fraction that should scatter toward, and arrive without collision at, the surface of the sphere. The DXTRAN method then puts this correct weight on the sphere. The source or collision event is sampled in the usual manner, except that the particle is killed if it tries to enter the sphere because all particles

entering the sphere have already been accounted for deterministically.

- m. Correlated sampling:* The sequence of random numbers in the Monte Carlo process is chosen so that statistical fluctuations in the problem solution will not mask small variations in that solution resulting from slight changes in the problem specification. The i^{th} history will always start at the same point in the random number sequence no matter what the previous $i - 1$ particles did in their random walks.

III. MCNP GEOMETRY

We will present here only basic information about geometry setup, surface specification, and cell and surface card input. Areas of further interest would be the complement operator, use of parentheses, and repeated structure and lattice definitions, found in Chapter 2. Chapter 4 contains geometry examples and is recommended as a next step. Chapter 3 has detailed information about the format and entries on cell and surface cards.

The geometry of MCNP treats an arbitrary three-dimensional configuration of user-defined materials in geometric cells bounded by first- and second-degree surfaces and fourth-degree elliptical tori. The cells are defined by the intersections, unions, and complements of the regions bounded by the surfaces. Surfaces are defined by supplying coefficients to the analytic surface equations or, for certain types of surfaces, known points on the surfaces.

MCNP has a more general geometry than is available in most combinatorial geometry codes. Rather than combining several predefined geometrical bodies as in a combinatorial geometry scheme, MCNP gives the user the added flexibility of defining geometrical regions from all the first and second degree surfaces of analytical geometry and elliptical tori and then of combining them with Boolean operators. The code does extensive internal checking to find input errors. In addition, the geometry-plotting capability in MCNP helps the user check for geometry errors.

MCNP treats geometric cells in a Cartesian coordinate system. The surface equations recognized by MCNP are listed in Table 3.1 on page 3-14. The particular Cartesian coordinate system used is arbitrary and user defined, but the right-handed system shown in Figure 1.2 is often chosen.

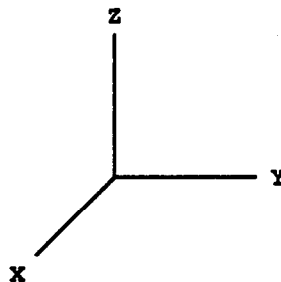


Figure 1.2

Using the bounding surfaces specified on cell cards, MCNP tracks particles through the geometry, calculates the intersection of a track's trajectory

CHAPTER 1

Geometry

with each bounding surface, and finds the minimum positive distance to an intersection. If the distance to the next collision is greater than this minimum distance and there are no DXTRAN spheres along the track, the particle leaves the current cell. At the appropriate surface intersection, MCNP finds the correct cell that the particle will enter by checking the sense of the intersection point for each surface listed for the cell. When a complete match is found, MCNP has found the correct cell on the other side and the transport continues.

A. Cells

When cells are defined, an important concept is that of the *sense* of all points in a cell with respect to a bounding surface. Suppose that $s = f(x, y, z) = 0$ is the equation of a surface in the problem. For any set of points (x, y, z) , if $s = 0$ the points are on the surface. However, for points not on the surface, if s is negative the points are said to have a negative sense with respect to that surface and, conversely, a positive sense if s is positive. For example, a point at $x = 3$ has a positive sense with respect to the plane $x - 2 = 0$. That is, the equation $x - D = 3 - 2 = s = 1$ is positive for $x = 3$ (where $D = \text{constant}$).

Cells are defined on cells cards. Each cell is described by a cell number, material number, and material density followed by a list of operators and signed surfaces that bound the cell. If the sense is positive, the sign can be omitted. The material number and material density can be replaced by a single zero to indicate a void cell. The cell number must begin in columns 1-5. The remaining entries follow, separated by blanks. A more complete description of the cell card format can be found on page 1-22. Each surface divides all space into two regions, one with positive sense with respect to the surface and the other with negative sense. The geometry description defines the cell to be the intersection, union, and/or complement of the listed regions.

The subdivision of the physical space into cells is not necessarily governed only by the different material regions, but may be affected by problems of sampling and variance reduction techniques (such as splitting and Russian roulette), the need to specify an unambiguous geometry, and the tally requirements. The tally segmentation feature may eliminate most of the tally requirements.

Be cautious about making any one cell very complicated. With the union operator and disjointed regions, a very large geometry can be set up with just one cell. The problem is that for each track flight between collisions in a cell, the intersection of the track with each bounding surface of the cell is calculated, a calculation that can be costly if a cell has many surfaces. As an example, consider Figure 1.3a. It is just a lot of parallel cylinders and is easy to set up. However, the cell containing all the little cylinders is bounded by fourteen surfaces (counting a top and bottom). A much more efficient geometry is seen in Figure 1.3b, where the large cell has been broken up into a number of smaller cells.

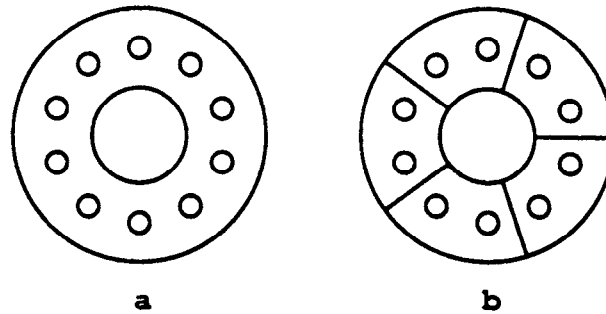


Figure 1.3

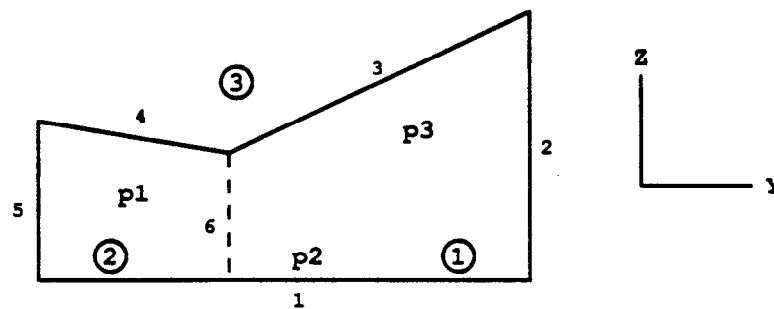


Figure 1.4

1. Cells Defined by Intersections of Regions of Space

The intersection operator in MCNP is implicit; it is simply the blank space between two surface numbers on the cell card.

If a cell is specified using only intersections, all points in the cell must have the same sense with respect to a given bounding surface. This means that, for each bounding surface of a cell, all points in the cell must remain on only one side of any particular surface. Thus, there can be no concave corners in a cell specified only by intersections. Figure 1.4, a cell formed by the intersection of five surfaces (ignore surface 6 for the time being), illustrates the problem of concave corners by allowing a particle (or point) to be on two sides of a surface in one cell.

Surfaces 3 and 4 form a concave corner in the cell such that points p_1 and p_2 are on the same side of surface 4 (that is, have the same sense with respect to 4) but point p_3 is on the other side of surface 4 (opposite sense). Points p_2 and p_3 have the same sense with respect to surface 3, but p_1 has the opposite sense. One way to remedy this dilemma (and there are others) is to add surface 6 between the 3/4 corner and surface 1 to divide the original cell into two cells.

With surface 6 added to Figure 1.4, the cell to the right of surface 6 is number 1 (cells indicated by circled numbers); to the left number 2; and the outside cell number 3. The cell cards (in two dimensions, all cells void) are

| | | | | | |
|---|---|---|----|----|---|
| 1 | 0 | 1 | -2 | -3 | 6 |
| 2 | 0 | 1 | -6 | -4 | 5 |

Cell 1 is a void and is formed by the intersection of the region above (positive sense) surface 1 with the region to the left (negative sense) of surface 2

CHAPTER 1

Geometry

intersected with the region below (negative sense) surface 3 and finally intersected with the region to the right (positive sense) of surface 6. Cell 2 is described similarly.

Cell 3 cannot be specified with the intersection operator. The following section about the union operator is needed to describe cell 3.

2. Cells Defined by Unions of Regions of Space

The union operator, signified by a colon on the cell cards, allows concave corners in cells and also cells that are completely disjoint. The intersection and union operators are binary Boolean operators, so their use follows Boolean algebra methodology; unions and intersections can be used in combination in any cell description.

Spaces on either side of the union operator are irrelevant, but remember that a space without the colon signifies an intersection. In the hierarchy of operations, intersections are performed first and then unions. There is no left to right ordering. Parentheses can be used to clarify operations and in some cases are required to force a certain order of operations. Innermost parentheses are cleared first. Spaces are optional on either side of a parenthesis. A parenthesis is equivalent to a space and signifies an intersection.

For example, let A and B be two regions of space. The region containing points that belong to both A and B is called the intersection of A and B. The region containing points that belong to A alone or to B alone or to both A and B is called the union of A and B. The lined area in Figure 1.5a represents the union of A and B (or $A : B$), and the lined area in Figure 1.5b represents the intersection of A and B (or $A B$). The only way regions of space can be added is with the union operator. An intersection of two spaces always results in a region no larger than either of the two spaces. Conversely, the union of two spaces always results in a region no smaller than either of the two spaces.

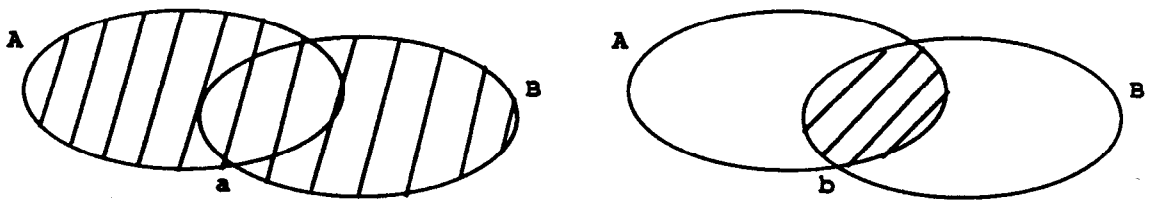


Figure 1.5

A simple example will further illustrate the concept of Figure 1.5 and the union operator to solidify the concept of adding and intersecting regions of space to define a cell. See also the second example in Chapter 4. In Figure 1.6 we have two infinite planes that meet to form two cells. Cell 1 is easy to define; it is everything in the universe to the right of surface 1 (that is, a positive sense) that is also in common with (or intersected with) everything in the universe below surface 2 (that is, a negative sense). Therefore, the surface relation of cell 1 is $1 - 2$.

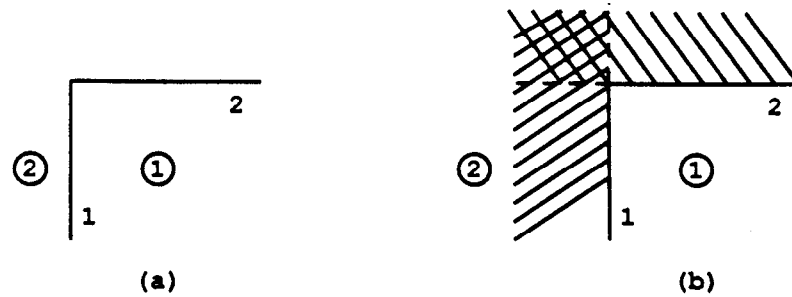


Figure 1.6

Cell 2 is everything in the universe to the left (negative sense) of surface 1 plus everything in the universe above (positive sense) surface 2, or $-1 : 2$, illustrated in Figure 1.6b by all the shaded regions of space. If cell 2 were specified as $-1 \ 2$, that would represent the region of space common to -1 and 2 , which is only the cross-hatched region in the figure and is obviously an improper specification for cell 2.

Returning to Figure 1.4 on page 1-15, if cell 1 is inside the solid black line and cell 2 is the entire region outside the solid line, then the MCNP cell cards in two dimensions are (assuming both cells are voids)

$$\begin{array}{r} 1 \quad 0 \quad 1 \quad -2 \quad (-3 \quad : \quad -4) \quad 5 \\ 2 \quad 0 \quad -5 \quad : \quad -1 \quad : \quad 2 \quad : \quad 3 \quad 4 \end{array}$$

Cell 1 is defined as the region above surface 1 intersected with the region to the left of surface 2, intersected with the union of regions below surfaces 3 and 4, and finally intersected with the region to the right of surface 5. Cell 2 contains four concave corners (all but between surfaces 3 and 4), and its specification is just the converse (or complement) of cell 1. Cell 2 is the space defined by the region to the left of surface 5 plus the region below 1 plus the region to the right of 2 plus the space defined by the intersections of the regions above surfaces 3 and 4.

A simple consistency check can be noted with the two cell cards above. All intersections for cell 1 become unions for cell 2 and vice versa. The senses are also reversed.

Note that in this example, all corners less than 180 degrees in a cell are handled by intersections and all corners greater than 180 degrees are handled by unions.

To illustrate some of the concepts about parentheses, assume an intersection is thought of mathematically as multiplication and a union is thought of mathematically as addition. Parentheses are removed first, with multiplication being performed before addition. The cell cards for the example cards above from Figure 1.4 may be written in the form

$$\begin{array}{r} 1 \quad a \cdot b \cdot (c + d) \cdot e \\ 2 \quad e + a + b + c \cdot d \end{array}$$

Note that parentheses are required for the first cell but not for the second, although the second could have been written as $e + a + b + (c \cdot d)$, $(e + a + b) + (c \cdot d)$, $(e) + (a) + (b) + (c \cdot d)$, etc.

CHAPTER 1 Geometry

Several more examples using the union operator are given in Chapter 4. Study them to get a better understanding of this powerful operator that can greatly simplify geometry setups.

B. Surface Type Specification

The first- and second-degree surfaces plus the fourth-degree elliptical and degenerate tori of analytical geometry are all available in MCNP. The surfaces are designated by mnemonics such as C/Z for a cylinder parallel to the z-axis. A cylinder at an arbitrary orientation is designated by the general quadratic GQ mnemonic. A paraboloid parallel to a coordinate axis is designated by the special quadratic SQ mnemonic. The 29 mnemonics representing various types of surfaces are listed in Table 3.1 on page 3–14.

C. Surface Parameter Specification

There are two ways to specify surface parameters in MCNP: (1) by supplying the appropriate coefficients needed to satisfy the surface equation, and (2) by specifying known geometrical points on a surface that is rotationally symmetric about a coordinate axis.

1. Coefficients for the Surface Equations

The first way to define a surface is to use one of the surface-type mnemonics from Table 3.1 on page 3–14 and to calculate the appropriate coefficients needed to satisfy the surface equation. For example, a sphere of radius 3.62-cm with the center located at the point (4,1,-3) is specified by

S 4 1 -3 3.62

An ellipsoid whose axes are not parallel to the coordinate axes is defined by the GQ mnemonic plus up to 10 coefficients of the general quadratic equation. Calculating the coefficients can be (and frequently is) nontrivial, but the task is greatly simplified by defining an auxiliary coordinate system whose axes coincide with the axes of the ellipsoid. The ellipsoid is easily defined in terms of the auxiliary coordinate system, and the relationship between the auxiliary coordinate system and the main coordinate system is specified on a TRn card, described on page 3–26.

The use of the SQ (special quadratic) and GQ (general quadratic) surfaces is determined by the orientation of the axes. One should always use the simplest possible surface in describing geometries; for example, using a GQ surface instead of an S to specify a sphere will require more computational effort for MCNP.

2. Points that Define a Surface

The second way to define a surface is to supply known points on the surface. This method is convenient if you are setting up a geometry from something like a blueprint where you know the coordinates of intersections of surfaces or points on the surfaces. When three or more surfaces intersect at a point, this second method also produces a more nearly perfect point of intersection if the common point is used in the surface specification. It is frequently difficult to get complicated surfaces to meet at one point if the

surfaces are specified by the equation coefficients. Failure to achieve such a meeting can result in the unwanted loss of particles.

There are, however, restrictions that must be observed when specifying surfaces by points that do not exist when specifying surfaces by coefficients. Surfaces described by points must be either skew planes or surfaces rotationally symmetric about the x, y, or z axes. They must be unique, real, and continuous. For example, points specified on both sheets of a hyperboloid are not allowed because the surface is not continuous. However, it is valid to specify points that are all on one sheet of the hyperboloid. (See the X,Y,Z, and P input cards description on page 3-16 for additional explanation.)

IV. MCNP INPUT FOR SAMPLE PROBLEM

The main input file for the user is the INP (the default name) file that contains the input information to describe the problem. We will present here only the subset of cards required to run the simple fixed source demonstration problem. All input cards are discussed in Chapter 3 and summarized in Table 3.6 starting on page 3-123.

MCNP does extensive input checking but is not foolproof. A geometry should be checked by looking at several different views with the geometry plotting option. You should also surround the entire geometry with a sphere and flood the geometry with particles from a source with an inward cosine distribution on the spherical surface, using a VOID card to remove all materials specified in the problem. If there are any incorrectly specified places in your geometry, this procedure will usually find them. Make sure the importance of the cell just inside the source sphere is not zero. Then run a short job and study the output to see if you are calculating what you think you are calculating.

The basic constants used in MCNP are printed in optional print table 98 in the output file. The units used are:

1. lengths in centimeters,
2. energies in MeV,
3. times in shakes (10^{-8} sec),
4. temperatures in MeV (kT),
5. atomic densities in units of atoms/barn-cm,
6. mass densities in g/cm^3 ,
7. cross sections in barns (10^{-24} cm^2),
8. heating numbers in MeV/collision, and
9. atomic weight ratio based on a neutron mass of 1.008664967. In these units, Avogadro's number is $0.59703109 \times 10^{-24}$.

A simple sample problem illustrated in Figure 1.7 is referred to throughout the remainder of this chapter. We wish to start 14-MeV neutrons at a point isotropic source in the center of a small sphere of oxygen that is embedded in a cube of carbon. A small sphere of iron is also embedded in the carbon. The carbon is a cube 10 cm on each side; the spheres have a 0.5-cm radius and are centered between the front and back faces of the cube.

CHAPTER 1

Input File

We wish to calculate the total and energy-dependent flux in increments of 1 MeV from 14 to 1 MeV

1. on the surface of the iron sphere and
2. averaged in the iron sphere volume.

Bin 1 will be the tally from 0 to 1 MeV.

This geometry has four cells, indicated by circled numbers, and eight surfaces—six planes and two spheres. Surface numbers are written next to the appropriate surfaces. Surface 5 comes out from the page in the $+x$ direction and surface 6 goes back into the page in the $-x$ direction.

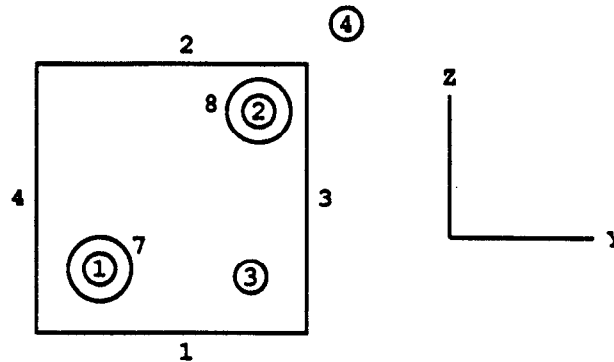


Figure 1.7

With knowledge of the cell card format, the sense of a surface, and the union and intersection operators, we can set up the cell cards for the geometry of our example problem. To simplify this step, assume the cells are void, for now. Cells 1 and 2 are described by the following cards:

```
1 0 -7
2 0 -8
```

where the negative signs denote the regions inside (negative sense) surfaces 7 and 8. Cell 3 is everything in the universe above surface 1 intersected with everything below surface 2 intersected with everything to the left of surface 3 and so forth for the remaining three surfaces. The region in common to all six surfaces is the cube, but we need to exclude the two spheres by intersecting everything outside surface 7 and outside surface 8. The card for cell 3 is

```
3 0 1 -2 -3 4 -5 6 7 8
```

Cell 4 requires the use of the union operator and is similar to the idea illustrated in Figure 1.6. Cell 4 is the outside world, has zero importance, and is defined as everything in the universe below surface 1 plus everything above surface 2 plus everything to the right of surface 3 and so forth. The cell card for cell 4 is

```
4 0 -1 : 2 : 3 : -4 : 5 : -6
```

A. INP File

An input file has the following form:

```

Message Block      } Optional
Blank Line Delimiter }
One Line Problem Title Card
Cell Cards
.
.
Blank Line Delimiter
Surface Cards
.
.
Blank Line Delimiter
Data Cards
.
.
Blank Line Terminator (optional)

```

All input lines are limited to 80 columns. Alphabetic characters can be upper, lower, or mixed case. A \$ (dollar sign) terminates data entry. Anything that follows the \$ is interpreted as a comment. Blank lines are used as delimiters and as an optional terminator. Data entries are separated by one or more blanks.

Comment cards can be used anywhere in the INP file after the problem title card and before the optional blank terminator card. Comment lines must have a C somewhere in columns 1-5 followed by at least one blank and can be a total of 80 columns long.

Cell, surface, and data cards must all begin within the first five columns. Entries are separated by one or more blanks. Numbers can be integer or floating point. MCNP makes the appropriate conversion. A data entry item, e.g., IMP:N or 1.1e2, must be completed on one line.

Blanks filling the first five columns indicate a continuation of the data from the last named card. An & (ampersand) ending a line indicates data will continue on the following card, where data on the continuation card can be in columns 1-80.

The optional message block, discussed in detail on page 3-1, is used to change file names and specify running options such as a continuation run. On most systems these options and files may alternatively be specified with an execution line message (see page 1-29). Message block entries supersede execution line entries. The blank line delimiter signals the end of the message block.

The first card in the file after the optional message block is the required problem title card. If there is no message block, this must be the first card in the INP file. It is limited to one 80-column line and is used as a title in various places in the MCNP output. It can contain any information you desire but usually contains information describing the particular problem.

CHAPTER 1

Input File

MCNP makes extensive checks of the input file for user errors. A FATAL error occurs if a basic constraint of the input specification is violated, and MCNP will terminate before running any particles. The first fatal error is real; subsequent error messages may or may not be real because of the nature of the first fatal message.

B. Cell Cards

The cell number is the first entry and must begin in the first five columns.

The next entry is the cell material number, which is arbitrarily assigned by the user. The material is described on a material card (Mn) that has the same material number (see page 1-27). If the cell is a void, a zero is entered for the material number. The cell and material numbers can not exceed 5 digits.

Next is the cell material density. A positive entry is interpreted as atom density in units of 10^{24} atoms/cm³. A negative entry is interpreted as mass density in units of g/cm³. No density is entered for a void cell.

A complete specification of the geometry of the cell follows. This specification includes a list of the signed surfaces bounding the cell where the sign denotes the sense of the regions defined by the surfaces. The regions are combined with the Boolean intersection and union operators. A space indicates an intersection and a colon indicates a union.

Optionally, after the geometry description, cell parameters can be entered. The form is keyword=value. The following line illustrates the cell card format:

```
1 1 -0.0014 -7 INP:N=1
```

Cell 1 contains material 1 with density 0.0014 g/cm³, is bounded by only one surface (7), and has an importance of 1. If cell 1 were a void, the cell card would be

```
1 0 -7 INP:N=1
```

The complete cell card input for this problem (with 2 comment cards) is

```
c cell cards for sample problem
1 1 -0.0014 -7
2 2 -7.86 -8
3 3 -1.60 1 -2 -3 4 -5 6 7 8
4 0 -1:2:3:-4:5:-6
c end of cell cards for sample problem
blank line delimiter
```

The blank line terminates the cell card section of the INP file. We strongly suggest that the cells be numbered sequentially starting with one. A complete explanation of the cell card input is found in Chapter 3, page 3-9.

C. Surface Cards

The surface number is the first entry. It must begin in columns 1-5 and not exceed 5 digits. The next entry is an alphabetic mnemonic indicating the surface type. Following the surface mnemonic are the numerical coefficients of the equation of the surface in the proper order. This simplified description

enables us to proceed with the example problem. For a full description of the surface card see page 3-12.

Our problem uses planes normal to the x, y, and z axes and two general spheres. The respective mnemonics are PX, PY, PZ, and S. Table 1.2 shows the equations that determine the sense of the surface for the cell cards and the entries required for the surface cards. A complete list of available surface equations is contained in Table 3.1 on page 3-14.

Table 1.2
Surface Equations

| Mnemonic | Equation | Card Entries |
|----------|---|-----------------------------|
| PX | $x - D = 0$ | D |
| PY | $y - D = 0$ | D |
| PZ | $z - D = 0$ | D |
| S | $(x - \bar{x})^2 + (y - \bar{y})^2 + (z - \bar{z})^2 - R^2 = 0$ | $\bar{x} \bar{y} \bar{z} R$ |

For the planes, D is the point where the plane intersects the axis. If we place the origin in the center of the 10-cm cube shown in Figure 1.7, the planes will be at $x = -5$, $x = 5$, etc. The two spheres are not centered at the origin or on an axis, so we must give the x,y,z of their center as well as their radii. The complete surface card input for this problem is shown below. A blank line terminates the surface card portion of the input.

C Beginning of surfaces for cube

- 1 PZ -5
- 2 PZ 5
- 3 PY 5
- 4 PY -5
- 5 PX 5
- 6 PX -5

C End of cube surfaces

- 7 S 0 -4 -2.5 .5 \$ oxygen sphere
- 8 S 0 4 4 .5 \$ iron sphere

blank line delimiter

D. Data Cards

The remaining data input for MCNP follow the second blank card delimiter, or third blank card if there is a message block. The card name is the first entry and must begin in the first five columns. The required entries follow, separated by one or more blanks.

Several of the data cards require a particle designator to distinguish between input data for neutrons, data for photons, and data for electrons. The particle designator consists of the symbol : (colon) and the letter N or P or E immediately following the name of the card. For example, to enter

CHAPTER 1

Input File

neutron importances, use an IMP:N card; enter photon importances on an IMP:P card; enter electron importances on an IMP:E card. No data card can be used more than once with the same mnemonic, that is, M1 and M2 are acceptable, but two M1 cards are not allowed. Defaults have been set for cards in some categories. A summary starting on page 3-123 shows which cards are required, which are optional, and whether defaults exist and if so, what they are. The sample problem will use cards in the following categories:

| | <u>MCNP card name</u> |
|---------------------------------|-----------------------|
| 1. mode, | MODE |
| 2. cell and surface parameters, | IMP:N |
| 3. source specification, | SDEF |
| 4. tally specification, | Fn, En |
| 5. material specification, and | Mn |
| 6. problem cutoffs. | NPS |

A complete description of the data cards is found on page 3-18 in Chapter 3.

1. MODE card

MCNP can be run in several different modes:

- Mode N - neutron transport only (default)
- N P - neutron and neutron-induced photon transport
- P - photon transport only
- E - electron transport only
- P E - photon and electron transport
- N P E - neutron, neutron-induced photon and electron transport

The MODE card consists of the mnemonic MODE followed by either an N, N P, P, E, P E, or N P E. If the MODE card is omitted, mode N is assumed.

Mode N P does not account for photo-neutrons but only neutron-induced photons. Photon-production cross sections do not exist for all nuclides. If they are not available for a Mode N P problem, MCNP will print out warning messages. To find out whether a particular table for a nuclide has photon-production cross sections available, check the Appendix G cross-section list.

Mode P or mode N P problems generate bremsstrahlung photons with a computationally expensive thick-target bremsstrahlung approximation. This approximation can be turned off with the PHYS:E card.

The sample problem is a neutron-only problem, so the MODE card can be omitted because MODE N is the default.

2. Cell and surface parameter cards

Most of these cards define values of cell parameters. Entries correspond in order to the cell or surface cards that appear earlier in the INP file. A listing of all available cell and surface parameter cards is found on page 3-28. A few examples are neutron and photon importance cards (IMP:N,IMP:P), weight window cards (WWE:N, WWE:P, WWNi:N, WWNi:P), etc. Some method of specifying relative cell importances is required; the majority of the other cell parameter cards are for optional variance reduction techniques. The number of entries on a cell or surface parameter card must equal the

number of cells or surfaces in the problem or MCNP prints out a WARNING or FATAL error message. In the case of a WARNING, MCNP assumes zeros.

The IMP:N card is used to specify relative cell importances in the sample problem. There are four cells in the problem, so the IMP:N card will have four entries. The IMP:N card is used (a) for terminating the particle's history if the importance is zero and (b) for geometry splitting and Russian roulette to help particles move more easily to important regions of the geometry. An IMP:N card for the sample problem is

```
IMP:N 1 1 1 0
```

Cell parameters also can be defined on cell cards using the keyword=value format. If a cell parameter is specified on **any** cell card, it must be specified **only** on cell cards and **not at all** in the data card section.

3. Source specification cards

A source definition card SDEF is one of four available methods of defining starting particles. Chapter 3 has a complete discussion of source specification. The SDEF card defines the basic source parameters, some of which are

| | |
|----------------------------|---|
| POS = x y z | default is 0 0 0; |
| CEL = starting cell number | |
| ERG = starting energy | default is 14 MeV; |
| WGT= starting weight | default is 1; |
| TME= time | default is 0; |
| PAR = source particle type | N for N, N P, N P E; P for P, P E; E for E. |

MCNP will determine the starting cell number for a point isotropic source, so the CEL entry is not always required. The default starting direction for source particles is isotropic.

For the example problem, a fully specified source card is

```
SDEF POS=0 -4 -2.5 CEL=1 ERG=14 WGT=1 TME=0 PAR=N
```

Neutron particles will start at the center of the oxygen sphere (0 -4 -2.5), in cell 1, with an energy of 14 MeV, and with weight 1 at time 0. All these source parameters except the starting position are the default values, so the most concise source card is

```
SDEF POS=0 -4 -2.5
```

If all the default conditions were satisfactory for the problem, only the mnemonic SDEF would be required.

4. Tally specification cards

The tally cards are used to specify what you want to learn from the Monte Carlo calculation, perhaps current across a surface, flux at a point, etc. You request this information with one or more tally cards. Tally specification cards are not required, but if none is supplied, no tallies will be printed when the problem is run and a warning message is issued. Many of the tally specification cards describe tally "bins." A few examples are energy (En), time (Tn), and cosine (Cn) cards.

CHAPTER 1

Input File

MCNP provides six standard neutron, six standard photon, and four standard electron tallies, all normalized to be per starting particle. Some tallies in criticality calculations are normalized differently. Chapter 2, page 2–66, discusses tallies more completely and Chapter 3, page 3–59, lists all the tally cards and fully describes each one.

| Tally Mnemonic | Description |
|------------------------|---|
| F1:N or F1:P or F1:E | Surface current |
| F2:N or F2:P or F2:E | Surface flux |
| F4:N or F4:P or F4:E | Track length estimate of cell flux |
| F5a:N or F5a:P | Flux at a point (point detector) |
| F6:N or F6:N,P or F6:P | Track length estimate of energy deposition |
| F7:N | Track length estimate of fission energy deposition |
| F8:P or F8:E or F8:P,E | Energy distribution of pulses created in a detector |

The tallies are identified by tally type and particle type. Tallies are given the numbers 1, 2, 4, 5, 6, 7, 8, or increments of 10 thereof, and are given the particle designator :N or :P or :E (or :N,P only in the case of tally type 6 or P,E only for tally type 8). Thus you may have as many of any basic tally as you need, each with different energy bins or flagging or anything else. F4:N, F14:N, F104:N, and F234:N are all legitimate neutron cell flux tallies; they could all be for the same cell(s) but with different energy or multiplier bins, for example. Similarly F5:P, F15:P, and F305:P are all photon point detector tallies. Having both an F1:N card and an F1:P card in the same INP file is not allowed. The tally number may not exceed three digits.

For our sample problem we will use Fn cards (Tally type) and En cards (Tally energy).

a. Tally (Fn) Cards: The sample problem has a surface flux tally and a track length cell flux tally. Thus, the tally cards for the sample problem shown in Figure 1.7 are

```
F2:N      8  $ flux across surface 8
F4:N      2  $ track length in cell 2
```

Printed out with each tally bin is the relative error of the tally corresponding to one estimated standard deviation. Read page 1–6 for an explanation of the relative error. Results are not reliable until they become stable as a function of the number of histories run. Much information is provided for one bin of each tally in the tally fluctuation charts at the end of the output file to help determine tally stability. The user is strongly encouraged to look at this information carefully.

b. Tally Energy (En) Card: We wish to calculate flux in increments of 1 MeV from 14 to 1 MeV. Another tally specification card in the sample input deck establishes these energy bins.

The entries on the En card are the upper bounds in MeV of the energy bins for tally n. The entries must be given in order of increasing magnitude.

If a particle has an energy greater than the last entry, it will not be tallied, and a warning is issued. MCNP automatically provides the total over all specified energy bins unless inhibited by putting the symbol NT as the last entry on the selected En card.

The following cards will create energy bins for the sample problem:

```
E2  1 2 3 4 5 6 7 8 9 10 11 12 13 14
E4  1 12I 14
```

If no En card exists for tally n, a single bin over all energy will be used. To change this default, an E0 (zero) card may be used to set up a default energy bin structure for all tallies. A specific En card will override the default structure for tally n. We could replace the E2 and E4 cards with one E0 card for the sample problem, thus setting up identical bins for both tallies.

5. Materials specification

The cards in this section specify both the isotopic composition of the materials and the cross-section evaluations to be used in the cells. For a comprehensive discussion of materials specification, see page 3-92.

a. Material (Mm) Card: The following card is used to specify a material for all cells containing material m, where m can not exceed 5 digits:

```
Mm      ZAID1  fraction1  ZAID2  fraction2  ...
```

The m on a material card corresponds to the material number on the cell card (see page 1-22). The consecutive pairs of entries on the material card consist of the identification number (ZAID) of the constituent element or nuclide followed by the atomic fraction (or weight fraction if entered as a negative number) of that element or nuclide, until all the elements and nuclides needed to define the material have been listed.

i. Nuclide Identification Number (ZAID). This number is used to identify the element or nuclide desired. The form of the number is ZZZAAA.nnX, where

- ZZZ is the atomic number of the element or nuclide,
- AAA is the mass number of the nuclide, ignored for photons and electrons,
- nn is the cross-section evaluation identifier; if blank or zero, a default cross-section evaluation will be used, and
- X is the class of data: C is continuous energy; D is discrete reaction; T is thermal; Y is dosimetry; P is photon; E is electron; and M is multigroup.

For naturally occurring elements, AAA=000. Thus ZAID=74182 represents the isotope $^{182}_{74}\text{W}$, and ZAID=74000 represents the element tungsten.

ii. Nuclide Fraction. The nuclide fractions may be normalized to 1 or left unnormalized. For example, if the material is H₂O the fractions can be entered as .667 and .333 or as 2 and 1 for H and O respectively. If the fractions are entered with negative signs, they are weight fractions; otherwise they are atomic fractions. Weight fractions and atomic fractions cannot be mixed on the same Mm card.

CHAPTER 1

Input File

The material cards for the sample problem are

```
M1  8016  1  $ oxygen 16
M2  26000 1  $ natural iron
M3  6000  1  $ carbon
```

b. VOID Card: The VOID card removes all materials and cross sections in a problem and sets all nonzero importances to unity. It is very effective for finding errors in the geometry description because many particles can be run in a short time. Flooding the geometry with many particles increases the chance of particles going to most parts of the geometry—in particular, to an incorrectly specified part of the geometry—and getting lost. The history of a lost particle often helps locate the geometry error. The other actions of and uses for the VOID card are discussed on page 3–96.

The sample input deck could have a VOID card while testing the geometry for errors. When you are satisfied that the geometry is error-free, remove the VOID card.

6. Problem Cutoffs

Problem cutoff cards are used to specify parameters for some of the ways to terminate execution of MCNP. The full list of available cards and a complete discussion of problem cutoffs is found on page 3–107. For our problem we will use only the history cutoff (NPS) card. The mnemonic NPS is followed by a single entry that specifies the number of histories to transport. MCNP will terminate after NPS histories unless it has terminated earlier for some other reason.

7. Sample Problem Summary

The entire input deck for the sample problem follows. Recall that the input can be upper, lower, or mixed case.

```
Sample Problem Input Deck
c  cell cards for sample problem
1  1 -0.0014 -7
2  2 -7.86 -8
3  3 -1.60 1 -2 -3 4 -5 6 7 8
4  0 -1:2:3:-4:5:-6
c  end of cell cards for sample problem
blank line delimiter
C  Beginning of surfaces for cube
1  PZ -5
2  PZ 5
3  PY 5
4  PY -5
5  PX 5
6  PX -5
C  End of cube surfaces
7  S 0 -4 -2.5 .5 $ oxygen sphere
8  S 0 4 4 .5 $ iron sphere
blank line delimiter
```

```

IMP:N 1 1 1 0
SDEF POS=0 -4 -2.5
F2:N 8 $ flux across surface 8
F4:N 2 $ brack length in cell 2
E0 1 12I 14
M1 8016 1 $ oxygen 16
M2 26000 1 $ natural iron
M3 6000 1 $ carbon
NPS 100000
blank line delimiter (optional)

```

V. HOW TO RUN MCNP

This section assumes a basic knowledge of UNIX. Lines the user will type are shown in **lower case typewriter style type**. Press the RETURN key after each input line. MCNP is the executable binary file and XSDIR is the cross-section directory. If XSDIR is not in your current directory, you may need to set the environmental variable:

```
setenv DATAPATH /ab/cd
```

where /ab/cd is the directory containing both XSDIR and the data libraries.

A. Execution Line

The MCNP execution line has the following form:

```
mcnp Files Options
```

Files and *Options* are described below. Their order on the execution line is irrelevant. If there are no changes in default file names, nothing need be entered for *Files* and *Options*.

1. Files

MCNP uses several files for input and output. The file names cannot be longer than eight characters. The files pertinent to the sample problem are shown in Table 1.3. File INP must be present as a local file. MCNP will create OUTP and RUNTPE.

Table 1.3
MCNP Files

| <u>Default File Name</u> | <u>Description</u> |
|--------------------------|-----------------------------|
| INP | Problem input specification |
| OUTP | BCD output for printing |
| RUNTPE | Binary start-restart data |
| XSDIR | Cross-section directory |

The default name of any of the files in Table 1.3 can be changed on the MCNP execution line by entering

```
default_file_name=newname
```


CHAPTER 1

Execution

For example, if you have an input file called MCIN and want the output file to be MCOU and the runtpe to be MCRUNTPE, the execution line is

```
mcnp inp=mcin outp=mcout runtpe=mcruntpe
```

Only enough letters of the default name are required to uniquely identify it. For example,

```
mcnp i=mcin o=mcout ru=mcrntpe
```

also works. If a file in your local file space has the same name as a file MCNP needs to create, the file is created with a different unique name by changing the last letter of the name of the new file to the next letter in the alphabet. For example, if you already have an OUP, MCNP will create OUTQ.

Sometimes it is useful for all files from one run to have similar names. If your input file is called JOB1, the following line

```
mcnp name=job1
```

will create an OUP file called JOB1O and a RUNTPE file called JOB1R. If these files already exist, MCNP will NOT overwrite them, but will issue a message that JOB1O already exists and then will terminate.

2. Options

There are two kinds of options: program module execution options and other options. The other options are: C m, DEBUG n, NOTEK, FATAL, PRINT, and TASKS m. Execution options are discussed next.

MCNP consists of five distinct execution operations, each given a module name. These operations, their corresponding module names, and a one-letter mnemonic for each operation are listed in Table 1.4.

Table 1.4
Execution Options

| <u>Mnemonic</u> | <u>Module</u> | <u>Operation</u> |
|-----------------|---------------|----------------------------|
| i | IMCN | Process problem input file |
| p | PLOT | Plot geometry |
| x | XACT | Process cross sections |
| r | MCRUN | Particle transport |
| z | MCPLLOT | Plot tally results |

When *Options* are omitted, the default is *ixr*. The execution of the modules is controlled by entering the proper mnemonic on the execution line. If more than one operation is desired, combine the single characters (in any order) to form a string. Examples of use are: *i* to look for input errors, *ip* to debug a geometry by plotting, *ix* to see how much cross-section space is required, and *z* to plot tally results from the RUNTPE file.

After a job has been run, the BCD print file OUP can be examined with an editor on the computer and/or sent to a printer. Numerous messages about the problem execution and statistical quality of the results are displayed at the terminal.

B. Interrupts

MCNP allows four interactive interrupts while it is running:

| | |
|------------------------|---|
| (ctrl c)<cr> (default) | MCNP status |
| (ctrl c)s | MCNP status |
| (ctrl c)m | Make interactive plots of tallies |
| (ctrl c)q | Terminate MCNP normally after current history |
| (ctrl c)k | Kill MCNP immediately |

The (ctrl c)s interrupt prints the computer time used so far, the number of particles run so far, and the number of collisions. In the IMCN module, it prints the input line being processed. In the XACT module, it prints the cross section being processed.

The (ctrl c)q interrupt has no effect until MCRUN is executed. (Ctrl c)q causes the code to stop after the current particle history, to terminate "gracefully," and to produce a final print output file and RUNTPE file.

The (ctrl c)k interrupt kills MCNP immediately, without normal termination. If (ctrl c)k fails, enter (ctrl c) three or more times in a row.

C. Running MCNP

To run the example problem, have the input file in your current directory. For illustration, assume the file is called SAMPLE. Type

```
mcnp n=sample
```

where n uniquely identifies NAME. MCNP will produce an output file SAMPLEO that you can examine at your terminal, send to a printer, or both. To look at the geometry with the PLOT module using an interactive graphics terminal, type in

```
mcnp ip n=sample
```

After the plot prompt *plot*> appears, type in

```
px=0 ex=20
```

This plot will show an intersection of the surfaces of the problem by the plane $X=0$ with an extent in the x-direction of 20 cm on either side of the origin. If you want to do more with PLOT, see the instructions on page B-1. Otherwise type *end* after the next prompt to terminate the session.

VI. TIPS FOR CORRECT AND EFFICIENT PROBLEMS

This section has a brief checklist of helpful hints that apply to three phases of your calculation: defining and setting up the problem, preparing for the long computer runs that you may require, and making the runs that will give you results. Not everything mentioned in the checklist has been covered in this chapter, but the list can serve as a springboard for further reading in preparation for tackling more difficult problems.

CHAPTER 1

Execution

A. Problem Setup

1. Model the geometry and source distribution accurately.
2. Use the best problem cutoffs.
3. Use zero (default) for the neutron energy cutoff (MODE N P).
4. Do not use too many variance reduction techniques.
5. Use the most conservative variance reduction techniques.
6. Do not use cells with many mean free paths.
7. Use simple cells.
8. Use the simplest surfaces.
9. Study warning messages.
10. Always plot the geometry.
11. Use the VOID card when checking geometry.
12. Use separate tallies for the fluctuation chart.
13. Generate the best output (consider PRINT card).
14. RECHECK the INP file (materials, densities, masses, sources, etc.).
15. GARBAGE into code = GARBAGE out of code.

B. Preproduction

1. Run some short jobs.
2. Examine the outputs carefully.
3. Study the summary tables.
4. Study the statistical checks on tally quality and the sources of variance.
5. Compare the figures of merit and variance of the variance.
6. Consider the collisions per source particle.
7. Examine the track populations by cell.
8. Scan the mean free path column.
9. Check detector diagnostic tables.
10. Understand large detector contributions.
11. Strive to eliminate unimportant tracks.
12. Check MODE N P photon production.
13. Do a back-of-the-envelope check of the results.
14. DO NOT USE MCNP AS A BLACK BOX.

C. Production

1. Save RUNTPE for expanded output printing, continue run, tally plotting.
2. Look at figure of merit stability.
3. Make sure answers seem reasonable.
4. Make continue runs if necessary.
5. See if stable errors decrease by $1/\sqrt{N}$ (that is, be careful of the brute force approach).
6. Remember, accuracy is only as good as the nuclear data, modeling, MCNP sampling approximations, etc.

VII. REFERENCES

1. R. Kinsey, "Data Formats and Procedures for the Evaluated Nuclear Data File, ENDF," Brookhaven National Laboratory report BNL-NCS-50496 (ENDF 102) 2nd Edition (ENDF/B-V) (October 1979).
2. R. J. Howerton, D. E. Cullen, R. C. Haight, M. H. MacGregor, S. T. Perkins, and E. F. Plechaty, "The LLL Evaluated Nuclear Data Library (ENDL): Evaluation Techniques, Reaction Index, and Descriptions of Individual Reactions," Lawrence Livermore National Laboratory report UCRL-50400, Vol. 15, Part A (September 1975).
3. M. A. Gardner and R. J. Howerton, "ACTL: Evaluated Neutron Activation Cross-Section Library—Evaluation Techniques and Reaction Index," Lawrence Livermore National Laboratory report UCRL-50400, Vol. 18 (October 1978).
4. E. D. Arthur and P. G. Young, "Evaluated Neutron-Induced Cross Sections for $^{54,56}\text{Fe}$ to 40 MeV," Los Alamos Scientific Laboratory report LA-8626-MS (ENDF-304) (December 1980).
5. D. G. Foster, Jr. and E. D. Arthur, "Average Neutronic Properties of "Prompt" Fission Products," Los Alamos National Laboratory report LA-9168-MS (February 1982).
6. E. D. Arthur, P. G. Young, A. B. Smith, and C. A. Philis, "New Tungsten Isotope Evaluations for Neutron Energies Between 0.1 and 20 MeV," *Trans. Am. Nucl. Soc.* **39**, 793 (1981).
7. R. E. MacFarlane, D. W. Muir, and R. M. Boicourt, "The NJOY Nuclear Data Processing System, Volume I: User's Manual," Los Alamos National Laboratory report LA-9303-M, Vol. I (ENDF-324) (May 1982).
R. E. MacFarlane, D. W. Muir, and R. M. Boicourt, "The NJOY Nuclear Data Processing System, Volume II: The NJOY, RECONR, BROADR, HEATR, and THERMR Modules," Los Alamos National Laboratory report LA-9303-M, Vol. II (ENDF-324) (May 1982).
8. R. A. Forster, R. C. Little, J. F. Briesmeister, and J. S. Hendricks, "MCNP Capabilities For Nuclear Well Logging Calculations," *IEEE Transactions on Nuclear Science*, **37** (3), 1378 (June 1990)

CHAPTER 1

CHAPTER 2 GEOMETRY, DATA, PHYSICS, AND MATHEMATICS

I. INTRODUCTION

Chapter 2 discusses the mathematics and physics of MCNP, including geometry, cross-section libraries, sources, variance reduction schemes, Monte Carlo simulation of neutron and photon transport, and tallies. This discussion is not meant to be exhaustive; many details of the particular techniques and of the Monte Carlo method itself will be found elsewhere. Carter and Cashwell's book *Particle-Transport Simulation with the Monte Carlo Method*,¹ a good general reference on radiation transport by Monte Carlo, is based upon what is in MCNP. A more recent reference is Lux and Koblinger's book, *Monte Carlo Particle Transport Methods: Neutron and Photon Calculations*.² Methods of sampling from standard probability densities are discussed in the Monte Carlo samplers by Everett and Cashwell.³

MCNP was originally developed by the Monte Carlo Group, currently the Radiation Transport Group, (Group X-6) in the Applied Theoretical Physics Division (X Division) at the Los Alamos National Laboratory. Group X-6 improves MCNP (releasing a new version every two to three years), maintains it at Los Alamos and at other laboratories where we have collaborators or sponsors, and provides limited free consulting and support for MCNP users. MCNP is distributed to other users through the Radiation Shielding Information Center (RSIC) at Oak Ridge, Tennessee, and the OECD/NEA data bank in Paris, France.

MCNP has approximately 40,000 lines of FORTRAN and 1000 lines of C source coding, including comments and with the COMMON blocks listed only once and not in every subroutine. There are about 350 subroutines. There is only one source code; it is used for all systems. At Los Alamos, there are about 200 active users. Worldwide, there are about 1000 active users at about 100 installations.

MCNP takes advantage of parallel computer architectures. It is supported in multitasking mode on the 8-processor Cray YMP and in multiprocessing mode on a cluster of 16 IBM RS-6000 workstations where the distributed processing uses the Parallel Virtual Machine (PVM) software from Oak Ridge.

MCNP has not been successfully vectorized because the overhead required to set up and break apart vector queues at random decision points is greater than the savings from vectorizing the simple arithmetic between the decision points. MCNP (and any general Monte Carlo code) is little more than a collection of random decision points with some simple arithmetic in between. Because MCNP does not take advantage of vectorization, it is fairly inefficient on vectorized computers. In particular, many workstations run MCNP as fast or faster than the Cray-YMP.⁴

MCNP has been made as system independent as possible to enhance its portability, and has been written to comply with the ANSI FORTRAN 77

CHAPTER 2

Introduction

standard. With one source code, MCNP is maintained on many platforms.

A. History

The Monte Carlo method is generally attributed to scientists working on the development of nuclear weapons in Los Alamos during the 1940s. However, its roots go back much farther.

Perhaps the earliest documented use of random sampling to solve a mathematical problem was that of Comte de Buffon in 1772.⁵ A century later people performed experiments in which they threw a needle in a haphazard manner onto a board ruled with parallel straight lines and inferred the value of π from observations of the number of intersections between needle and lines.^{6,7} Laplace suggested in 1886 that π could be evaluated by random sampling.⁸ Lord Kelvin appears to have used random sampling to aid in evaluating some time integrals of the kinetic energy that appear in the kinetic theory of gasses⁹ and acknowledged his secretary for performing calculations for more than 5000 collisions.¹⁰

According to Emilio Segrè, Enrico Fermi's student and collaborator, Fermi invented a form of the Monte Carlo method when he was studying the moderation of neutrons in Rome.^{10,11} Though Fermi did not publish anything, he amazed his colleagues with his predictions of experimental results. After indulging himself, he would reveal that his "guesses" were really derived from the statistical sampling techniques that he performed in his head when he couldn't fall asleep.

During World War II at Los Alamos, Fermi joined many other eminent scientists to develop the first atomic bomb. It was here that Stan Ulam became impressed with electromechanical computers used for implosion studies. Ulam realized that statistical sampling techniques were considered impractical because they were long and tedious, but with the development of computers they could become practical. Ulam discussed his ideas with others like John von Neumann and Nicholas Metropolis. Statistical sampling techniques reminded everyone of games of chance, where randomness would statistically become resolved in predictable probabilities. It was Nicholas Metropolis who noted that Stan had an uncle who would borrow money from relatives because he "just had to go to Monte Carlo" and thus named the mathematical method "Monte Carlo."¹¹

Meanwhile, a team of wartime scientists headed by John Mauchly was working to develop the first electronic computer at the University of Pennsylvania in Philadelphia. Mauchly realized that if Geiger counters in physics laboratories could count, then they could also do arithmetic and solve mathematical problems. When he saw a seemingly limitless array of women cranking out firing tables with desk calculators at the Ballistic Research Laboratory at Aberdeen, he proposed¹¹ that an electronic computer be built to deal with these calculations. The result was ENIAC (Electronic Numerical Integrator and Computer), the world's first computer, built for Aberdeen at the University of Pennsylvania. It had 18,000 double triode vacuum tubes in a system with 500,000 solder joints.¹¹

CHAPTER 2 Introduction

John von Neumann was a consultant to both Aberdeen and Los Alamos. When he heard about ENIAC, he convinced the authorities at Aberdeen that he could provide a more exhaustive test of the computer than mere firing-table computations. In 1945 John von Neumann, Stan Frankel, and Nicholas Metropolis visited the Moore School of Electrical Engineering at the University of Pennsylvania to explore using ENIAC for thermonuclear weapon calculations with Edward Teller at Los Alamos.¹¹ After the successful testing and dropping of the first atomic bombs a few months later, work began in earnest to calculate a thermonuclear weapon. On March 11, 1947, John von Neumann sent a letter to Robert Richtmyer, leader of the Theoretical Division at Los Alamos, proposing use of the statistical method to solve neutron diffusion and multiplication problems in fission devices.¹¹ His letter was the first formulation of a Monte Carlo computation for an electronic computing machine. In 1947, while in Los Alamos, Fermi invented a mechanical device called FERMIAC¹² to trace neutron movements through fissionable materials by the Monte Carlo Method.

By 1948 Stan Ulam was able to report to the Atomic Energy Commission that not only was the Monte Carlo method being successfully used on problems pertaining to thermonuclear as well as fission devices, but also it was being applied to cosmic ray showers and the study of partial differential equations.¹¹ In the late 1940s and early 1950s, there was a surge of papers describing the Monte Carlo method and how it could solve problems in radiation or particle transport and other areas.^{13,14,15} Many of the methods described in these papers are still used in Monte Carlo today, including the method of generating random numbers¹⁶ used in MCNP. Much of the interest was based on continued development of computers such as the Los Alamos MANIAC (Mechanical Analyzer, Numerical Integrator, and Computer) in March, 1952.

The Atomic Energy Act of 1946 created the Atomic Energy Commission to succeed the Manhattan Project. In 1953 the United States embarked upon the "Atoms for Peace" program with the intent of developing nuclear energy for peaceful applications such as nuclear power generation. Meanwhile, computers were advancing rapidly. These factors led to greater interest in the Monte Carlo method. In 1954 the first comprehensive review of the Monte Carlo method was published by Herman Kahn¹⁷ and the first book was published by Cashwell and Everett¹⁸ in 1959.

At Los Alamos, Monte Carlo computer codes developed along with computers. The first Monte Carlo code was the simple 19-step computing sheet in John von Neumann's letter to Richtmyer. But as computers became more sophisticated, so did the codes. At first the codes were written in machine language and each code would solve a specific problem. In the early 1960s, better computers and the standardization of programming languages such as FORTRAN made possible more general codes. The first Los Alamos general-purpose particle transport Monte Carlo code was MCS,¹⁹ written in 1963. Scientists who were not necessarily experts in computers and Monte Carlo mathematical techniques now could take advantage of

CHAPTER 2

Introduction

the Monte Carlo method for radiation transport. They could run the MCS code to solve modest problems without having to do either the programming or the mathematical analysis themselves. MCS was followed by MCN²⁰ in 1965. MCN could solve the problem of neutrons interacting with matter in a three-dimensional geometry and used physics data stored in separate, highly-developed libraries.

In 1973 MCN was merged with MCG,²¹ a Monte Carlo gamma code that treated higher energy photons, to form MCNG, a coupled neutron-gamma code. In 1977 MCNG was merged with MCP,²¹ a Monte Carlo Photon code with detailed physics treatment down to 1 keV, to accurately model neutron-photon interactions. The code has been known as MCNP ever since. Though at first MCNP stood for Monte Carlo Neutron Photon, now it stands for Monte Carlo N-Particle. Other major advances in the 70s included the present generalized tally structure, automatic calculation of volumes, and a Monte Carlo eigenvalue algorithm to determine k_{eff} for nuclear criticality (KCODE).

In 1983 MCNP3 was released, entirely rewritten in ANSI standard FORTRAN 77. MCNP3 was the first MCNP version internationally distributed through the Radiation Shielding and Information Center at Oak Ridge, Tennessee. Other 1980s versions of MCNP were MCNP3A (1986) and MCNP3B (1988), that included tally plotting graphics (MCPLLOT), the present generalized source, surface sources, repeated structures/lattice geometries, and multigroup/adjoint transport.

MCNP4 was released in 1990 and was the first UNIX version of the code. It accommodated N-particle transport and multitasking on parallel computer architectures. MCNP4 added electron transport (patterned after the Integrated TIGER Series (ITS) continuous-slowing-down approximation physics),²² the pulse height tally (F8), a thick-target bremsstrahlung approximation for photon transport, enabled detectors and DXTRAN with the $S(\alpha, \beta)$ thermal treatment, provided greater random number control, and allowed plotting of tally results while the code was running.

MCNP4A, released in 1993, featured enhanced statistical analysis, distributed processor multitasking for running in parallel on a cluster of scientific workstations, new photon libraries, ENDF/B-VI capabilities, color X-Windows graphics, dynamic memory allocation, expanded criticality output, periodic boundaries, plotting of particle tracks via SABRINA, improved tallies in repeated structures, and many smaller improvements.

Large production codes such as MCNP have revolutionized science — not only in the way it is done, but also by becoming the repositories for physics knowledge. MCNP represents about 400 person-years of sustained effort. The knowledge and expertise contained in MCNP is formidable.

Current MCNP development is characterized by a strong emphasis on quality control, documentation, and research. New features continue to be added to the code to reflect new advances in computer architecture, improvements in Monte Carlo methodology, and better physics models. MCNP has a proud history and a promising future.

B. MCNP Structure

MCNP is written in the style of Dr. Thomas N. K. Godfrey, the principal MCNP programmer from 1975 - 1989. Variable dimensions for arrays are achieved by massive use of EQUIVALENCE statements and offset indexing. All variables local to a routine are no more than two characters in length, and all COMMON variables are between three and six characters in length. The code strictly complies with the ANSI FORTRAN 77 standard. The principal characteristic of Tom Godfrey's style is its terseness. Everything is accomplished in as few lines of code as possible. Thus MCNP does more than some other codes that are more than ten times larger. It was Godfrey's philosophy that anyone can understand code at the highest level by making a flow chart and anyone can understand code at the lowest level (one FORTRAN line); it is the intermediate level that is most difficult. Consequently, by using a terse programming style, subroutines could fit within a few pages and be most easily understood. Tom Godfrey's style is clearly counter to modern computer science programming philosophies, but it has served MCNP well and is preserved to provide stylistic consistency throughout.

The general structure of MCNP is as follows:

Initiation (IMCN):

- Read input file (INP) to get dimensions (PASS1);
- Set up variable dimensions or dynamically allocated storage (SETDAS);
- Re-read input file (INP) to load input (RDPROB);
- Process source (ISOURC);
- Process tallies (ITALLY);
- Process materials specifications (STUFF) including masses but without loading in the data files;
- Calculate cell volumes and surface areas (VOLUME).

Interactive Geometry Plot (PLOT).

Cross Section Processing (XACT):

- Load libraries (GETXST);
- Eliminate excess neutron data outside problem energy range (EXPUNG);
- Doppler broaden elastic and total cross sections to the proper temperature if the problem temperature is higher than the library temperature (BROADN);
- Process multigroup libraries (MGXSPT);
- Process electron libraries (XSGEN) including calculation of range tables, straggling tables, scattering angle distributions, and bremsstrahlung.

MCRUN sets up multitasking and multiprocessing, runs histories (by calling TRNSPT, which calls HISTORY), and returns to OUTPUT to print, write RUNTPE dumps, or process another criticality (KCODE) cycle.

Under MCRUN, MCNP runs neutron, photon, or electron histories (HISTORY), calling ELECTR for electron tracks:

- Start a source particle (STARTP);

CHAPTER 2

Introduction

- Find the distance to the next boundary (TRACK), cross the surface (SURFAC) and enter the next cell (NEWCEL);
- Find the total neutron cross section (ACETOT) and process neutron collisions (COLIDN) producing photons as appropriate (ACEGAM);
- Find the total photon cross section (PHOTOT) and process photon collisions (COLIDP) producing electrons as appropriate (EMAKER);
- Use the optional thick-target bremsstrahlung approximation if no electron transport (TTBR);
- Follow electron tracks (ELECTR);
- Process optional multigroup collisions (MGCOLN, MGCOLP, MGCOL);
- Process detector tallies (TALLYD) or DXTRAN;
- Process surface, cell, and pulse height tallies (TALLY).

Periodically write output file, restart dumps, update to next criticality (KCODE) cycle, rendezvous for multitasking and updating detector and DXTRAN Russian roulette criteria, etc. (OUTPUT):

- Go to the next criticality cycle (KCALC);
- Print output file summary tables (SUMARY, ACTION);
- Print tallies (TALLYP);
- Generate weight windows (OUTWWG).

Plot tallies (MC PLOT).

GKS graphics simulation routines.

PVM distributed processor multiprocessing routines.

Random number generator and control (RANDOM).

Mathematics, character manipulation, and other slave routines.

C. History Flow

The basic flow of a particle history for a coupled neutron/photon/electron problem is handled in subroutine HSTORY. HSTORY is called from TRNSPT after the random number sequence is set up and the number of the history, NPS, is incremented. The flow of HSTORY is then as follows.

First, STARTP is called. The flag IPT is set for the type of particle being run: 1 for a neutron, 2 for a photon, and 3 for an electron. Some arrays and variables (such as NBNK, the number of particles in the bank) are initialized to zero. The starting random number is saved (RANB, RANS, RNRTC0), and the branch of the history, NODE, is set to 1.

Next, the appropriate source routine is called. Source options are the standard fixed sources (SOURCB), the surface source (SURSRC), the KCODE criticality source (SOURCK), or a user-provided source (SOURCE). All of the parameters describing the particle are set in these source routines, including position, direction of flight, energy, weight, time, and starting cell (and possibly surface), by sampling the various distributions described on the source input control cards. Several checks are made at this time to verify

that the particle is in the correct cell or on the correct surface, and directed toward the correct cell; then control is returned to STARTP.

Next in STARTP, the initial parameters of the first fifty particle histories are printed. Then some of the summary information is incremented (see Appendix E for an explanation of these arrays). Energy, time, and weight are checked against cutoffs. A number of error checks are made. TALLYD is called to score any detector contributions, and then DXTRAN is called (if used in the problem) to create particles on the spheres. The particles are saved with BANKIT for later tracking. TALPH is called to start the bookkeeping for the pulse height cell tally energy balance. The weight window game is played, with any additional particles from splitting put into the bank and any losses to Russian roulette terminated. Control is returned to HSTORY.

Back in HSTORY, the actual particle transport is started. For an electron source, ELECTR is called and electrons are run separately. For a neutron or photon source, TRACK is called to calculate the intersection of the particle trajectory with each bounding surface of the cell. The minimum positive distance DLS to the cell boundary indicates the next surface JSU the particle is heading toward. The distance to the nearest DXTRAN sphere DXL is calculated, as is the distance to time cutoff DTC, and energy boundary for multigroup charged particles DEB. The cross sections for cell ICL are calculated using a binary table lookup in ACETOT for neutrons and in PHOTOT for photons. The total cross section is modified in EXTRAN by the exponential transformation if necessary. The distance PMF to the next collision is determined (if a forced collision is required, FORCOL is called and the uncollided part is banked). The track length D of the particle in the cell is found as the minimum of the distance PMF to collision, the distance DLS to the surface JSU, the distance DXL to a DXTRAN sphere, the distance DTC to time cutoff, or the distance DEB to energy boundary. TALLY then is called to increment any track length cell tallies. Some summary information is incremented. The particle's parameters (time, position, and energy) are then updated. If the particle's distance DXL to a DXTRAN sphere (of the same type as the current particle) is equal to the minimum track length D, the particle is terminated because particles reaching the DXTRAN sphere are already accounted for by the DXTRAN particles from each collision. If the particle exceeds the time cutoff, the track is terminated. If the particle was detected leaving a DXTRAN sphere, the DXTRAN flag IDX is set to zero and the weight cutoff game is played. The particle is either terminated to weight cutoff or survives with an increased weight. Weight adjustments then are made for the exponential transformation.

If the minimum track length D is equal to the distance-to-surface crossing DLS, the particle is transported distance D to surface JSU and SURFAC is called to cross the surface and do any surface tallies (by calling TALLY) and to process the particle across the surface into the next cell by calling NEWCEL. It is in SURFAC that reflecting surfaces, periodic boundaries, geometry splitting, Russian roulette from importance sampling, and loss to

CHAPTER 2

Introduction

escape are treated. For splitting, one bank entry of NPA particle tracks is made in BANKIT for an (NPA+1)-for-1 split. The bank is the IBNK array, and entries or retrievals are made with the GPBLCM and JPBLCM arrays (the bank operates strictly on a last-in, first-out basis). The history is continued by going back to HSTORY and calling TRACK.

If the distance to collision PMF is less than the distance to surface DLS, or if a multigroup charged particle reaches the distance to energy boundary DEB, the particle undergoes a collision. Everything about the collision is determined in COLIDN for neutrons and COLIDP for photons. COLIDN determines which nuclide is involved in the collision, samples the target velocity of the collision nuclide by calling TGTVEL for the free gas thermal treatment, generates and banks any photons (ACEGAM), handles analog capture or capture by weight reduction, plays the weight cutoff game, handles $S(\alpha, \beta)$ thermal collisions (SABCOL) and elastic or inelastic scattering (ACECOL). For criticality problems, COLIDK is called to store fission sites for subsequent generations. Any additional tracks generated in the collision are put in the bank. ACECAS and ACECOS determine the energies and directions of particles exiting the collision. Multigroup and multigroup/adjoint collisions are treated separately in MGCOLN and MGACOL that are called from COLIDN. The collision process and thermal treatments are described in more detail later in this chapter (see page 2-27).

COLIDP for photons is similar to COLIDN, and it covers the simple or the detailed physics treatments. The simple physics treatment is better for free electrons; the detailed treatment is the default and includes form factors for electron binding effects, coherent (Thomson) scatter, and fluorescence from photoelectric capture (see page 2-50). COLIDP samples for the collision nuclide, treats photoelectric absorption, or capture (with fluorescence in the detailed physics treatment), incoherent (Compton) scatter (with form factors in the detailed physics treatment to account for electron binding), coherent (Thomson) scatter for the detailed physics treatment only (again with form factors), and pair production. Electrons are generated (EMAKER) for incoherent scatter, pair production, and photoelectric absorption. These electrons may be assumed to instantly deposit all their energy if IDES=1 on the PHYS:P card, or they may produce electrons with the thick-target bremsstrahlung approximation (default for MODE P problems, IDES=0 on the PHYS:P card), or they may undergo full electron transport (default for MODE P E problems, IDES=0 on the PHYS:P card.) Multigroup or multigroup/adjoint photons are treated separately in MGCOLP or MGACOL.

After the surface crossing or collision is processed, control returns to HSTORY and transport continues by calling TRACK, where the distance to cell boundary is calculated. Or if the particle involved in the collision was killed by capture or variance reduction, the bank is checked for any remaining progeny, and if none exists, the history is terminated. Appropriate summary information is incremented, the tallies of this particular history are added to the total tally data by TALSHF, and a return is made to TRNSPT.

In TRNSPT, checks are made to see if output is required or if the job

should be terminated because enough histories have been run or too little time remains to continue. For continuation, HISTORY is called again. Otherwise a return is made to MCRUN. MCRUN calls OUTPUT, which calls SUMARY to print the summary information. Then SUMARY calls TALLYP to print the tally data. Appendix E defines all of the MCNP variables that are in COMMON as well as detailed descriptions of some important arrays.

II. GEOMETRY

The basic MCNP geometry concepts, discussed in Chapter 1, include the sense of a cell, the intersection and union operators, and surface specification. Covered in this section are the complement operator; the repeated structure capability; an explanation of two surfaces, the cone and the torus; and a description of ambiguity, reflecting, white, and periodic boundary surfaces.

A. Complement Operator

This operator provides no new capability over the intersection and union operators; it is just a shorthand cell-specifying method that implicitly uses the intersection and union operators.

The symbol # is the complement operator and can be thought of as standing for *not in*. There are two basic uses of the operator:

#*n* means that the description of the current cell is the complement of the description of cell *n*.

#(...) means complement the portion of the cell description in the parentheses (usually just a list of surfaces describing another cell).

In the first of the two above forms, MCNP performs five operations: (1) the symbol # is removed, (2) parentheses are placed around *n*, (3) any intersections in *n* become unions, (4) any unions in *n* are replaced by back-to-back parentheses)(which is an intersection, and (5) the senses of the surfaces defining *n* are reversed.

A simple example is a cube. We define a two-cell geometry with six surfaces, where cell 1 is the cube and cell 2 is the outside world:

```
1    0 -1  2 -3  4 -5  6
2    0  1:-2: 3:-4: 5:-6
```

Note that cell 2 is everything in the universe that is *not in* cell 1, or

```
2    0 #1
```

The form #(*n*) is not allowed; it is functionally available as the equivalent of -*n*.

CAUTION: Using the complement operator can destroy some of the necessary conditions for some cell volume and surface area calculations by MCNP. See page 4-14 for an example.

CHAPTER 2 Geometry

The complement operator can be easily abused if it is used indiscriminately. A simple example can best illustrate the problems. Fig. 2.1 consists of two concentric spheres inside a box. Cell 4 can be described using the complement operator as

```
4    0  #3 #2 #1
```

Although cells 1 and 2 do not touch cell 4, to omit them would be incorrect. If they were omitted, the description of cell 4 would be everything in the universe that is not in cell 3. Since cells 1 and 2 are not part of cell 3, they would be included in cell 4. Even though surfaces 1 and 2 do not physically bound cell 4, using the complement operator as in this example causes MCNP to think that all surfaces involved with the complement do bound the cell. Even though this specification is correct and required by MCNP, the disadvantage is that when a particle enters cell 4 or has a collision in cell 4, MCNP must calculate the intersection of the particle's trajectory with all real bounding surfaces of cell 4 plus any extraneous ones brought in by the complement operator. This intersection calculation is very expensive and can add significantly to the required computer time.

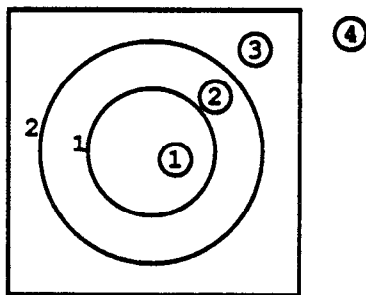


Figure 2.1

A better description of cell 4 would be to complement the description of cell 3 (omitting surface 2) by reversing the senses and interchanging union and intersection operators as illustrated in the cell cards that describe the simple cube in the preceding paragraphs.

B. Repeated Structure Geometry

The repeated structure geometry feature is explained in detail starting on page 3–21. The capabilities are only introduced here. Examples are shown in Chapter 4. The cards associated with the repeated structure feature are U (universe), FILL, TRCL, and LAT (lattice) and cell cards with LIKE m BUT.

The repeated structure feature makes it possible to describe only once the cells and surfaces of any structure that appears more than once in a geometry. This unit then can be replicated at other xyz locations by using the “LIKE m BUT” construct on a cell card. The user specifies that a cell is filled with something called a universe. The U card identifies the universe, if any, to which a cell belongs. The FILL card specifies with which universe

a cell is to be filled. A universe is either a lattice or an arbitrary collection of cells. The two types of lattice shapes, hexagonal prisms and hexahedra, need not be rectangular nor regular, but they must fill space exactly. Several concepts and cards combine in order to use this capability.

C. Surfaces

1. Explanation of Cone and Torus

Two surfaces, the cone and torus, require more explanation. The quadratic equation for a cone describes a cone of two sheets (just like a hyperboloid of two sheets)—one sheet is a cone of positive slope, and the other has a negative slope. A cell whose description contains a two-sheeted cone may require an ambiguity surface to distinguish between the two sheets. MCNP provides the option to select either of the two sheets; this option frequently simplifies geometry setups and eliminates any ambiguity. The +1 or the -1 entry on the cone surface card causes the one sheet cone treatment to be used. If the sign of the entry is positive, the specified sheet is the one that extends to infinity in the positive direction of the coordinate axis to which the cone axis is parallel. The converse is true for a negative entry. This feature is available only for cones whose axes are parallel to the coordinate axes of the problem.

The treatment of fourth degree surfaces in Monte Carlo calculations has always been difficult because of the resulting fourth order polynomial (“quartic”) equations. These equations must be solved to find the intersection of a line of flight of a particle with a toroidal surface. In MCNP these equations must also be solved to find the intersection of surfaces to compute the volumes and surface areas of geometric regions of a given problem. In either case, the quartic equation,

$$x^4 + Bx^3 + Cx^2 + Dx + E = 0$$

is difficult to solve on a computer because of roundoff errors. For many years the MCNP toroidal treatment required 30 decimal digits (CDC double-precision) accuracy to solve quartic equations. Even then there were roundoff errors that had to be corrected by Newton-Raphson iterations. Schemes using a single-precision quartic formula solver followed by a Newton-Raphson iteration were inadequate because if the initial guess of roots supplied to the Newton-Raphson iteration is too inaccurate, the iteration will often diverge when the roots are close together.

The single-precision quartic algorithm in MCNP basically follows the quartic solution of Cashwell and Everett.²³ When roots of the quartic equation are well separated, a modified Newton-Raphson iteration quickly achieves convergence. But the key to this method is that if the roots are double roots or very close together, they are simply thrown out because a double root corresponds to a particle’s trajectory being tangent to a toroidal surface, and it is a very good approximation to assume that the particle then has no contact with the toroidal surface. In extraordinarily rare cases where this is

CHAPTER 2 Geometry

not a good assumption, the particle would become “lost.” Additional refinements to the quartic solver include a carefully selected finite size of zero, the use of a cubic rather than a quartic equation solver whenever a particle is transported from the surface of a torus, and a gross quartic coefficient check to ascertain the existence of any real positive roots. As a result, the single-precision quartic solver is substantially faster than double-precision schemes, portable, and also somewhat more accurate.

In MCNP, elliptical tori symmetric about any axis parallel to a coordinate axis may be specified. The volume and surface area of various tallying segments of a torus usually will be calculated automatically.

2. Ambiguity Surfaces

The description of the geometry of a cell must eliminate any ambiguities as to which region of space is included in the cell. That is, a particle entering a cell should be able to uniquely determine which cell it is in from the senses of the bounding surfaces. This is not possible in a geometry such as shown in Fig. 2.2 unless an *ambiguity surface* is specified. Suppose the figure is rotationally symmetric about the y -axis.

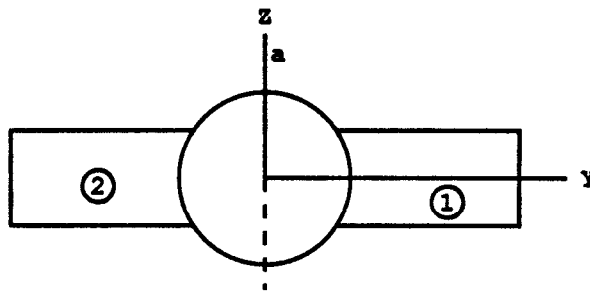


Figure 2.2

A particle entering cell 2 from the inner spherical region might think it was entering cell 1 because a test of the senses of its coordinates would satisfy the description of cell 1 as well as that of cell 2. In such cases, an ambiguity surface is introduced such as a , the plane $y = 0$. An ambiguity surface need not be a bounding surface of a cell, but it may be and frequently is. It can also be the bounding surface of some cell other than the one in question. However, the surface must be listed among those in the problem and must not be a reflecting surface (see page 2–13). The description of cells 1 and 2 in Fig. 2.2 is augmented by listing for each its sense relative to surface a as well as that of each of its other bounding surfaces. A particle in cell 1 cannot have the same sense relative to surface a as does a particle in cell 2. More than one ambiguity surface may be required to define a particular cell.

A second example may help to clarify the significance of ambiguity surfaces. We would like to describe the geometry of Fig. 2.3a. Without the use of an ambiguity surface, the result will be Fig. 2.3b. Surfaces 1 and 3 are spheres about the origin, and surface 2 is a cylinder around the y -axis.

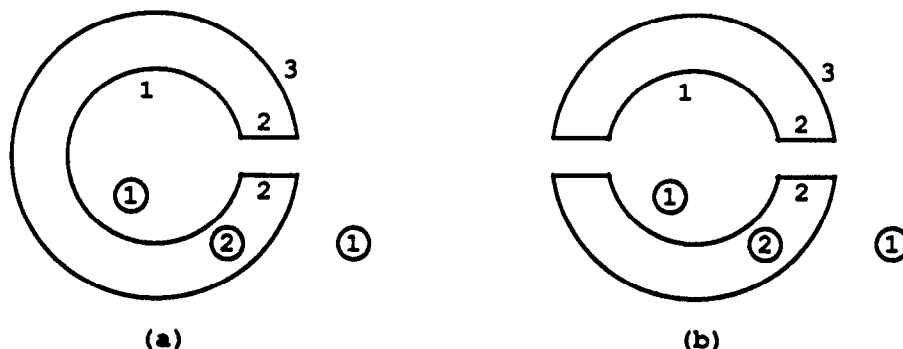


Figure 2.3

Cell 1 is both the center and outside world of the geometry connected by the region interior to surface 2.

At first glance it may appear that cell 1 can easily be specified by $-1 : -2 : 3$ whereas cell 2 is simply $\#1$. This results in Figure 2.3b, in which cell 1 is everything in the universe interior to surface 1 plus everything in the universe interior to surface 2 (remember the cylinder goes to plus and minus infinity) plus everything in the universe exterior to surface 3.

An ambiguity surface (a plane at $y=0$) will solve the problem. Everything in the universe to the right of the ambiguity surface (call it surface 4) *intersected* with everything in the universe interior to the cylinder is a cylindrical region that goes to plus infinity but terminates at $y=0$. Therefore, $-1 : (4 - 2) : 3$ defines cell 1 as desired in Figure 2.3a. The parentheses in this last expression are not required because intersections are done before unions. Another expression for cell 2 rather than $\#1$ is $1 - 3 \#(4 - 2)$.

For the user, ambiguity surfaces are specified the same way as any other surface—simply list the signed surface number as an entry on the cell card. For MCNP, if a particular ambiguity surface appears on cell cards with only one sense, it is treated as a true ambiguity surface. Otherwise, it still functions as an ambiguity surface but the TRACK subroutine will try to find intersections with it, thereby using a little more computer time.

3. Reflecting Surfaces

A surface can be designated a reflecting surface by preceding its number on the surface card with an asterisk. Any particle hitting a reflecting surface is specularly (mirror) reflected. Reflecting planes are valuable because they can simplify a geometry setup (and also tracking) in a problem. They can, however, make it difficult (or even impossible) to get the correct answer. The user is cautioned to check the source weight and tallies to ensure that the desired result is achieved. Any tally in a problem with reflecting planes should have the same expected result as the tally in the same problem without reflecting planes. Detectors or DXTRAN used with reflecting surfaces give wrong answers (see page 2-79).

The following example illustrates the above points and hopefully makes

CHAPTER 2

Geometry

you very cautious in the use of reflecting surfaces; they should never be used in any situation without a lot of thought.

Consider a cube of carbon 10 cm on a side sitting on top of a 5-MeV neutron source distributed uniformly in volume. The source cell is a 1-cm-thick void completely covering the bottom of the carbon cube and no more. The average neutron flux across any one of the sides (but not top or bottom) is calculated to be 0.150 ($\pm 0.5\%$) per cm^2 per starting neutron from an MCNP F2 tally, and the flux at a point at the center of the same side is $1.55\text{E}-03$ n/ cm^2 ($\pm 1\%$) from an MCNP F5 tally.

The cube can be modeled by half a cube and a reflecting surface. All dimensions remain the same except the distance from the tally surface to the opposite surface (which becomes the reflecting surface) is 5 cm. The source cell is cut in half also. Without any source normalization, the flux across the surface is now 0.302 ($\pm 0.5\%$), which is twice the flux in the nonreflecting geometry. The detector flux is $2.58\text{E}-03$ ($\pm 1\%$), which is *less* than twice the point detector flux in the nonreflecting problem.

The problem is that for the surface tally to be correct, the starting weight of the source particles has to be normalized; it should be half the weight of the nonreflected source particles. The detector results will always be wrong (and lower) for the reason discussed on page 2-79.

In this particular example, the normalization factor for the starting weight of source particles should be 0.5 because the source volume is half of the original volume. Without the normalization, the full weight of source particles is started in only half the volume. These normalization factors are problem dependent and should be derived very carefully.

Another way to view this problem is that the tally surface has doubled because of the reflecting surface; two scores are being made across the tally surface when one is made across each of two opposite surfaces in the nonreflecting problem. The detector has doubled, too—except that the contributions to it from beyond the reflecting surface are not being made, as explained on page 2-79.

4. White Boundaries

A surface can be designated a white boundary surface by preceding its number on the surface card with a plus. Any particle hitting a white boundary is isotropically reflected. White boundary surfaces are useful for comparing MCNP results with other codes that have white boundary conditions. They also can be used to approximate a boundary with an infinite scatterer. They make absolutely no sense in problems with next event estimators such as detectors or DXTRAN (see page 2-79) and should always be used with caution.

5. Periodic Boundaries

Periodic boundary conditions can be applied to pairs of planes to simulate an infinite lattice. Although the same effect can be achieved with an

infinite lattice, the periodic boundary is easier to use, simplifies comparison with other codes having periodic boundaries, and can save considerable computation time. There is approximately a 55% run time penalty associated with repeated structures and lattices that can be avoided with periodic boundaries. However, collisions and other aspects of the Monte Carlo random walk usually dominate running time, so the savings realized by using periodic boundaries are usually much smaller. A simple periodic boundary problem is illustrated in Figure 2.3c.

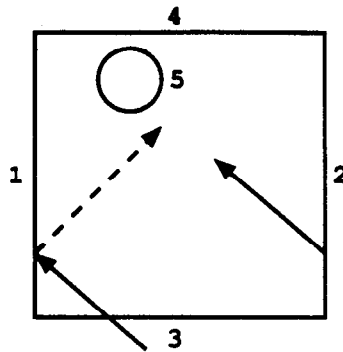


Figure 2.3(c)

It consists of a square reactor lattice infinite in the z direction and 10 cm on a side in the x and y directions with an off-center 1-cm-radius cylindrical fuel pin. The MCNP surface cards are:

```

1 -2 px -5
2 -1 px 5
3 -4 py -5
4 -3 py 5
5 c/z -2 4 1

```

The negative entry before the surface mnemonic specifies periodic boundaries. Card one says that surface 1 is periodic with surface 2 and is a px plane. Card two says that surface 2 is periodic with surface 1 and is a px plane. Card three says that surface 3 is periodic with surface 4 and is a py plane. Card four says that surface 4 is periodic with surface 3 and is a py plane. Card five says that surface 5 is an infinite cylinder parallel to the z -axis. A particle leaving the lattice out the left side (surface 1) re-enters on the right side (surface 2). If the surfaces were reflecting, the re-entering particle would miss the cylinder, shown by the dotted line. In a fully specified lattice and in the periodic geometry, the re-entering particle will hit the cylinder as it should.

Much more complicated examples are possible, particularly hexagonal prism lattices. In all cases, MCNP checks that the periodic surface pair matches properly and performs all the necessary surface rotations and translations to put the particle in the proper place on the corresponding periodic plane.

The following limitations apply:

CHAPTER 2

Cross Sections

- Periodic boundaries cannot be used with next event estimators such as detectors or DXTRAN (see page 2–79);
- All periodic surfaces must be planes;
- Periodic planes cannot also have a surface transformation;
- The periodic cells may be infinite or bounded by planes on the top or bottom that must be periodic, reflecting, or white boundaries;
- Periodic planes can only bound other periodic planes or top and bottom planes;
- A zero-importance cell must be on exactly one side of each periodic plane;
- All periodic planes must have a common rotational vector normal to the geometry top and bottom.

III. CROSS SECTIONS

The MCNP code package is incomplete without the associated nuclear data tables. The kinds of tables available and their general features are outlined in this section. The manner in which information contained on nuclear data tables is used in MCNP is described in Sec. IV of this chapter.

There are two broad objectives in preparing nuclear data tables for MCNP. First, it is our responsibility to ensure that the data available to MCNP reproduce the original evaluated data as much as is practical. Second, new data should be brought into the MCNP package in a timely fashion, thereby giving users access to the most recent evaluations.

Eight classes of nuclear data tables exist for MCNP. They are: (1) continuous-energy neutron interaction data, (2) discrete reaction neutron interaction data, (3) photon interaction data, (4) neutron dosimetry cross sections, (5) neutron $S(\alpha, \beta)$ thermal data (6) multigroup neutron, coupled neutron/photon, and charged particles masquerading as neutrons, (7) multigroup photon, and (8) electron interaction data. It is understood that photon and electron data are atomic rather than nuclear. In Mode N problems, one continuous-energy or discrete-reaction neutron interaction table is required for each isotope or element in the problem. Likewise, one photon interaction table is required for each element in a Mode P problem, and one electron interaction table is required for each element in a Mode E problem. Dosimetry and thermal data are optional. Cross sections from dosimetry tables can be used as response functions with the FM card to determine reaction rates. Thermal $S(\alpha, \beta)$ tables are appropriate if the neutrons are transported at sufficiently low energies where molecular binding effects are important.

MCNP can read from data tables in any of three formats. Data tables are transmitted between computer installations in 80-column card-image BCD format (Type-1 format). An auxiliary processing code, MAKXSF, converts the BCD files to standard unformatted binary files (Type-2 format), allowing more economical access during execution of MCNP. At Los Alamos ACE (A Compact ENDF) tables (Type-3 format) are available. The data contained on a table for a specific Z Aid (10-character name for a nuclear data table) are independent of the format of the table.

The format of nuclear data tables is given in considerable detail in Appendix F. This appendix may be useful for users making extensive modifications to MCNP involving cross sections or for users debugging MCNP at a fairly high level.

The available nuclear data tables are listed in Appendix G. Each nuclear data table is identified by a ZAID. The general form of a ZAID is ZZZAAA.nnX, where ZZZ is the atomic number, AAA is the atomic weight, nn is the evaluation identifier, and X indicates the class of data. For elemental evaluations AAA=000. Nuclear data tables are selected by the user with the Mn and MTn cards.

In the remainder of this section we describe several characteristics of each class of data such as evaluated sources, processing tools, and any differences between data on the original evaluation and on the MCNP data tables. The means of accessing each class of data through MCNP input will be detailed and some hints will be provided on how to select the appropriate data tables.

A. Neutron Interaction Data: Continuous-Energy and Discrete Reaction

In neutron problems, one neutron interaction table is required for each isotope or element in the problem. The form of the ZAIDs is ZZZAAA.nnC for a continuous-energy table and ZZZAAA.nnD for a discrete reaction table. The neutron interaction tables available to MCNP are listed in Table G.2 of Appendix G. (It should be noted that although all nuclear data tables in Appendix G are available to users at Los Alamos, users at other installations will generally have only a subset of the tables available.)

For most materials there are many cross-section sets available (represented by different values of nn in the ZAIDs) because of multiple sources of evaluated data and different parameters used in processing the data. An evaluated nuclear data set is produced by analyzing experimentally measured cross sections and combining those data with the predictions of nuclear model calculations in an attempt to extract the most accurate cross-section information. Preparing evaluated cross-section sets has become a discipline in itself and has developed since the early 1960s. People in most of the national laboratories and several of the commercial reactor design firms are involved in such work. American evaluators joined forces in the mid-1960s to create the national ENDF system.²⁴ The ENDF contributors collaborate through the Cross Section Evaluation Working Group (CSEWG).

In recent years the primary evaluated source of neutron interaction data for MCNP has been the ENDF/B system. Recently evaluated neutron interaction data tables are also extracted from two other sources: Lawrence Livermore National Laboratory's Evaluated Nuclear Data Library (ENDL),²⁵ and supplemental evaluations performed in the Applied Nuclear Science Group at Los Alamos.^{26,27,28} Older evaluations come from previous versions of ENDF/B and ENDL, the Los Alamos Master Data File,²⁹ and the Atomic Weapons Research Establishment in Great Britain.

CHAPTER 2

Cross Sections

MCNP does not access evaluated data directly; these data must first be processed into ACE format. The very complex processing codes used for this purpose include NJOY³⁰ for evaluated data in ENDF/B format and MCPOINT³¹ for ENDL data.

Data on the MCNP neutron interaction tables include cross sections and much more. Cross sections for all reactions given in the evaluated data are specified. For a particular table, the cross sections for each reaction are given on one energy grid that is sufficiently dense that linear-linear interpolation between points reproduces the evaluated cross sections within a specified tolerance that is generally 1% or less. Depending primarily on the number of resolved resonances for each isotope, the resulting energy grid may contain as few as ~ 250 points (for example, H-1) or as many as $\sim 22,500$ points (for example, the ENDF/B-V version of Au-197). Other information, including the total absorption cross section, the total photon production cross section, and the average heating number (for energy deposition calculations), is also tabulated on the same energy grid.

Angular distributions of scattered neutrons are included in the neutron interaction tables for all nonabsorption reactions. The distributions are given in the center-of-mass system for elastic scattering, discrete-level inelastic scattering, and for some ENDF/B-VI scattering laws. They are given in the laboratory system for all other inelastic reactions. Angular distributions are given on a reaction-dependent grid of incident neutron energies. These tables are sampled to conserve energy for many collisions but will not necessarily conserve energy for a single collision; that is, energy is conserved on average.

The sampled angle of scattering uniquely determines the secondary energy for elastic scattering and discrete-level inelastic scattering. For other inelastic reactions, energy distributions of the scattered neutrons are provided in the neutron interaction tables. As with angular distributions, the energy distributions are given on a reaction-dependent grid of incident neutron energies.

When evaluations contain data about secondary photon production, that information appears in the MCNP neutron interaction tables. Many processed data sets contain photon production cross sections, photon angular distributions, and photon energy distributions for each neutron reaction that produces secondary photons. The information is given in a manner similar to that described in the last few paragraphs for neutron cross sections and secondary neutron distributions.

Other miscellaneous information on the neutron interaction tables includes the atomic weight ratio of the target nucleus, the Q-values of each reaction, and $\bar{\nu}$ data (the average number of neutrons per fission) for fissionable isotopes. In many cases both prompt and total $\bar{\nu}$ are given. Prompt $\bar{\nu}$ is the default for all but KCODE criticality problems and total $\bar{\nu}$ is the default for KCODE criticality problems. The TOTNU input card can be used to change the default.

Approximations must be made when processing an evaluated data set into ACE format. As mentioned above, cross sections are reproduced only

within a certain tolerance, generally $< 1\%$; to decrease it further would result in excessively large data tables. For many nuclides, a "thinned" neutron interaction table is available with a coarse tolerance, $> 1\%$, that greatly reduces the library size. Smaller library sizes also can be obtained by using discrete reaction tables or higher temperature data. Evaluated angular distributions for secondary neutrons and photons are approximated on MCNP data tables by 32 equally probable cosine bins. This approximation is clearly necessary when contrasted to the alternative that might involve sampling from a 20th-order Legendre polynomial distribution. Secondary neutron energy distributions given in tabular form by evaluators are sometimes approximated on MCNP data tables by 32 equally probable energy bins. Older cross-section tables include a 30×20 matrix approximation of the secondary photon energy spectra (described on page 2-32). On the whole, the approximations are small, and MCNP neutron interaction data tables are extremely faithful representations of evaluated data.

Discrete-reaction tables are identical to continuous-energy tables except that in the discrete reaction tables all cross sections have been averaged into 262 groups. The averaging is done with a flat weighting function. This is not a multigroup representation; the cross sections are simply given as histograms rather than as continuous curves. The remaining data (angular distributions, energy distributions, \bar{v} , etc.) are identical in discrete-reaction and continuous-energy tables. Discrete-reaction tables are provided primarily as a method of shrinking the required data storage to enhance the ability to run MCNP on small machines or in a time-sharing environment. The tables may also be useful for preliminary scoping studies or for isotopes that exist only in trace quantities in a problem. They are not, however, recommended as a substitute for the continuous-energy tables when performing final calculations, particularly for problems involving transport through the resonance region.

The matter of how to select the appropriate neutron interaction tables for your calculation is now discussed. Multiple tables for the same isotope are differentiated by the "nn" portion of the ZAID. The easiest choice for the user, although by no means the recommended one, is not to enter the nn at all. MCNP will select the first match found in the directory file XSDIR. The default nnX can be changed for all isotopes of a material by the NLIB keyword entry on the Mm card. The default will be overridden by fully specifying the ZAID. Default continuous-energy neutron interaction tables are accessed by entering ZZZAAA for the ZAID. Including a DRXS card in the input file will force MCNP to choose the default discrete reaction tables.

Careful users will want to think about what neutron interaction tables to choose. There is, unfortunately, no strict formula for guidance in choosing the tables. The following guidelines and observations are the best that can be offered:

1. Users should be aware of the differences between the ".50C" series of data tables and the ".51C" series. Both are derived from ENDF/B-V. The ".50C" series is the most faithful reproduction of the evaluated data. The

CHAPTER 2

Cross Sections

“.51C” series, also called the “thinned” series, has been processed with a less rigid tolerance than the “.50C” series. As with discrete reaction data tables, although by no means to the same extent, users should be careful when using the “thinned” data for transport through the resonance region.

2. Consider differences in evaluators’ philosophies. The Physical Data Group at Livermore is justly proud of its extensive cross-section efforts; their evaluations manifest a philosophy of reproducing the data with the fewest number of points. Livermore evaluations are available mainly in the “.40C” series. We at Los Alamos are particularly proud of the evaluation work being carried out in the Applied Nuclear Science Group T-2; generally, these evaluations are the most complex because they are the most thorough. Recent evaluations from Los Alamos are available in the “.55C” series.

3. Be aware of the neutron energy spectrum in your problem. For high-energy problems, the “thinned” and discrete reaction data are probably not bad approximations. Conversely, it is essential to use the most detailed continuous-energy set available for problems influenced strongly by transport through the resonance region.

4. Check the temperature at which various data tables have been processed. Do not use a set that is Doppler broadened to 12000000K for a room temperature calculation.

5. Consider checking the sensitivity of the results to various sets of nuclear data. Try, for example, a calculation with ENDF/B-V cross sections, and then another with ENDL cross sections. If the results of a problem are extremely sensitive to the choice of nuclear data, it is advisable to find out why.

6. For a coupled neutron/photon problem, be careful that the tables you choose have photon production data available. If possible, use the more-recent sets that have been processed into expanded photon production format.

7. Frequently, data tables are recommended that are not the defaults, leading to questions about what is wrong with the defaults. The answer is that nothing is wrong with them. They are frequently the very best evaluated data sets we have to offer. In other cases they are not, because of size limitations imposed on the default library at Los Alamos. In still other cases, a nondefault data table may be appropriate for one or more of the reasons given in the previous paragraphs.

8. Usually, use the best data you can afford. It is understood that the latest evaluations tend to be more complex and therefore require more memory and longer execution times. If you are limited by available memory, try to use smaller data tables such as thinned or discrete reaction for the minor isotopes in the calculation. Discrete reaction data tables might be used for a parameter study, followed by a calculation with the full continuous-energy data tables for confirmation.

To select the neutron interaction data tables, the nn portion of the ZAIDs must be entered on the Mn card(s). For a continuous-energy set, ZZZAAA.nn is equivalent to ZZZAAA.nnC. To use a discrete reaction table (unless there

is a DRXS card in the input) the full ZAID, ZZZAAA.nnD, must be entered.

In conclusion, the additional time necessary to choose appropriate neutron interaction data tables rather than simply to accept the defaults often will be well worth it in gaining understanding of your calculation.

B. Photon Interaction Data

Photon interaction cross sections are required for all photon problems. The form of the ZAID is ZZZ000.nnP. There are two photon interaction data libraries: nn = 01 and nn = 02.

For the ZAID=ZZZ000.01P library, the photon interaction tables for Z=84, 85, 87, 88, 89, 91, and 93 are based on the compilation of Storm and Israel³² from 1 keV to 15 MeV. For all other elements from Z=1 through Z=94 the photon interaction tables are based on evaluated data from ENDF³³ from 1 keV to 100 MeV. Fluorescence data are taken from work by Everett and Cashwell.³⁴ Energy grids are tailored specifically for each element and contain ~40-60 points.

The ZAID = ZZZ000.02P library is a superset of the ZAID = ZZZ000.01P library with pair production thresholds added for the Storm-Israel data. Data above 15 MeV for the Storm-Israel data and above 100 MeV for the ENDF data come from adaptation of the Livermore Evaluated Photon Data Library (EPDL)³⁵ and go up to 100 GeV. However, it usually is impractical to run above 1 GeV with MCNP because electron data only go to 1 GeV. The energy grid for the ZAID=ZZZ000.02P library contains ~100 points.

For each nuclide the photon interaction libraries contain an energy grid (logarithms of energies), including the photoelectric edges and the pair production threshold. These energies are tailored specifically for each element. The logarithmic energies are followed by tables of incoherent form factors and coherent form factors that are tabulated as a function of momentum transfer. The next tables are logarithms of the incoherent scattering, coherent scattering, photoelectric, and pair production cross sections, followed by the photon heating numbers. The total cross section is not stored, but rather summed from the other cross sections during transport.

The determination of directions and energies of scattered photons requires information different from the sets of angular and energy distributions found on neutron interaction tables. Angular distributions of secondary photons are isotropic for photoelectric effect, fluorescence, and pair production, and come from sampling the well-known Thomson and Klein-Nishina formulas for coherent and incoherent scattering. The energy of an incoherently scattered photon is calculated from the sampled scattering angle. Values of the integrated coherent form factor are tabulated on the photon interaction tables for use with next event estimators such as point detectors.

Very few approximations are made in the various processing codes used to transfer photon data from ENDF into the format of MCNP photon interaction tables. Cross sections are reproduced exactly as given. Form factors and scattering functions are reproduced as given; however, the momentum transfer grid on which they are tabulated may be different from that of the

CHAPTER 2

Cross Sections

original evaluation. Heating numbers are calculated values, not given in evaluated sets, but inferred from them. Fluorescence data are not provided in ENDF; therefore the data for MCNP are extracted from a variety of sources as described in Ref. 32.

To select photon interaction data, specific ZAID identifiers can be used, such as ZAID=ZZZ000.02P, or selections from a library can be used by specifying PLIB=nnP on the M card. The PLIB=specification on the M card is the preferred method because the ZAID entries may already be used to specify neutron libraries and, unlike neutrons, it usually is desirable to pick all photon data from the same library. A specification on the Mn card for a neutron interaction table with ZAID=ZZZAAA.nnC or ZAID=ZZZAAA.nnD immediately causes a photon interaction table with ZAID=ZZZ000.nnP to be accessed as well, where nn is the first photon data encountered for ZZZ000 on the XSDIR cross section directory file or nn comes from PLIB=nn. The data table required for ZAID=ZZZAAA.nnP is identical to that required for ZAID=ZZZ000.nnP; however, the atomic weight used in the calculation will likely be different.

C. Electron Interaction Data

Electron interaction data tables are required both for problems in which electrons are actually transported, and for photon problems in which the thick-target bremsstrahlung model is used. Electron data tables are identified by ZAIDs of the form ZZZ000.nnE, and are selected by default when the problem mode requires them. There is only one electron interaction data library: nn = 01.

The electron library contains data on an element-by-element basis for atomic numbers $Z = 1-94$. As is the case with photons, there is no distinction between isotopes for a given element. The data contain energies for tabulation, bremsstrahlung production cross sections, bremsstrahlung energy distributions, X-ray production probabilities, K-edge energies and fluorescent probabilities, electron stopping powers and ranges, and parameters for the evaluation of the Goudsmit-Saunders theory for angular deflections and the Landau-Blunck-Leisegang theory of energy-loss fluctuations. Discussions of the theoretical basis for these data and references to the relevant literature are presented in Section IV-E of this chapter.

Only the nn = 01 library is currently available, but to support the use of alternate libraries in the future, MCNP implements a hierarchy of rules identical to that for photons. Thus, one may select a specific ZAID, such as ZZZ000.01E, and that choice will override any defaults. Alternatively, a default electron library for a given material may be chosen by specifying ELIB = nnE on the M card. In the absence of either of these specifications, MCNP will use the first electron data table listed in the XSDIR cross section directory file for the relevant element.

D. Neutron Dosimetry Cross Sections

Dosimetry cross-section tables cannot be used for transport through material. These incomplete cross-section sets provide energy-dependent neutron cross sections to MCNP for use as response functions with the FM tally feature. ZAIDs of dosimetry tables are of the form ZZZAAA.nnY. Remember, dosimetry cross-section tables have no effect on the particle transport of a problem.

The available dosimetry cross sections are from three sources: ENDF/B-V Dosimetry Tape 531, ENDF/B-V Activation Tape 532, and ACTL³⁶—an evaluated neutron activation cross-section library from the Lawrence Livermore National Laboratory. Various codes have been used to process evaluated dosimetry data into the format of MCNP dosimetry tables.

Data on dosimetry tables are simply energy-cross-section pairs for one or more reactions. The energy grids for all reactions are independent of each other. Interpolation between adjacent energy points can be specified as histogram, linear-linear, linear-log, log-linear, or log-log. With the exception of the tolerance involved in any reconstruction of pointwise cross sections from resonance parameters, evaluated dosimetry cross sections can be reproduced on the MCNP data tables with no approximation.

ZAIDs for dosimetry tables must be entered on material cards that are referenced by FM cards, not on Mm cards referenced by cell cards. The complete ZAID, ZZZAAA.nnY, must be given; there are no defaults for dosimetry tables.

E. Neutron Thermal $S(\alpha, \beta)$ Tables

Thermal $S(\alpha, \beta)$ tables are not required, but they are absolutely essential to get correct answers in problems involving neutron thermalization. Thermal tables have ZAIDs of the form XXXXXX.nnT, where XXXXXX is a mnemonic character string. The data on these tables encompass those required for a complete representation of thermal neutron scattering by molecules and crystalline solids. The source of $S(\alpha, \beta)$ data is a special set of ENDF tapes.³⁷ The THERMR and ACER modules of the NJOY³⁰ system have been used to process the evaluated thermal data into a format appropriate for MCNP.

Data are for neutron energies generally less than 4 eV. Cross sections are tabulated on table-dependent energy grids; inelastic scattering cross sections are always given and elastic scattering cross sections are sometimes given. Correlated energy-angle distributions are provided for inelastically scattered neutrons. A set of equally probable final energies is tabulated for each of several initial energies. Further, a set of equally probable cosines or cosine bins is tabulated for each combination of initial and final energies. Elastic scattering data can be derived from either an incoherent or a coherent approximation. In the incoherent case, equally probable cosines or cosine bins are tabulated for each of several incident neutron energies. In the coherent case, scattering cosines are determined from a set of Bragg energies derived

CHAPTER 2

Neutrons

from the lattice parameters. During processing, approximations to the evaluated data are made when constructing equally probable energy and cosine distributions.

ZAIDs for the thermal tables are entered on an MTn card that is associated with an existing Mn card. The thermal table generally will provide data for one component of a material; for example, hydrogen in light water. Thermal ZAIDs may be entered on the MTn card(s) as XXXXXX, XXXXXX.nn, or XXXXXX.nnT.

F. Multigroup Tables

Multigroup cross section libraries are the only libraries allowed in multigroup/adjoint problems. Neutron multigroup problems cannot be supplemented with $S(\alpha, \beta)$ thermal libraries; the thermal effects must be included in the multigroup neutron library. Photon problems cannot be supplemented with electron libraries; the electrons must be part of the multigroup library containing the photon data. The form of the ZAID is ZZZAAA.nnM.

Although continuous-energy data are more accurate than multigroup data, the multigroup option is useful for a number of important applications: (1) comparison of deterministic (S_n) transport codes to Monte Carlo; (2) use of adjoint calculations in problems where the adjoint method is more efficient; (3) generation of adjoint importance functions; (4) cross section sensitivity studies; (5) solution of problems for which continuous-cross sections are unavailable; and (6) charged particle transport using the Boltzmann-Fokker-Planck algorithm in which charged particles masquerade as neutrons.

Multigroup cross sections are very problem dependent. Some multigroup libraries are available from the Radiation Transport Group at Los Alamos but must be used with caution. Users are encouraged to generate or get their own multigroup libraries and then use the supplementary code CRSRD³⁸ to convert them to MCNP format. Reference 38 describes the conversion procedure. This report also describes how to use both the multigroup and adjoint methods in MCNP and presents several benchmark calculations demonstrating the validity and effectiveness of the multigroup/adjoint method.

IV. PHYSICS

The physics of neutron, photon, and electron interactions is the very essence of MCNP. This section may be considered a software requirements document in that it describes the equations MCNP is intended to solve. All the sampling schemes essential to the random walk are presented or referenced. But first, particle weight and particle tracks, two concepts that are important for setting up the input and for understanding the output, are discussed in the following sections.

A. Particle Weight

If MCNP were used only to simulate exactly physical transport, then each MCNP particle would represent one physical particle and would have unit weight. However, for computational efficiency, MCNP allows many techniques that do not exactly simulate physical transport. For instance, each MCNP particle might represent a number w of particles emitted from a source. This number w is the initial weight of the MCNP particle. The w physical particles all would have different random walks, but the one MCNP particle representing these w physical particles will only have one random walk. Clearly this is not an exact simulation; however, the true number of physical particles is preserved in MCNP in the sense of statistical averages and therefore in the limit of large particle numbers (of course including particle production or loss if they occur). Each MCNP particle result is multiplied by the weight so that the full results of the w physical particles represented by each MCNP particle are exhibited in the final results (tallies). This procedure allows users to normalize their calculations to whatever source strength they desire. The default normalization is to weight one per MCNP particle. A second normalization to the number of Monte Carlo histories is made in the results so that the expected means will be independent of the number of source particles actually initiated in the MCNP calculation.

The utility of particle weight, however, goes far beyond simply normalizing the source. Every Monte Carlo biasing technique alters the probabilities of random walks executed by the particles. The purpose of such biasing techniques is to increase the number of particles that sample some part of the problem of special interest (1) without increasing (sometimes actually decreasing) the sampling of less interesting parts of the problem, and (2) without erroneously affecting the expected mean physical result (tally). This procedure, properly applied, increases precision in the desired result compared to an unbiased calculation taking the same computing time. For example, if an event is made $\sqrt{2}$ times as likely to occur (as it would occur without biasing), the tally ought to be multiplied by $1/\sqrt{2}$ so that the expected average tally is unaffected. This tally multiplication can be accomplished by multiplying the particle weight by $1/\sqrt{2}$ because the tally contribution by a particle is always multiplied by the particle weight in MCNP. Note that weights need not be integers.

In short, particle weight is a number carried along with each MCNP particle, representing that particle's relative contribution to the final tallies. Its magnitude is determined to ensure that whenever MCNP deviates from an exact simulation of the physics, the expected physical result nonetheless is preserved in the sense of statistical averages, and therefore in the limit of large MCNP particle numbers. Its utility is in the manipulation of the number of particles, sampling just a part of the problem to improve the precision of selected results obviating a full unbiased calculation—with its added cost in computing time—to achieve the same results and precision.

CHAPTER 2

Neutrons

B. Particle Tracks

When a particle starts out from a source, a particle track is created. If that track is split 2 for 1 at a splitting surface, a second track is created and there are now two tracks from the original source particle, each with half the single track weight. If one of the tracks has an (n,2n) reaction, one more track is started for a total of three. A track refers to each component of a source particle during its history. Track length tallies use the length of a track in a given cell to determine a quantity of interest, such as fluence, flux, or energy deposition. Tracks crossing surfaces are used to calculate fluence, flux, or pulse-height energy deposition (surface estimators). Tracks undergoing collisions are used to calculate multiplication and criticality (collision estimators).

Within a given cell of fixed composition, the method of sampling a collision along the track is determined using the following theory. The probability of a first collision for a particle between l and $l + dl$ along its line of flight is given by

$$p(l)dl = e^{-\Sigma_t l} \Sigma_t dl,$$

where Σ_t is the macroscopic total cross section of the medium and is interpreted as the probability per unit length of a collision. Setting ξ the random number on $[0,1)$, to be

$$\xi = \int_0^l e^{-\Sigma_t s} \Sigma_t ds = 1 - e^{-\Sigma_t l},$$

it follows that

$$l = -\frac{1}{\Sigma_t} \ln(1 - \xi).$$

But, because $1 - \xi$ is distributed in the same manner as ξ and hence may be replaced by ξ , we obtain the well-known expression for the distance to collision,

$$l = -\frac{1}{\Sigma_t} \ln(\xi).$$

C. Neutron Interactions

When a particle (representing any number of neutrons, depending upon the particle weight) collides with a nucleus, the following sequence occurs:

1. the collision nuclide is identified;
2. either the $S(\alpha, \beta)$ treatment is used or the velocity of the target nucleus is sampled for low-energy neutrons;
3. photons are optionally generated for later transport;
4. neutron capture (that is, neutron disappearance by any process) is modeled;

5. unless the $S(\alpha, \beta)$ treatment is used, either elastic scattering or an inelastic reaction is selected, and the new energy and direction of the outgoing track(s) are determined;
6. if the energy of the neutron is low enough and an appropriate $S(\alpha, \beta)$ table is present, the collision is modeled by the $S(\alpha, \beta)$ treatment instead of by step 5.

1. Selection of Collision Nuclide

If there are n different nuclides forming the material in which the collision occurred, and if ξ is a random number on the unit interval $[0,1)$, then the k^{th} nuclide is chosen as the collision nuclide if

$$\sum_{i=1}^{k-1} \Sigma_{ti} < \xi \sum_{i=1}^n \Sigma_{ti} \leq \sum_{i=1}^k \Sigma_{ti},$$

where Σ_{ti} is the macroscopic total cross section of nuclide i . If the energy of the neutron is low enough (below about 4 eV) and the appropriate $S(\alpha, \beta)$ table is present, the total cross section is the sum of the capture cross section from the regular cross-section table and the elastic and inelastic scattering cross sections from the $S(\alpha, \beta)$ table. Otherwise, the total cross section is taken from the regular cross-section table and is adjusted for thermal effects as described below.

2. Free Gas Thermal Treatment

A collision between a neutron and an atom is affected by the thermal motion of the atom, and in most cases, the collision is also affected by the presence of other atoms nearby. The thermal motion cannot be ignored in many applications of MCNP without serious error. The effects of nearby atoms are also important in some applications. MCNP uses a thermal treatment based on the free gas approximation to account for the thermal motion. It also has an explicit $S(\alpha, \beta)$ capability that takes into account the effects of chemical binding and crystal structure for incident neutron energies below about 4 eV, but is available for only a limited number of substances and temperatures. The $S(\alpha, \beta)$ capability is described later on page 2-49.

The free gas thermal treatment in MCNP assumes that the medium is a free gas and also that, in the range of atomic weight and neutron energy where thermal effects are significant, the elastic scattering cross section at zero temperature is nearly independent of the energy of the neutron, and that the reaction cross sections are nearly independent of temperature. These assumptions allow MCNP to have a thermal treatment of neutron collisions that runs almost as fast as a completely nonthermal treatment and that is adequate for most practical problems.

With the above assumptions, the free gas thermal treatment consists of adjusting the elastic cross section and taking into account the velocity of the target nucleus when the kinematics of a collision are being calculated. Note that Doppler broadening of the inelastic cross sections is assumed to have

CHAPTER 2

Neutrons

already been done in the processing of the cross section libraries. The free gas thermal treatment effectively applies to elastic scattering only.

a. Adjusting the Elastic Cross Section: The first aspect of the free gas thermal treatment is to adjust the zero-temperature elastic cross section by raising it by the factor

$$F = (1 + 0.5/a^2) \operatorname{erf}(a) + \exp(-a^2)/(a\sqrt{\pi}),$$

where $a = \sqrt{AE/kT}$, A = atomic weight, E = neutron energy, and T = temperature. For speed, F is approximated by $F = 1 + 0.5/a^2$ when $a \geq 2$ and by linear interpolation in a table of 51 values of aF when $a < 2$. Both approximations have relative errors less than 0.0001. The total cross section also is increased by the amount of the increase in the elastic cross section.

The adjustment to the elastic and total cross sections is done partly in the setup of a problem and partly during the actual transport calculation. No adjustment is made if the elastic cross section in the data library was already processed to the temperature that is needed in the problem. If all of the cells that contain a particular nuclide have the same temperature, constant in time, that is different from the temperature of the library, the elastic and total cross sections for that nuclide are adjusted to that temperature during the setup so that the transport will run a little faster. Otherwise, these cross sections are reduced, if necessary, to zero temperature during the setup and the thermal adjustment is made when the cross sections are used. For speed, the thermal adjustment is omitted if the neutron energy is greater than $500 kT/A$. At that energy the adjustment of the elastic cross section would be less than 0.1%.

b. Sampling the Velocity of the Target Nucleus: The second aspect of the free gas thermal treatment consists of taking into account the velocity of the target nucleus when the kinematics of a collision are being calculated. The target velocity is sampled and subtracted from the velocity of the neutron to get the relative velocity. The collision is sampled in the target-at-rest frame and the outgoing velocities are transformed to the laboratory frame by adding the target velocity.

There are different schools of thought as to whether the relative energy between the neutron and target, E_r , or the laboratory frame incident neutron energy (target-at-rest), E_o , should be used for all the kinematics of the collision. E_o is used in MCNP to obtain the distance-to-collision, select the collision nuclide, determine energy cutoffs, generate photons, generate fission sites for the next generation of a KCODE criticality problem, for $S(\alpha, \beta)$ scattering, and for capture. E_r is used for everything else in the collision process, namely elastic and inelastic scattering, including fission and (n,xn) reactions. It is shown in Eqn. 2.1 that E_r is based upon v_{rel} that is based upon the elastic scattering cross section, and, therefore, E_r is truly valid only for elastic scatter. However, the only significant thermal reactions for stable isotopes are absorption, elastic scattering, and fission. ^{181}Ta has a 6 keV threshold inelastic reaction; all other stable isotopes have higher inelas-

tic thresholds. Metastable nuclides like ^{242m}Am have inelastic reactions all the way down to zero, but these inelastic reaction cross sections are neither constant nor $1/v$ cross sections and these nuclides are generally too massive to be affected by the thermal treatment anyway. Furthermore, fission is very insensitive to incident neutron energy at low energies. The fission secondary energy and angle distributions are nearly flat or constant for incident energies below about 500 keV. Therefore, it makes no significant difference if E_r is used only for elastic scatter or for other inelastic collisions as well. At thermal energies, whether E_r or E_0 is used only makes a difference for elastic scattering.

If the energy of the neutron is greater than $400 kT$ and the target is not ^1H , the velocity of the target is set to zero. Otherwise, the target velocity is sampled as follows.

The free-gas kernel is a thermal interaction model that results in a good approximation to the thermal flux spectrum in a variety of applications and can be sampled without tables. The effective scattering cross section in the laboratory system for a neutron of kinetic energy E is

$$\sigma_s^{eff}(E) = \frac{1}{v_n} \iint \sigma_s(v_{rel}) v_{rel} p(V) dV \frac{d\mu_t}{2}. \quad (2.1)$$

Here, v_{rel} is the relative velocity between a neutron moving with a scalar velocity v_n and a target nucleus moving with a scalar velocity V , and μ_t is the cosine of the angle between the neutron and the target direction-of-flight vectors. The equation for v_{rel} is

$$v_{rel} = (v_n^2 + V^2 - 2v_n V \mu_t)^{\frac{1}{2}}.$$

The scattering cross section at the relative velocity is denoted by $\sigma_s(v_{rel})$, and $p(V)$ is the probability density function for the Maxwellian distribution of target velocities,

$$p(V) = \frac{4}{\pi^{1/2}} \beta^3 V^2 e^{-\beta^2 V^2}$$

with β defined as

$$\beta = \left(\frac{AM_n}{2kT} \right)^{1/2},$$

where A is the mass of a target nucleus in units of the neutron mass, M_n is the neutron mass in $\text{MeV}\cdot\text{sh}^2/\text{cm}^2$, and kT is the equilibrium temperature of the target nuclei in MeV.

The most probable scalar velocity V of the target nuclei is $1/\beta$, which corresponds to a kinetic energy of kT for the target nuclei. This is not the average kinetic energy of the nuclei, which is $3kT/2$. The quantity that MCNP expects on the TMPn input card is kT and not just T (see page 3–105). Note that kT is not a function of the particle mass and is therefore the kinetic energy at the most probable velocity for particles of any mass.

CHAPTER 2
Neutrons

Equation (2.1) implies that the probability distribution for a target velocity V and cosine μ_t is

$$P(V, \mu_t) = \frac{\sigma_s(v_{rel})v_{rel}P(V)}{2\sigma_s^{eff}(E)v_n}$$

It is assumed that the variation of $\sigma_s(v_{rel})$ with target velocity can be ignored. The justification for this approximation is that (1) for light nuclei, $\sigma_s(v_{rel})$ is slowly varying with velocity, and (2) for heavy nuclei, where $\sigma_s(v_{rel})$ can vary rapidly, the moderating effect of scattering is small so that the consequences of the approximation will be negligible. As a result of the approximation, the probability distribution actually used is

$$P(V, \mu_t) \propto \sqrt{v_n^2 + V^2 - 2Vv_n\mu_t} V^2 e^{-\beta^2 V^2}$$

Note that the above expression can be written as

$$P(V, \mu_t) \propto \frac{\sqrt{v_n^2 + V^2 - 2Vv_n\mu_t}}{v_n + V} (V^3 e^{-\beta^2 V^2} + v_n V^2 e^{-\beta^2 V^2})$$

As a consequence, the following algorithm is used to sample the target velocity.

1. With probability $\alpha = 1/(1 + (\sqrt{\pi}\beta v_n/2))$, the target velocity V is sampled from the distribution $P_1(V) = 2\beta^4 V^3 e^{-\beta^2 V^2}$. The transformation $V = \sqrt{y}/\beta$ reduces this distribution to the sampling distribution for $P(y) = ye^{-y}$.
2. With probability $1 - \alpha$, the target velocity is sampled from the distribution $P_2(V) = (4\beta^3/\sqrt{\pi})V^2 e^{-\beta^2 V^2}$. Substituting $V = y/\beta$ reduces the distribution to the sampling distribution for y : $P(y) = (4/\sqrt{\pi})y^2 e^{-y^2}$.
3. The cosine of the angle between the neutron velocity and the target velocity is sampled uniformly on the interval $-1 \leq \mu_t \leq +1$.
4. The rejection function $R(V, \mu_t)$ is computed using

$$R(V, \mu_t) = \frac{\sqrt{v_n^2 + V^2 - 2Vv_n\mu_t}}{v_n + V} \leq 1$$

With probability $R(V, \mu_t)$, the sampling is accepted; otherwise, the sampling is rejected and the procedure is repeated. The minimum efficiency of this rejection algorithm averaged over μ_t is 68% and approaches 100% as either the incident neutron energy approaches zero or becomes much larger than kT .

3. Optional Generation of Photons

Photons are generated if the problem is a combined neutron/photon run and if the collision nuclide has a nonzero photon production cross section.

The number of photons produced is a function of neutron weight, neutron source weight, photon weight limits (entries on the PWT card), photon production cross section, neutron total cross section, cell importance, and the importance of the neutron source cell. No more than 10 photons may be born from any neutron collision.

Because of the many low-weight photons typically created by neutron collisions, Russian roulette is played for particles with weight below the bounds specified on the PWT card, resulting in fewer particles, each having a larger weight. The created photon weight before Russian roulette is

$$W_p = \frac{W_n \sigma_\gamma}{\sigma_T},$$

where W_p = photon weight
 W_n = neutron weight
 σ_γ = photon production cross section
 σ_T = total neutron cross section.

Both σ_γ and σ_T are evaluated at the incoming neutron energy without the effects of the thermal free gas treatment because nonelastic cross sections are assumed independent of temperature.

The Russian roulette game is played according to neutron cell importances for the collision and source cell. For a photon produced in cell i where the minimum weight set on the PWT card is W_i^{min} , let I_i be the neutron importance in cell i and let I_s be the neutron importance in the source cell. If $W_p > W_i^{min} * I_s / I_i$, one or more photons will be produced. The number of photons created is N_p , where $N_p = (W_p * I_i) / (5 * W_i^{min} * I_s) + 1$. $N_p \leq 10$. Each photon is stored in the bank with weight W_p / N_p . If $W_p < W_i^{min} * I_s / I_i$, Russian roulette is played and the photon survives with probability $W_p * I_i / (W_i^{min} * I_s)$ and is given the weight $W_i^{min} * I_s / I_i$.

If weight windows are not used and if the weight of the starting neutrons is not unity, setting all the W_i^{min} on the PWT card to negative values will make the photon minimum weight relative to the neutron source weight. This will make the number of photons being created roughly proportional to the biased collision rate of neutrons. It is recommended for most applications that negative numbers be used and be chosen to produce from one to four photons per source neutron. The default values for W_i^{min} on the PWT card are -1 , which should be adequate for most problems using cell importances.

If energy-independent weight windows are used, the entries on the PWT card should be the same as on the WWN1:P card. If energy-dependent photon weight windows are used, the entries on the PWT card should be the minimum WWNn:P entry for each cell, where n refers to the photon weight window energy group. This will cause most photons to be born within the weight window bounds.

Any photons generated at neutron collision sites are temporarily stored in the bank. There are two methods for determining the exiting energies and directions, depending on the form in which the processed photon production data are stored in a library. The first method has the evaluated photon pro-

CHAPTER 2

Neutrons

duction data processed into an “expanded format.”³⁹ In this format, energy-dependent cross sections, energy distributions, and angular distributions are explicitly provided for every photon-producing neutron interaction. In the second method, used with data processed from older evaluations, the evaluated photon production data have been collapsed so that the only information about secondary photons is in a matrix of 20 equally probable photon energies for each of 30 incident neutron energy groups. The sampling techniques used in each method are now described.

a. Expanded Photon Production Method: In the expanded photon production method, the reaction n responsible for producing the photon is sampled from

$$\sum_{i=1}^{n-1} \sigma_i < \xi \sum_{i=1}^N \sigma_i \leq \sum_{i=1}^n \sigma_i,$$

where ξ is a random number on the interval $[0,1)$, N is the number of photon production reactions, and σ_i is the photon production cross section for reaction i at the incident neutron energy. Note that there is no correlation between the sampling of the type of photon production reaction and the sampling of the type of neutron reaction described on page 2–34.

Just as every neutron reaction (for example, $(n, 2n)$) has associated energy-dependent angular and energy distributions for the secondary neutrons, every photon production reaction (for example, $(n, p\gamma)$) has associated energy-dependent angular and energy distributions for the secondary photons. The photon distributions are sampled in much the same manner as their counterpart neutron distributions.

All nonisotropic secondary photon angular distributions are represented by 32 equiprobable cosine bins. The distributions are given at a number of incident neutron energies. All photon-scattering cosines are sampled in the laboratory system. The sampling procedure is identical to that described for secondary neutrons on page 2–35.

Secondary photon energy distributions are also a function of incident neutron energy. There are two representations of secondary photon energy distributions allowed in ENDF/B format: tabulated spectra and discrete (line) photons. Correspondingly, there are three laws used in MCNP for the determination of secondary photon energies. Law 4 is an exact representation of tabulated photon spectra. Law 2 is used for discrete photons. Law 44 is for discrete photon lines with a continuous background. These laws are described beginning on page 2–39.

The expanded photon production method has clear advantages over the original 30 x 20 matrix method described below. In coupled neutron/photon problems, users should attempt to specify data sets that contain photon production data in expanded format. Such data sets are identified by “YES P(E)” entries in the GPD column in Table G.2 in Appendix G.

b. 30 x 20 Photon Production Method: For lack of better terminology, we will refer to the photon production data contained on older libraries

as “30 x 20 photon production” data. In contrast to expanded photon production data, there is no information about individual photon production reactions in the 30 x 20 data.

The only secondary photon data are a 30 x 20 matrix of photon energies; that is, for each of 30 incident neutron energy groups there are 20 equally probable exiting photon energies. There is no information regarding secondary photon angular distributions; therefore, all photons are taken to be produced isotropically in the laboratory system.

There are several problems associated with 30 x 20 photon production data. The 30 x 20 matrix is an inadequate representation of the actual spectrum of photons produced. In particular, discrete photon lines are not well represented, and the high-energy tail of a photon continuum energy distribution is not well sampled. Also, the multigroup representation is not consistent with the continuous-energy nature of MCNP. Finally, not all photons should be produced isotropically. None of these problems exist for data processed into the expanded photon production format.

4. Capture

Capture is treated in one of two ways: analog or implicit. Either way, the incident incoming neutron energy does not include the relative velocity of the target nucleus from the free gas thermal treatment because nonelastic reaction cross sections are assumed to be nearly independent of temperature. That is, only the scattering cross section is affected by the free gas thermal treatment.

a. Analog Capture: In analog capture, the particle is killed with probability σ_a/σ_T , where σ_a and σ_T are the absorption and total cross sections of the collision nuclide at the incoming neutron energy. The absorption cross section is specially defined for MCNP as the sum of all (n, x) cross sections, where x is anything except neutrons. Thus σ_a is the sum of $\sigma_{n,\gamma}$, $\sigma_{n,\alpha}$, $\sigma_{n,d}$, ... etc. For all particles killed by analog capture, the entire particle energy and weight are deposited in the collision cell.

b. Implicit Capture: For implicit capture, the neutron weight W_n is reduced to W'_n as follows:

$$W'_n = \left(1 - \frac{\sigma_a}{\sigma_T}\right) * W_n.$$

If the new weight, W'_n , is below the problem weight cutoff (specified on the CUT card), Russian roulette is played, resulting overall in fewer particles with larger weight.

For implicit capture, a fraction σ_a/σ_T of the incident particle weight and energy is deposited in the collision cell corresponding to that portion of the particle that was captured. Implicit capture is the default method of neutron capture in MCNP.

c. Implicit Capture Along a Flight Path: Implicit capture also can be done continuously along the flight path of a particle trajectory as is the

CHAPTER 2
Neutrons

common practice in astrophysics. In this case, the distance to scatter, rather than the distance to collision, is sampled. The distance to scatter is

$$l = -\frac{1}{\Sigma_s} \ln(1 - \xi).$$

The particle weight at the scattering point is reduced by the capture loss,

$$W' = W e^{-\Sigma_a l} ,$$

where W' = reduced weight after capture loss,
 W = weight before capture along flight path,
 σ_a = absorption cross section,
 σ_s = scattering cross section,
 $\sigma_t = \sigma_s + \sigma_a$ = total cross section,
 l = distance to scatter, and
 ξ = random number.

Implicit capture along a flight path is a special form of the exponential transformation coupled with implicit capture at collisions. (See the description of the exponential transform on page 2-125.) The path length is stretched in the direction of the particle, $\mu = 1$, and the stretching parameter is $p = \Sigma_a / \Sigma_t$. Using these values the exponential transform and implicit capture at collisions yield the identical equations as does implicit capture along a flight path.

Implicit capture along a flight path is invoked in MCNP as a special option of the exponential transform variance reduction method. It is most useful in highly absorbing media, that is, Σ_a / Σ_t approaches 1. When almost every collision results in capture, it is very inefficient to sample distance to collision. However, implicit capture along a flight path is discouraged. In highly absorbing media, there is usually a superior set of exponential transform parameters. In relatively nonabsorbing media, it is better to sample the distance to collision than the distance to scatter.

5. Elastic and Inelastic Scattering

If the conditions for the $S(\alpha, \beta)$ treatment are not met, the particle undergoes either an elastic or inelastic collision. The selection of an elastic collision is made with probability

$$\frac{\sigma_{el}}{\sigma_{in} + \sigma_{el}} = \frac{\sigma_{el}}{\sigma_T - \sigma_a}$$

where

- σ_{el} is the elastic scattering cross section.
- σ_{in} is the inelastic cross section; includes any neutron-out process— (n, n') , (n, f) , (n, np) , etc.
- σ_a is the absorption cross section; $\Sigma\sigma(n, x)$, $\neq n$, that is, all neutron disappearing reactions.
- σ_T is the total cross section, $\sigma_T = \sigma_{el} + \sigma_{in} + \sigma_a$.

Both σ_{el} and σ_T are adjusted for the free gas thermal treatment at thermal energies.

The selection of an inelastic collision is made with the remaining probability

$$\frac{\sigma_{in}}{\sigma_T - \sigma_a}$$

If the collision is determined to be inelastic, the type of inelastic reaction, n , is sampled from

$$\sum_{i=1}^{n-1} \sigma_i < \xi \sum_{i=1}^N \sigma_i \leq \sum_{i=1}^n \sigma_i \quad ,$$

where ξ is a random number on the interval $[0,1)$ N is the number of inelastic reactions, and the σ_i 's are the inelastic reaction cross sections at the incident neutron energy.

For both elastic and inelastic scattering, the direction of exiting particles usually is determined by sampling angular distribution tables from the cross-section files. This process is described shortly. For elastic collisions and discrete inelastic scattering from levels, the exiting particle energy is determined from two body kinematics based upon the center-of-mass cosine of the scattering angle. For other inelastic processes, the energy of exiting particles is determined from secondary energy distribution laws from the cross-section files, which vary according to the particular inelastic collision modeled.

a. Sampling of Angular Distributions: The direction of emitted particles is sampled in the same way for most elastic and inelastic collisions. The cosine of the angle between incident and exiting particle directions, μ , is sampled from angular distribution tables in the collision nuclide's cross-section library. The angular distribution tables consist of 32 equiprobable cosine bins and are given at a number of different incident neutron energies. The cosines are either in the center-of-mass or target-at-rest system, depending on the type of reaction. If E is the incident neutron energy, if E_n is the energy of table n , and if E_{n+1} is the energy of table $n + 1$, then a value of μ is sampled from table $n + 1$ with probability $(E - E_n)/(E_{n+1} - E_n)$ and from table n with probability $(E_{n+1} - E)/(E_{n+1} - E_n)$. A random number ξ on the interval $[0,1)$ is then used to select the i^{th} cosine bin such that $i = 32\xi + 1$. The value of μ is then computed as

$$\mu = \mu_i + (32\xi - i)(\mu_{i+1} - \mu_i) \quad .$$

If, for some incident neutron energy, the emitted angular distribution is isotropic, μ is chosen from $\mu = \xi'$, where ξ' is a random number on the interval $[-1,1)$. (Strictly, in MCNP random numbers are always furnished on the interval $[0,1)$. Thus, to compute ξ' on $[-1,1)$ we calculate $\xi' = 2\xi - 1$, where ξ is a random number on $[0,1)$.)

CHAPTER 2
Neutrons

For elastic scattering, inelastic level scattering, and some ENDF/B-VI inelastic reactions, the scattering cosine is chosen in the center-of-mass system. Conversion must then be made to μ_{lab} , the cosine in the target-at-rest system. For other inelastic reactions, the scattering cosine is sampled directly in the target-at-rest system.

The incident particle direction cosines, (u_o, v_o, w_o) , are rotated to new outgoing target-at-rest system cosines, (u, v, w) , through a polar angle whose cosine is μ_{lab} , and through an azimuthal angle sampled uniformly. For random numbers ξ_1 and ξ_2 on the interval $[-1,1)$ with rejection criterion $\xi_1^2 + \xi_2^2 \leq 1$, the rotation scheme is (Ref. 2, pg. 54):

$$\begin{aligned} u &= u_o \mu_{lab} + \frac{\sqrt{1 - \mu_{lab}^2} (\xi_1 u_o w_o - \xi_2 v_o)}{\sqrt{(\xi_1^2 + \xi_2^2)(1 - w_o^2)}} \\ v &= v_o \mu_{lab} + \frac{\sqrt{1 - \mu_{lab}^2} (\xi_1 v_o w_o + \xi_2 u_o)}{\sqrt{(\xi_1^2 + \xi_2^2)(1 - w_o^2)}} \\ w &= w_o \mu_{lab} - \frac{\xi_1 \sqrt{(1 - \mu_{lab}^2)(1 - w_o^2)}}{\sqrt{(\xi_1^2 + \xi_2^2)}} \end{aligned}$$

If $1 - w_o^2 \sim 0$, then

$$\begin{aligned} u &= u_o \mu_{lab} + \frac{\sqrt{1 - \mu_{lab}^2} (\xi_1 u_o v_o + \xi_2 w_o)}{\sqrt{(\xi_1^2 + \xi_2^2)(1 - v_o^2)}} \\ v &= v_o \mu_{lab} - \frac{\xi_1 \sqrt{(1 - \mu_{lab}^2)(1 - v_o^2)}}{\sqrt{(\xi_1^2 + \xi_2^2)}} \\ w &= w_o \mu_{lab} + \frac{\sqrt{1 - \mu_{lab}^2} (\xi_1 w_o v_o - \xi_2 u_o)}{\sqrt{(\xi_1^2 + \xi_2^2)(1 - v_o^2)}} \end{aligned}$$

If the scattering distribution is isotropic in the target-at-rest system, it is possible to use an even simpler formulation that takes advantage of the exiting direction cosines, (u, v, w) , being independent of the incident direction cosines, (u_o, v_o, w_o) . In this case,

$$\begin{aligned}
 u &= 2\xi_1^2 + 2\xi_2^2 - 1 \\
 v &= \xi_1 \sqrt{\frac{1-u^2}{\xi_1^2 + \xi_2^2}} \\
 w &= \xi_2 \sqrt{\frac{1-u^2}{\xi_1^2 + \xi_2^2}} \quad ,
 \end{aligned}$$

where ξ_1 and ξ_2 are rejected if $\xi_1^2 + \xi_2^2 > 1$.

b. Elastic Scattering: The particle direction is sampled from the appropriate angular distribution tables, and the exiting energy, E_{out} , is dictated by two-body kinematics:

$$\begin{aligned}
 E_{out} &= \frac{1}{2} E_{in} [(1 - \alpha)\mu_{cm} + 1 + \alpha] \\
 &= E_{in} \left[\frac{1 + A^2 + 2A\mu_{cm}}{(1 + A)^2} \right] \quad ,
 \end{aligned}$$

where E_{in} = incident neutron energy

μ_{cm} = center-of-mass cosine of the angle between incident and exiting particle directions

$$\alpha = \left(\frac{A - 1}{A + 1} \right)^2$$

and A = mass of collision nuclide in units of the mass of a neutron
(atomic weight ratio)

c. Inelastic Scattering: The treatment of inelastic scattering depends upon the particular inelastic reaction chosen. Inelastic reactions are defined as (n, y) reactions such as (n, n') , $(n, 2n)$, (n, f) , $(n, n'\alpha)$ in which y includes at least one neutron.

For many inelastic reactions, such as $(n, 2n)$, more than one neutron can be emitted for each incident neutron. The weight of each exiting particle is always the same as the weight of the incident particle minus any implicit capture. The energy of exiting particles is governed by various scattering laws that are sampled independently from the cross-section files for each exiting particle. Which law is used is prescribed by the particular cross-section evaluation used. In fact, more than one law can be specified, and the particular one used at a particular time is decided with a random number. In an $(n, 2n)$ reaction, for example, the first particle emitted may have an energy sampled from one or more laws, but the second particle emitted may have an energy sampled from one or more different laws, depending upon specifications in the nuclear data library. Because emerging energy and scattering angle is sampled independently for each particle, there is no correlation between the emerging particles. Hence energy is not conserved in an individual reaction because, for example, a 14-MeV particle could conceivably produce

CHAPTER 2
Neutrons

two 12-MeV particles in a single reaction. But the net effect of many particle histories is unbiased because on the average the correct amount of energy is emitted. Results are biased only when quantities that depend upon the correlation between the emerging particles are being estimated.

Users should note that MCNP follows a very particular convention. The exiting particle energy and direction are always given in the target-at-rest (laboratory) coordinate system. For the kinematical calculations in MCNP to be performed correctly, the angular distributions for elastic, discrete inelastic level scattering, and some ENDF/B-VI inelastic reactions *must* be given in the center-of-mass system, and the angular distributions for all other reactions *must* be given in the target-at-rest system. MCNP does not stop if this convention is not adhered to, but the results will be erroneous. In the checking of the cross-section libraries prepared for MCNP at Los Alamos, however, careful attention has been paid to ensure that these conventions are followed.

The exiting particle energy and direction in the target-at-rest (laboratory) coordinate system are related to the center-of-mass energy and direction as follows:¹

$$E' = E'_{cm} + \left[\frac{E + 2\mu_{cm}(A+1)\sqrt{E E'_{cm}}}{(A+1)^2} \right]; \text{ and}$$

$$\mu_{lab} = \mu_{cm} \sqrt{\frac{E'_{cm}}{E'}} + \frac{1}{A+1} \sqrt{\frac{E}{E'}}$$

where E' = exiting particle energy (laboratory),
 E'_{cm} = exiting particle energy (center-of-mass),
 E = incident particle energy (laboratory),
 μ_{cm} = cosine of center-of-mass scattering angle,
 μ_{lab} = cosine of laboratory scattering angle,
 A = atomic weight ratio (mass of nucleus divided by mass of incident particle.)

For point detectors it is necessary to convert

$$p(\mu_{lab}) = p(\mu_{cm}) \frac{d\mu_{cm}}{d\mu_{lab}},$$

where

$$\mu_{cm} = \mu_{lab} \sqrt{\frac{E'}{E'_{cm}}} - \frac{1}{A+1} \sqrt{\frac{E}{E'_{cm}}} \quad \text{and}^1$$

$$\frac{d\mu_{cm}}{d\mu_{lab}} = \frac{E'/E'_{cm}}{\sqrt{\frac{E'}{E'_{cm}}} - \frac{\mu_{lab}}{A+1} \sqrt{\frac{E}{E'_{cm}}}}$$

$$= \frac{\sqrt{\frac{E'}{E'_{cm}}}}{1 - \frac{\mu_{lab}}{A+1} \sqrt{\frac{E}{E'_{cm}}}}.$$

d. Nonfission Inelastic Scattering and Emission Laws: Nonfission inelastic reactions are handled differently from fission inelastic reactions. For each nonfission reaction N_p particles are emitted, where N_p is an integer quantity specified for each reaction in the cross-section data library of the collision nuclide. The direction of each emitted particle is independently sampled from the appropriate angular distribution table, as was described earlier. The energy of each emitted particle is independently sampled from one of the following scattering or emission laws. Energy and angle are correlated only for ENDF/B-VI laws 44 and 67. For completeness and convenience we list all the laws together, regardless of whether the law is appropriate for nonfission inelastic scattering (for example, Law 3), fission spectra (for example, Law 11), both (for example, Law 9), or neutron-induced photon production (for example, Law 2). The conversion from center-of-mass to target-at-rest (laboratory) coordinate systems is as above.

Law 1 (ENDF law 1): Equiprobable energy bins.

The index i and the interpolation fraction r are found on the incident energy grid for the incident energy E_{in} such that

$$E_i < E_{in} < E_{i+1} \quad \text{and}$$

$$E_{in} = E_i + r(E_{i+1} - E_i).$$

A random number on the unit interval ξ_1 is used to select an equiprobable energy bin k from the K equiprobable outgoing energies E_{ik}

$$k = \xi_1 K + 1.$$

Then scaled interpolation is used with random numbers ξ_2 and ξ_3 on the unit interval. Let

$$E_1 = E_{i,1} + r(E_{i+1,1} - E_{i,1}) \quad \text{and}$$

$$E_K = E_{i,K} + r(E_{i+1,K} - E_{i,K}); \quad \text{and}$$

$$l = i \text{ if } \xi_3 > r \quad \text{or}$$

$$l = i + 1 \text{ if } \xi_3 < r \quad \text{and}$$

$$E' = E_{l,k} + \xi_2(E_{l,k+1} - E_{l,k}); \quad \text{then}$$

$$E_{out} = E_1 + \frac{(E' - E_{l,1})(E_K - E_1)}{E_{l,K} - E_{l,1}}.$$

Law 2 Discrete photon energy.

The value provided in the library is E_g . The secondary photon energy

CHAPTER 2
Neutrons

E_{out} is either

$$E_{out} = E_g \text{ for non-primary photons or}$$

$$E_{out} = E_g + [A/(A + 1)]E_{in} \text{ for primary photons,}$$

where A is the atomic weight to neutron weight ratio of the target and E_{in} is the incident neutron energy.

Law 3 (ENDF law 3): Inelastic scattering (n, n') from nuclear levels. The value provided in the library is Q .

$$E_{out} = \left(\frac{A}{A + 1} \right)^2 \left[E_{in} - \frac{Q(A + 1)}{A} \right]$$

Law 4 Tabular distribution (ENDF law 4).

For each incident neutron energy E_i there is a pointer to a table of secondary energies $E_{i,k}$, probability density functions $p_{i,k}$, and cumulative density functions $c_{i,k}$. The index i and the interpolation fraction r are found on the incident energy grid for the incident energy E_{in} such that

$$E_i < E_{in} < E_{i+1} \quad \text{and}$$

$$E_{in} = E_i + r(E_{i+1} - E_i).$$

A random number on the unit interval ξ_1 is used to sample a secondary energy bin k from the cumulative density function

$$c_{i,k} + r(c_{i+1,k} - c_{i,k}) < \xi_1 < c_{i,k+1} + r(c_{i+1,k+1} - c_{i,k+1}).$$

If these are discrete line spectra, then the sampled energy E' is interpolated between incident energy grids as

$$E' = E_{i,k} + r(E_{i+1,k} - E_{i,k}).$$

It is possible to have all discrete lines, all continuous spectra, or a mixture of discrete lines superimposed on a continuous background. For continuous distributions, the secondary energy bin k is sampled from

$$c_{l,k} < \xi_1 < c_{l,k+1},$$

where $l = i$ if $\xi_2 > r$ and $l = i + 1$ if $\xi_2 < r$, and ξ_2 is a random number on the unit interval. For histogram interpolation the sampled energy is

$$E' = E_{l,k} + \frac{(\xi_1 - c_{l,k})}{p_{l,k}}.$$

For linear-linear interpolation the sampled energy is

$$E' = E_{l,k} + \left\{ \frac{\sqrt{p_{l,k}^2 + 2 \left[\frac{p_{l,k+1} - p_{l,k}}{E_{l,k+1} - E_{l,k}} \right] (\xi_1 - c_{l,k}) - p_{l,k}}}{\left[\frac{p_{l,k+1} - p_{l,k}}{E_{l,k+1} - E_{l,k}} \right]} \right\}$$

For neutron-induced photons, $E_{out} = E'$ and the angle is selected as described on page 2-35. That is, the photon secondary energy is sampled from either of the two bracketing incident energy bins, $l = i$ or $l = i + 1$.

The neutron secondary energy must be interpolated between the incident energy bins i and $i + 1$ to properly preserve thresholds. Let

$$E_1 = E_{i,1} + r(E_{i+1,1} - E_{i,1}) \quad \text{and}$$

$$E_K = E_{i,K} + r(E_{i+1,K} - E_{i,K}); \quad \text{then}$$

$$E_{out} = E_1 + \frac{(E' - E_{l,1})(E_K - E_1)}{(E_{l,K} - E_{l,1})}$$

The outgoing neutron energy is then adjusted to the laboratory system, if it is in the center-of-mass system, and the outgoing angle is selected as described on page 2-35.

Law 5 (ENDF law 5): General evaporation spectrum.

The function $g(x)$ is tabulated versus χ and the energy is tabulated versus incident energy E_{in} . The law is then

$$f(E_{in} \rightarrow E_{out}) = g\left(\frac{E_{out}}{T(E_{in})}\right)$$

This density function is sampled by

$$E_{out} = \chi(\xi)T(E_{in}),$$

where $T(E_{in})$ is a tabulated function of the incident energy and $\chi(\xi)$ is a table of equiprobable χ values.

Law 7 (ENDF law 7): Simple Maxwell Fission Spectrum.

$$f(E_{in} \rightarrow E_{out}) = C * \sqrt{E_{out}} e^{-E_{out}/T(E_{in})}$$

The nuclear temperature $T(E_{in})$ is a tabulated function of the incident energy. The normalization constant C is given by

$$C^{-1} = T^{3/2} \left[\left(\frac{\sqrt{\pi}}{2} \right) \operatorname{erf} \left(\sqrt{\frac{(E_{in} - U)}{T}} \right) - \sqrt{\frac{(E_{in} - U)}{T}} e^{-(E_{in} - U)/T} \right]$$

CHAPTER 2
Neutrons

U is a constant provided in the library and limits E_{out} to $0 \leq E_{out} \leq E_{in} - U$. In MCNP this density function is sampled by the rejection scheme

$$E_{out} = -T(E_{in}) \left[\frac{\xi_1^2 \ln \xi_3}{\xi_1^2 + \xi_2^2} + \ln \xi_4 \right] ,$$

where ξ_1 , ξ_2 , ξ_3 , and ξ_4 are random numbers on the unit interval. ξ_1 and ξ_2 are rejected if $\xi_1^2 + \xi_2^2 > 1$.

Law 9 (ENDF law 9): Evaporation spectrum.

$$f(E_{in} \rightarrow E_{out}) = C E_{out} e^{-E_{out}/T(E_{in})} ,$$

where the nuclear temperature $T(E_{in})$ is a tabulated function of the incident energy. The energy U is provided in the library and is assigned so that E_{out} is limited by $0 \leq E_{out} \leq E_{in} - U$. The normalization constant C is given by

$$C^{-1} = T^2 \left[1 - e^{-(E_{in}-U)/T} (1 + (E_{in} - U)/T) \right] .$$

In MCNP this density function is sampled by

$$E_{out} = -T(E_{in}) \ln(\xi_1 \xi_2) ,$$

where ξ_1 and ξ_2 are random numbers on the unit interval, and ξ_1 and ξ_2 are rejected if $E_{out} > E_{in} - U$.

Law 11 (ENDF law 11): Energy Dependent Watt Spectrum.

$$f(E_{in} \rightarrow E_{out}) = C e^{-E_{out}/a(E_{in})} \sinh \sqrt{b(E_{in}) E_{out}} .$$

The constants a and b are tabulated functions of incident energy and U is a constant from the library. The normalization constant C is given by

$$C^{-1} = \frac{1}{2} \sqrt{\frac{\pi a^3 b}{4}} \exp\left(\frac{ab}{4}\right) \left[\operatorname{erf}\left(\sqrt{\frac{(E_{in}-U)}{a}} - \sqrt{\frac{ab}{4}}\right) + \operatorname{erf}\left(\sqrt{\frac{(E_{in}-U)}{a}} + \sqrt{\frac{ab}{4}}\right) \right] \\ - a \exp\left[-\frac{(E_{in}-U)}{a}\right] \sinh \sqrt{b(E_{in}-U)} ,$$

where the constant U limits the range of outgoing energy so that $0 \leq E_{out} \leq E_{in} - U$. This density function is sampled as follows. Let

$$g = \sqrt{\left(1 + \frac{ab}{8}\right)^2 - 1 + \left(1 + \frac{ab}{8}\right)} . \quad \text{Then} \quad E_{out} = -ag \ln \xi_1 .$$

E_{out} is rejected if

$$[(1 - g)(1 - \ln \xi_1) - \ln \xi_2]^2 > bE_{out},$$

where ξ_1 and ξ_2 are random numbers on the unit interval.

Law 22 (UK law 2): Tabular linear functions of incident energy out. Tables of P_{ij} , C_{ij} , and T_{ij} are given at a number of incident energies E_i . If $E_i \leq E_{in} < E_{i+1}$ then the i^{th} P_{ij} , C_{ij} , and T_{ij} tables are used.

$$E_{out} = C_{ik}(E_{in} - T_{ik}),$$

where k is chosen according to

$$\sum_{j=1}^k P_{ij} < \xi \leq \sum_{j=1}^{k+1} P_{ij} \quad ,$$

where ξ is a random number on the unit interval [0,1).

Law 24 (UK law 6): Equiprobable energy multipliers. The law is

$$E_{out} = E_{in}T(E_{in})$$

The library provides a table of K equiprobable energy multipliers $T_{i,k}$ for a grid of incident neutron energies E_i . For incident energy E_{in} such that

$$E_i < E_{in} < E_{i+1} \quad ,$$

the random numbers ξ_1 and ξ_2 on the unit interval are used to find T :

$$k = \xi_1 K + 1$$

$$T = T_{i,k} + \xi_2(T_{i,k+1} - T_{i,k}) \quad \text{and then}$$

$$E_{out} = E_{in} T$$

Law 44 Tabular Distribution (ENDF/B-VI file 6 law=1 lang=2, Kalbach-87 correlated energy-angle scattering). Law 44 is a generalization of law 4. For each incident neutron energy E_i there is a pointer to a table of secondary energies $E_{i,k}$, probability density functions $p_{i,k}$, cumulative density functions $c_{i,k}$, precompound fractions $R_{i,k}$, and angular distribution slope values $A_{i,k}$. The index i and the interpolation fraction r are found on the incident energy grid for the incident energy E_{in} such that

$$E_i < E_{in} < E_{i+1} \quad \text{and}$$

$$E_{in} = E_i + r(E_{i+1} - E_i).$$

CHAPTER 2
Neutrons

A random number on the unit interval ξ_1 is used to sample a secondary energy bin k from the cumulative density function

$$c_{i,k} + r(c_{i+1,k} - c_{i,k}) < \xi_1 < c_{i,k+1} + r(c_{i+1,k+1} - c_{i,k+1}).$$

If these are discrete line spectra, then the sampled energy E' is interpolated between incident energy grids as

$$E' = E_{i,k} + r(E_{i+1,k} - E_{i,k}).$$

It is possible to have all discrete lines, all continuous spectra, or a mixture of discrete lines superimposed on a continuous background. For continuous distributions, the secondary energy bin k is sampled from

$$c_{l,k} < \xi_1 < c_{l,k+1},$$

where $l = i$ if $\xi_2 > r$ and $l = i+1$ if $\xi_2 < r$, and ξ_2 is a random number on the unit interval. For histogram interpolation the sampled energy is

$$E' = E_{l,k} + \frac{(\xi_1 - c_{l,k})}{p_{l,k}}.$$

For linear-linear interpolation the sampled energy is

$$E' = E_{l,k} + \left\{ \frac{\sqrt{p_{l,k}^2 + 2 \left[\frac{p_{l,k+1} - p_{l,k}}{E_{l,k+1} - E_{l,k}} \right] (\xi_1 - c_{l,k}) - p_{l,k}}}{\left[\frac{p_{l,k+1} - p_{l,k}}{E_{l,k+1} - E_{l,k}} \right]} \right\}.$$

Unlike Law 4, the sampled energy is interpolated between the incident energy bins i and $i+1$ for both neutron-induced photons and neutrons. Let

$$E_1 = E_{i,1} + r(E_{i+1,1} - E_{i,1}) \quad \text{and}$$

$$E_K = E_{i,K} + r(E_{i+1,K} - E_{i,K}); \quad \text{then}$$

$$E_{out} = E_1 + \frac{(E' - E_{l,1})(E_K - E_1)}{(E_{l,K} - E_{l,1})}.$$

For neutron-induced photons, the outgoing angle is selected as described on page 2-35. For neutrons, E_{out} is always in the center-of-mass system and must be adjusted to the laboratory system. The outgoing neutron center-of-mass scattering angle μ is sampled from the Kalbach-87 density function

$$p(\mu, E_{in}, E_{out}) = \frac{1}{2} \frac{A}{\sinh(A)} [\cosh(A\mu) + R \sinh(A\mu)]$$

using the random numbers ξ_3 and ξ_4 on the unit interval as follows. If $\xi_3 > R$, then let

$$T = (2\xi_4 - 1) \sinh(A) \quad \text{and}$$

$$\mu = \ln(T + \sqrt{T^2 + 1}) / A,$$

or if $\xi_3 < R$, then

$$\mu = \ln [\xi_4 e^A + (1 - \xi_4) e^{-A}] / A.$$

R and A are interpolated on both the incident and outgoing energy grids. For discrete spectra,

$$A = A_{i,k} + r(A_{i+1,k} - A_{i,k}),$$

$$R = R_{i,k} + r(R_{i+1,k} - R_{i,k}).$$

For continuous spectra with histogram interpolation,

$$A = A_{l,k},$$

$$R = R_{l,k}.$$

For continuous spectra with linear-linear interpolation,

$$A = A_{l,k} + (A_{l,k+1} - A_{l,k})(E' - E_{l,k}) / (E_{l,k+1} - E_{l,k}),$$

$$R = R_{l,k} + (R_{l,k+1} - R_{l,k})(E' - E_{l,k}) / (E_{l,k+1} - E_{l,k}).$$

The Kalbach-87 formalism (Law 44) is also characterized by an energy-dependent multiplicity in which the number of neutrons emerging from a collision varies. If the number is less than one, Russian roulette is played and the collision can result in a capture. If the number is greater than one, the usual MCNP approach is taken whereby the additional particles are banked and only the first one contributes to detectors and DXTRAN.

Law 66 N-body phase space distribution (ENDF/B-VI file 6 law 6).

The phase space distribution for particle i in the center-of-mass coordinate system is:

$$P_i(\mu, E_{in}, E_{out}) = C_n \sqrt{E_{out}} (E_i^{max} - E_{out})^{3n/2-4},$$

where all energies and angles are also in the center-of-mass system and E_i^{max} is the maximum possible energy for particle i , μ and E_{out} . The C_n normalization constants for $n = 3, 4, 5$ are:

CHAPTER 2
Neutrons

$$C_3 = \frac{4}{\pi(E_i^{max})^2} \quad ,$$

$$C_4 = \frac{105}{32(E_i^{max})^{7/2}} \quad , \text{ and}$$

$$C_5 = \frac{256}{14\pi(E_i^{max})^5} \quad .$$

E_i^{max} is a fraction of the energy available, E_a ,

$$E_i^{max} = \frac{M - m_i}{M} E_a \quad ,$$

where M is the total mass of the n particles being treated, m_i is the mass of particle i , and

$$E_a = \frac{m_T}{m_p + m_T} E_{in} + Q \quad ,$$

where m_T is the target mass and m_p is the projectile mass. For neutrons,

$$\frac{m_T}{m_p + m_T} = \frac{A}{A + 1}$$

and for a total mass ratio $A_p = M/m_i$,

$$\frac{M - m_i}{M} = \frac{A_p - 1}{A_p} \quad .$$

Thus,

$$E_i^{max} = \frac{A_p - 1}{A_p} \left(\frac{A}{A + 1} E_{in} + Q \right) \quad .$$

The total mass A_p and the number of particles in the reaction n are provided in the data library. The outgoing energy is sampled as follows.

Let ξ_i , $i = 1, 9$ be random numbers on the unit interval. Then from rejection technique R28 from the Monte Carlo Sampler,³ accept ξ_1 and ξ_2 if

$$\xi_1^2 + \xi_2^2 \leq 1$$

and accept ξ_3 and ξ_4 if

$$\xi_3^2 + \xi_4^2 \leq 1 \quad .$$

Then let

$$p = \xi_5 \quad \text{if} \quad n = 3 \quad ,$$

$$p = \xi_5 \xi_6 \quad \text{if } n = 4 \quad , \quad \text{and}$$

$$p = \xi_5 \xi_6 \xi_7 \xi_8 \quad \text{if } n = 5 \quad ,$$

and let

$$x = \frac{-\xi_1 \ln(\xi_1^2 + \xi_2^2)}{(\xi_1^2 + \xi_2^2)} - \ln \xi_9 \quad ,$$

$$y = \frac{-\xi_3 \ln(\xi_3^2 + \xi_4^2)}{(\xi_3^2 + \xi_4^2)} - \ln p \quad , \quad \text{and}$$

$$T = \frac{x}{x + y} \quad ;$$

then

$$E_{out} = T E_i^{max} \quad .$$

The cosine of the scattering angle is always sampled isotropically in the center-of-mass system using another random number ξ_2 on the unit interval:

$$\mu = 2\xi_2 - 1 \quad .$$

Law 67 Correlated energy-angle scattering (ENDF/B-VI file 6 law 7).

For each incident neutron energy, first the exiting particle direction μ is sampled as described on page 2-35. In other Law data, first the exiting particle energy is sampled and then the angle is sampled. The index i and the interpolation fraction r are found on the incident energy grid for the incident energy E_{in} , such that

$$E_i < E_{in} < E_{i+1} \quad \text{and}$$

$$E_{in} = E_i + r(E_{i+1} - E_i).$$

For each incident energy E_i there is a table of exiting particle direction cosines $\mu_{i,j}$ and locators $L_{i,j}$. This table is searched to find which ones bracket μ , namely,

$$\mu_{i,j} < \mu < \mu_{i,j+1}.$$

Then the secondary energy tables at $L_{i,j}$ and $L_{i,j+1}$ are sampled for the outgoing particle energy. The secondary energy tables consist of a secondary energy grid $E_{i,j,k}$, probability density functions $p_{i,j,k}$, and cumulative density functions $c_{i,j,k}$. A random number ξ_1 on the unit interval is used to pick between incident energy indices: if $\xi_1 < r$ then $l = i + 1$; otherwise, $l = i$. Two more random numbers ξ_2 and

CHAPTER 2
Neutrons

ξ_3 on the unit interval are used to determine interpolation energies. If $\xi_2 < (\mu - \mu_{i,j})/(\mu_{i,j+1} - \mu_{i,j})$, then

$$E_{i,k} = E_{i,j+1,k} \quad \text{and} \quad m = j + 1, \quad \text{if} \quad l = i.$$

Otherwise,

$$E_{i,k} = E_{i,j,k} \quad \text{and} \quad m = j, \quad \text{if} \quad l = i.$$

If $\xi_3 < (\mu - \mu_{i+1,j})/(\mu_{i+1,j+1} - \mu_{i+1,j})$, then

$$E_{i+1,k} = E_{i+1,j+1,k} \quad \text{and} \quad m = j + 1, \quad \text{if} \quad l = i + 1.$$

Otherwise,

$$E_{i+1,k} = E_{i+1,j,k} \quad \text{and} \quad m = j, \quad \text{if} \quad l = i + 1.$$

A random number ξ_4 on the unit interval is used to sample a secondary energy bin k from the cumulative density function

$$c_{l,m,k} < \xi_4 < c_{l,m,k+1}.$$

For histogram interpolation the sampled energy is

$$E' = E_{l,m,k} + \frac{(\xi_4 - c_{l,m,k})}{p_{l,m,k}}.$$

For linear-linear interpolation the sampled energy is

$$E' = E_{l,m,k} + \left\{ \frac{\sqrt{p_{l,m,k}^2 + 2 \left[\frac{p_{l,m,k+1} - p_{l,m,k}}{E_{l,m,k+1} - E_{l,m,k}} \right] (\xi_4 - c_{l,m,k}) - p_{l,m,k}}}{\left[\frac{p_{l,m,k+1} - p_{l,m,k}}{E_{l,m,k+1} - E_{l,m,k}} \right]} \right\}.$$

The final outgoing energy E_{out} uses scaled interpolation. Let

$$E_1 = E_{i,1} + r(E_{i+1,1} - E_{i,1})$$

$$\text{and} \quad E_K = E_{i,K} + r(E_{i+1,K} - E_{i,K}).$$

$$\text{Then} \quad E_{out} = E_1 + \frac{(E' - E_{l,1})(E_K - E_1)}{(E_{l,K} - E_{l,1})}.$$

e. Fission Inelastic Scattering: For any fission reaction a number of neutrons, N_p , are emitted according to the value of $\bar{\nu}(E_{in})$. The average number of neutrons per fission, $\bar{\nu}(E_{in})$, is either a tabulated function of energy or a polynomial function of energy. If I is the largest integer less than $\nu(E_{in})$, then

$$\begin{aligned} N_p &= I + 1 && \text{if } \xi \leq \bar{\nu}(E_{in}) - I \\ N_p &= I && \text{if } \xi > \bar{\nu}(E_{in}) - I, \text{ where } \xi \text{ is a random number.} \end{aligned}$$

The direction of each emitted neutron is sampled independently from the appropriate angular distribution table by the procedure described on page 2-35.

The energy of each fission neutron is determined from the appropriate (that is, as specified in the evaluation) emission law. The three laws used for fission neutron spectra are 7, 9, and 11. These laws are discussed in the preceding section, starting on page 2-41. MCNP then models the transport of the first neutron out after storing all other neutrons in the bank.

6. The $S(\alpha, \beta)$ treatment

The $S(\alpha, \beta)$ thermal scattering treatment is a complete representation of thermal neutron scattering by molecules and crystalline solids. Two processes are allowed: (1) inelastic scattering with cross section σ_{in} and a coupled energy-angle representation derived from an ENDF/B $S(\alpha, \beta)$ scattering law, and (2) elastic scattering with no change in the outgoing neutron energy for solids with cross section σ_{el} and an angular treatment derived from lattice parameters. The elastic scattering treatment is chosen with probability $\sigma_{el}/(\sigma_{el} + \sigma_{in})$. This thermal scattering treatment also allows the representation of scattering by multiatomic molecules (for example, BeO).

For the inelastic treatment, the distribution of secondary energies is represented by a set of equally probable final energies (typically 16 or 32) for each member of a grid of initial energies from an upper limit of typically 4 eV down to 10^{-5} eV, along with a set of angular data for each initial and final energy. The selection of a final energy E' given an initial energy E can be characterized by sampling from the distribution

$$p(E' | E_i < E < E_{i+1}) = \frac{1}{N} \sum_{j=1}^N \delta [E' - \rho E_{i,j} - (1 - \rho)E_{i+1,j}] \quad ,$$

where E_i and E_{i+1} are adjacent elements on the initial energy grid,

$$\rho = \frac{E_{i+1} - E}{E_{i+1} - E_i} \quad ,$$

N is the number of equally probable final energies, and $E_{i,j}$ is the j^{th} discrete final energy for incident energy E_i .

There are two allowed schemes for the selection of a scattering cosine following selection of a final energy and final energy index j . In each case, the $(i, j)^{\text{th}}$ set of angular data is associated with the energy transition $E = E_i \rightarrow E' = E_{i,j}$.

- (1) The data consist of sets of equally probable discrete cosines $\mu_{i,j,k}$ for $k = 1, \dots, \nu$ with ν typically 4 or 8. An index k is selected with probability $1/\nu$, and μ is obtained by the relation

$$\mu = \rho \mu_{i,j,k} + (1 - \rho) \mu_{i+1,j,k} \quad .$$

CHAPTER 2

Photons

- (2) The data consist of bin boundaries of equally probable cosine bins. In this case, random linear interpolation is used to select one set or the other, with ρ being the probability of selecting the set corresponding to incident energy E_i . The subsequent procedure consists of sampling for one of the equally probable bins and then choosing μ uniformly in the bin.

For elastic scattering, the above two angular representations are allowed for data derived by an incoherent approximation. In this case, one set of angular data appears for each incident energy and is used with the interpolation procedures on incident energy described above.

For elastic scattering, when the data have been derived in the coherent approximation, a completely different representation occurs. In this case, the data actually stored are the set of parameters D_k , where

$$\begin{aligned}\sigma_{el} &= D_k/E && \text{for } E_{Bk} \leq E < E_{Bk+1} \\ \sigma_{el} &= 0 && \text{for } E < E_{B1}\end{aligned}$$

and E_{Bk} are Bragg energies derived from the lattice parameters. For incident energy E such that $E_{Bk} \leq E \leq E_{Bk+1}$,

$$P_i = D_i/D_k \text{ for } i = 1, \dots, k$$

represents a discrete cumulative probability distribution that is sampled to obtain index i , representing scattering from the i^{th} Bragg edge. The scattering cosine is then obtained from the relationship

$$\mu = 1 - 2E_{Bi}/E$$

Using next event estimators such as point detectors with $S(\alpha, \beta)$ scattering cannot be done exactly because of the discrete scattering angles. MCNP uses an approximate scheme^{40,41} that in the next event estimation calculation replaces discrete lines with histograms of width

$$\delta\mu < .1$$

See also page 2-82.

D. Photon Interactions

Sampling of a collision nuclide, analog capture, implicit capture, and many other aspects of photon interactions such as variance reduction, are the same as for neutrons. The collision physics are completely different.

MCNP has two photon interaction models: simple and detailed.

The simple physics treatment ignores coherent (Thomson) scattering and fluorescent photons from photoelectric absorption. It is intended for high-energy photon problems or problems where electrons are free and is also important for next event estimators such as point detectors, where scattering can be nearly straight ahead with coherent scatter. The simple physics treatment uses implicit capture unless overridden with the CUT:P card, in which case it uses analog capture.

CHAPTER 2

Errors

bins will be for positrons (positive scores), electrons (negative scores), and total. The total bin will be the same as the single bin with the first ELC option above (usually with negative scores because there are more electrons than positrons).

5. User modification

If the above capabilities do not provide the user with exactly what is desired, tallies can be modified by a user-supplied TALLYX subroutine (FU card). As with a user-supplied SOURCE subroutine, which lets the user provide his own specialized source, the TALLYX subroutine lets the user modify any tally, with all the programming changes conveniently located in a single subroutine.

6. Tally output format

Not only can users change the contents of MCNP tallies, the output format can be modified as well. Any desired descriptive comment can be added to the tally title by the tally comment (FC) card. The printing order can be changed (FQ card) so that instead of, for instance, getting the default output blocks in terms of time vs energy, they could be printed in blocks of segment vs cosine. The tally bin that is monitored for the tally fluctuation chart printed at the problem end and used in the statistical analysis of the tally can be selected (TF card). Detector tally diagnostic prints are controlled with the DD card. Finally, the PRINT card controls what optional tables are displayed in the output file.

VI. ESTIMATION OF THE MONTE CARLO PRECISION

Monte Carlo results represent an average of the contributions from many histories sampled during the course of the problem. An important quantity equal in stature to the Monte Carlo answer (or tally) itself is the statistical error or uncertainty associated with the result. The importance of this error and its behavior vs the number of histories cannot be overemphasized because the user not only gains insight into the quality of the result, but also can determine if a tally appears statistically well behaved. If a tally is not well behaved, the estimated error associated with the result generally will not reflect the true confidence interval of the result and, thus, the answer could be completely erroneous. MCNP contains several quantities that aid the user in assessing the quality of the confidence interval.

The purpose of this section is to educate MCNP users about the proper interpretation of the MCNP estimated mean, relative error, variance of the variance, and history score probability density function. Carefully check tally results and the associated tables in the tally fluctuation charts to ensure a well-behaved and properly converged tally.

A. Monte Carlo Means, Variances, and Standard Deviations

Monte Carlo results are obtained by sampling possible random walks and assigning a score x_i (for example, x_i = energy deposited by the i^{th} random walk) to each random walk. Random walks typically will produce a range of scores depending on the tally selected and the variance reduction chosen.

Suppose $f(x)$ is the history score probability density function for selecting a random walk that scores x to the tally being estimated. The true answer (or mean) is the expected value of x , $E(x)$, where

$$E(x) = \int x f(x) dx = \text{true mean.}$$

The function $f(x)$ is seldom explicitly known; thus, $f(x)$ is implicitly sampled by the Monte Carlo random walk process. The true mean then is estimated by the sample mean \bar{x} where

$$\bar{x} = \frac{1}{N} \sum_{i=1}^N x_i \quad , \quad (2.15)$$

where x_i is the value of x selected from $f(x)$ for the i^{th} history and N is the number of histories calculated in the problem. The Monte Carlo mean \bar{x} is the average value of the scores x_i for all the histories calculated in the problem. The relationship between $E(x)$ and \bar{x} is given by the Strong Law of Large Numbers¹ that states that if $E(x)$ is finite, \bar{x} tends to the limit $E(x)$ as N approaches infinity.

The variance of the population of x values is a measure of the spread in these values and is given by¹

$$\sigma^2 = \int (x - E(x))^2 f(x) dx = E(x^2) - (E(x))^2$$

The square root of the variance is σ , which is called the standard deviation of the population of scores. As with $E(x)$, σ is seldom known but can be estimated by Monte Carlo as S , given by (for large N)

$$S^2 = \frac{\sum_{i=1}^N (x_i - \bar{x})^2}{N - 1} \sim \overline{x^2} - \bar{x}^2 \quad (2.16a)$$

and

$$\overline{x^2} = \frac{1}{N} \sum_{i=1}^N x_i^2 \quad (2.16b)$$

The quantity S is the estimated standard deviation of the population of x based on the values of x_i that were actually sampled.

The estimated variance of \bar{x} is given by

$$S_{\bar{x}}^2 = \frac{S^2}{N} \quad (2.17)$$

CHAPTER 2

Errors

These formulae do not depend on any restriction on the distribution of x or \bar{x} (such as normality) beyond requiring that $E(x)$ and σ^2 exist and are finite. The estimated standard deviation of the mean \bar{x} is given by $S_{\bar{x}}$.

It is important to note that $S_{\bar{x}}$ is proportional to $1/\sqrt{N}$, which is the inherent drawback to the Monte Carlo method. To halve $S_{\bar{x}}$, four times the original number of histories must be calculated, a calculation that can be computationally expensive. The quantity $S_{\bar{x}}$ can also be reduced for a specified N by making S smaller, reducing the inherent spread of the tally results. This can be accomplished by using variance reduction techniques such as those discussed in section VII of this chapter.

B. Precision and Accuracy

There is an extremely important difference between precision and accuracy of a Monte Carlo calculation. As illustrated in Fig. 2.10, precision is the uncertainty in \bar{x} caused by the statistical fluctuations of the x_i 's for the portion of physical phase space sampled by the Monte Carlo process. Important portions of physical phase space might not be sampled because of problem cutoffs in time or energy, inappropriate use of variance reduction techniques, or an insufficient sampling of important low-probability events. Accuracy is a measure of how close the expected value of \bar{x} , $E(x)$, is to the true physical quantity being estimated. The difference between this true value and $E(x)$ is called the systematic error, which is seldom known. Error or uncertainty estimates for the results of Monte Carlo calculations refer only to the precision of the result and not to the accuracy. It is quite possible to calculate a highly precise result that is far from the physical truth because nature has not been modeled faithfully.

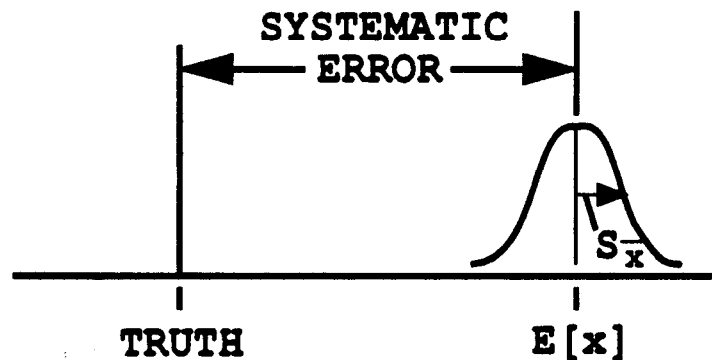


Figure 2.10

1. Factors Affecting Problem Accuracy

Three factors affect the accuracy of a Monte Carlo result: (1) the code, (2) problem modeling, and (3) the user. Code factors encompass: the physics features included in a calculation as well as the mathematical models used;

uncertainties in the data, such as the transport and reaction cross sections, Avogadro's number, atomic weights, etc.; the quality of the representation of the differential cross sections in energy and angle; and coding errors (bugs). All of the applicable physics must be included in a calculation to produce accurate results. Even though the evaluations are not perfect, more faithful representation of the evaluator's data should produce more accurate results. The descending order of preference for Monte Carlo data for calculations is continuous energy, thinned continuous energy, discrete reaction, and multi-group. Coding errors can always be a problem because no large code is bug-free. MCNP, however, is a very mature, heavily used production code. With steadily increasing use over the years, the likelihood of a serious coding error continues to diminish.

The second area, problem-modeling factors, can quite often contribute to a decrease in the accuracy of a calculation. Many calculations produce seemingly poor results because the model of the energy and angular distribution of the radiation source is not adequate. Two other problem-modeling factors affecting accuracy are the geometrical description and the physical characteristics of the materials in the problem.

The third general area affecting calculational accuracy involves user errors in the problem input or in user-supplied subroutines and patches to MCNP. The user can also abuse variance reduction techniques such that portions of the physical phase space are not allowed to contribute to the results. Checking the input and output carefully can help alleviate these difficulties. A last item that is often overlooked is a user's thorough understanding of the relationship of the Monte Carlo tallies to any measured quantities being calculated. Factors such as detector efficiencies, data reduction and interpretation, etc., must be completely understood and included in the calculation, or the comparison is not meaningful.

2. Factors Affecting Problem Precision

The precision of a Monte Carlo result is affected by four user-controlled choices: (1) forward vs adjoint calculation, (2) tally type, (3) variance reduction techniques, and (4) number of histories run.

The choice of a forward vs adjoint calculation depends mostly on the relative sizes of the source and detector regions. Starting particles from a small region is easy to do, whereas transporting particles to a small region is generally hard to do. Because forward calculations transport particles from source to detector regions, forward calculations are preferable when the detector (or tally) region is large and the source region is small. Conversely, because adjoint calculations transport particles backward from the detector region to the source region, adjoint calculations are preferable when the source (or tally) region is large and the detector region is small. MCNP can be run in multigroup adjoint mode. There is no continuous-energy adjoint capability.

As alluded to above, the smaller the tally region, the harder it becomes to get good tally estimates. An efficient tally will average over as large a

CHAPTER 2
Errors

region of phase space as practical. In this connection, tally dimensionality is extremely important. A one-dimensional tally is typically 10 to 100 times easier to estimate than a two-dimensional tally, which is 10 to 100 times easier than a three-dimensional tally. This fact is illustrated in Fig. 2.15 later in this section.

Variance reduction techniques can be used to improve the precision of a given tally by increasing the nonzero tallying efficiency and by decreasing the spread of the nonzero history scores. These two components are depicted in a hypothetical $f(x)$ shown in Fig. 2.11. See page 2-99 for more discussion about the empirical $f(x)$ for each tally fluctuation chart bin. A calculation will be more precise when the history-scoring efficiency is high and the variance of the nonzero scores is low. The user should strive for these conditions in difficult Monte Carlo calculations. Examples of these two components of precision are given on page 2-95.

More histories can be run to improve precision (see section C following). Because the precision is proportional to $1/\sqrt{N}$, running more particles is often costly in computer time and therefore is viewed as the method of last resort for difficult problems.

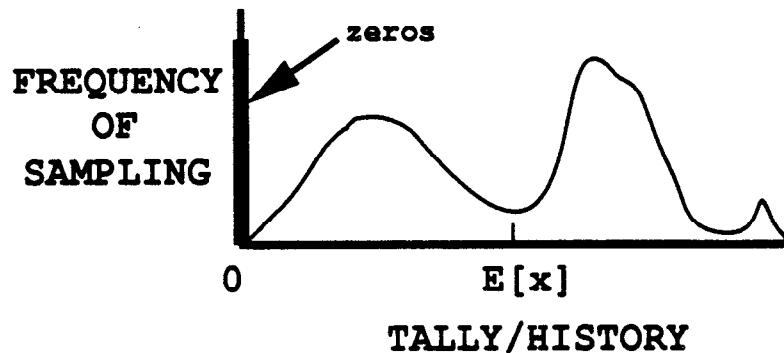


Figure 2.11

C. The Central Limit Theorem and Monte Carlo Confidence Intervals

To define confidence intervals for the precision of a Monte Carlo result, the Central Limit Theorem¹ of probability theory is used, stating that

$$\lim_{N \rightarrow \infty} \Pr \left[E(x) + \alpha \frac{\sigma}{\sqrt{N}} < \bar{x} < E(x) + \beta \frac{\sigma}{\sqrt{N}} \right] = \frac{1}{\sqrt{2\pi}} \int_{\alpha}^{\beta} e^{-t^2/2} dt \quad ,$$

where α and β can be any arbitrary values and $\Pr[Z]$ means the probability of Z . In terms of the estimated standard deviation of \bar{x} , $S_{\bar{x}}$, this may be rewritten in the following approximation for large N :

$$\Pr \left[\alpha S_{\bar{x}} < \frac{\bar{x} - E(x)}{\sigma \sqrt{N}} < \beta S_{\bar{x}} \right] \sim \frac{1}{\sqrt{2\pi}} \int_{\alpha}^{\beta} e^{-t^2/2} dt \quad .$$

This crucial theorem states that for large values of N (that is, as N tends to infinity) and identically distributed independent random variables x_i with finite means and variances, the distribution of the \bar{x} 's approaches a normal distribution. Therefore, for any distribution of tallies (an example is shown in Fig. 2.11), the distribution of resulting \bar{x} 's will be approximately normally distributed, as shown in Fig. 2.10, with a mean of $E(x)$. If S is approximately equal to σ , which is valid for a statistically significant sampling of a tally (i.e, N has tended to infinity), then

$$\bar{x} - S_{\bar{x}} < E(x) < \bar{x} + S_{\bar{x}}, \sim 68\% \text{ of the time} \quad (2.18a)$$

and

$$\bar{x} - 2S_{\bar{x}} < E(x) < \bar{x} + 2S_{\bar{x}}, \sim 95\% \text{ of the time} \quad (2.18b)$$

from standard tables for the normal distribution function. Eq. (2.18a) is a 68% confidence interval and Eq. (2.18b) is a 95% confidence interval.

The key point about the validity of these confidence intervals is that the physical phase space must be adequately sampled by the Monte Carlo process. If an important path in the geometry or a window in the cross sections, for example, has not been well sampled, both \bar{x} and $S_{\bar{x}}$ will be unknowingly incorrect and the results will be wrong, usually tending to be too small. The user must take great care to be certain that adequate sampling of the source, transport, and any tally response functions have indeed taken place. Additional statistical quantities to aid in the assessment of proper confidence intervals are described in later portions of section VI.

D. Estimated Relative Errors in MCNP

All standard MCNP tallies are normalized to be per starting particle history (except for some criticality calculations) and are printed in the output with a second number, which is the estimated relative error defined as

$$R \equiv S_{\bar{x}}/\bar{x} \quad (2.19a)$$

The relative error is a convenient number because it represents statistical precision as a fractional result with respect to the estimated mean.

Combining Eqs. (2.15), (2.16), and (2.17), R can be written (for large N) as

$$R = \left[\frac{1}{N} \left(\frac{\overline{x^2}}{\bar{x}^2} - 1 \right) \right]^{1/2} = \left[\frac{\sum_{i=1}^N x_i^2}{\left(\sum_{i=1}^N x_i \right)^2} - \frac{1}{N} \right]^{1/2} \quad (2.19b)$$

Several important observations about the relative error can be made from Eq. (2.19b). First, if all the x_i 's are nonzero and equal, R is zero. Thus, low-variance solutions should strive to reduce the spread in the x_i 's. If the x_i 's are all zero, R is defined to be zero. If only one nonzero score is made,

CHAPTER 2

Errors

R approaches unity as N becomes large. Therefore, for x_i 's of the same sign, $S_{\bar{x}}$ can never be greater than \bar{x} because R never exceeds unity. For positive and negative x_i 's, this is not true. The range of R values for x_i 's of the same sign is therefore between zero and unity.

To determine what values of R lead to results that can be stated with confidence using Eqs. (2.6), consider Eq. (2.19b) for a difficult problem in which nonzero scores occur very infrequently. In this case,

$$\frac{1}{N} \ll \frac{\sum_{i=1}^N x_i^2}{\left(\sum_{i=1}^N x_i\right)^2} \quad (2.20a)$$

For clarity, assume that there are n out of N ($n \ll N$) nonzero scores that are identical and equal to x . With these two assumptions, R for "difficult problems" becomes

$$R_{D.P.} \sim \left[\frac{nx^2}{n^2x^2} \right]^{1/2} = \frac{1}{\sqrt{n}}, n \ll N \quad (2.20b)$$

This result is expected because the limiting form of a binomial distribution with infrequent nonzero scores and large N is the Poisson distribution, which is the form in Eq. (2.20b) used in detector "counting statistics."

Table 2.2

Estimated Relative Error R vs Number of Identical Tallies n for Large N

| | | | | | | |
|-----|-----|-----|------|------|------|------|
| n | 1 | 4 | 16 | 25 | 100 | 400 |
| R | 1.0 | 0.5 | 0.25 | 0.20 | 0.10 | 0.05 |

Through use of Eqs. (2.8), a table of R values versus the number of tallies or "counts" can be generated as shown in Table 2.2. A relative error of 0.5 is the equivalent of four counts, which is hardly adequate for a statistically significant answer. Sixteen counts is an improvement, reducing R to 0.25, but still is not a large number of tallies. The same is true for n equals 25. When n is 100, R is 0.10, so the results should be much improved. With 400 tallies, an R of 0.05 should be quite good indeed.

Based on this qualitative analysis and the experience of Monte Carlo practitioners, Table 2.3 presents the recommended interpretation of the estimated 1σ confidence interval $\bar{x}(1 \pm R)$ for various values of R associated with an MCNP tally. These guidelines were determined empirically, based on years of experience using MCNP on a wide variety of problems. Just before the tally fluctuation charts, a "Status of Statistical Checks" table prints how many tally bins of each tally have values of R exceeding these recommended guidelines.

Point detector tallies generally require a smaller value of R for valid confidence interval statements because some contributions, such as those near the detector point, are usually extremely important and may be difficult to sample well. Experience has shown that for R less than 0.05, point detector

Table 2.3
Guidelines for Interpreting the Relative Error R^a

| Range of R | Quality of the Tally |
|--------------|---|
| 0.5 to 1 | Garbage |
| 0.2 to 0.5 | Factor of a few |
| 0.1 to 0.2 | Questionable |
| < 0.10 | Generally reliable except for point detector |
| < 0.05 | Generally reliable for point detector |

^a $R = S_{\bar{x}}/\bar{x}$ and represents the estimated statistical relative error at the 1σ level. These interpretations of R assume that all portions of the problem phase space have been well sampled by the Monte Carlo process.

results are generally reliable. For an R of 0.10, point detector tallies may only be known within a factor of a few and sometimes not that well (see the pathological example on page 2-109.)

MCNP calculates the relative error for each tally bin in the problem using Eq. (2.19b). Each x_i is defined as the total contribution from the i^{th} starting particle and all resulting progeny. This definition is important in many variance reduction methods, multiplying physical processes such as fission or (n, xn) neutron reactions that create additional neutrons, and coupled neutron/photon/electron problems. The i^{th} source particle and its offspring may thus contribute many times to a tally and all of these contributions are correlated because they are from the same source particle.

Figure 2.12 represents the MCNP process of calculating the first and second moments of each tally bin and relevant totals using three tally storage blocks of equal length for each tally bin. The hypothetical grid of tally bins in the bottom half of Fig. 2.12 has 24 tally bins including the time and energy totals. During the course of the i^{th} history, sums are performed in the first MCNP tally storage block. Some of the tally bins receive no contributions and others receive one or more contributions. At the conclusion of the i^{th} history, the sums are added to the second MCNP tally storage block. The sums in the first MCNP tally storage block are squared and added to the third tally storage block. The first tally storage block is then filled with zeros and history $i + 1$ begins. After the last history N , the estimated tally means are computed using the second MCNP tally storage block and Eq. (2.15). The estimated relative errors are calculated using the second and third MCNP tally storage blocks and Eq. (2.19b). This method of estimating the statistical uncertainty of the result produces the best estimate because the batch size is one, which minimizes the variance of the variance.^{64,65}

Note that there is no guarantee that the estimated relative error will decrease inversely proportional to the \sqrt{N} as required by the Central Limit

CHAPTER 2
Errors

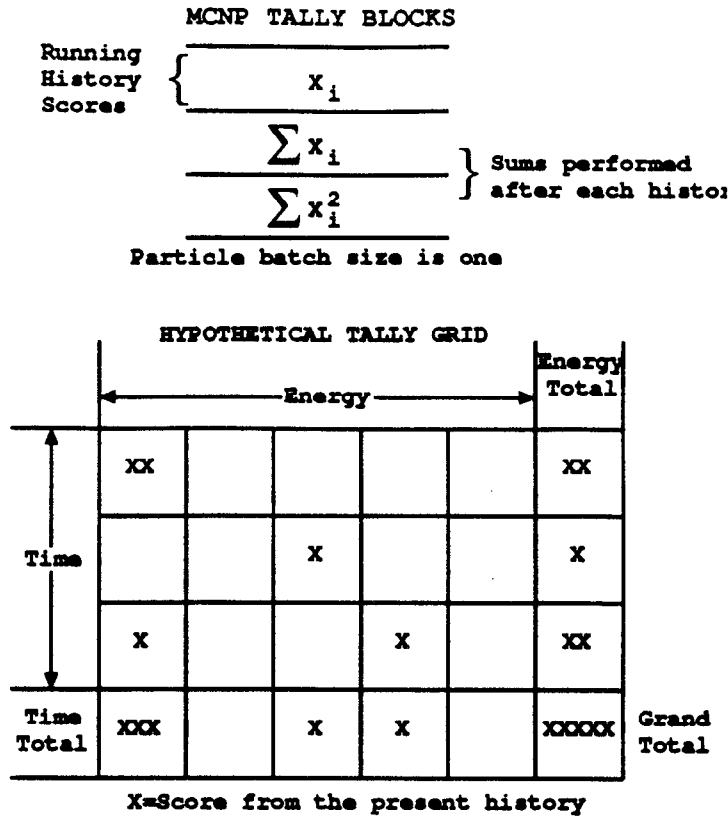


Figure 2.12

Theorem because of the statistical nature of the tallies. Early in the problem, R will generally have large statistical fluctuations. Later, infrequent large contributions may cause fluctuations in $S_{\bar{x}}$ and to a lesser extent in \bar{x} and therefore in R . MCNP calculates a FOM for one bin of each numbered tally to aid the user in determining the statistical behavior as a function of N and the efficiency of the tally.

E. MCNP Figure of Merit

The estimated relative error squared R^2 should be proportional to $1/N$, as shown by Eq. (2.19a). The computer time T used in an MCNP problem should be directly proportional to N ; therefore, R^2T should be approximately a constant within any one Monte Carlo run. It is convenient to define a figure of merit (FOM) of a tally to be

$$FOM \equiv \frac{1}{R^2T} \quad (2.21a)$$

MCNP prints the FOM for one bin of each numbered tally as a function of N , where the unit of computer time T is minutes. The table is printed in particle increments of 1000 up to 20 000 histories. Between 20 000 and 40 000 histories, the increment is doubled to 2000. This trend continues, producing a table of up to 20 entries. The default increment can be changed by the 5th entry on the PRDMP card.

The *FOM* is a very important statistic about a tally bin and should be studied by the user. It is a tally reliability indicator in the sense that if the tally is well behaved, the *FOM* should be approximately a constant with the possible exception of statistical fluctuations very early in the problem. An order-of-magnitude estimate of the expected fractional statistical fluctuations in the *FOM* is $2R$. This result assumes that both the relative statistical uncertainty in the relative error is of the order of the relative error itself and the relative error is small compared to unity. The user should always examine the tally fluctuation charts at the end of the problem to check that the *FOMs* are approximately constant as a function of the number of histories for each tally.

The numerical value of the *FOM* can be better appreciated by considering the relation

$$R = 1/\sqrt{FOM * T} \quad (2.21b)$$

Table 2.4 shows the expected value of R that would be produced in a one-minute problem ($T = 1$) as a function of the value of the *FOM*. It is clearly advantageous to have a large *FOM* for a problem because the computer time required to reach a desired level of precision is proportionally reduced. Examination of Eq. (2.21b) shows that doubling the *FOM* for a problem will reduce the computer time required to achieve the same R by a factor of two.

Table 2.4
R Values as a Function of the *FOM* for $T = 1$ Minute

| | | | | | |
|------------|-----|------|------|-------|-------|
| <i>FOM</i> | 1 | 10 | 100 | 1000 | 10000 |
| <i>R</i> | 1.0 | 0.32 | 0.10 | 0.032 | 0.010 |

In summary, the *FOM* has three uses. The most important use is as a tally reliability indicator. If the *FOM* is not approximately a constant (except for statistical fluctuations early in the problem), the confidence intervals may not overlap the expected score value, $E(x)$, the expected fraction of the time. A second use for the *FOM* is to optimize the efficiency of the Monte Carlo calculation by making several short test runs with different variance reduction parameters and then selecting the problem with the largest *FOM*. Remember that the statistical behavior of the *FOM* (i.e., R) for a small number of histories may cloud the selection of techniques competing at the same level of efficiency. A third use for the *FOM* is to estimate the computer time required to reach a desired value of R by using $T \sim 1/R^2 FOM$.

F. Separation of Relative Error into Two Components

Three factors that affect the efficiency of a Monte Carlo problem are (1) history-scoring efficiency, (2) dispersions in nonzero history scores, and (3) computer time per history. All three factors are included in the *FOM*. The first two factors control the value of R ; the third is T .

CHAPTER 2
Errors

The relative error can be separated into two components: the nonzero history-scoring efficiency component R_{eff}^2 and the intrinsic spread of the nonzero x_i scores R_{int}^2 . Defining q to be the fraction of histories producing nonzero x_i 's, Eq. 2.19b can be rewritten as

$$R = \frac{\sum_{i=1}^N x_i^2}{\left(\sum_{i=1}^N x_i\right)^2} - \frac{1}{N} = \frac{\sum_{x_i \neq 0} x_i^2}{\left(\sum_{x_i \neq 0} x_i\right)^2} - \frac{1}{N} = \frac{\sum_{x_i \neq 0} x_i^2}{\left(\sum_{x_i \neq 0} x_i\right)^2} - \frac{1}{qN} + \frac{1-q}{qN} \quad (2.22a)$$

Note by Eq. 2.19b that the first two terms are the relative error of the qN nonzero scores. Thus defining,

$$R_{int}^2 = \frac{\sum_{x_i \neq 0} x_i^2}{\left(\sum_{x_i \neq 0} x_i\right)^2} - \frac{1}{qN} \quad \text{and} \quad (2.22b)$$

$$R_{eff}^2 = (1-q)/(qN) \quad \text{yields} \quad (2.22c)$$

$$R^2 = R_{eff}^2 + R_{int}^2 \quad (2.22d)$$

For identical nonzero x_i 's, R_{int}^2 is zero and for a 100% scoring efficiency, R_{eff}^2 is zero. It is usually possible to increase q for most problems using one or more of the MCNP variance reduction techniques. These techniques alter the random walk sampling to favor those particles that produce a nonzero tally. The particle weights are then adjusted appropriately so that the expected tally is preserved. This topic is described in Sec. VII (Variance Reduction) beginning on page 2-112. The sum of the two terms of Eq. (2.22d) produces the same result as Eq. (2.19b). Both R_{int}^2 and R_{eff}^2 are printed for the tally fluctuation chart bin of each tally so that the dominant component of R can be identified as an aid to making the calculation more efficient.

These equations can be used to better understand the effects of scoring inefficiency; that is, those histories that do not contribute to a tally. Table 2.5 shows the expected values of R_{eff} as a function of q and the number of histories N . This table is appropriate for identical nonzero scores and represents the theoretical minimum relative error possible for a specified q and N . It is no surprise that small values of q require a compensatingly large number of particles to produce precise results.

Table 2.5
Expected Values of R_{eff} as a Function of q and N

| q | 0.001 | 0.01 | 0.1 | 0.5 |
|--------|-------|-------|-------|-------|
| N | | | | |
| 10^3 | 0.999 | 0.315 | 0.095 | 0.032 |
| 10^4 | 0.316 | 0.099 | 0.030 | 0.010 |
| 10^5 | 0.100 | 0.031 | 0.009 | 0.003 |
| 10^6 | 0.032 | 0.010 | 0.003 | 0.001 |

A practical example of scoring inefficiency is the case of infrequent high-energy particles in a down-scattering-only problem. If only a small fraction of all source particles has an energy in the highest energy tally bin, the dominant component of the relative error will probably be the scoring efficiency because only the high-energy source particles have a nonzero probability of contributing to the highest energy bin. For problems of this kind, it is often useful to run a separate problem starting only high-energy particles from the source and to raise the energy cutoff. The much-improved scoring efficiency will result in a much larger *FOM* for the high-energy tally bins.

To further illustrate the components of the relative error, consider the five examples of selected discrete probability density functions shown in Fig. 2.13. Cases I and II have no dispersion in the nonzero scores, cases III and IV have 100% scoring efficiency, and case V contains both elements contributing to *R*. The most efficient problem is case III. Note that the scoring inefficiency contributes 75% to *R* in case V, the second worst case of the five.

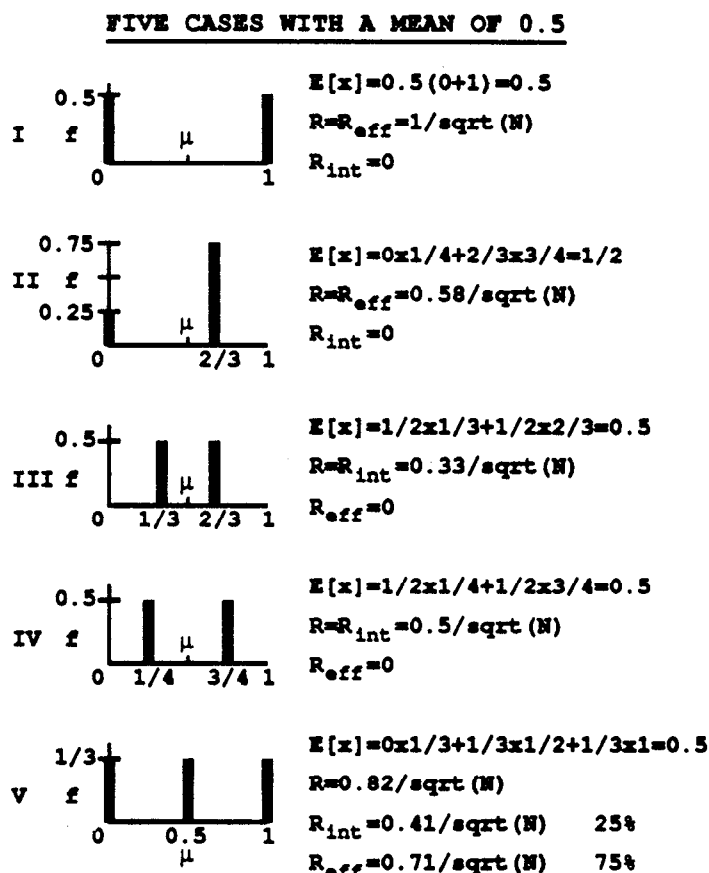


Figure 2.13

G. Variance of the Variance

Previous sections have discussed the relative error *R* and figure of merit *FOM* as measures of the quality of the mean. A quantity called the relative variance of the variance (*VOV*) is another useful tool that can assist

CHAPTER 2

Errors

the user in establishing more reliable confidence intervals. The VOV is the estimated relative variance of the estimated R. The VOV involves the estimated third and fourth moments of the empirical history score probability density function (PDF) $f(x)$ and is much more sensitive to large history score fluctuations than is R. The magnitude and NPS behavior of the VOV are indicators of tally fluctuation chart (TFC) bin convergence. Early work was done by Estes and Cashwell⁶⁴ and Pederson⁶⁶ later reinvestigated this statistic to determine its usefulness.

The VOV is a quantity that is analogous to the square of the R of the mean, except it is for R instead of the mean. The estimated relative VOV of the mean is defined as

$$VOV = S^2(S_{\bar{x}}^2)/S_{\bar{x}}^4$$

where $S_{\bar{x}}^2$ is the estimated standard deviation of \bar{x} and $S^2(S_{\bar{x}}^2)$ is the estimated variance in $S_{\bar{x}}^2$. The VOV is a measure of the relative statistical uncertainty in the estimated R and is important because S must be a good approximation of σ to use the Central Limit Theorem to form confidence intervals.

The VOV for a tally bin⁶⁶ is

$$VOV = \sum (x_i - \bar{x})^4 / (\sum (x_i - \bar{x})^2)^2 - 1/N. \quad (2.23)$$

This is the fourth central moment minus the second central moment squared normed by the product of N and the second central moment squared.

When Eq. (2.23) is expanded in terms of sums of powers of x_i , it becomes

$$VOV = \frac{\sum x_i^4 - 4 \sum x_i \sum x_i^3/N + 6 \sum x_i^2 (\sum x_i)^2/N^2 - 3(\sum x_i)^4/N^3}{(\sum x_i^2 - (\sum x_i)^2/N)^2} - \frac{1}{N}$$

or

$$VOV = \frac{\sum x_i^4 - 4 \sum x_i \sum x_i^3/N + 8 \sum x_i^2 (\sum x_i)^2/N^2 - 4(\sum x_i)^4/N^3 - (\sum x_i^2)^2/N}{(\sum x_i^2 - (\sum x_i)^2/N)^2} \quad (2.24)$$

Now consider the truncated Cauchy formula for the following analysis. The truncated Cauchy is similar in shape to some difficult Monte Carlo tallies. After numerous statistical experiments on sampling a truncated positive Cauchy distribution

$$Cauchy f(x) = 2/\pi(1+x^2), 0 \leq x \leq x_{max}, \quad (2.25)$$

it is concluded that the VOV should be below 0.1 to improve the probability of forming a reliable confidence interval. The quantity 0.1 is a convenient value and is why the VOV is used for the statistical check and not the square root of the VOV (R of the R). Multiplying numerator and denominator of Eq. (2.24) by $1/N$ converts the terms into \bar{x}^n averages and shows that the VOV is expected to decrease as $1/N$.

It is interesting to examine the VOV for the n identical history scores x ($n \ll N$) that were used to analyze R in Table 2.2, page 2–92. The VOV behaves as $1/n$ in this limit. Therefore, ten identical history scores would be enough to satisfy the VOV criterion, a factor of at least ten less than the R criterion. There are two reasons for this phenomenon: 1) it is more important to know R well than the VOV in forming confidence intervals; and 2) the history scores will ordinarily not be identical and thus the fourth moment terms in the VOV will increase rapidly over the second moment terms in R.

The behavior of the VOV as a function of N for the TFC bin is printed in the OUTF file. Because the VOV involves third and fourth moments, the VOV is a much more sensitive indicator to large history scores than the R, which is based on first and second moments. The desired VOV behavior is to decrease inversely with N . This criterion is deemed to be a necessary, but not sufficient, condition for a statistically well-behaved tally result. A tally with a VOV that matches this criteria is NOT guaranteed to produce a high quality confidence interval because undersampling of high scores will also underestimate the higher score moments.

To optionally calculate the VOV of every tally bin, put a nonzero 15th entry on the DBCN card. This option creates two additional history score moment tables each of length MXF in the TAL array to sum x_i^3 and x_i^4 (see Fig. 2.12). This option is not the default because the amount of tally storage will increase by 2/5, which could be prohibitive for a problem with many tally bins. The magnitude of the VOV in each tally bin is reported in the “Status of Statistical Checks” table. History-dependent checks of the VOV of all tally bins can be done by printing the tallies to the output file at some frequency using the PRDMP card.

H. Empirical History Score Probability Density Function $f(x)$

1. Introduction

This section discusses another statistic that is useful in assessing the quality of confidence intervals from Monte Carlo calculations. Consider a generic Monte Carlo problem with difficult to sample, but extremely important, large history scores. This type of problem produces three possible scenarios.

The first, and obviously desired, case is a correctly converged result that produces a statistically correct confidence interval. The second case is the sampling of an infrequent, but very large, history score that causes the mean and R to increase and the FOM to decrease significantly. This case is easily detectable by observing the behavior of the FOM and the R in the TFCs.

The third and most troublesome case yields an answer that appears statistically converged based on the accepted guidelines described previously, but in fact may be substantially smaller than the correct result because the large history tallies were not well sampled. This situation of too few large history tallies is difficult to detect. The following sections discuss the use of the empirical history score probability density function (PDF) $f(x)$ to gain

CHAPTER 2

Errors

insight into the TFC bin result. A pathological example to illustrate the third case follows.

2. The History Score Probability Density Function $f(x)$

A history score posted to a tally bin can be thought of as having been sampled from an underlying and generally unknown history score PDF $f(x)$, where the random variable x is the score from one complete particle history to a tally bin. The history score can be either positive or negative. The quantity $f(x)dx$ is the probability of selecting a history score between x and $x + dx$ for the tally bin. Each tally bin will have its own $f(x)$.

The most general form for expressing $f(x)$ mathematically is

$$f(x) = f_c(x) + \sum_{i=1}^n p_i \delta(x - x_i),$$

where $f_c(x)$ is the continuous nonzero part and $\sum_{i=1}^n p_i \delta(x - x_i)$ represents the n different discrete components occurring at x_i with probability p_i . An $f(x)$ could be composed of either or both parts of the distribution. A history score of zero is included in $f(x)$ as the discrete component $\delta(x - 0)$.

By the definition of a PDF,

$$\int_{-\infty}^{\infty} f(x)dx \equiv 1.$$

As discussed on page 2-87, $f(x)$ is used to estimate the mean, variance, and higher moment quantities such as the VOV.

3. The Central Limit Theorem and $f(x)$

As discussed on page 2-90, the Central Limit Theorem (CLT) states that the estimated mean will appear to be sampled from a normal distribution with a KNOWN standard deviation σ/\sqrt{N} when N approaches infinity. In practice, σ is NOT known and must be approximated by the estimated standard deviation S . The major difficulty in applying the CLT correctly to a Monte Carlo result to form a confidence interval is knowing when N has approached infinity.

The CLT requires the first two moments of $f(x)$ to exist. Nearly all MCNP tally estimators (except point detectors with zero neighborhoods in a scattering material and some exponential transform problems) satisfy this requirement. Therefore, the history score PDF $f(x)$ also exists. One can also examine the behavior of $f(x)$ for large history scores to assess if $f(x)$ appears to have been "completely" sampled. If "complete" sampling has occurred, the largest values of the sampled x 's should have reached the upper bound (if such a bound exists) or should decrease faster than $1/x^3$ so that $E(x^2) = \int_{-\infty}^{\infty} x^2 f(x)dx$ exists (σ is assumed to be finite in the CLT). Otherwise, N is assumed not to have approached infinity in the sense of the CLT. This is the basis for the use of the empirical $f(x)$ to assess Monte Carlo tally convergence.

The argument should be made that since S must be a good estimate of σ , the expected value of the fourth history score moment $E(x^4) = \int_{-\infty}^{\infty} x^4 f(x) dx$ should exist. It will be assumed that only the second moment needs to exist so that the $f(x)$ convergence criterion will be relaxed somewhat. Nevertheless, this point should be kept in mind.

4. Analytic Study of $f(x)$ for Two-State Monte Carlo Problems

Booth^{67,68} examined the distribution of history scores analytically for both an analog two-state splitting problem and two exponential transform problems. This work provided the theoretical foundation for statistical studies⁶⁹ on relevant analytic functions to increase understanding of confidence interval coverage rates for Monte Carlo calculations.

It was found that the two-state splitting problem $f(x)$ decreases geometrically as the score increases by a constant increment. This is equivalent to a negative exponential behavior for a continuous $f(x)$. The $f(x)$ for the exponential transform problem decreases geometrically with geometrically increasing x . Therefore, the splitting problem produces a linearly decreasing $f(x)$ for the history score on a lin-log plot of the score probability versus score. The exponential transform problem generates a linearly decreasing score behavior (with high score negative exponential roll off) on a log-log plot of the score probability versus score plot. In general, the exponential transform problem is the more difficult to sample because of the larger impact of the low probability high scores.

The analytic shapes were compared with a comparable problem calculated with a modified version of MCNP. These shapes of the analytic and empirical $f(x)$ s were in excellent agreement.⁶⁹

5. Proposed Uses for the Empirical $f(x)$ in Each TFC Bin

Few papers discuss the underlying or empirical $f(x)$ for Monte Carlo transport problems.⁷⁰ MCNP provides a visual inspection and analysis of the empirical $f(x)$ for the TFC bin of each tally. This analysis helps to determine if there are any unsampled regions (holes) or spikes in the empirical history score PDF $f(x)$ at the largest history scores.

The most important use for the empirical $f(x)$ is to help determine if N has approached infinity in the sense of the CLT so that valid confidence intervals can be formed. It is assumed that the underlying $f(x)$ satisfies the CLT requirements; therefore, so should the empirical $f(x)$. Unless there is a largest possible history score, the empirical $f(x)$ must eventually decrease more steeply than x^{-3} for the second moment ($\int_{-\infty}^{\infty} x^2 f(x) dx$) to exist. It is postulated⁷¹ that if such decreasing behavior in the empirical $f(x)$ with no upper bound has not been observed, then N is not large enough to satisfy the CLT because $f(x)$ has not been completely sampled. Therefore, a larger N is required before a confidence interval can be formed. It is important to note that this convergence criterion is NOT affected by any correlations that may exist between the estimated mean and the estimated R. In principle,

CHAPTER 2

Errors

this lack of correlation should make the $f(x)$ diagnostic robust in assessing “complete” sampling.

Both the analytic and empirical history score distributions suggest that large score fill-in and one or more extrapolation schemes for the high score tail of the $f(x)$ could provide an estimate of scores not yet sampled to help assess the impact of the unsampled tail on the mean. The magnitude of the unsampled tail will surely affect the quality of the tally confidence interval.

6. Creation of $f(x)$ for TFC Bins

The creation of the empirical $f(x)$ in MCNP automatically covers nearly all TFC bin tallies that a user might reasonably be expected to make, including the effect of large and small tally multipliers. A logarithmically spaced grid is used for accumulating the empirical $f(x)$ because the tail behavior is assumed to be of the form $1/x^n$, $n > 3$ (unless an upper bound for the history scores exists). This grid produces an equal width histogram straight line for $f(x)$ on a log-log plot that decreases n decades in $f(x)$ per decade increase in x .

Ten bins per x decade are used and cover the unnormalized tally range from 10^{-30} to 10^{30} . The term “unnormalized” indicates that normalizations that are not performed until the end of the problem, such as cell volume or surface area, are not included in $f(x)$. The user can multiply this range at the start of the problem by the 16th entry on the DBCN card when the range is not sufficient. Both history score number and history score for the TFC bin are tallied in the x grid.

With this x grid in place, the average empirical $f(\bar{x}_i)$ between x_i and x_{i+1} is defined to be

$$f(\bar{x}_i) = (\text{number of history scores in } i^{\text{th}} \text{ score bin}) / (N(x^{i+1} - x^i)),$$

where $x^{i+1} = 1.2589x^i$. The quantity 1.2589 is $10^{0.1}$ and comes from 10 equally spaced log bins per decade. The calculated $f(\bar{x}_i)$ s are available on printed plots or by using the “z” plot option (MC PLOT) with the TFC command mnemonics. Any history scores that are outside the x grid are counted as either above or below to provide this information to the user.

Negative history scores can occur for some electron charge deposition tallies. The MCNP default is that any negative history score will be lumped into one bin below the lowest history score in the built-in grid (the default is 1×10^{-30}). If DBCN(16) is negative, $f(-x)$ will be created from the negative scores and the absolute DBCN(16) value will be used as the score grid multiplier. Positive history scores then will be lumped into the lowest bin because of the sign change.

Figures 2.14 and 2.15 show two simple examples of empirical $f(x)$ s from MCNP for 10 million histories each. Figure 2.14 is from an energy leakage tally directly from a source that is uniform in energy from 0 to 10 MeV. The analytic $f(x)$ is a constant 0.1 between 0 and 10 MeV. The empirical $f(x)$ shows the sampling, which is 0.1 with statistical noise at the lower x bins where fewer samples are made in the smaller bins.

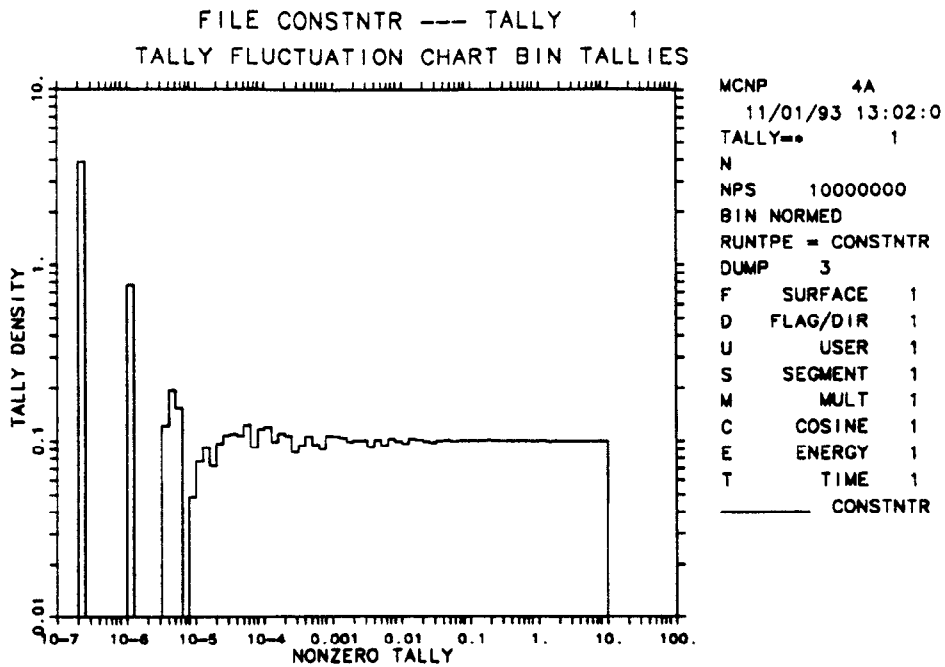


Figure 2.14

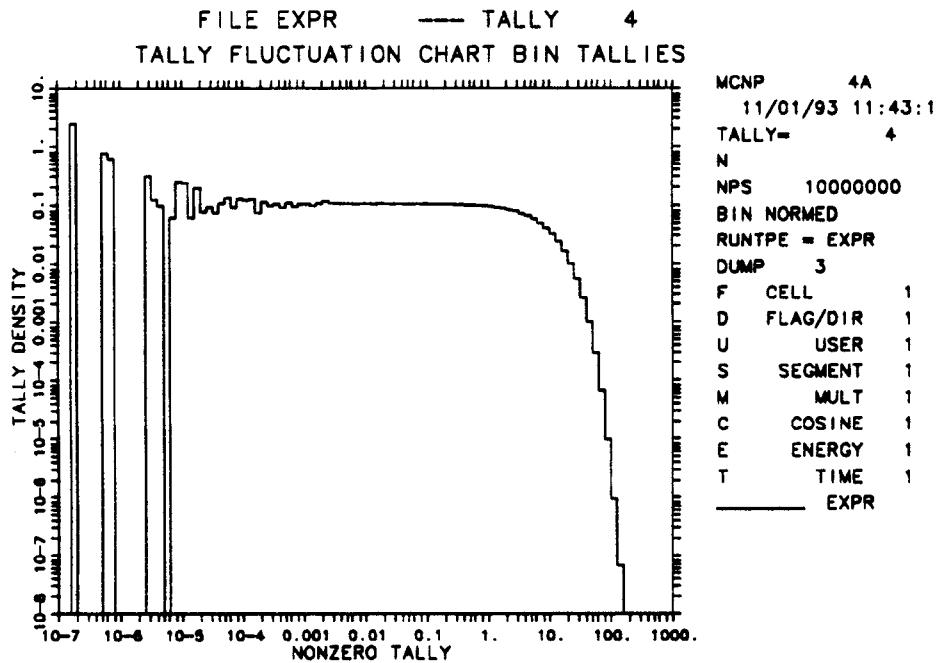


Figure 2.15

Figure 2.15 shows the sampled distance to first collision in a material that has a macroscopic cross section of about 0.1 cm^{-1} . This analytic function is a negative exponential given by $f(x) = \Sigma \exp^{-\Sigma x}$ (see page 2-26) with a mean of 10. The empirical $f(x)$ transitions from a constant 0.1 at values of x less than unity to the expected negative exponential behavior.

CHAPTER 2

Errors

7. Pareto Fit to the Largest History Scores for the TFC Bin

The slope n in $1/x^n$ of the largest history tallies x must be estimated to determine if and when the largest history scores decrease faster than $1/x^3$. The 201 largest history scores for each TFC bin are continuously updated and saved during the calculation. A generalized Pareto function⁷²

$$\text{Pareto } f(x) = a^{-1}(1 + kx/a)^{-(1/k)-1}$$

is used to fit the largest x 's. This function fits a number of extreme value distributions including $1/x^n$, exponential ($k = 0$), and constant ($k = -1$). The large history score tail fitting technique uses the robust "simplex" algorithm,⁷³ which finds the values of a and k that best fit the largest history scores by maximum likelihood estimation.

The number of history score tail points used for the Pareto fit is a maximum of 201 points because this provides about 10% precision⁷² in the slope estimator at $n = 3$. The precision increases for smaller values of n and vice versa. The number of points actually used in the fit is the lesser of 5% of the nonzero history scores or 201. The minimum number of points used for a Pareto fit is 25 with at least two different values, which requires 500 nonzero history scores with the 5% criterion. If less than 500 history scores are made in the TFC bin, no Pareto fit is made.

From the Pareto fit, the slope of $f(x_{large})$ is defined to be

$$\text{SLOPE} \equiv (1/k) + 1.$$

A SLOPE value of zero is defined to indicate that not enough $f(x_{large})$ tail information exists for a SLOPE estimate. The SLOPE is not allowed to exceed a value of 10 (a "perfect score"), which would indicate an essentially negative exponential decrease. If the 100 largest history scores all have values with a spread of less than 1%, an upper limit is assumed to have been reached and the SLOPE is set to 10. The SLOPE should be greater than 3 to satisfy the second moment existence requirement of the CLT. Then, $f(x)$ will appear to be "completely" sampled and hence N will appear to have approached infinity.

A printed plot of $f(x)$ is automatically generated in the OUTF file if the SLOPE is less than 3 (or if any of the other statistical checks described in the next section do not pass). If $0 < \text{SLOPE} < 10$, several "S's" appear on the printed plot to indicate the Pareto fit, allowing the quality of the fit to the largest history scores to be assessed visually. If the largest scores are not Pareto in shape, the SLOPE value may not reflect the best estimate of the largest history score decrease. A new SLOPE can be estimated graphically. A blank or 162 on the PRINT card also will cause printed plots of the first two cumulative moments of the empirical $f(x)$ to be made. Graphical plots of various $f(x)$ quantities can be made using the "z" plot option (MCPLLOT) with the TFC plot command. These plots should be examined for unusual behavior in the empirical $f(x)$, including holes or spikes in the tail. MCNP tries to assess both conditions and prints a message if either condition is found.

I. Forming Statistically Valid Confidence Intervals

The ultimate goal of a Monte Carlo calculation is to produce a valid confidence interval for each tally bin. Section VI has described different statistical quantities and the recommended criteria to form a valid confidence interval. Detailed descriptions of the information available in the output for all tally bins and the TFC bins are now discussed.

1. Information Available for Forming Statistically Valid Confidence Intervals for All Tally Bins

The R is calculated for every user-specified tally bin in the problem. The VOV and the shifted confidence interval center, discussed below, can be obtained for all bins with a nonzero entry for the 15th entry on the DBCN card at problem initiation.

a. R Magnitude Comparisons With MCNP Guidelines: The quality of MCNP Monte Carlo tallies historically has been associated with two statistical checks that have been the responsibility of the user: 1) for all tally bins, the estimated relative error magnitude rules-of-thumb that are shown in Fig. 2.3 (i.e., $R < 0.1$ for nonpoint detector tallies and $R < 0.05$ for point detector tallies); and 2) a statistically constant FOM in the user-selectable (TFn card) TFC bin so that the estimated R is decreasing by $1/\sqrt{N}$ as required by the CLT.

In an attempt to make the user more aware of the seriousness of checking these criteria, MCNP provides checks of the R magnitude for all tally bins. A summary of the checks is printed in the "Status of Statistical Checks" table. Messages are provided to the user giving the results of these checks.

b. Asymmetric Confidence Intervals: A correlation exists between the estimated mean and the estimated uncertainty in the mean.⁶⁶ If the estimated mean is below the expected value, the estimated uncertainty in the mean $S_{\bar{x}}$ will most likely be below its expected value. This correlation is also true for higher moment quantities such as the VOV. The worst situation for forming valid confidence intervals is when the estimated mean is much smaller than the expected value, resulting in smaller than predicted coverage rates. To correct for this correlation and improve coverage rates, one can estimate a statistic shift in the midpoint of the confidence interval to a higher value. The estimated mean is unchanged.

The shifted confidence interval midpoint is the estimated mean plus a term proportional to the third central moment. The term arises from an Edgeworth expansion⁶⁶ to attempt to correct the confidence interval for non-normality effects in the estimate of the mean. The adjustment term is given by

$$SHIFT = \sum (x_i - \bar{x})^3 / (2S^2N).$$

Substituting for the estimated mean and expanding produces

$$SHIFT = \left(\sum x_i^3 - 3 \sum x_i^2 \sum x_i / N + 2 \left(\sum x_i \right)^3 / N^2 \right) / \left(2 \left(N \sum x_i^2 - \left(\sum x_i \right)^2 \right) \right).$$

CHAPTER 2

Errors

The *SHIFT* should decrease as $1/N$. This term is added to the estimated mean to produce the midpoint of the now asymmetric confidence interval about the mean. This value of the confidence interval midpoint can be used to form the confidence interval about the estimated mean to improve coverage rates of the true, but unknown, mean $E(x)$. The estimated mean plus the *SHIFT* is printed automatically for the TFC bin for all tallies. A nonzero entry for the 15th DBCN card entry produces the shifted value for all tally bins.

This correction approaches zero as N approaches infinity, which is the condition required for the CLT to be valid. Kalos⁷⁴ uses a slightly modified form of this correction to determine if the requirements of the CLT are “substantially satisfied”. His relation is

$$|\sum(x_i - \bar{x})^3| \ll S^3\sqrt{N},$$

which is equivalent to

$$SHIFT \ll S_{\bar{x}}/2.$$

The user is responsible for applying this check.

c. Forming Valid Confidence Intervals for Non-TFC Bins: The amount of statistical information available for non-TFC bins is limited to the mean and R. The VOV and the center of the asymmetric confidence can be obtained for all tally bins with a nonzero 15th entry on the DBCN card in the initial problem. The magnitude criteria for R (and the VOV, if available) should be met before forming a confidence interval. If the shifted confidence interval center is available, it should be used to form asymmetric confidence intervals about the estimated mean.

History dependent information about R (and the VOV, if available) for non-TFC bins can be obtained by printing out the tallies periodically during a calculation using the PRDMP card. The N -dependent behavior of R can then be assessed. The complete statistical information available can be obtained by creating a new tally and selecting the desired tally bin with the TFn card.

2. Information Available for Forming Statistically Valid Confidence Intervals for TFC Bins

Additional information about the statistical behavior of each TFC bin result is available. A TFC bin table is produced by MCNP after each tally to provide the user with detailed information about the apparent quality of the TFC bin result. The contents of the table are discussed in the following subsections, along with recommendations for forming valid confidence intervals using this information.

a. TFC Bin Tally Information: The first part of the TFC bin table contains information about the TFC bin result including the mean, R, scoring efficiency, the zero and nonzero history score components of R (see page

2-95), and the shifted confidence interval center. The two components of R can be used to improve the problem efficiency by either improving the history scoring efficiency or reducing the range of nonzero history scores.

b. The Largest TFC Bin History Score Occurs on the Next History:

There are occasions when the user needs to make a conservative estimate of a tally result. Conservative is defined so that the results will not be less than the expected result. One reasonable way to make such an estimate is to assume that the largest observed history score would occur again on the very next history, $N + 1$.

MCNP calculates new estimated values for the mean, R , VOV, FOM, and shifted confidence interval center for the TFC bin result for this assumption. The results of this proposed occurrence are summarized in the TFC bin information table. The user can assess the impact of this hypothetical happening and act accordingly.

c. Description of the 10 Statistical Checks for the TFC Bin: MCNP prints the results of ten statistical checks of the tally in the TFC bin at each print. In a "Status of Statistical Checks" table, the results of these ten checks are summarized at the end of the output for all TFC bin tallies. The quantities involved in these checks are the estimated mean, R , VOV, FOM, and the large history score behavior of $f(x)$. Passing all of the checks should provide additional assurance that any confidence intervals formed for a TFC bin result will cover the expected result the correct fraction of the time. At a minimum, the results of these checks will provide the user with more information about the statistical behavior of the result in the TFC bin of each tally.

The following 10 statistical checks are made on the TFCs printed at the end of the output for desirable statistical properties of Monte Carlo solutions:

MEAN

- (1) a nonmonotonic behavior (no up or down trend) in the estimated mean as a function of the number histories N for the last half of the problem;

R

- (2) an acceptable magnitude of the estimated R of the estimated mean (< 0.05 for a point detector tally or < 0.10 for a non-point detector tally);
- (3) a "monotonically" decreasing R as a function of the number histories N for the last half of the problem;
- (4) a $1/\sqrt{N}$ decrease in the R as a function of N for the last half of the problem;

VOV

- (5) the magnitude of the estimated VOV should be less than 0.10 for all types of tallies;
- (6) a "monotonically" decreasing VOV as a function of N for the last half of the problem;
- (7) a $1/N$ decrease in the VOV as a function of N for the last half of the problem;

CHAPTER 2

Errors

FOM

- (8) a statistically constant value of the FOM as a function of N for the last half of the problem;
- (9) a non-monotonic behavior in the FOM as a function of N for the last half of the problem; and

$f(x)$

- (10) the SLOPE (see page 2-104) of the 25 to 201 largest positive (negative with a negative DBCN(16) entry) history scores x should be greater than 3.0 so that the second moment $\int_{-\infty}^{\infty} x^2 f(x) dx$ will exist if the SLOPE is extrapolated to infinity.

The seven N -dependent checks for the TFC bin are for the last half of the problem. The last half of the problem should be well behaved in the sense of the CLT to form the most valid confidence intervals. "Monotonically decreasing" in checks 3 and 5 allows for some increases in both R and the VOV. Such increases in adjacent TFC entries are acceptable and usually do not, by themselves, cause poor confidence intervals. A TFC bin R that does not pass check 3, by definition in MCNP, does not pass check 4. Similarly, a TFC bin VOV that does not pass check 6, by definition, does not pass check 7.

A table is printed after each tally for the TFC bin result that summarizes the results and the pass or no pass status of the checks. Both asymmetric and symmetric confidence intervals are printed for the one, two, and three σ levels when all of the statistical checks are passed. These intervals can be expected to be correct with improved probability over historical rules of thumb. This is NOT A GUARANTEE, however; there is always a possibility that some as-yet-unsampled portion of the problem would change the confidence interval if more histories were calculated. A WARNING is printed if one or more of these ten statistical checks is not passed, and one page of printed plot information about $f(x)$ is produced for the user to examine.

An additional information-only check is made on the largest five $f(x)$ score grid bins to determine if there are bins that have no samples or if there is a spike in an $f(x)$ that does not appear to have an upper limit. The result of the check is included in the TFC summary table for the user to consider. This check is not a pass or no pass test because a hole in the tail may be appropriate for a discrete $f(x)$ or an exceptional sample occurred with so little impact that none of the ten checks was affected. The empirical $f(x)$ should be examined to assess the likelihood of "complete" sampling.

d. Forming Valid TFC Bin Confidence Intervals: For TFC bin results, the highest probability of creating a valid confidence interval occurs when all of the statistical checks are passed. Not passing several of the checks is an indication that the confidence interval is less likely to be correct. A monotonic trend in the mean for the last half of the problem is a strong indicator that the confidence interval is likely to produce incorrect coverage rates. The magnitudes of R and the VOV should be less than the recommended values to increase the likelihood of a valid confidence interval. Small jumps in the R , VOV, and/or the FOM as a function of N are not threat-

ening to the quality of a result. The slope of $f(x)$ is an especially strong indicator that N has not approached infinity in the sense of the CLT. If the slope appears too shallow (< 3), check the printed plot of $f(x)$ to see that the estimated Pareto fit is adequate. The use of the shifted confidence interval is recommended, although it will be a small effect for a well-converged problem.

The last half of the problem is determined from the TFC. The more information available about the last half of the problem, the better the N -dependent checks will be. Therefore, a problem that has run 40,000 histories will have 20 TFC N entries, which is more N entries than a 50,000 history problem with 13 entries. It is possible that a problem that passes all tests at 40,000 may not pass all the tests at 40,001. As is always the case, the user is responsible for deciding when a confidence interval is valid. These statistical diagnostics are designed to aid in making this decision.

J. A Statistically Pathological Output Example

A statistically pathological test problem is discussed in this section. The problem calculates the surface neutron leakage flux above 12 MeV from an isotropic 14 MeV neutron point source of unit strength at the center of a 30 cm thick concrete shell with an outer radius of 390 cm. Point and ring detectors were deliberately used to estimate the surface neutron leakage flux with highly inefficient, long-tailed $f(x)$ s. The input is shown on page 5–50 if you want to run this problem yourself.

The variance reduction methods used were implicit capture with weight cutoff, low-score point detector Russian roulette, and a 0.5 mean free path (4 cm) neighborhood around the detectors to produce large, but finite, higher moments. Other tallies or variance reduction methods could be used to make this calculation much more efficient, but that is not the object of this example. A surface flux estimator would have been over a factor of 150 to 30,000 times more efficient than ring and point detectors, respectively.

Figure 2.16 shows MCNP plots of the estimated mean, R, VOV and slope of the history score PDF as a function of N values of 20,000 (left column) and 5 million (right column). The ring detector results are shown as the solid line and the point detector result is the dashed line.

Column 1 shows the results as a function of N for 20,000 histories. The point detector result at 14,000 histories (not shown) was 1.41×10^{-8} n/cm²/s ($R=0.041$). The FOM varied somewhat randomly between about 800 and 1160 for the last half of the problem. With no other information, this result could be accepted by even a careful Monte Carlo practitioner. However, the VOV never gets close to the required 0.1 value and the slope of the unbounded $f(x)$ is less than 1.4. This slope could not continue indefinitely because even the mean of $f(x)$ would not exist. Therefore, a confidence interval should not be formed for this tally. At 20,000 histories, R increases substantially and the FOM crashes, indicating serious problems with the result.

The ring detector result is having problems of its own. The ring detector result for 14,000 histories was 4.60×10^{-8} n/cm²/s ($R=0.17$, $VOV=0.35$,

CHAPTER 2
Errors

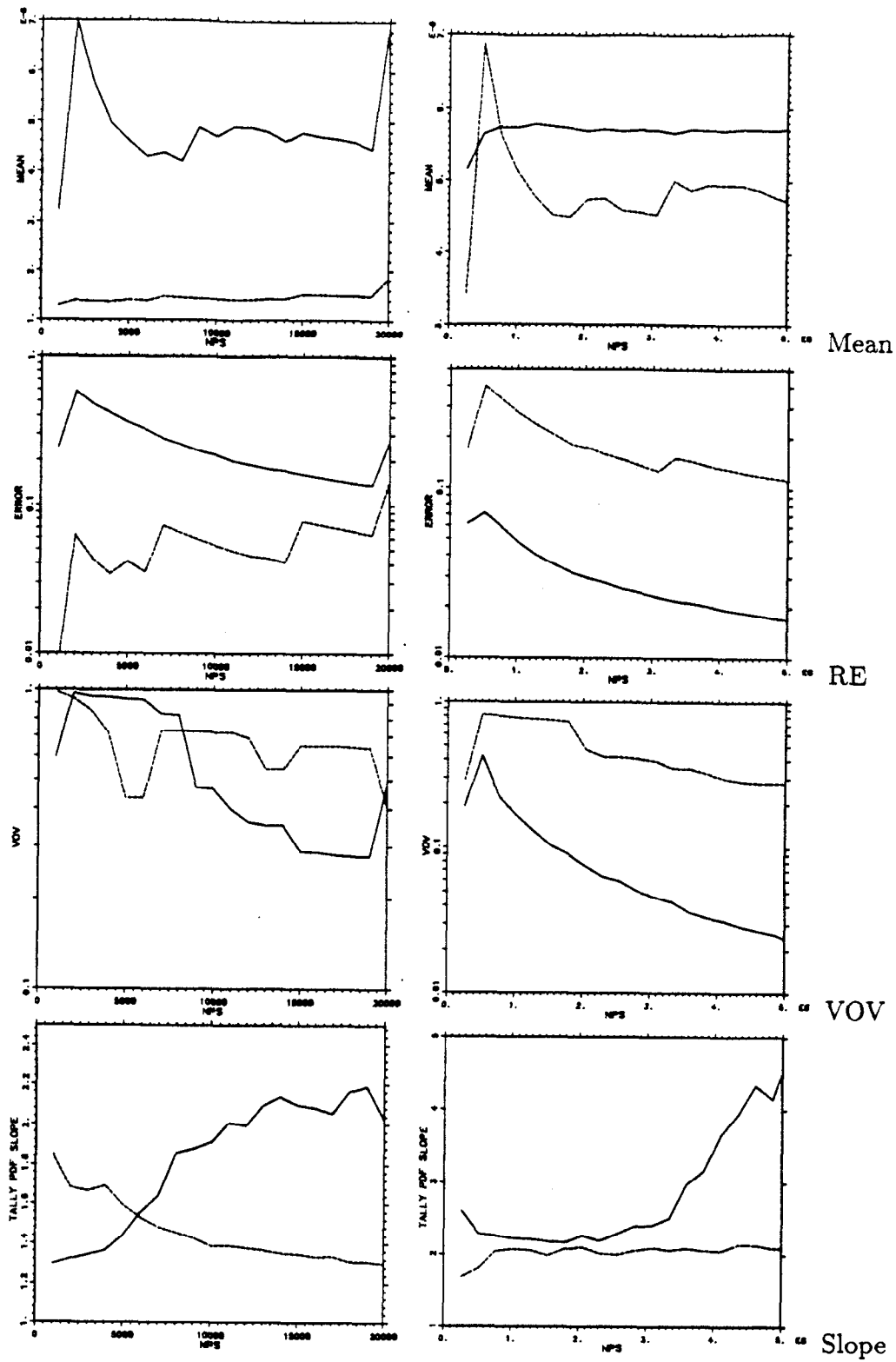


Figure 2.16

slope=2.1, FOM=67). None of the plotted quantities satisfies the required convergence criteria.

The correct detector result, obtained from a 5 million history ring detector tally, is 5.72×10^{-8} n/cm²/s (R=0.0169, VOV=0.023, slope=4.6, FOM=19). The apparently converged 14,000 history point detector result is a factor of four below the correct result!

If you were to run 200,000 histories, you would see the point detector result increasing to 3.68×10^{-8} n/cm²/s (R=0.20, VOV=0.30, slope=1.6, FOM=1.8). The magnitudes of R and the VOV are much too large for the point detector result to be accepted. The slope of $f(x)$ is slowly increasing, but has only reached a value of 1.6. This slope is still far too shallow compared to the required value of 3.0.

The ring detector result of 5.06×10^{-8} n/cm²/s (R=0.0579, VOV=0.122, slope=2.8, FOM=22) at 192,000 histories is interesting. All of these values are close to being acceptable, but just miss the requirements. The ring detector result is more than two estimated standard deviations below the correct result.

Column 2 shows the results as a function of N for 5 million histories. The ring detector result of 5.72×10^{-8} n/cm²/s (R=0.0169, VOV=0.023, slope=4.6, FOM=19) now appears very well behaved in all categories. This tally passed all 10 statistical checks. There appears to be no reason to question the validity of this tally. The point detector result is 4.72×10^{-8} n/cm²/s (R=0.11, VOV=0.28, slope=2.1, FOM=0.45). The result is clearly improving, but does not meet the acceptable criteria for convergence. This tally did not pass 3 out 10 statistical checks.

When you compare the empirical point detector $f(x)$ s for 14,000 and 200 million histories you see that the 14,000 history $f(x)$ clearly has unsampled regions in the tail, indicating incomplete $f(x)$ sampling.⁷¹ For the point detector, seven decades of x have been sampled by 200 million histories compared to only three decades for 14,000 histories. The largest x 's occur from the extremely difficult to sample histories that have multiple small energy loss collisions close to the detector. The 200 million history point detector result is 5.41×10^{-8} n/cm²/s (R=0.035, VOV=0.60, slope=2.4, FOM=0.060). The point detector $f(x)$ slope is increasing, but still is not yet completely sampled. This tally did not pass 6 of 10 checks with 200 million histories. The result is about 1.5 estimated standard deviations below the correct answer. It is important to note that calculating a large number of histories DOES NOT guarantee a precise result. The more compact empirical ring $f(x)$ for 20 million histories appears to be completely sampled because of the large slope.

For difficult to sample problems such as this example, it is possible that an even larger history score could occur that would cause the VOV and possibly the slope to have unacceptable values. The mean and RE will be much less affected than the VOV. The additional running time required to reach acceptable values for the VOV and the slope could be prohibitive. The large history score should NEVER be discarded from the tally result. It is impor-

CHAPTER 2

Variance Reduction

tant that the cause for the large history score be completely understood. If the score was created by a poorly sampled region of phase space, the problem should be modified to provide improved phase space sampling. It is also possible that the large score was created by an extremely unlikely set of circumstances that occurred "early" in the calculation. In this situation, if the RE is within the guidelines, the empirical $f(x)$ appears to be otherwise completely sampled, and the largest history score appears to be a once in a lifetime occurrence, a good confidence interval can still be formed. If a conservative (large) answer is required, the printed result that assumes the largest history score occurs on the very next history can be used.

Comparing several empirical $f(x)$ s for the above problem with 200 million histories that have been normalized so that the mean of each $f(x)$ is unity, you see that the point detector at 390 cm clearly is quite Cauchy-like (see Eq. (2.25) for many decades.⁷⁰ The point detector at 4000 cm is a much easier tally (by a factor of 10,000) as exhibited by the much more compact empirical $f(x)$. The large-score tail decreases in a manner similar to the negative exponential $f(x)$. The surface flux estimator is the most compact $f(x)$ of all. The blip on the high-score tail is caused by the average cosine approximation of 0.05 between cosines of 0 and 0.1 (see page 2-70). This tally is 30,000 times more efficient than the point detector tally.

VII. VARIANCE REDUCTION

A. General Considerations

1. Variance Reduction and Accuracy

Variance-reducing techniques in Monte Carlo calculations reduce the computer time required to obtain results of sufficient precision. Note that precision is only one requirement for a good Monte Carlo calculation. Even a zero variance calculation cannot accurately predict natural behavior if other sources of error are not minimized. Factors affecting accuracy were discussed in Section VI beginning on page 2-86.

2. Two Choices That Affect Efficiency

The efficiency of a Monte Carlo calculation is affected by two choices, tally type and random walk sampling. The tally choice (for example, point detector flux tally vs surface crossing flux tally) amounts to trying to obtain the best results from the random walks sampled. The chosen random walk sampling amounts to preferentially sampling "important" random walks at the expense of "unimportant" random walks. (A random walk is important if it has a large affect on a tally.) These two choices usually affect the time per history and the history variance as described in Sec. 3 below.

MCNP estimates tallies of the form

$$\langle T \rangle = \int d\vec{r} \int d\vec{v} \int dt N(\vec{r}, \vec{v}, t) T(\vec{r}, \vec{v}, t)$$

Correlated sampling should not be confused with more elaborate Monte Carlo perturbation schemes that calculate differences and their variances directly. MCNP has no such scheme at present.

VIII. CRITICALITY CALCULATIONS

Nuclear criticality, the ability to sustain a chain reaction by fission neutrons, is characterized by k_{eff} , the eigenvalue to the neutron transport equation. In reactor theory, k_{eff} is thought of as the ratio between the number of neutrons in successive generations, with the fission process regarded as the birth event that separates generations of neutrons.⁸⁰ For critical systems, $k_{eff} = 1$ and the chain reaction will just sustain itself. For subcritical systems, $k_{eff} < 1$ and the chain reaction will not sustain itself. For supercritical systems, $k_{eff} > 1$ and the number of fissions in the chain reaction will increase with time. In addition to the geometry description and material cards, all that is required to run a criticality problem is a KCODE card, described below, and an initial spatial distribution of fission points using either the KSRC card, the SDEF card, or an SRCTP file.

Calculating k_{eff} consists of estimating the mean number of fission neutrons produced in one generation per fission neutron started. A generation is the life of a neutron from birth in fission to death by escape, parasitic capture, or absorption leading to fission. In MCNP, the computational equivalent of a fission generation is a k_{eff} cycle; i.e., a cycle is a computed estimate of an actual fission generation. Processes such as $(n, 2n)$ and $(n, 3n)$ are considered internal to a cycle and do not act as termination. Because fission neutrons are terminated in each cycle to provide the fission source for the next cycle, a single history can be viewed as continuing from cycle to cycle. The effect of the delayed neutrons is included by using the total $\bar{\nu}$. The spectrum of delayed neutrons is assumed to be the same as neutrons from prompt fission. MCNP uses three different estimators for k_{eff} . We recommend using, for the final k_{eff} result, the statistical combination of all three.⁸¹

It is extremely important to emphasize that the result from a criticality calculation is a confidence interval for k_{eff} that is formed using the final estimated k_{eff} and the estimated standard deviation. A properly formed confidence interval from a valid calculation should include the true answer the fraction of time used to define the confidence interval. There will always be some probability that the true answer lies outside of a confidence interval.

Reference 92 is an introduction to using MCNP for criticality calculations, focusing on the unique aspects of setting up and running a criticality problem and interpreting the results. A quickstart chapter gets the new MCNP user on the computer running a simple criticality problem as quickly as possible.

A. Criticality Program Flow

Because the calculation of k_{eff} entails running successive fission cycles, criticality calculations have a different program flow than MCNP fixed source

CHAPTER 2

KCODE

problems. They require a special criticality source that is incompatible with the surface source and user-supplied sources. Unlike fixed source problems, where the source being sampled throughout the problem never changes, the criticality source changes from cycle to cycle.

1. Criticality Problem Definition

To set up a criticality calculation, the user initially supplies an INP file that includes the KCODE card with the following information:

- a) the nominal number of source histories, N , per k_{eff} cycle;
- b) an initial guess of k_{eff} ;
- c) the number of source cycles, I_c , to skip before k_{eff} accumulation;
- d) the total number of cycles, I_t , in the problem.

Other KCODE entries are discussed in Chapter 3, page 3–57. The initial spatial distribution of fission neutrons can be entered by using (1) the KSRC card with sets of x, y, z point locations, (2) the SDEF card to define points uniformly in volume, or (3) a file (SRCTP) from a previous MCNP criticality calculation. If the SDEF card is used, the default WGT value should not be changed. Any KSRC points in geometric cells that are void or have zero importance are rejected. The remaining KSRC points are duplicated or rejected enough times so the total number of points M in the source spatial distribution is approximately the nominal source size N . The energy of each source particle for the first k_{eff} cycle is selected from a generic Watt thermal fission distribution if it is not available from the SRCTP file.

2. Particle Transport for Each k_{eff} Cycle

In each k_{eff} cycle, M source particles are started isotropically. For the first cycle, these M points come from one of three user selected source possibilities. For subsequent cycles, these points are the ones written at collision sites from neutron transport in the previous cycle. The weight of each source particle is N/M , so all normalizations occur as if N rather than M particles started in each cycle.

Source particles are transported through the MCNP geometry by the standard random walk process, except that fission is treated as capture, either analog or implicit as defined on the PHYS:N card. At each collision point the following four steps are performed for the cycle:

- 1) the prompt neutron lifetimes by absorption and collision estimates are accumulated;
- 2) if fission is possible, the three k_{eff} estimates are accumulated; and
- 3) if fission is possible, $n \geq 0$ fission sites (including the sampled outgoing energy of the fission neutron) at each collision are stored for use as source points in the next cycle,

where $n = W\bar{\nu}(\sigma_f/\sigma_t)(1/k_{eff}) + \text{random number}$;

W = particle weight (before implicit capture weight reduction or analog capture);

$\bar{\nu}$ = average number of neutrons produced by fission at the

incident energy of this collision, with either prompt $\bar{\nu}$ or total $\bar{\nu}$ (default) used;

σ_f = microscopic material fission cross section;

σ_t = microscopic material total cross section; and

k_{eff} = estimated collision k_{eff} from previous cycle.

For first cycle, the second KCODE card entry.

$M = \sum n$ = number of fission source points to be used in next cycle. The number of fission sites n stored at each collision is rounded up or down to an integer (including zero) with a probability proportional to its closeness to that integer. If the initial guess of k_{eff} is too low or too high, the number of fission sites written as source points for the next cycle will be, respectively, too high or too low relative to the desired nominal number N . A bad initial guess of k_{eff} causes only this consequence.

A very poor initial guess for the spatial distribution of fissions can cause the first cycle estimate of k_{eff} to be extremely low. This situation can occur when only a fraction of the fission source points enter a cell with a fissionable material. As a result, one of two error messages can be printed: (1) no new source points were generated, or (2) the new source has overrun the old source. The second message occurs when the MCNP storage for the fission source points is exceeded because the small k_{eff} that results from a poor initial source causes n to become very large.

The fission energy of the next-cycle neutron is sampled separately for each source point and stored for the next cycle. It is sampled from the same distributions as fissions would be sampled in the random walk based on the incident neutron energy and fissionable isotope. The geometric coordinates and cell of the fission site are also stored.

- 4) The collision nuclide and reaction are sampled (after steps 1, 2, and 3) but the fission reaction is not allowed to occur because fission is treated as capture. The fission neutrons that would have been created are accrued in three different ways to estimate k_{eff} for this cycle.

3. k_{eff} Cycle Termination

At the end of each k_{eff} cycle, a new set of M source particles has been written from fissions in that cycle. The number M varies from cycle to cycle but the total starting weight in each cycle is a constant N . These M particles are written to the SRCTP file at certain cycle intervals. The SRCTP file can be used as the initial source in a subsequent criticality calculation with a similar, though not necessarily identical, geometry. Also, k_{eff} quantities are accumulated, as is described below.

The first I_c cycles in a criticality calculation are inactive cycles, where the spatial source changes from the initial definition to the correct distribution for the problem. No k_{eff} or tally information is accrued for inactive cycles. I_c is an input parameter on the KCODE card for the number of k_{eff} cycles to be skipped before k_{eff} and tally accumulation. After the first I_c cycles, the fission source spatial distribution is assumed to have achieved equilibrium,

CHAPTER 2 KCODE

active cycles begin, and k_{eff} and tallies are accumulated. Cycles are run until either a time limit is reached or the total cycles on the KCODE card in the problem have been completed.

B. Estimation of k_{eff} Confidence Intervals and Prompt Neutron Lifetimes

The criticality eigenvalue k_{eff} and various prompt neutron lifetimes, along with their standard deviations, are automatically estimated in every criticality calculation in addition to any user-requested tallies. k_{eff} and the lifetimes are estimated for every active cycle, as well as averaged over all active cycles. k_{eff} is estimated in three different ways; the lifetimes are estimated in two ways. These estimates are combined⁸¹ using observed statistical correlations to provide the optimum final estimate of k_{eff} and its standard deviation.

It is known⁸² that the power iteration method with a fixed source size produces a very small negative bias Δk_{eff} in k_{eff} that is proportional to $1/N$. This bias is negligible⁸² for all practical problems where N is greater than about 200 neutrons per cycle and as long as too many active cycles are not used. It has been shown⁸² that this bias is less, probably much less, than one-half of one standard deviation for 400 active cycles when the ratio of the true k_{eff} standard deviation to k_{eff} is 0.0025 at the problem end.

1. Collision Estimators

The collision estimate for k_{eff} for any active cycle is:

$$k_{eff}^C = \frac{1}{N} \sum_i W_i \left[\frac{\sum_k f_k \bar{\nu}_k \sigma_{Fk}}{\sum_k f_k \sigma_{Tk}} \right],$$

where i is summed over all collisions in a cycle where fission is possible;

k is summed over all isotopes of the material involved in the i^{th} collision;

σ_{Tk} = total microscopic cross section;

σ_{Fk} = microscopic fission cross section;

$\bar{\nu}_k$ = average number of prompt or total neutrons produced per fission by the collision isotope at the incident energy;

f_k = atomic fraction for nuclide k ;

N = nominal source size for cycle; and

W_i = weight of particle entering collision.

Because W_i represents the number of neutrons entering the i^{th} collision,

$$W_i \left[\frac{\sum_k f_k \bar{\nu}_k \sigma_{Fk}}{\sum_k f_k \sigma_{Tk}} \right]$$

is the expected number of neutrons to be produced from all fission processes in the collision. Thus k_{eff}^C is the mean number of fission neutrons produced per cycle. The collision estimator tends to be best, sometimes only marginally so, in very large systems.

The collision estimate of the removal lifetime for any active cycle is

$$R_c = \frac{1}{N} \left[\sum_i W_i T_i \left[\frac{\sum_k f_k (\sigma_{A_k} + \sigma_{F_k})}{\sum_k f_k \sigma_{T_k}} \right] + \sum W_e T_e \right] ,$$

where σ_{A_k} is the microscopic absorption cross section excluding fission, T_i is the time from birth of the particle to the collision, W_e is the weight from particle birth to escape, summed over histories that escape, and T_e is elapsed time from particle birth to escape, summed over histories that escape.

The removal lifetime is simply the average time required for a fission source neutron to be removed from the system by either absorption, fission, or escape. The absorption, fission, or escape lifetimes are similar, except the time for each designated process is used.

2. Absorption Estimators

The absorption estimators for k_{eff} are made when a neutron interacts with a fissionable isotope. The estimators differ for analog capture and implicit capture. For analog capture,

$$k_{eff}^A = \frac{1}{N} \sum_i W_i \bar{\nu}_k \frac{\sigma_{F_k}}{\sigma_{A_k} + \sigma_{F_k}} ,$$

where i is summed over each analog capture event in the k^{th} isotope. Note that in analog capture, the weight is the same both before and after the collision. Because analog capture includes fission in criticality calculations, the frequency of analog capture at each collision with isotope k is $(\sigma_{A_k} + \sigma_{F_k})/\sigma_{T_k}$. The analog absorption k_{eff} estimate is very similar to the collision estimator of k_{eff} except that only the k^{th} absorbing nuclide, as sampled in the collision, is used rather than averaging over all nuclides.

For implicit capture, the following is accumulated:

$$k_{eff}^A = \frac{1}{N} \sum_i W'_i \bar{\nu}_k \frac{\sigma_{F_k}}{\sigma_{A_k} + \sigma_{F_k}} ,$$

where i is summed over all collisions in which fission is possible and $W'_i = W_i(\sigma_{A_k} + \sigma_{F_k})/\sigma_{T_k}$ is the weight absorbed in the implicit capture. The difference between the implicit absorption estimator k_{eff}^A and the collision estimator k_{eff}^C is that only the nuclide involved in the collision is used for the absorption k_{eff} estimate rather than an average of all nuclides in the material for the collision k_{eff} estimator.

The absorption estimator with analog capture is likely to produce the smallest statistical uncertainty of the three for systems where the ratio $\bar{\nu}_k \sigma_{F_k}/(\sigma_{A_k} + \sigma_{F_k})$ is nearly constant. Such would be the case for a thermal system with a dominant fissile isotope such that the 1/velocity cross section variation would tend to cancel.

CHAPTER 2

KCODE

For analog capture, the absorption removal lifetime is accumulated as $R_A = (1/N) \sum_i W_i T_i$ at analog capture events and system leakage. For implicit capture, the absorption removal lifetime is accumulated as $R_A = (1/N) \sum_i W_i' T_i$ at all collisions and system leakage, using the appropriate time.

3. Track Length Estimator of k_{eff}

The track length estimator of k_{eff} is accumulated every time the neutron traverses a distance d in a fissionable material cell:

$$k_{eff}^{TL} = \frac{1}{N} \sum_i W_i \rho d \sum_k f_k \bar{v}_k \sigma_{Fk} \quad ,$$

where i is summed over all neutron trajectories,

ρ is the atomic density in the cell, and

d is the trajectory track length from the last event.

Because $\rho d \sum_k f_k \bar{v}_k \sigma_{Fk}$ is the expected number of fission neutrons produced along trajectory d , k_{eff}^{TL} is a third estimate of the mean number of fission neutrons produced in a cycle per nominal fission source neutron.

The track length estimator tends to display the lowest variance for optically thin fuel cells (e.g., plates) and fast systems where large cross-section variations because of resonances may cause high variances in the other two estimators.

There is no track length estimator for neutron lifetimes.

4. Combined k_{eff} Estimators

MCNP provides a number of combined k_{eff} estimators that are combinations of the three individual k_{eff} estimators using two at a time or all three. The combined k_{eff} s are computed by using a maximum likelihood estimate, as outlined by Halperin⁸³ and discussed further by Urbatsch.⁸¹ This technique, which is a generalization of the inverse variance weighting for uncorrelated estimators, produces the maximum likelihood estimate for the combined average k_{eff} , which, for multivariate normality, is the almost-minimum variance estimate. It is "almost" because the covariance matrix is not known exactly and must be estimated. The three-combined k_{eff} estimator is the best final estimate from an MCNP calculation.⁸¹

This method of combining estimators can exhibit one feature that is disconcerting: sometimes (usually with highly positively correlated estimators) the combined estimate will lie outside the interval defined by the two or three individual average estimates. Statisticians at Los Alamos have shown⁸¹ that this is the best estimate to use for a final k_{eff} value. Reference 81 shows the results of one study of 500 samples from three highly positively correlated normal distributions, all with a mean of zero. In 319 samples, all three estimators fell on the same side of the expected value. This type of behavior occurs with high positive correlation because if one estimator is above or below the expected value, the others have a good probability of being on the

same side of the expected value. The advantage of the three-combined estimator is that the Halperin algorithm correctly predicts that the true value will lie outside of the range.

5. k_{eff} Error Estimation and Estimator Combination

After the first I_c inactive cycles, during which the fission source spatial distribution is allowed to come into spatial equilibrium, MCNP begins to accumulate the estimates of k_{eff} and the prompt neutron lifetimes with those estimates from previous active (after the inactive) cycles. The relative error R of each quantity is estimated in the usual way as

$$R = \frac{1}{\bar{x}} \sqrt{\frac{\overline{x^2} - \bar{x}^2}{M - 1}}$$

where M = the number of active cycles,

$$\bar{x} = \frac{1}{M} \sum_m x_m, \quad \text{and} \quad \overline{x^2} = \frac{1}{M} \sum_m x_m^2,$$

where x_m = a quantity, such as k_{eff}^C , from cycle m . This assumes that the cycle-to-cycle estimates of each k_{eff} are uncorrelated. This assumption generally is good for k_{eff} , but not for the eigenfunction (fluxes) of optically large systems.⁸⁴

MCNP also combines the three estimators in all possible ways and determines the covariance and correlations. The simple average of two estimators is defined as $x^{ij} = (1/2)(x^i + x^j)$, where, for example, x^i may be the collision estimator k_{eff}^C and x^j may be the absorption estimator k_{eff}^A .

The "combined average" of two estimators is weighted by the covariances as

$$x^{ij} = x^i - \frac{(x^i - x^j)(C_{ii} - C_{ij})}{(C_{ii} + C_{jj} - 2C_{ij})} = \frac{(C_{jj} - C_{ij})x^i + (C_{ii} - C_{ij})x^j}{(C_{ii} + C_{jj} - 2C_{ij})},$$

where the covariance C_{ij} is

$$C_{ij} = \frac{1}{M} \sum_m x_m^i x_m^j - \left(\frac{1}{M} \sum_m x_m^i \right) \left(\frac{1}{M} \sum_m x_m^j \right).$$

Note that $C_{ii} = \overline{x^2} - \bar{x}^2$ for estimator i .

The "correlation" between two estimators is a function of their covariances and is given by

$$\text{correlation} = \frac{C_{ij}}{\sqrt{|C_{ii}C_{jj}|}}$$

The correlation will be between unity (perfect positive correlation) and minus one (perfect anti or negative correlation). If the correlation is one, no

CHAPTER 2

KCODE

new information has been gained by the second estimator. If the correlation is zero, the two estimators appear statistically independent and the combined estimated standard deviation should be significantly less than either. If the correlation is negative one, even more information is available because the second estimator will tend to be low, relative to the expected value, when the first estimator is high and vice versa. Even larger improvements in the combined standard deviation should occur.

The combined average k_{eff} and the estimated standard deviation of all three k_{eff} estimators are based on the method of Halperin⁸³ and is much more complicated than the two combination case. The improvements to the standard deviation of the three combined estimator will depend on the magnitude and sign of the correlations as discussed above. The details and analysis of this method are given in Ref. 81.

For many problems, all three estimators are positively correlated. The correlation will depend on what variance reduction (e.g., implicit or analog capture) is used. Occasionally, the absorption estimator may be only weakly correlated with either the collision or track length estimator. It is possible for the absorption estimator to be significantly anticorrelated with the other two estimators for some fast reactor compositions and large thermal systems. Except in the most heterogeneous systems, the collision and track length estimators are likely to be strongly positively correlated.

There may be a negative bias⁸² in the estimated standard deviation of k_{eff} for systems with dominance ratios (second largest to largest eigenvalue) close to unity. These systems are typically large with small neutron leakage. The magnitude of this effect can be estimated by batching the cycle k_{eff} values in batch sizes much greater than one cycle,⁸² which MCNP provides automatically. For problems where there is a reason to suspect the results, a more accurate calculation of this effect can be done by making several independent calculations of the same problem (using different random number sequences) and observing the variance of the population of independent k_{eff} s. The larger the number of independent calculations that can be made, the better the distribution of k_{eff} values can be assessed.

6. Creating and Interpreting k_{eff} Confidence Intervals

The result of a Monte Carlo criticality calculation (or any other type of Monte Carlo calculation) is a confidence interval. For criticality, this means that the result is not just k_{eff} , but k_{eff} plus and minus some number of estimated standard deviations to form a confidence interval (based on the Central Limit Theorem) in which the true answer is expected to lie a certain fraction of the time. The number of standard deviations used (e.g., from a Student's t Table) determines the fraction of the time that the confidence interval will include the true answer, for a selected confidence level. For example, a valid 99% confidence interval should include the true result 99% of the time. There is always some probability (in this example, 1%) that the true result will lie outside of the confidence interval. To reduce this probability to an acceptable level, either the confidence interval must be

increased according to the desired Student's t percentile, or more histories need to be run to get a smaller estimated standard deviation.

MCNP uses three different estimators for k_{eff} . The advantages of each estimator vary with the problem: no one estimator will be the best for all problems. All estimators and their estimated standard deviations are valid under the assumption that they are unbiased and consistent, therefore representative of the true parameters of the population. This statement has been validated empirically⁸¹ for all MCNP estimators for small dominance ratios. The batched k_{eff} results table should be used to estimate if the calculated batch-size-of-one k_{eff} standard deviation appears to be adequate.

The confidence interval based on the three statistically combined k_{eff} estimator is the recommended result to use for all final k_{eff} confidence interval quotations because all of the available information has been used in the final result. This estimator often has a lower estimated standard deviation than any of the three individual estimators and therefore provides the smallest valid confidence interval as well. The final estimated k_{eff} value, estimated standard deviation, and the estimated 68%, 95%, and 99% confidence intervals (using the correct number of degrees of freedom) are presented in the box on the k_{eff} results summary page of the output. If other confidence intervals are wanted, they can be formed from the estimated standard deviation of k_{eff} . At least 30 active cycles need to be run for the final k_{eff} results box to appear. Thirty cycles are required so that there are enough degrees of freedom to form confidence intervals using the well known estimated standard deviation multipliers. (When constructing a confidence interval using any single k_{eff} estimator, its standard deviation, and a Student's t Table, there are $I_t - I_c - 1$ degrees of freedom. For the two and three combined k_{eff} estimators, there are $I_t - I_c - 2$ and $I_t - I_c - 3$ degrees of freedom, respectively.)

All of the k_{eff} estimators and combinations by two or three are provided in MCNP so that the user can make an alternate choice of confidence interval if desired. Based on statistical studies, using the individual k_{eff} estimator with the smallest estimated standard deviation is not recommended. Its use can lead to confidence intervals that do not include the true result the correct fraction of the time.⁸¹ The studies have shown that the standard deviation of the three combined k_{eff} estimator provides the correct coverage rates, assuming that the estimated standard deviations in the individual k_{eff} estimators are accurate. This accuracy can be verified by checking the batched k_{eff} results table. When significant anti-correlations occur among the estimators, the resultant much smaller estimated standard deviation of the three combined average has been verified⁸¹ by analyzing a number of independent criticality calculations.

7. Analysis to Assess the Validity of a Criticality Calculation

The two most important requirements for producing a valid criticality calculation for a specified geometry are sampling all of the fissionable material well and ensuring that the fundamental spatial mode was achieved before

CHAPTER 2 KCODE

and maintained during the active k_{eff} cycles. MCNP has checks to assess the fulfillment of both of these conditions.

MCNP verifies that at least one fission source point was generated in each cell containing fissionable material. A WARNING message is printed on the k_{eff} results summary page that includes a list of cells that did not have any particles entering, and/or no collisions, and/or no fission source points. For repeated structures geometries, a source point in any one cell that is repeated will satisfy this test. For example, assume a problem with a cylinder and a cube that are both filled with the same universe, namely a sphere of uranium and the space outside the sphere. If a source point is placed in the sphere inside the cylinder but not in the sphere inside the cube, the test will be satisfied.

One basic assumption that is made for a good criticality calculation is that the normal spatial mode for the fission source has been achieved after I_c cycles were skipped. MCNP attempts to assess this condition in several ways. The estimated combined k_{eff} and its estimated standard deviation for the first and second active cycle halves of the problem are compared. A WARNING message is issued if either the difference of the two values of combined col/abs/track-length k_{eff} does not appear to be zero or the ratio of the larger to the smaller estimated standard deviations of the two col/abs/track-length k_{eff} is larger than expected. Failure of either or both checks implies that the two active halves of the problem do not appear to be the same and the output from the calculation should be inspected carefully.

MCNP checks to determine which number of cycles skipped produces the minimum estimated standard deviation for the combined k_{eff} estimator. If this number is larger than I_c , it may indicate that not enough inactive cycles were skipped. The table of combined k_{eff} -by-number-of-cycles skipped should be examined to determine if enough inactive cycles were skipped.

It is assumed that N is large enough so that the collection of active cycle k_{eff} estimates for each estimator will be normally distributed if the fundamental spatial mode has been achieved in I_c cycles and maintained for the rest of the calculation. To test this assumption, MCNP performs normality checks^{85,86} on each of the three k_{eff} estimator cycle data at the 95% and 99% confidence levels. A WARNING message is issued if an individual k_{eff} data set does not appear to be normally distributed at the 99% confidence level. This condition will happen to good data about 1% of the time. Unless there is a high positive correlation among the three estimators, it is expected to be rare that all three k_{eff} estimators will not appear normally distributed at the 99% confidence level when the normal spatial mode has been achieved and maintained. When the condition that all three sets of k_{eff} estimators do not appear to be normal at the 99% confidence level occurs, the box with the final k_{eff} will not be printed. The final confidence interval results are available elsewhere in the output. Examine the calculation carefully to see if the normal mode was achieved before the active cycles began. The normality checks are also made for the batched- k_{eff} and k_{eff} -by-cycles-skipped tables so that normality behavior can be studied by batch size and I_c .

These normality checks test the assumption that the individual cycle k_{eff} values behave in the assumed way. Even if the underlying individual cycle k_{eff} values are not normally distributed, the three *average* k_{eff} values and the combined k_{eff} estimator will be normally distributed if the conditions required by the Central Limit Theorem are met for the average. If required, this assumption can be tested by making several independent calculations to verify empirically that the population of average k_{eff} s appears to be normally distributed with the same population variance as estimated by MCNP.

MCNP tests for a monotonic trend of the three combined k_{eff} estimator over the last ten active cycles. This type of behavior is not expected in a well converged solution for k_{eff} and could indicate a problem with achieving or maintaining the normal spatial mode. A WARNING message is printed if such a monotonic trend is observed.

8. Normalization of Standard Tallies in a Criticality Calculation

Track length fluxes, surface currents, surface fluxes, heating and detectors—all the standard MCNP tallies—can be made during a criticality calculation. The tallies are for one fission neutron generation. Biases may exist in these criticality results, but appear to be smaller than statistical uncertainties.⁸² These tallied quantities are accumulated only after the I_c inactive cycles are finished. The tally normalization is per active source weight w , where $w = N * (I_t - I_c)$, and N is the nominal source size (from the KCODE card); I_t is the total number of cycles in the problem; and I_c is the number of inactive cycles (from KCODE card). The number w is appropriately adjusted if the last cycle is only partially completed. If the tally normalization flag (on the KCODE card) is turned on, the tally normalization is the actual number of starting particles during the active cycles rather than the nominal weight above. Bear in mind, however, that the source particle weights are all set to $W = N/M$ so that the source normalization is based upon the nominal source size N for each cycle.

An MCNP tally in a criticality calculation is for one fission neutron being born in the system at the start of a cycle. The tally results must be scaled either by the total number of neutrons in a burst or by the neutron birth rate to produce, respectively, either the total result or the result per unit time of the source. The scaling factor is entered on the Fm card.

The statistical errors that are calculated for the tallies assume that all the neutron histories are independent. They are not independent because of the cycle-to-cycle correlations that become worse as the dominance ratio approaches one. In this limit, each k_{eff} cycle effectively provides no new source information. For extremely large systems (dominance ratio ≥ 0.995), the estimated standard deviation for a tally that involves only a portion of the problem could be underestimated by a factor of five or more (see Ref. 84, page 42–44). This value also is a function of the size of the tally region. In the Ref. 84 slab reactor example, the entire problem (i.e., k_{eff}) standard deviation was not underestimated at all. An MCNP study⁸⁷ of the FFTF

CHAPTER 2

KCODE

fast reactor with a smaller dominance ratio indicates that 90% coverage rates for flux tallies are good, but that 2 out of 300 tallies were beyond four estimated standard deviations. Independent runs can be made to study the real eigenfunction distribution (i.e., tallies) and the estimated standard deviations for difficult criticality calculations. This method is the only way to determine accurately these confidence intervals for large dominance ratio problems.

9. Neutron Tallies and the MCNP Net Multiplication Factor

The MCNP net multiplication factor M printed out on the problem summary page differs from the k_{eff} from the criticality code. We will examine a simple model to illustrate the approximate relationship between these quantities and compare the tallies between standard and criticality calculations.

Assume we run a standard MCNP calculation using a fixed neutron source distribution identical in space and energy to the source distribution obtained from the solution of an eigenvalue problem with $k_{eff} < 1$. Each generation will have the same space and energy distribution as the source. The contribution to an estimate of any quantity from one generation is reduced by a factor of k_{eff} from the contribution in the preceding generation. The estimate E_k of a tally quantity obtained in a criticality eigenvalue calculation is the contribution for one generation produced by a unit source of fission neutrons. An estimate for a standard MCNP fixed source calculation, E_s , is the sum of contributions for all generations starting from a unit source.

$$E_s = E_k + k_{eff}E_k + k_{eff}^2E_k + k_{eff}^3E_k + \dots = E_k/(1 - k_{eff}) \quad (2.26)$$

Note that $1/(1 - k_{eff})$ is the true system multiplication. The above result depends on our assumptions about the unit fission source used in the standard MCNP run. Usually, E_s will vary considerably from the above result, depending on the difference between the fixed source and the eigenmode source generated in the eigenvalue problem. E_s will be a fairly good estimate if the fixed source is a distributed source roughly approximating the eigenmode source. Tallies from a criticality calculation are appropriate only for a critical system and the tally results can be scaled to a desired fission neutron source (power) level or total neutron pulse strength.

In a fixed source MCNP problem, the net multiplication M is defined to be unity plus the gain G_f in neutrons from fission plus the gain G_x from nonfission multiplicative reactions. Using neutron weight balance (creation equals loss),

$$M = 1 + G_f + G_x = W_e + W_c \quad , \quad (2.27)$$

where W_e is the weight of neutrons escaped per source neutron and W_c is the weight of neutrons captured per source neutron. In a criticality calculation, fission is treated as an absorptive process; the corresponding relationship for the net multiplication is then

$$M^o = 1 + G_x^o = W_e^o + W_c^o + W_f^o \quad , \quad (2.28)$$

where the superscript *o* designates results from the criticality calculation and W_f^o is the weight of neutrons causing fission per source neutron. Because k_{eff} is the number of fission neutrons produced in a generation per source neutron, we can also write

$$k_{eff} = \bar{\nu} W_f^o \quad , \quad (2.29)$$

where $\bar{\nu}$ is the average number of neutrons emitted per fission for the entire problem. Making the same assumptions as above for the fixed source used in the standard MCNP calculation and using equations (2.26), (2.27), and (2.28), we obtain

$$M = W_e + W_c = \frac{W_e^o + W_c^o}{1 - k_{eff}} = \frac{M^o - W_f^o}{1 - k_{eff}}$$

or, by using (2.28) and (2.29),

$$M = \frac{M^o - \frac{k_{eff}}{\bar{\nu}}}{1 - k_{eff}} = \frac{1 - \frac{k_{eff}}{\bar{\nu}} + G_x^o}{1 - k_{eff}}$$

Often, the nonfission multiplicative reactions $G_x^o \ll 1$. This implies that k_{eff} can be **approximated** by k_{eff}^{FS} (from an appropriate **Fixed Source** calculation)

$$k_{eff} \approx k_{eff}^{FS} = \frac{M - 1}{M - \frac{1}{\bar{\nu}}} \quad , \quad (2.30)$$

when the two fission neutron source distributions are nearly the same. The average value of $\bar{\nu}$ in a problem can be calculated by dividing the fission neutrons gained by the fission neutrons lost as given in the totals of the neutron weight balance for physical events. Note, however, that the above estimate is subject to the same limitations as described in Eq. 2.26.

C. Recommendations for Making a Good Criticality Calculation

1. Problem Set-Up

As with any calculation, the geometry must be adequately and correctly specified to represent the true physical situation. Geometry plots should be made and cells, materials, and masses checked for correctness. The appropriate nuclear data, including $S(\alpha, \beta)$ thermal data, at the correct material temperatures should be specified. Do as good a job as possible to put initial fission source points in every cell with fissionable material. Try running short problems with both analog and implicit capture (see the PHYS:N card) to improve the figure of merit for the combined k_{eff} and any tallies being made. Follow the tips for good calculations listed at the end of Chapter 1.

CHAPTER 2
KCODE

2. Number of Neutrons per Cycle and Number of Cycles

Criticality calculations can suffer from two potential problems. The first is the failure to sufficiently converge the spatial distribution of the fission source from its initial guess to a distribution fluctuating around the fundamental eigenmode solution. It is recommended that you make an initial run with a relatively small number of source particles per generation (perhaps 500) and generously allow a large enough number of cycles so that the eigenvalue appears to be fluctuating about a constant value. You should examine the results and continue the calculation if any trends in the eigenvalue are noticeable. The SRCTP file from the last k_{eff} cycle of the initial run can then be used as the source for the final production run to be made with a larger number of histories per cycle.

This convergence procedure can be extended for very slowly convergent problems, typically large, thermal, low-leakage systems, where a convergence run might be made with 500 histories per cycle. Then a second convergence run would be made with 1000 histories per cycle, using the SRCTP file from the first run as an initial fission source guess. If the results from the second run appear satisfactory, then a final run might be made using 4000 particles per cycle with the SRCTP file from the second run as an initial fission source guess. In the final run, only a few cycles should need to be skipped. The bottom line is this: skip enough cycles so that the normal spatial mode is achieved.

The second potential problem arises from the fact that the criticality algorithm produces a very small negative bias in the estimated eigenvalue. The bias depends upon $1/N$, where N is the number of source particles per generation. Thus it is desirable to make N as large as possible. Any value of $N > 200$ should be sufficient to reduce the bias to a small level.

The eigenvalue bias Δk_{eff} has been shown⁸² to be

$$-\Delta k_{eff} = \frac{(I_t - I_c)}{2k_{eff}} (\sigma_{k_{eff}}^2 - \sigma_{approx}^2) \quad , \quad (2.31)$$

where $\sigma_{k_{eff}}$ is the true standard deviation for the final k_{eff} ,
 σ_{approx} is the approximate standard deviation computed assuming
the individual k_{eff} values are statistically independent, and
 $\sigma_{k_{eff}}^2 > \sigma_{approx}^2$.

The standard deviations are computed at the end of the problem. Because the σ^2 s decrease as $1/(I_t - I_c)$, Δk_{eff} is independent of the number of active cycles. Recall that Δk_{eff} is proportional to $1/N$, the number of neutrons per k_{eff} cycle.

Eqn. (2.31) can be written⁸² as the following inequality:

$$\frac{|\Delta k_{eff}|}{\sigma_{k_{eff}}} < \frac{(I_t - I_c)\sigma_{k_{eff}}}{2k_{eff}} \quad . \quad (2.32)$$

This inequality is useful for determining an upper limit to the number of active cycles that should be used for a calculation without having Δk_{eff}

dominate $\sigma_{k_{eff}}$. If $\sigma_{k_{eff}}/k_{eff}$ is 0.0025, which is a reasonable value for criticality calculations, and $I_t - I_c$ is 400, then $|\Delta k_{eff}|/\sigma_{k_{eff}} < 0.5$ and Δk_{eff} will not dominate the k_{eff} confidence interval. If $\sigma_{k_{eff}}$ is reasonably well approximated by MCNP's estimated standard deviation, this ratio will be much less than 0.5.

The total running time for the active cycles is proportional to $N(I_t - I_c)$, and the standard deviation in the estimated eigenvalue is proportional to $1/\sqrt{N(I_t - I_c)}$. From the results of the convergence run, the total number of histories needed to achieve the desired standard deviation can be estimated.

It is recommended that 200 to 400 active cycles be used, assuming that the above $|\Delta k_{eff}|/\sigma_{k_{eff}}$ is much less than unity in doing so. This large number of cycles will provide large batch sizes of k_{eff} cycles (e.g., 40 batches of 10 cycles each for 400 active cycles) to compare estimated standard deviations with those obtained for a batch size of one k_{eff} cycle. For example, for 400 active cycles, 40 batches of 10 k_{eff} s are created and analyzed for a new average k_{eff} and a new estimated standard deviation. The behavior of the average k_{eff} by a larger number of cycles can also be observed to ensure a good normal spatial mode. Fewer than 30 active cycles is not recommended because trends in the average k_{eff} may not have enough cycles to develop.

3. Analysis of Criticality Problem Results

The goal of the calculation is to produce a k_{eff} confidence interval that includes the true result the desired fraction of the time. Check all WARNING messages. Understand their significance to the calculation. Study the results of the checks that MCNP makes that were described starting on page 2-149.

The criticality problem output contains a lot of useful information. Study it to make sure that: 1) the problem terminated properly; 2) enough cycles were skipped to ensure that the normal spatial mode for fission sources was achieved; 3) all cells with fissionable material were sampled; 4) the average combined k_{eff} appears to be varying randomly about the average value for the active cycles; 5) the average combined k_{eff} -by-cycles-skipped does not exhibit a trend during the latter stages of the calculation; 6) the confidence intervals for the batched (with at least 30 batch values) combined k_{eff} do not differ significantly from the final result; 7) the impact of having the largest of each of the three k_{eff} estimators occurring on the next cycle is not too great on the final confidence interval; and 8) the combined k_{eff} figure of merit should be stable. The combined k_{eff} figure of merit should be reasonably stable, but not as stable as a tally figure of merit because the number of histories for each cycle is not exactly the same and combined k_{eff} relative error may experience some changes because of changes in the estimated covariance matrix for the three individual estimators.

Plots (using the z option) can be made of the three individual and average k_{eff} estimators by cycle, as well as the three estimator combined k_{eff} . Use these plots to better understand the results.

If there is concern about a calculation, the k_{eff} -by-cycles-skipped table presents the results that would be obtained in the final result box for differing

CHAPTER 2

Volume/Area

numbers of cycles skipped. This information can provide insight into fission source spatial convergence, normality of the k_{eff} data sets, and changes in the 95% and 99% confidence intervals. If concern persists, a problem could be run that tallies the track length estimator k_{eff} using an F4:n tally and an FM card using the -6 and -7 reaction multipliers (see Chapter 4 for an example). In the most drastic cases, several independent calculations can be made and the variance of the k_{eff} values (and any other tallies) could be computed from the individual values.

If a conservative (too large) k_{eff} confidence interval is desired, the results from the largest k_{eff} occurring on the next cycle table can be used. This situation could occur with a maximum probability of $1/(I_t - I_c)$ for highly positively correlated k_{eff} s to $1/(I_t - I_c)^3$ for no correlation.

Finally, keep in mind the discussion in starting on page 2-151. For large systems with a dominance ratio close to one, the estimated standard deviations for tallies could be much smaller than the true standard deviation. The cycle-to-cycle correlations in the fission sources are not taken into account, especially for any tallies that are not made over the entire problem. The only way to obtain the correct statistical errors in this situation is to run a series of independent problems using different random number sequences and analyze the sampled tally results to estimate the statistical uncertainties.

IX. VOLUMES AND AREAS⁸⁸

The particle flux in Monte Carlo transport problems often is estimated as the track length per unit volume or the number of particles crossing a surface per unit area. Therefore, knowing the volumes and surface areas of the geometric regions in a Monte Carlo problem is essential. Knowing volumes is useful in calculating the masses and densities of cells and thus in calculating volumetric or mass heating. Furthermore, calculation of the mass of a geometry is frequently a good check on the accuracy of the geometry setup when the mass is known by other means.

Calculating volumes and surface areas in modern Monte Carlo transport codes is nontrivial. MCNP allows the construction of cells from unions and/or intersections of regions defined by an arbitrary combination of second-degree surfaces, toroidal fourth-degree surfaces, or both. These surfaces can have different orientations or be segmented for tallying purposes. The cells they form even can consist of several disjoint subcells. Cells can be constructed from quadrilateral or hexagonal lattices or can be embedded in repeated structures universes. Although such generality greatly increases the flexibility of MCNP, computing cell volumes and surface areas understandably requires increasingly elaborate computational methods.

MCNP automatically calculates volumes and areas of polyhedral cells and of cells or surfaces generated by surfaces of revolution about any axis, even a skew axis. If a tally is segmented, the segment volumes or areas are computed. For nonrotationally symmetric or nonpolyhedral cells, a stochastic volume and surface area method that uses ray tracing is available. See page 2-158.

CHAPTER 3 DESCRIPTION OF MCNP INPUT

Input to MCNP consists of several files, but the main one supplied by the user is the INP (the default name) file, which contains the input information necessary to describe the problem. Only a small subset of all available input cards will be needed in any particular problem. The input cards are summarized by card type on page 3-123. The word "card" is used throughout this manual to describe a single line of input up to 80 characters.

Maximum dimensions exist for some MCNP input items; they are summarized on page 3-126. The user can increase any of these maximum values by altering the code and recompiling.

All features of MCNP should be used with caution and knowledge. This is especially true of detectors and variance reduction schemes; you are encouraged to read the appropriate sections of Chapter 2 before using them.

The units used throughout MCNP are given in Chapter 1 on page 1-19.

I. INP FILE

The INP file can have two forms, initiate-run and continue-run. Either can contain an optional message block that replaces or supplements the MCNP execution line information.

A. Message Block

A user may optionally put a set of cards called the message block before the problem identification title card in the INP file. In computer environments where there are no execution line messages, the message block is the only means for giving MCNP an execution message. Less crucially, it is a convenient way to avoid retyping an often-repeated message. The message block starts with the string MESSAGE: and is limited to columns 1-80. Alphabetic characters can be upper, lower, or mixed case. All cards before the blank line delimiter are continuation cards. A \$ and & in the message block are end-of-line markers. The message block ends with a blank line delimiter before the title card. The syntax of the message is the same as for the regular execution line message discussed on page 1-29. The meanings of the components of the message are the same as for the execution line message, subject to the following rules, which are needed to resolve conflicts between the message block and execution line message if the two are used simultaneously. Information in the execution line takes precedence over the same information in the message block, in particular:

- a. $INP = filename$ is not a legitimate entry in the message block. The name INP may be changed on the MCNP execution line only.
- b. In the case of $A = B$ (filename substitution), if the construct $A =$ appears in both the execution line message and in the message block, the message block entry is ignored.

function 5 describes the required surface transformations. According to the SI5 card, surfaces 6 and 7 are related to surfaces 3 and 2, respectively, by transformation TR4; surfaces 12 and 13 are related to 3 and 2 by TR5. The physical probability of starting on surfaces 6 and 7 is 40% according to the SP5 card, and the physical probability of starting on surfaces 12 and 13 is 60%. The SB5 card causes the particles from surfaces 3 and 2 to be started on surfaces 6 and 7 30% of the time with weight multiplier 4/3 and to be started on surfaces 12 and 13 70% of the time with weight multiplier 6/7.

Example 2: Original run: SSW 3 SYM 1
 Current run: SSR AXS 0 0 1 EXT D99
 SI99 -1 .5 1
 SP99 C .75 1
 SB99 0 .5 .5

All particles written to surface 3 in the original problem will be started on surface 3 in the new problem, which must be exactly the same because no OLD, NEW, COL, or TR keywords are present. Because this is a spherically symmetric problem, indicated by the SYM 1 flag in the original run, the position on the sphere can be biased. It is biased in the z -direction with a cone bias described by distribution 99.

9. KCODE Criticality Source Card

Form: KCODE NSRCK RKK IKZ KCT MSRK KNRM MRKP

NSRCK = nominal source size per cycle
 RKK = initial guess for k_{eff}
 IKZ = number of cycles to be skipped before beginning
 tally accumulation
 KCT = number of cycles to be done
 MSRK = number of source points to allocate storage for
 KNRM = method of tally normalization.
 0 means normalize tallies by weight
 not zero means normalize tallies to number of particles
 MRKP = number of k_{eff} cycle values stored in RKPL array

Defaults: NSRCK=no default; RKK=1.0; IKZ=5; KCT=0, that is, do not terminate on the number of cycles; MSRK=4500 or 1.5*NSRCK, whichever is larger; KNRM=0; and MRKP=201 or 2*KCT, whichever is larger.

Use: This card is required for criticality calculations.

The KCODE card specifies the MCNP criticality source that is used for determining k_{eff} . The criticality source uses total fission nuubar values unless overridden by a TOTNU NO card. The KCODE source applies only to neutron problems. See Chapter 1 for further information.

CHAPTER 3

Source Cards

The NSRCK entry is the nominal source size for each cycle and is frequently taken to be in the range of $300 < \text{NSRCK} \leq 3000$. The IKZ entry is the number of cycles to skip before beginning tally accumulation (this is important if the initial source guess is poor). The KCT entry specifies the number of cycles to be done before the problem ends. A zero entry means never terminate on the number of cycles but terminate on time. The MSRK is the maximum number of source points for which storage will be allocated. If an SRCTP file with a larger value of MSRK is read for the initial source, the larger value is used.

Fission sites for each cycle are those points generated by the previous cycle. For the initial cycle, fission sites can come from an SRCTP file from a similar geometry, from a KSRC card, or from a volume distribution specified by an SDEF card.

If in the first cycle the source being generated overruns the current source, the initial guess (RKK) is probably too low. The code then proceeds to print a comment, continues without writing a new source, calculates k'_{eff} , reads the initial source back in, and begins the problem using k'_{eff} instead of RKK. If the generated source again overruns the current source after the first cycle, the job terminates and either a better initial guess (RKK) or more source space (MSRK) should be specified on the next try.

10. KSRC Source Points for KCODE Calculation

Form: KSRC $x_1 y_1 z_1 x_2 y_2 z_2 \dots$

x_i, y_i, z_i = location of initial source points

Default: None. If this card is absent, an SRCTP source file or SDEF card must be supplied to provide initial source points for a criticality calculation.

Use: Optional card for use with criticality calculations.

This card contains up to NSRCK (x, y, z) triplets, which are locations of initial source points for a KCODE criticality calculation. At least one point must be in a cell containing fissile material. The points must be away from cell boundaries. It is not necessary to input all NSRCK coordinate points. MCNP will start approximately (NSRCK/number of points) particles at each point. Usually one point in each fissile region is adequate, because MCNP will quickly calculate and use the new fission source distribution. The energy of each particle in the initial source is sampled from a Watt fission spectrum hardwired into MCNP, with the values $a = 0.965\text{MeV}$ and $b = 2.29\text{MeV}^{-1}$.

An SRCTP file from a previous criticality calculation may be used instead of a KSRC card. If the current problem has a lot in common with the previous problem, using the SRCTP file may save some computer time. Even if the problems are quite different, the SRCTP file may still be usable if some of the points in the SRCTP file are in cells containing fissile material in the current problem. Points in void or zero importance cells will be deleted.

The number of particles actually started at each point will be such as to produce approximately NSRCK initial source particles.

An SDEF card also can be used to sample initial source points in fissile material regions. The SDEF card parameters applicable to volume sampling can be used: CEL, POS, RAD, EXT, AXS, X, Y, Z; and CCC, ERG, and EFF. If a uniform volume distribution is chosen, the early values of k_{eff} will likely be low because too many particles are put near where they can escape, just the opposite of the usual situation with the KSRC card. Do not change the default value of WGT for a KCODE calculation.

11. Subroutines SOURCE and SRCDX

If SDEF, SSR, or KCODE cards are not present in the INP file, a user supplied source is assumed and is implemented by calling subroutine SOURCE, which the user must provide. Chapter 4 has examples of a SOURCE subroutine and discusses the SRCDX subroutine. The parameters that must be specified within the subroutine are listed and defined on page 3-39.

Prior to calling subroutine SOURCE, isotropic direction cosines u, v, w (UUU,VVV,WWW) are calculated. Therefore, you need not specify the direction cosines if you want an isotropic distribution.

The SIn, SPn, and SBn cards also can be used with the SOURCE subroutine, although modifications to other parts of MCNP may be required for proper initialization and to set up storage. A random number generator RANG() is available for use by SOURCE for generating random numbers between 0 and 1. Up to 50 numerical entries can be entered on each of the IDUM and RDUM cards for use by SOURCE. The IDUM entries must be integers and the RDUM entries floating point numbers.

If you are using a detector or DXTRAN and your source has an anisotropic angular distribution, you will need to supply an SRCDX subroutine to specify PSCs for each detector or DXTRAN sphere (see Chapters 2 and 4).

There are unused variables stored in the particle bank that are reserved for the user called SPARE(M), M=1,MSPARE, where MSPARE=3. Depending on the application, you may need to reset them to 0 in SOURCE for each history; MCNP does not reset them.

E. Tally Specification

The tally cards are used to specify what type of information the user wants to gain from the Monte Carlo calculation; that is, current across a surface, flux at a point, heating in a region, etc. This information is requested by the user by using a combination of the following cards. To obtain tally results, only the Fn card is required; the other tally cards provide various optional features.

CHAPTER 3 Material Cards

1. Mm Material Card

Form: Mm $ZAID_1$ $fraction_1$ $ZAID_2$ $fraction_2$... keyword=value ...

m corresponds to the material number on the cell cards

$ZAID_i$ = either a full ZZZAAA.nnX or partial ZZZAAA element or nuclide identifier for constituent i where ZZZ is the atomic number, AAA is the atomic mass, nn is the library identifier, and X is the class of data

$fraction_i$ = atomic fraction (or weight fraction if entered as a negative number) of constituent i in the material.

keyword = value, where = sign is optional. Keywords are:

GAS = m flag for density-effect correction to electron stopping power.

$m = 0$ calculation appropriate for material in the condensed (solid or liquid) state used.

$m = 1$ calculation appropriate for material in the gaseous state used.

ESTEP = n causes the number of electron substeps per energy step to be increased to n for the material. If n is smaller than the built-in default found for this material, the entry is ignored. Both the default value and the ESTEP value actually used are printed in Table 85.

NLIB = id changes the default neutron table identifier to the string id . The neutron default is a blank string, which selects the first matching entry in XSDIR.

PLIB = id changes the default photon table identifier to id .

ELIB = id changes the default electron table identifier to id .

Default: None for ZAID fraction; GAS=0; ESTEP internally set; NLIB, PLIB, and ELIB=first match in XSDIR.

Use: Optional, but required if you want materials in cells.

Neutrons. For naturally occurring elements, AAA = 000. Thus, ZAID = 74182.01 represents the isotope ^{182}W and ZAID = 74000.01 represents the element tungsten. Natural elements not available from among those listed in Appendix G must be constructed on an Mm card by adding together the individual isotopes if they are available.

If the density for cells with AAA = 000 is input in g/cm^3 , MCNP will assume the atomic weight for the natural element.

The ZZZ and AAA quantities are determined for neutrons by looking at the list of cross sections in Appendix G and finding the appropriate ZAID associated with an evaluation that you want.

Photons and electrons. If neutrons are not being run, the AAA can be set to 000 and the nnX can be omitted. Cross sections are specified exactly like the neutron cross sections, but ZZZAAA.nnX equals ZZZ000. There

is no distinction between isotope and element for photons and electrons. However, if the isotopic distribution for the element differs from the natural element, the atom density should be entered on the cell cards to ensure the correct atom density for these cells.

Nuclide Fraction. The nuclide fractions may be normalized to 1.0 or left unnormalized. For instance, if the material is H₂O the atom fractions can be entered as 0.667 and 0.333 or as 2 and 1 for H and O respectively. If the fractions are entered with negative signs they are assumed to be weight fractions. Weight fractions and atom fractions cannot be mixed on the same Mm card.

There is no limit to the number of "nuclide fraction" entries or the total number of different cross-section tables allowed.

Default Library Hierarchy. When NLIB=*id* is included on an Mm card, the default neutron table identifier for that material is changed to *id*. Fully specifying a ZAIID on that Mm card, ZZZAAA.nnX, overrides the NLIB=*id* default.

Example: M1 NLIB=50D 1001 2 8016.50C 1 6012 1
This material consists of three isotopes. Hydrogen (1001) and carbon (6012) are not fully specified and will use the default neutron table that has been defined by the NLIB entry to be 50D, the discrete reaction library. Oxygen (8016.50C) is fully specified and will use the continuous energy library. The same default override hierarchy also applies to photon and electron specifications.

2. DRXS Discrete Reaction Cross-Section Card

Form: DRXS ZAIID₁ ZAIID₂ ... ZAIID_i ...
or blank

ZAIID_i= Identifying number of the form ZZAAA.nn, where ZZ is the atomic number, AAA the mass number, and nn the neutron library identifier.

Default: Continuous-energy cross-section treatment if DRXS is absent.

Use: Optional. Applies only to neutron cross sections.

Nuclides listed on the optional DRXS card are given a discrete energy treatment instead of the regular fully continuous-energy cross-section treatment if the necessary discrete data are available. Check the list in Appendix G for availability. If the DRXS card is present but has no entries after the mnemonic, discrete cross sections will be used for every nuclide, if available.

Unless you are transporting neutrons in an energy region where resonances and hence self-shielding are of little importance, it is not recommended that this card be used. However, if the problem under consideration

CHAPTER 3

Material Cards

meets this criterion, using the DRXS card can reduce computer storage requirements and enhance timesharing.

All discrete reaction libraries are based on a 262 energy group structure. Groups below 1 eV make the discrete treatment appropriate for thermal neutron problems near room temperature. Also, all discrete reaction libraries (except for DRL79) have photon production data given in expanded format.

Use of these discrete cross sections will not result in the calculation being what is commonly referred to as a multigroup Monte Carlo calculation because the only change is that the cross sections are represented in a histogram form rather than a continuous-energy form. The angular treatment used for scattering, energy sampling after scattering, etc., is performed using identical procedures and data as in the continuous-energy treatment. The user wanting to make a truly multigroup Monte Carlo calculation should use the MGOPT card multigroup capability.

3. TOTNU Total Fission Card

Form: TOTNU NO
or blank

Default: If the TOTNU card is absent, prompt $\bar{\nu}$ is used for non-KCODE calculations and total $\bar{\nu}$ is used for KCODE calculations.

Use: All steady-state problems should use this card.

In a non-KCODE problem, the absence of a TOTNU card causes prompt $\bar{\nu}$ to be used for all fissionable nuclides for which prompt $\bar{\nu}$ values are available. If a TOTNU card is present but has no entry after it, total $\bar{\nu}$ will be used for those fissionable nuclides for which total values are available. A TOTNU card with NO as the entry is the same as if the card were absent, that is, prompt $\bar{\nu}$ is used.

In a KCODE calculation, the absence of a TOTNU card causes total $\bar{\nu}$ to be used for all fissionable nuclides for which total values are available. If a TOTNU card is present but has no entry after it, total $\bar{\nu}$ is again used. A TOTNU card with NO as the entry causes prompt $\bar{\nu}$ to be used for all fissionable nuclides for which prompt values are available.

The nuclide list of Appendix G indicates data available for each fissionable nuclide. The MCNP neutron cross-section summary print from XACT will show whether prompt or total was used.

4. NONU Fission Turnoff Card

Form: NONU $a_1 a_2 \dots a_i \dots a_{mza}$
or blank

$a_i = 0$ fission in cell i treated as capture; gammas produced
= 1 fission in cell i treated as real; gammas produced
= 2 fission in cell i treated as capture; gammas not produced

$mxa =$ number of cells in the problem

Default: If the NONU card is absent, fission is treated as real fission.

Use: Optional, as needed.

This card allows turning off fission in any cell. The fission is then treated as simple capture and accounted for on the loss side of the problem summary as the "Loss to fission" entry. If the NONU card is not used, all cells are given their regular treatment of real fission, that is, the same as if all entries were one. If the NONU card is present but blank, all a_i 's are assumed to be zero and fission in all cells is treated like capture. The NONU card cannot be added to a continue-run.

Sometimes it is desirable to run a problem with a fixed source in a multiplying medium. For example, an operating reactor power distribution could be specified as a function of position in the core either by an SDEF source description or by writing the fission source from a KCODE calculation to a WSSA file with a CEL option on an SSW card. The non-KCODE calculation would be impossible to run because of the criticality of the system and because fission neutrons have already been accounted for. Using the NONU card in the non-KCODE mode allows this problem to run correctly by treating fission as simple capture.

A value of 2 treats fission as capture and, in addition, no fission gamma rays are produced. This option should be used with KCODE fission source problems written to surface source files. Suppressing the creation of new fission neutrons and photons is important because they are already accounted for in the source.

5. AWTAB Atomic Weight Card

Form: AWTAB $ZAID_1 AW_1 ZAID_2 AW_2 \dots$

$ZAID_i = ZAID$ used on the Mm material card but not including the nn specification.

$AW_i =$ atomic weight ratios.

Default: If the AWTAB card is absent, MCNP will use the atomic weight ratios from the cross-section directory file XSDIR and cross-section tables.

Use: Optional, as needed.

Entries on this card override the existing atomic weight ratios as contained in both the cross-section directory file XSDIR and the cross-section tables. The AWTAB card is needed when atomic weights are not available in an XSDIR file. Also, for fission products, $ZAID=50120.35$, the atomic weight of tin ($^{120}_{50}\text{Sn}$) will be used, so the following AWTAB card is needed:

AWTAB 50120.35 116.490609

CHAPTER 3
Material Cards

WARNING: Using atomic weight ratios different from the ones in the cross-section tables in a neutron problem can lead to negative neutron energies, which will cause the problem to terminate prematurely.

6. XS_n Cross-Section File Card

Use: Optional, as an alternative to the directory part of the XSDIR file.

The XS_n card can be used to load cross-section evaluations not listed in the XSDIR file directory. You can use XS_n cards in addition to the XSDIR file. Each XS_n card, with $n = 1$ to 999, is used to describe one cross section table. The entries for the XS_n card are identical to those in XSDIR except that the + is not used for continuation. A detailed description of the required entries is provided in Appendix F.

7. VOID Material Void Card

Form: VOID no entries
or: VOID $C_1 C_2 \dots C_i$

C_i = cell number

Default: None.

Use: Debugging geometry and calculating volumes.

The first form is used when calculating volumes stochastically (see page 2-158) and in checking for geometry errors (see page 3-8). When there are no entries on the VOID card, all cells in the problem are made void by setting the material number and density to zero, FM cards are turned off, heating tallies are turned into flux tallies, and, if there is no NPS card, the effect of an NPS 100000 card is created. If there is a TALLYX subroutine, it may need to be changed, too.

The second form is used to selectively void cells instead of replacing the material number and density on each selected cell card by a zero by hand. It can be a convenience if you want to check whether the presence of some object in your geometry makes any significant difference in the answers.

8. PIKMT Photon-Production Bias Card

Form: PIKMT Z_1 IPIK₁ MT_{1,1} PMT_{1,1} ... MT_{1,IPIK₁} PMT_{1,IPIK₁}
 Z_n IPIK_n MT_{n,1} PMT_{n,1} ... MT_{n,IPIK_n} PMT_{n,IPIK_n}

Z_i = the ZAID of the i^{th} entry. Full or partial ZAIDs can be specified, that is, 29000 is equivalent to 29000.50.

IPIK_i = the parameter that controls the biasing for ZAID_i.
If IPIK_i = 0, there is no biasing for ZAID_i; photons from ZAID_i are produced with the normal sampling technique.

If $IPIK_i = -1$, no photons are produced from $ZAID_i$.

This is the default, so that if no entries are made on the PIKMT card for a particular Z Aid, there will be no photons produced from that Z Aid.

If $IPIK_i > 0$, there is biasing for $ZAID_i$. The value of $IPIK_i$ is the number of partial photon-production reactions to be sampled.

$MT_{i,j}$ and $PMT_{i,j}$ are only required for ZAIDs with $IPIK_i > 0$. In these cases, $IPIK_i$ pairs of entries of MTs and PMTs are necessary. The MTs are the identifiers for the partial photon-production reactions to be sampled. The PMTs control, to a certain extent, the frequency with which the specified MTs are sampled. The entries need not be normalized. For a Z Aid with a positive value of $IPIK$, any reaction that is not identified with its MT on the PIKMT card will not be sampled.

Default: If the PIKMT card is absent, there is no biasing of neutron-induced photons.

Use: Optional; see caveats below.

For several classes of coupled neutron-photon calculations, the desired result is the intensity of a small subset of the entire photon energy spectrum. Two examples are discrete-energy (line) photons and the high-energy tail of a continuum spectrum. In such cases, it may be profitable to bias the spectrum of neutron-induced photons to produce only those that are of interest.

1. The most important thing to realize when using the PIKMT card is that nonzero probability events may be completely excluded. In other words, the biasing game is not necessarily a fair one. While neutron tallies will be unaffected (within statistics), the only reliable photon tallies will be those with energy bins immediately around the energies of the discrete photons produced.
2. Users need information about the MT identifiers of the reactions that produce discrete-energy photons. This information is available for Los Alamos users in a document stored on the CFS as /X6XS/CTSS /DISCEGAM. Send the file to the HSP with the -V, -UC and -CC options.
3. The feature is also useful for biasing the neutron-induced photon spectrum to produce very high energy photons (for example, $E_\gamma \geq 10$ MeV). Without biasing, these high-energy photons are produced very infrequently; therefore, it is difficult to extract reliable statistical information about them. An energy cutoff can be used to terminate a track when it falls below the energy range of interest. See Ref. 4 when using the PIKMT card for this application.

CHAPTER 3 Material Cards

Example: PIKMT 26000.55 1 102001 1 7014 0
 29000 2 3001 2 3002 1
 8016 -1

This example results in normal sampling of all photon-production reactions for ^{14}N . All photons from neutron collisions with Fe are from the reaction with MT identifier 102001. Two photon-production reactions with Cu are allowed. Because of the PMT parameters the reaction with MT identifier 3001 is sampled twice as frequently relative to the reaction with MT identifier 3002 than otherwise would be the case. No photons are produced from ^{16}O or from any other isotopes in the problem that are not listed on the PIKMT card.

9. MGOPT Multigroup Adjoint Transport Option

Form: MGOPT MCAL IGM IPLT ISB ICW FNW RIM

- MCAL = F for forward problem
 A for adjoint problem
- IGM = the total number of energy groups for all kinds of particles in the problem. A negative total indicates a special electron-photon problem.
- IPLT = indicator of how weight windows are to be used.
 = 0 means that IMP values set cell importances. Weight windows, if any, are ignored for cell importance splitting and Russian roulette.
 = 1 means that weight windows must be provided and are transformed into energy-dependent cell importances. A zero weight-window lower bound produces an importance equal to the lowest nonzero importance for that energy group.
 = 2 means that weight-windows do what they normally do.
- ISB = Controls adjoint biasing for adjoint problems only (MCAL=A).
 = 0 means collisions are biased by infinite-medium fluxes.
 = 1 means collisions are biased by functions derived from weight-windows, which must be supplied.
 = 2 means collisions are not biased.
- ICW = name of the reference cell for generated weight windows.
 = 0 means weight windows are not generated.
 $\neq 0$ requires volumes be supplied or calculated for all cells of nonzero importance.
- FNW = normalization value for generated weight windows. The value of the weight-window lower bound in the most important energy group in cell ICW is set to FNW.
- RIM = compression limit for generated weight windows. Before generated weight windows are printed out, the weight

windows in each group separately are checked to see that the ratio of the highest to the lowest is less than RIM. If not, they are compressed.

Default: IPLT=0, ISB=0, ICW=0, FNW=1, RIM=1000. MCAL and IGM must be specified.

Use: Required for multigroup calculation.

MCAL and IGM are required parameters. The others are optional. "J" is not an acceptable value for any of the parameters.

At this time, the standard MCNP multigroup neutron cross sections are given in 30 groups and photons are given in 12 groups. Thus, an existing continuous-energy input file can be converted to a multigroup input file simply by adding one of the following cards:

```

MGOPT F 30 $MODE N
MGOPT F 42 $MODE N P
MGOPT F 12 $MODE P

```

A negative IGM value allows a single cross-section table to include data for more than one sort of particle. This feature applies currently to electron/photon multigroup calculations only. A problem with 50 electron groups followed by 30 photon groups in one table would have IGM=-80. A negative IGM value also means that the energy variable in the source and in tallies is group number rather than MeV. The particles can be separated in tallies by using the PTT option on the FTn tally card.

An input file for an adjoint problem can have both an IMP card and weight window cards (IPLT=0 ISB=1). The entries on the weight window cards are not weight windows in the normal sense but biasing functions. If IPLT=1 the values on a weight window card become energy-dependent cell importances. Until now, importances have been energy independent.

See Appendix G for a more complete discussion of multigroup libraries.

G. Energy and Thermal Treatment Specification

The following cards control energy and other physics aspects of MCNP:

| <u>Mnemonic</u> | <u>Card Type</u> | <u>Page</u> |
|-----------------|-------------------------------|-------------|
| PHYS | Energy physics cutoff | 3-100 |
| ESPLT | Energy splitting and roulette | 3-104 |
| TMP | Free-gas thermal temperature | 3-105 |
| THTME | Thermal times | 3-105 |
| MTm | $S(\alpha, \beta)$ material | 3-106 |

All energy entries on these cards are in units of MeV, and all times are in shakes.

CHAPTER 3
Cutoff Cards

Default: Zero; temperature is not time dependent.

Use: Optional. Use with TMP card.

The THTME card specifies the times at which the thermal temperatures on the TMPn cards are provided. The temperatures on the TMP1 card are at time t_1 on the THTME card, the temperatures on the TMP2 card are at time t_2 on the THTME card, etc. The times must be monotonically increasing: $t_n < t_{n+1}$. For each entry on the THTME card there must be a TMPn card.

5. MTm $S(\alpha, \beta)$ Material Card

Form: MTm $X_1 X_2 \dots$

$X_i = S(\alpha, \beta)$ identifier corresponding to a particular component on the Mm card.

Default: None.

Use: Optional, as needed.

For any material defined on an Mn card, a particular component of that material (represented by a *Z A I D* number) may be associated through an MTm card with an $S(\alpha, \beta)$ data set if that data set exists. The $S(\alpha, \beta)$ data for that *Z A I D* are used in every cell in which that material is specified. For a particular *Z A I D* in a material, the free-gas treatment may be used down to the energy where $S(\alpha, \beta)$ data are available. At that point, the $S(\alpha, \beta)$ treatment automatically overrides the free-gas treatment (that is, there is no mixing of the two treatments for the same *Z A I D* in the same material at a given energy).

Typically the free-gas model will be used for a particular *Z A I D* of a material down to 4 eV and then the $S(\alpha, \beta)$ treatment will take over. In general, $S(\alpha, \beta)$ effects are most significant below 2 eV.

The $S(\alpha, \beta)$ treatment is invoked by identifiers on MTm cards. The m refers to the material m defined on a regular Mm card. The appearance of an MTm card will cause the loading of the corresponding $S(\alpha, \beta)$ data from the thermal data file.

The currently available $S(\alpha, \beta)$ identifiers for the MTm card are listed in Table G.1 of Appendix G.

$S(\alpha, \beta)$ contributions to detectors or DXTRAN spheres are approximate.

| | | | | |
|-----------|------|---------|--------|--------------|
| Examples: | M1 | 1001 2 | 8016 1 | light water |
| | MT1 | LWTR.07 | | |
| | M14 | 1001 2 | 6012 1 | polyethylene |
| | MT14 | POLY.03 | | |
| | M8 | 6012 1 | | graphite |
| | MT8 | GRPH.01 | | |

CHAPTER 5

KCODE

IV. KCODE

The problem selected to illustrate the output from a criticality calculation is the one-dimensional model of the GODIVA critical assembly, composed of about 94% ^{235}U . This assembly is one of several fast neutron critical assemblies discussed in LA-4208 entitled "Reevaluated Critical Specifications of Some Los Alamos Fast-Neutron Systems" by G. E. Hansen and H. C. Paxton (September 1964).

An MCNP input file that models GODIVA and performs only the criticality calculation with no separate tallies would be only 11 lines long. The KCODE card indicates that the problem is a criticality calculation for the k_{eff} eigenvalue. To perform this same calculation with neutron-induced photon production, add the MODE N P card. Any tallies that are made in a criticality problem are normalized to the starting weight (default) or number of particles as defined by the user (see Chapter 2, section VIII for details). Tallies should be scaled for the appropriate steady state neutron generation rate.

Following is a partial listing of the output from a KCODE calculation. The pages selected emphasize the criticality aspects of the problem.

CHAPTER 5
KCODE

lmcnp version 4a ld=10/01/93 10/01/93 11:04:27

 probid = 10/01/93 11:04:27

inp=godiva

N1 1- bare u(94) sphere ref. la-4208, g. e. hansen and h. c. parxon, 1969, page 4
 2- 1 10 0.048146 -1
 3- 2 0 1
 4-
 5- 1 so 8.7037
 6-
 7- imp:n 1 0
 8- m10 92235.50c 0.045217 92238.50c 0.0024355 92234.50c 0.0004935
 N2 9- kccde 3000 1. 5 35
 N3 warning. tallies are normed per fission neutron for one generation.
 N4 10- ksrc 0. 0. 0.
 11- print
 12- c
 13- c tallies
 14- c
 15- f1:n 1
 16- f2:n 1
 17- f4:n 1
 18- f14:n 1
 19- fc14 total neutron fluence, total fissions, total fission neutrons,
 20- total neutron absorptions, and neutron heating (mev/gram)
 21- fq14 e m
 N5 22- fm14 (2761.85) (-2761.85 10 (-6) (-6 -7) (-2)) (-0.053183 10 1 -4)
 23- f24:n 1
 24- fc24 total neutron fluence, total fissions, total fission neutrons,
 25- total neutron absorptions, and neutron heating (mev/gram)
 26- e24 1.67-4 4.54e-4 1.235e-3 3.35-3 9.12-3 0.0248 0.0676 0.184
 27- 0.303 0.50 0.823 1.353 1.738 2.232 2.865 3.68
 28- 6.07 7.79 10.0 12.0 13.5 15.0 20.0
 29- fq24 e m
 30- fm24 (2761.85) (-2761.85 10 (-6) (-6 -7) (-2)) (-0.053183 10 1 -4)
 31- f6:n 1
 32- f7:n 1

CHAPTER 5
KCODE

33- c
 34- c use the sixteen group hansen-roach energy structure as the default
 35- c
 N6 36- e0 1-7 4-7 1-6 3-6 1-5 3-5 1-4 5.5-4 3-3 1.7-2 0.1 0.4 0.9 1.4 3 20
 37-

N7 1 initial source from ksrc card. print table 90
 original number of points 1
 points not in any cell 0
 points in cells of zero importance 0
 points in void cells 0
 points in ambiguous cells 0
 total points rejected 0
 points remaining 1
 points after expansion or contraction 3000
 nominal source size 3000
 initial guess for k(eff.) 1.000000
 cycles to skip before tallying 5
 number of keff cycles that can be stored 201
 total fission nubar data are being used.

SKIP 198 LINES IN OUTPUT

N8 1material composition print table 40
 material
 number component nuclide, atom fraction
 10 92235, 0.93916 92238, 0.05059 92234, 0.01025
 material
 number component nuclide, mass fraction
 10 92235, 0.93860 92238, 0.05120 92234, 0.01020

N9 1cell volumes and masses print table 50

| cell | atom density | gram density | input volume | calculated volume | mass | pieces | reason volume not calculated |
|------|---------------|--------------|--------------|-------------------|-------------|--------|------------------------------|
| 1 | 1 4.81460E-02 | 1.88030E+01 | 0.00000E+00 | 2.76185E+03 | 5.19311E+04 | 1 | |
| 2 | 2 0.00000E+00 | 0.00000E+00 | 0.00000E+00 | 0.00000E+00 | 0.00000E+00 | 0 | infinite |

SKIP 67 LINES IN OUTPUT

N10 1cross-section tables print table 100
 table length
 tables from file endf5p2

CHAPTER 5
KCODE

warning. nubar of 92234.50c may be either prompt or total.

```

92234.50c  89429  njoy                ( 1394)   79/10/17.
           tables from file rmccs2
92235.50c  49913  njoy                total nu   ( 1395)   79/09/12.
92238.50c  75725  njoy                total nu   ( 1398)   79/09/13.
total      215067

```

warning. neutron energy cutoff is below some cross-section tables.

decimal words of dynamically allocated storage

```

general      42654
tallies      24548
bank         3902
N11 cross sections 215067
total       286171

```

```

dump no. 1 on file runtpe      nps =      0      coll =      0      ctm = 0.00      nrn =      0
N12 source distribution written to file srctp      cycle = 0
      3 warning messages so far.

```

```

N13 1 starting mcrun.      field length =      0      cp0 = 0.01      print table 110
      bare u(94) sphere ref. la-4208, g. e. hansen and h. c. parxon, 1969, page 4

```

| nps | x | y | z | cell | surf | u | v | w | energy | weight | time |
|-----|-----------|-----------|-----------|------|------|------------|------------|------------|-----------|-----------|-----------|
| 1 | 0.000E+00 | 0.000E+00 | 0.000E+00 | 1 | 0 | 5.085E-01 | 4.733E-01 | 7.193E-01 | 2.209E+00 | 1.000E+00 | 0.000E+00 |
| 2 | 0.000E+00 | 0.000E+00 | 0.000E+00 | 1 | 0 | 8.952E-01 | -4.447E-01 | -2.944E-02 | 4.904E+00 | 1.000E+00 | 0.000E+00 |
| 3 | 0.000E+00 | 0.000E+00 | 0.000E+00 | 1 | 0 | -6.184E-01 | -4.495E-01 | 6.446E-01 | 3.809E-01 | 1.000E+00 | 0.000E+00 |
| 4 | 0.000E+00 | 0.000E+00 | 0.000E+00 | 1 | 0 | 9.710E-01 | -5.665E-02 | -2.323E-01 | 1.331E+00 | 1.000E+00 | 0.000E+00 |
| 5 | 0.000E+00 | 0.000E+00 | 0.000E+00 | 1 | 0 | 5.861E-01 | 1.496E-01 | -7.963E-01 | 1.902E+00 | 1.000E+00 | 0.000E+00 |
| 6 | 0.000E+00 | 0.000E+00 | 0.000E+00 | 1 | 0 | -6.489E-02 | -1.626E-01 | 9.845E-01 | 4.410E-01 | 1.000E+00 | 0.000E+00 |
| 7 | 0.000E+00 | 0.000E+00 | 0.000E+00 | 1 | 0 | -7.068E-02 | 3.263E-02 | -9.970E-01 | 4.750E-01 | 1.000E+00 | 0.000E+00 |
| 8 | 0.000E+00 | 0.000E+00 | 0.000E+00 | 1 | 0 | -3.915E-01 | 4.664E-01 | -7.932E-01 | 4.136E+00 | 1.000E+00 | 0.000E+00 |
| 9 | 0.000E+00 | 0.000E+00 | 0.000E+00 | 1 | 0 | -2.368E-01 | 9.215E-01 | -3.079E-01 | 7.453E-02 | 1.000E+00 | 0.000E+00 |
| 10 | 0.000E+00 | 0.000E+00 | 0.000E+00 | 1 | 0 | 1.946E-01 | -3.204E-01 | 9.271E-01 | 3.128E+00 | 1.000E+00 | 0.000E+00 |
| 11 | 0.000E+00 | 0.000E+00 | 0.000E+00 | 1 | 0 | -6.698E-01 | -7.177E-01 | -1.905E-01 | 1.014E+00 | 1.000E+00 | 0.000E+00 |
| 12 | 0.000E+00 | 0.000E+00 | 0.000E+00 | 1 | 0 | -8.398E-01 | -4.129E-01 | 3.524E-01 | 1.395E+00 | 1.000E+00 | 0.000E+00 |
| 13 | 0.000E+00 | 0.000E+00 | 0.000E+00 | 1 | 0 | -1.714E-01 | -8.572E-01 | 4.857E-01 | 7.748E-01 | 1.000E+00 | 0.000E+00 |
| 14 | 0.000E+00 | 0.000E+00 | 0.000E+00 | 1 | 0 | -2.489E-01 | -5.118E-01 | -8.222E-01 | 1.101E+00 | 1.000E+00 | 0.000E+00 |
| 15 | 0.000E+00 | 0.000E+00 | 0.000E+00 | 1 | 0 | -2.959E-01 | 2.119E-01 | 9.314E-01 | 1.951E+00 | 1.000E+00 | 0.000E+00 |
| 16 | 0.000E+00 | 0.000E+00 | 0.000E+00 | 1 | 0 | 1.395E-01 | -9.829E-01 | 1.202E-01 | 2.186E+00 | 1.000E+00 | 0.000E+00 |

CHAPTER 5
KCODE

| | | | | | | | | | | | |
|----|-----------|-----------|-----------|---|---|------------|------------|------------|-----------|-----------|-----------|
| 17 | 0.000E+00 | 0.000E+00 | 0.000E+00 | 1 | 0 | 6.909E-01 | -7.110E-01 | 1.307E-01 | 1.865E+00 | 1.000E+00 | 0.000E+00 |
| 18 | 0.000E+00 | 0.000E+00 | 0.000E+00 | 1 | 0 | -6.580E-01 | 5.320E-01 | -5.329E-01 | 1.229E+00 | 1.000E+00 | 0.000E+00 |
| 19 | 0.000E+00 | 0.000E+00 | 0.000E+00 | 1 | 0 | -9.903E-01 | -1.380E-01 | 1.353E-02 | 1.305E+00 | 1.000E+00 | 0.000E+00 |
| 20 | 0.000E+00 | 0.000E+00 | 0.000E+00 | 1 | 0 | 7.462E-01 | 4.859E-01 | -4.551E-01 | 1.000E+00 | 1.000E+00 | 0.000E+00 |
| 21 | 0.000E+00 | 0.000E+00 | 0.000E+00 | 1 | 0 | -1.977E-01 | 9.797E-01 | 3.360E-02 | 3.990E+00 | 1.000E+00 | 0.000E+00 |
| 22 | 0.000E+00 | 0.000E+00 | 0.000E+00 | 1 | 0 | -9.117E-01 | -3.647E-01 | -1.891E-01 | 2.665E-01 | 1.000E+00 | 0.000E+00 |
| 23 | 0.000E+00 | 0.000E+00 | 0.000E+00 | 1 | 0 | -4.287E-01 | 8.361E-01 | -3.423E-01 | 1.156E+00 | 1.000E+00 | 0.000E+00 |
| 24 | 0.000E+00 | 0.000E+00 | 0.000E+00 | 1 | 0 | 1.080E-01 | 3.412E-01 | -9.338E-01 | 2.669E+00 | 1.000E+00 | 0.000E+00 |
| 25 | 0.000E+00 | 0.000E+00 | 0.000E+00 | 1 | 0 | -9.111E-01 | -9.012E-03 | -4.122E-01 | 2.185E+00 | 1.000E+00 | 0.000E+00 |
| 26 | 0.000E+00 | 0.000E+00 | 0.000E+00 | 1 | 0 | -2.568E-01 | -6.391E-01 | -7.249E-01 | 4.225E+00 | 1.000E+00 | 0.000E+00 |
| 27 | 0.000E+00 | 0.000E+00 | 0.000E+00 | 1 | 0 | -2.912E-01 | 8.086E-01 | 5.113E-01 | 1.079E+00 | 1.000E+00 | 0.000E+00 |
| 28 | 0.000E+00 | 0.000E+00 | 0.000E+00 | 1 | 0 | 1.472E-01 | -9.514E-01 | 2.705E-01 | 3.461E+00 | 1.000E+00 | 0.000E+00 |
| 29 | 0.000E+00 | 0.000E+00 | 0.000E+00 | 1 | 0 | -6.135E-01 | -7.645E-01 | -1.978E-01 | 1.836E+00 | 1.000E+00 | 0.000E+00 |
| 30 | 0.000E+00 | 0.000E+00 | 0.000E+00 | 1 | 0 | -5.702E-01 | 5.651E-01 | -5.963E-01 | 4.556E-01 | 1.000E+00 | 0.000E+00 |
| 31 | 0.000E+00 | 0.000E+00 | 0.000E+00 | 1 | 0 | -6.607E-01 | 5.373E-01 | -5.242E-01 | 6.415E-01 | 1.000E+00 | 0.000E+00 |
| 32 | 0.000E+00 | 0.000E+00 | 0.000E+00 | 1 | 0 | -9.742E-02 | -3.639E-01 | -9.263E-01 | 2.764E+00 | 1.000E+00 | 0.000E+00 |
| 33 | 0.000E+00 | 0.000E+00 | 0.000E+00 | 1 | 0 | -1.965E-01 | -3.145E-01 | -9.287E-01 | 2.785E-01 | 1.000E+00 | 0.000E+00 |
| 34 | 0.000E+00 | 0.000E+00 | 0.000E+00 | 1 | 0 | 4.097E-01 | 8.465E-01 | -3.399E-01 | 9.097E-01 | 1.000E+00 | 0.000E+00 |
| 35 | 0.000E+00 | 0.000E+00 | 0.000E+00 | 1 | 0 | -4.048E-02 | 8.831E-01 | 4.675E-01 | 3.360E-01 | 1.000E+00 | 0.000E+00 |
| 36 | 0.000E+00 | 0.000E+00 | 0.000E+00 | 1 | 0 | 3.371E-01 | -9.269E-01 | -1.652E-01 | 6.376E-01 | 1.000E+00 | 0.000E+00 |
| 37 | 0.000E+00 | 0.000E+00 | 0.000E+00 | 1 | 0 | -1.867E-01 | 9.756E-01 | -1.155E-01 | 2.186E+00 | 1.000E+00 | 0.000E+00 |
| 38 | 0.000E+00 | 0.000E+00 | 0.000E+00 | 1 | 0 | -2.616E-01 | 2.336E-01 | -9.365E-01 | 7.314E-01 | 1.000E+00 | 0.000E+00 |
| 39 | 0.000E+00 | 0.000E+00 | 0.000E+00 | 1 | 0 | 9.780E-01 | -7.641E-02 | -1.939E-01 | 2.997E-01 | 1.000E+00 | 0.000E+00 |
| 40 | 0.000E+00 | 0.000E+00 | 0.000E+00 | 1 | 0 | 2.580E-01 | -7.076E-01 | 6.578E-01 | 1.444E+00 | 1.000E+00 | 0.000E+00 |
| 41 | 0.000E+00 | 0.000E+00 | 0.000E+00 | 1 | 0 | -3.212E-01 | -7.678E-01 | -5.543E-01 | 1.914E+00 | 1.000E+00 | 0.000E+00 |
| 42 | 0.000E+00 | 0.000E+00 | 0.000E+00 | 1 | 0 | 5.039E-01 | -1.460E-01 | 8.513E-01 | 1.502E+00 | 1.000E+00 | 0.000E+00 |
| 43 | 0.000E+00 | 0.000E+00 | 0.000E+00 | 1 | 0 | 6.080E-01 | 5.487E-01 | 5.738E-01 | 5.971E+00 | 1.000E+00 | 0.000E+00 |
| 44 | 0.000E+00 | 0.000E+00 | 0.000E+00 | 1 | 0 | -2.932E-01 | 9.304E-01 | -2.199E-01 | 1.827E+00 | 1.000E+00 | 0.000E+00 |
| 45 | 0.000E+00 | 0.000E+00 | 0.000E+00 | 1 | 0 | -8.475E-01 | -3.993E-01 | -3.497E-01 | 1.928E+00 | 1.000E+00 | 0.000E+00 |
| 46 | 0.000E+00 | 0.000E+00 | 0.000E+00 | 1 | 0 | 1.200E-01 | -9.195E-01 | -3.743E-01 | 1.351E+00 | 1.000E+00 | 0.000E+00 |
| 47 | 0.000E+00 | 0.000E+00 | 0.000E+00 | 1 | 0 | 7.085E-01 | 5.879E-01 | 3.904E-01 | 2.288E+00 | 1.000E+00 | 0.000E+00 |
| 48 | 0.000E+00 | 0.000E+00 | 0.000E+00 | 1 | 0 | 4.261E-01 | 9.046E-01 | 9.254E-03 | 1.230E+00 | 1.000E+00 | 0.000E+00 |
| 49 | 0.000E+00 | 0.000E+00 | 0.000E+00 | 1 | 0 | 5.431E-01 | 4.270E-01 | -7.230E-01 | 1.433E+00 | 1.000E+00 | 0.000E+00 |
| 50 | 0.000E+00 | 0.000E+00 | 0.000E+00 | 1 | 0 | -1.053E-01 | -9.805E-01 | 1.658E-01 | 6.572E-01 | 1.000E+00 | 0.000E+00 |

Estimated keff results by cycle

print table 175

cycle 1 k(collision) 1.368849 removal lifetime(abs) 8.1998E-01 source points generated 4120

CHAPTER 5
KCODE

| | | | | | | | | | |
|---|-------|--------------|------------|-----------------------|------------------|-------------------------|-------------------|--------|--|
| cycle | 2 | k(collision) | 1.149004 | removal lifetime(abs) | 6.6818E-01 | source points generated | 2514 | | |
| cycle | 3 | k(collision) | 1.064388 | removal lifetime(abs) | 5.9757E-01 | source points generated | 2715 | | |
| cycle | 4 | k(collision) | 1.027978 | removal lifetime(abs) | 5.7907E-01 | source points generated | 2895 | | |
| cycle | 5 | k(collision) | 0.998419 | removal lifetime(abs) | 5.6734E-01 | source points generated | 2928 | | |
| N14 cycle | 6 | k(collision) | 1.004871 | removal lifetime(abs) | 5.5494E-01 | source points generated | 3043 | | |
| estimator | cycle | 7 | ave of | 2 cycles | combination | simple average | combined average | corr | |
| k(collision) | | 0.996358 | 1.000614 | 0.0043 | k(col/abs) | 0.000000 0.0000 | 0.000000 0.0000 | 0.0000 | |
| k(absorption) | | 0.995886 | 1.000718 | 0.0048 | k(abs/tk ln) | 0.000000 0.0000 | 0.000000 0.0000 | 0.0000 | |
| k(trk length) | | 0.986257 | 0.995187 | 0.0090 | k(tk ln/col) | 0.000000 0.0000 | 0.000000 0.0000 | 0.0000 | |
| rem life(col) | | 5.7053E-01 | 5.6276E-01 | 0.0138 | | | | | |
| rem life(abs) | | 5.7000E-01 | 5.6247E-01 | 0.0134 | life(col/abs) | 0.0000E+00 0.0000 | 0.0000E+00 0.0000 | 0.0000 | |
| source points generated 2995 | | | | | | | | | |
| estimator | cycle | 8 | ave of | 3 cycles | combination | simple average | combined average | corr | |
| k(collision) | | 0.986610 | 0.995946 | 0.0053 | k(col/abs) | 0.995736 0.0056 | 0.999506 0.0007 | 1.0000 | |
| k(absorption) | | 0.985140 | 0.995526 | 0.0059 | k(abs/tk ln) | 0.995011 0.0050 | 0.994857 0.0070 | 0.5862 | |
| k(trk length) | | 0.993112 | 0.994495 | 0.0052 | k(tk ln/col) | 0.995221 0.0047 | 0.995196 0.0068 | 0.5793 | |
| rem life(col) | | 5.6716E-01 | 5.6423E-01 | 0.0084 | | | | | |
| rem life(abs) | | 5.6740E-01 | 5.6411E-01 | 0.0082 | life(col/abs) | 5.6417E-01 0.0083 | 5.6343E-01 0.0119 | 0.9990 | |
| source points generated 2970 | | | | | | | | | |
| estimator | cycle | 9 | ave of | 4 cycles | combination | simple average | combined average | corr | |
| k(collision) | | 0.972349 | 0.990047 | 0.0071 | k(col/abs) | 0.990069 0.0070 | 0.990168 0.0084 | 0.9959 | |
| k(absorption) | | 0.973789 | 0.990091 | 0.0069 | k(abs/tk ln) | 0.989256 0.0068 | 0.989477 0.0086 | 0.8635 | |
| k(trk length) | | 0.970192 | 0.988420 | 0.0072 | k(tk ln/col) | 0.989233 0.0069 | 0.989354 0.0088 | 0.8834 | |
| rem life(col) | | 5.4357E-01 | 5.5906E-01 | 0.0110 | k(col/abs/tk ln) | 0.989519 0.0068 | 0.989164 0.0117 | | |
| rem life(abs) | | 5.4411E-01 | 5.5911E-01 | 0.0107 | life(col/abs) | 5.5909E-01 0.0108 | 5.6007E-01 0.0092 | 0.9997 | |
| source points generated 2982 | | | | | | | | | |
| estimator | cycle | 10 | ave of | 5 cycles | combination | simple average | combined average | corr | |
| k(collision) | | 1.014685 | 0.994974 | 0.0074 | k(col/abs) | 0.995188 0.0074 | 0.993642 0.0087 | 0.9968 | |
| k(absorption) | | 1.016646 | 0.995402 | 0.0075 | k(abs/tk ln) | 0.993627 0.0068 | 0.991426 0.0085 | 0.8923 | |
| k(trk length) | | 1.005583 | 0.991852 | 0.0065 | k(tk ln/col) | 0.993413 0.0068 | 0.991464 0.0085 | 0.9105 | |
| rem life(col) | | 5.6633E-01 | 5.6052E-01 | 0.0089 | k(col/abs/tk ln) | 0.994076 0.0070 | 0.991424 0.0104 | | |
| rem life(abs) | | 5.6772E-01 | 5.6084E-01 | 0.0088 | life(col/abs) | 5.6068E-01 0.0088 | 5.6121E-01 0.0113 | 0.9979 | |
| source points generated 3221 | | | | | | | | | |
| source distribution written to file srctp | | | | | cycle = | 10 | | | |
| SKIP 190 LINES IN OUTPUT | | | | | | | | | |
| estimator | cycle | 34 | ave of | 29 cycles | combination | simple average | combined average | corr | |

CHAPTER 5
KCODE

| | | | | | | | | | |
|--|------------|------------|--------|------------------|-------------|----------------|------------------|--------|--------|
| k(collision) | 1.019305 | 1.001219 | 0.0024 | k(col/abs) | 1.001031 | 0.0024 | 1.001208 | 0.0025 | 0.9906 |
| k(absorption) | 1.020357 | 1.000843 | 0.0024 | k(abs/tk ln) | 0.999958 | 0.0024 | 1.000343 | 0.0024 | 0.7067 |
| k(trk length) | 0.999241 | 0.999072 | 0.0027 | k(tk ln/col) | 1.000145 | 0.0024 | 1.000668 | 0.0024 | 0.7217 |
| rem life(col) | 5.6280E-01 | 5.6736E-01 | 0.0047 | k(col/abs/tk ln) | 1.000378 | 0.0023 | 1.000605 | 0.0025 | |
| rem life(abs) | 5.6314E-01 | 5.6739E-01 | 0.0047 | life(col/abs) | 5.6737E-01 | 0.0047 | 5.6744E-01 | 0.0048 | 0.9989 |
| source points generated 3102 | | | | | | | | | |
| N15 estimator | cycle | 35 | ave of | 30 cycles | combination | simple average | combined average | corr | |
| k(collision) | 1.001426 | 1.001225 | 0.0023 | k(col/abs) | 1.001080 | 0.0023 | 1.001219 | 0.0024 | 0.9900 |
| k(absorption) | 1.003589 | 1.000934 | 0.0023 | k(abs/tk ln) | 0.999984 | 0.0023 | 1.000394 | 0.0023 | 0.7055 |
| k(trk length) | 0.997927 | 0.999034 | 0.0026 | k(tk ln/col) | 1.000130 | 0.0023 | 1.000664 | 0.0023 | 0.7215 |
| rem life(col) | 5.5761E-01 | 5.6703E-01 | 0.0046 | k(col/abs/tk ln) | 1.000398 | 0.0022 | 1.000615 | 0.0024 | |
| rem life(abs) | 5.5822E-01 | 5.6708E-01 | 0.0046 | life(col/abs) | 5.6706E-01 | 0.0046 | 5.6719E-01 | 0.0047 | 0.9989 |
| source points generated 2814 | | | | | | | | | |
| source distribution written to file srctp cycle = 35 | | | | | | | | | |
| !problem summary | | | | | | | | | |

N16 run terminated when 35 kcode cycles were done.

+

bare u(94) sphere ref. la-4208, g. e. hansen and h. c. parton, 1969, page 4

10/01/93 11:10:32

probid = 10/01/93 11:04:27

0

| neutron creation | tracks | weight | energy | neutron loss | tracks | weight | energy |
|-------------------|--------|-----------------------|------------|-------------------|--------|-----------------------|------------|
| | | (per source particle) | | | | (per source particle) | |
| source | 105024 | 9.9977E-01 | 2.0208E+00 | escape | 90246 | 5.6753E-01 | 9.4295E-01 |
| | | | | energy cutoff | 0 | 0. | 0. |
| | | | | time cutoff | 0 | 0. | 0. |
| weight window | 0 | 0. | 0. | weight window | 0 | 0. | 0. |
| cell importance | 0 | 0. | 0. | cell importance | 0 | 0. | 0. |
| weight cutoff | 0 | 3.3083E-02 | 1.7558E-02 | weight cutoff | 15112 | 3.3216E-02 | 1.6986E-02 |
| energy importance | 0 | 0. | 0. | energy importance | 0 | 0. | 0. |
| dxtran | 0 | 0. | 0. | dxtran | 0 | 0. | 0. |
| forced collisions | 0 | 0. | 0. | forced collisions | 0 | 0. | 0. |
| exp. transform | 0 | 0. | 0. | exp. transform | 0 | 0. | 0. |
| upacattering | 0 | 0. | 0. | downscattering | 0 | 0. | 4.2719E-01 |
| | | | | capture | 0 | 4.3242E-02 | 3.1207E-02 |
| (n,xn) | 668 | 3.8288E-03 | 2.3678E-03 | loss to (n,xn) | 334 | 1.9144E-03 | 1.4723E-02 |
| fission | 0 | 0. | 0. | loss to fission | 0 | 3.9078E-01 | 6.0765E-01 |
| total | 105692 | 1.0367E+00 | 2.0407E+00 | total | 105692 | 1.0367E+00 | 2.0407E+00 |

CHAPTER 5
KCODE

| | | | | | | | | |
|---|-------------------|-------------------------------|------------------|-----------------------------------|------------------------|------------------------|---------------------------------|------------------------|
| number of neutrons banked | 334 | average lifetime, shakes | | cutoffs | | | | |
| neutron tracks per source particle | 1.0064E+00 | escape | 5.8357E-01 | tco | 1.0000+120 | | | |
| neutron collisions per source particle | 3.9639E+00 | capture | 5.6931E-01 | eco | 0.0000E+00 | | | |
| total neutron collisions | 416304 | capture or escape | 5.7739E-01 | wc1 | -5.0000E-01 | | | |
| net multiplication | 1.0019E+00 0.0002 | any termination | 6.2340E-01 | wc2 | -2.5000E-01 | | | |
| computer time so far in this run | 5.24 minutes | maximum number ever in bank | 1 | | | | | |
| computer time in mcrun | 5.23 minutes | bank overflows to backup file | 0 | | | | | |
| source particles per minute | 2.0094E+04 | field length | 0 | | | | | |
| random numbers generated | 5016855 | most random numbers used was | 490 in history | 19010 | | | | |
| range of sampled source weights = 7.2816E-01 to 1.1933E+00 | | | | | | | | |
| neutron activity in each cell print table 126 | | | | | | | | |
| cell | tracks entering | population | collisions | collisions * weight (per history) | number weighted energy | flux weighted energy | average track weight (relative) | average track mfp (cm) |
| 1 1 | 105024 | 105358 | 416304 | 2.6059E+00 | 9.5293E-01 | 1.5486E+00 | 6.7268E-01 | 2.6767E+00 |
| total | 105024 | 105358 | 416304 | 2.6059E+00 | | | | |
| neutron weight balance in each cell -- external events print table 130 | | | | | | | | |
| cell | entering | source | energy cutoff | time cutoff | exiting | total | | |
| 1 1 | 0.0000E+00 | 9.9977E-01 | 0.0000E+00 | 0.0000E+00 | -5.6753E-01 | 4.3224E-01 | | |
| total | 0.0000E+00 | 9.9977E-01 | 0.0000E+00 | 0.0000E+00 | -5.6753E-01 | 4.3224E-01 | | |
| neutron weight balance in each cell -- variance reduction events print table 130 | | | | | | | | |
| cell | weight window | cell importance | weight cutoff | energy importance | dxtran | forced collision | exponential transform | total |
| 1 1 | 0.0000E+00 | 0.0000E+00 | -1.3279E-04 | 0.0000E+00 | 0.0000E+00 | 0.0000E+00 | 0.0000E+00 | -1.3279E-04 |
| total | 0.0000E+00 | 0.0000E+00 | -1.3279E-04 | 0.0000E+00 | 0.0000E+00 | 0.0000E+00 | 0.0000E+00 | -1.3279E-04 |
| neutron weight balance in each cell -- physical events print table 130 | | | | | | | | |
| cell | (n,xn) | fission | capture | loss to (n,xn) | loss to fission | total | | |
| 1 1 | 3.8288E-03 | 0.0000E+00 | -4.3242E-02 | -1.9144E-03 | -3.9078E-01 | -4.3211E-01 | | |
| total | 3.8288E-03 | 0.0000E+00 | -4.3242E-02 | -1.9144E-03 | -3.9078E-01 | -4.3211E-01 | | |
| neutron activity of each nuclide in each cell, per source particle print table 140 | | | | | | | | |
| cell | nuclides | atom fraction | total collisions | collisions * weight | weight lost to capture | weight loss to fission | weight gain by (n,xn) | |
| 1 1 | 92235.50c | 9.3916E-01 | 389868 | 2.4408E+00 | 4.1064E-02 | 3.8375E-01 | 1.7571E-03 | |
| | 92238.50c | 5.0586E-02 | 21744 | 1.3579E-01 | 1.4638E-03 | 3.6179E-03 | 1.5430E-04 | |

CHAPTER 5
KCODE

| | | | | | | | |
|---------------------------------------|-----------|------------|------------|------------|-------------|-------------|-------------|
| | 92234.50c | 1.0250E-02 | 4692 | 2.9368E-02 | 7.1442E-04 | 3.4110E-03 | 3.0589E-06 |
| total | | | 416304 | 2.6059E+00 | 4.3242E-02 | 3.9078E-01 | 1.9144E-03 |
| total over all cells for each nuclide | | | total | collisions | weight lost | weight loss | weight gain |
| | | | collisions | * weight | to capture | to fission | by (n,xn) |
| | 92234.50c | | 4692 | 2.9368E-02 | 7.1442E-04 | 3.4110E-03 | 3.0589E-06 |
| | 92235.50c | | 389868 | 2.4408E+00 | 4.1064E-02 | 3.8375E-01 | 1.7571E-03 |
| | 92238.50c | | 21744 | 1.3579E-01 | 1.4638E-03 | 3.6179E-03 | 1.5430E-04 |

N17 1keff results for: bare u(94) sphere ref. la-4208, g. e. hansen and h. c. paxton, 1969, page 4 probid = 10/01/93 11:04:27

the initial fission neutron source distribution used the 1 source points that were input on the ksrc card.
the criticality problem was scheduled to skip 5 cycles and run a total of 35 cycles with nominally 3000 neutrons per cycle.
this problem has run 5 inactive cycles with 15244 neutron histories and 30 active cycles with 89780 neutron histories.
this calculation has completed the requested number of keff cycles using a total of 105024 fission neutron source histories.
all cells with fissionable material were sampled and had fission neutron source points.
the results of the w test for normality applied to the individual collision, absorption, and track-length keff cycle values are:
the k(collision) cycle values appear normally distributed at the 95 percent confidence level
the k(absorption) cycle values appear normally distributed at the 95 percent confidence level
the k(trk length) cycle values appear normally distributed at the 95 percent confidence level

| the final estimated combined collision/absorption/track-length keff = 1.00061 with an estimated standard deviation of 0.00242 |
| the estimated 68, 95, & 99 percent keff confidence intervals are 0.99816 to 1.00307, 0.99565 to 1.00558, and 0.99391 to 1.00732 |
| the estimated collision/absorption neutron removal lifetime = 5.67E-09 seconds with an estimated standard deviation of 2.65E-11 |

the estimated average keffs, one standard deviations, and 68, 95, and 99 percent confidence intervals are:

| keff estimator | keff | standard deviation | 68 | 95 | 99 |
|-----------------|---------|--------------------|--------------------|--------------------|--------------------|
| collision | 1.00123 | 0.00230 | 0.99890 to 1.00355 | 0.99653 to 1.00592 | 0.99489 to 1.00756 |
| absorption | 1.00093 | 0.00232 | 0.99859 to 1.00328 | 0.99619 to 1.00568 | 0.99454 to 1.00733 |
| track length | 0.99903 | 0.00264 | 0.99636 to 1.00171 | 0.99363 to 1.00444 | 0.99175 to 1.00632 |
| col/absorp | 1.00122 | 0.00237 | 0.99882 to 1.00362 | 0.99637 to 1.00607 | 0.99467 to 1.00777 |
| abs/trk len | 1.00039 | 0.00233 | 0.99803 to 1.00276 | 0.99562 to 1.00517 | 0.99395 to 1.00684 |
| col/trk len | 1.00066 | 0.00234 | 0.99829 to 1.00303 | 0.99587 to 1.00546 | 0.99420 to 1.00713 |
| col/abs/trk len | 1.00061 | 0.00242 | 0.99816 to 1.00307 | 0.99565 to 1.00558 | 0.99391 to 1.00732 |

N18 if the largest of each keff occurred on the next cycle, the keff results and 68, 95, and 99 percent confidence intervals would be:

CHAPTER 5
KCODE

| keff estimator | keff | standard deviation | 68 | | |
|-----------------|---------|--------------------|--------------------|--------------------|--------------------|
| collision | 1.00185 | 0.00231 | 0.99951 to 1.00418 | 0.99714 to 1.00656 | 0.99551 to 1.00819 |
| absorption | 1.00158 | 0.00233 | 0.99922 to 1.00394 | 0.99681 to 1.00634 | 0.99516 to 1.00799 |
| track length | 1.00005 | 0.00275 | 0.99727 to 1.00283 | 0.99443 to 1.00566 | 0.99249 to 1.00760 |
| col/abs/trk len | 1.00154 | 0.00244 | 0.99907 to 1.00400 | 0.99655 to 1.00651 | 0.99481 to 1.00824 |

N19 the estimated collision/absorption neutron lifetimes, one standard deviations, and 68, 95, and 99 percent confidence intervals are:

| type | lifetime(sec) | standard deviation | 68 | | |
|---------|---------------|--------------------|--------------------------|--------------------------|--------------------------|
| removal | 5.6719E-09 | 2.6470E-11 | 5.6451E-09 to 5.6987E-09 | 5.6176E-09 to 5.7261E-09 | 5.5987E-09 to 5.7450E-09 |
| capture | 5.6113E-09 | 3.6592E-11 | 5.5743E-09 to 5.6484E-09 | 5.5363E-09 to 5.6863E-09 | 5.5102E-09 to 5.7125E-09 |
| fission | 5.2657E-09 | 3.2574E-11 | 5.2327E-09 to 5.2987E-09 | 5.1989E-09 to 5.3324E-09 | 5.1756E-09 to 5.3557E-09 |
| escape | 5.6896E-09 | 2.1967E-11 | 5.6673E-09 to 5.7118E-09 | 5.6445E-09 to 5.7346E-09 | 5.6288E-09 to 5.7503E-09 |

N20 average keff results summed over 2 cycles each to form 15 batch values of keff print table 178

| batch number | start cycle | end cycle | keff estimators by batch | | | average keff estimators and deviations | | | | | | col/abs/tl keff | | |
|--------------|-------------|-----------|--------------------------|---------|----------|--|---------|---------|---------|----------|---------|-----------------|---------|--|
| | | | k(coll) | k(abs) | k(track) | k(coll) | st dev | k(abs) | st dev | k(track) | st dev | k(c/a/t) | st dev | |
| 1 | 6 | 7 | 1.00061 | 1.00072 | 0.99519 | | | | | | | | | |
| 2 | 8 | 9 | 0.97948 | 0.97946 | 0.98165 | 0.99005 | 0.01057 | 0.99009 | 0.01063 | 0.98842 | 0.00677 | | | |
| 3 | 10 | 11 | 1.00951 | 1.01006 | 0.99964 | 0.99654 | 0.00891 | 0.99675 | 0.00905 | 0.99216 | 0.00541 | | | |
| 4 | 12 | 13 | 1.00480 | 1.00380 | 0.99834 | 0.99860 | 0.00663 | 0.99851 | 0.00664 | 0.99371 | 0.00412 | 0.98551 | 0.00100 | |
| 5 | 14 | 15 | 0.99192 | 0.99146 | 0.99297 | 0.99727 | 0.00531 | 0.99710 | 0.00533 | 0.99356 | 0.00320 | 0.98819 | 0.00272 | |
| 6 | 16 | 17 | 0.99957 | 0.99857 | 1.01380 | 0.99765 | 0.00435 | 0.99735 | 0.00436 | 0.99693 | 0.00427 | 0.99537 | 0.00593 | |
| 7 | 18 | 19 | 0.99460 | 0.99387 | 0.99978 | 0.99721 | 0.00370 | 0.99685 | 0.00372 | 0.99734 | 0.00363 | 0.99528 | 0.00500 | |
| 8 | 20 | 21 | 0.99490 | 0.99460 | 0.99091 | 0.99692 | 0.00322 | 0.99657 | 0.00323 | 0.99654 | 0.00324 | 0.99478 | 0.00448 | |
| 9 | 22 | 23 | 1.00139 | 1.00089 | 0.99663 | 0.99742 | 0.00288 | 0.99705 | 0.00289 | 0.99655 | 0.00286 | 0.99480 | 0.00408 | |
| 10 | 24 | 25 | 0.98633 | 0.98548 | 0.98452 | 0.99631 | 0.00281 | 0.99589 | 0.00283 | 0.99534 | 0.00283 | 0.99518 | 0.00439 | |

| | | | | | | | | | | | | | | |
|----|----|----|---------|---------|---------|---------|---------|---------|---------|---------|---------|---------|---------|--|
| 11 | 26 | 27 | 1.01106 | 1.01117 | 1.00458 | 0.99765 | 0.00287 | 0.99728 | 0.00291 | 0.99618 | 0.00269 | 0.99693 | 0.00428 | |
| 12 | 28 | 29 | 1.00710 | 1.00636 | 1.00877 | 0.99844 | 0.00274 | 0.99804 | 0.00277 | 0.99723 | 0.00267 | 0.99735 | 0.00432 | |
| 13 | 30 | 31 | 1.01596 | 1.01259 | 1.01737 | 0.99979 | 0.00285 | 0.99916 | 0.00278 | 0.99878 | 0.00290 | 0.99554 | 0.00341 | |
| 14 | 32 | 33 | 1.01079 | 1.01300 | 1.00278 | 1.00057 | 0.00276 | 1.00015 | 0.00276 | 0.99907 | 0.00270 | 0.99838 | 0.00318 | |
| 15 | 34 | 35 | 1.01037 | 1.01197 | 0.99858 | 1.00123 | 0.00265 | 1.00093 | 0.00269 | 0.99903 | 0.00252 | 0.99881 | 0.00301 | |

average keff results summed over 3 cycles each to form 10 batch values of keff

| batch number | start cycle | end cycle | keff estimators by batch | | | average keff estimators and deviations | | | | | | col/abs/tl keff | | |
|--------------|-------------|-----------|--------------------------|---------|----------|--|---------|---------|---------|----------|---------|-----------------|--------|--|
| | | | k(coll) | k(abs) | k(track) | k(coll) | st dev | k(abs) | st dev | k(track) | st dev | k(c/a/t) | st dev | |
| 1 | 6 | 8 | 0.99595 | 0.99553 | 0.99450 | | | | | | | | | |
| 2 | 9 | 11 | 0.99712 | 0.99797 | 0.98982 | 0.99654 | 0.00059 | 0.99675 | 0.00122 | 0.99216 | 0.00234 | | | |
| 3 | 12 | 14 | 0.99996 | 0.99861 | 0.99858 | 0.99768 | 0.00119 | 0.99737 | 0.00094 | 0.99430 | 0.00253 | | | |

CHAPTER 5
KCODE

| | | | | | | | | | | | | | |
|----|----|----|---------|---------|---------|---------|---------|---------|---------|---------|---------|---------|---------|
| 4 | 15 | 17 | 0.99757 | 0.99728 | 1.00483 | 0.99765 | 0.00084 | 0.99735 | 0.00067 | 0.99693 | 0.00318 | 0.99721 | 0.00125 |
| 5 | 18 | 20 | 0.99357 | 0.99237 | 0.99540 | 0.99683 | 0.00104 | 0.99635 | 0.00112 | 0.99663 | 0.00248 | 0.99676 | 0.00180 |
| 6 | 21 | 23 | 1.00035 | 1.00054 | 0.99615 | 0.99742 | 0.00104 | 0.99705 | 0.00115 | 0.99655 | 0.00203 | 0.99740 | 0.00157 |
| 7 | 24 | 26 | 0.99759 | 0.99622 | 0.99574 | 0.99744 | 0.00088 | 0.99693 | 0.00098 | 0.99643 | 0.00172 | 0.99740 | 0.00136 |
| 8 | 27 | 29 | 1.00541 | 1.00579 | 1.00284 | 0.99844 | 0.00125 | 0.99804 | 0.00139 | 0.99723 | 0.00169 | 0.99889 | 0.00171 |
| 9 | 30 | 32 | 1.01525 | 1.01393 | 1.01730 | 1.00031 | 0.00217 | 0.99980 | 0.00215 | 0.99946 | 0.00268 | 0.99995 | 0.00329 |
| 10 | 33 | 35 | 1.00949 | 1.01111 | 0.99519 | 1.00123 | 0.00215 | 1.00093 | 0.00223 | 0.99903 | 0.00244 | 1.00057 | 0.00323 |

average keff results summed over 5 cycles each to form 6 batch values of keff

| batch number | start cycle | end cycle | keff estimators by batch | | | average keff estimators and deviations | | | | | | col/abs/tl keff | |
|--------------|-------------|-----------|--------------------------|---------|----------|--|---------|---------|---------|----------|---------|-----------------|---------|
| number | cycle | cycle | k(coll) | k(abs) | k(track) | k(coll) | st dev | k(abs) | st dev | k(track) | st dev | k(c/a/t) | st dev |
| 1 | 6 | 10 | 0.99497 | 0.99540 | 0.99185 | | | | | | | | |
| 2 | 11 | 15 | 0.99956 | 0.99880 | 0.99527 | 0.99727 | 0.00229 | 0.99710 | 0.00170 | 0.99356 | 0.00171 | | |
| 3 | 16 | 20 | 0.99597 | 0.99485 | 1.00276 | 0.99683 | 0.00139 | 0.99635 | 0.00124 | 0.99663 | 0.00322 | | |
| 4 | 21 | 25 | 0.99474 | 0.99451 | 0.99149 | 0.99631 | 0.00111 | 0.99589 | 0.00099 | 0.99534 | 0.00261 | 0.99451 | 0.00157 |
| 5 | 26 | 30 | 1.00985 | 1.00875 | 1.00620 | 0.99902 | 0.00284 | 0.99846 | 0.00268 | 0.99752 | 0.00297 | 0.99309 | 0.00356 |
| 6 | 31 | 35 | 1.01226 | 1.01328 | 1.00663 | 1.00123 | 0.00320 | 1.00093 | 0.00330 | 0.99903 | 0.00286 | 0.99931 | 0.00503 |

average keff results summed over 6 cycles each to form 5 batch values of keff

| batch number | start cycle | end cycle | keff estimators by batch | | | average keff estimators and deviations | | | | | | col/abs/tl keff | |
|--------------|-------------|-----------|--------------------------|---------|----------|--|---------|---------|---------|----------|---------|-----------------|---------|
| number | cycle | cycle | k(coll) | k(abs) | k(track) | k(coll) | st dev | k(abs) | st dev | k(track) | st dev | k(c/a/t) | st dev |
| 1 | 6 | 11 | 0.99654 | 0.99675 | 0.99216 | | | | | | | | |
| 2 | 12 | 17 | 0.99876 | 0.99795 | 1.00170 | 0.99765 | 0.00111 | 0.99735 | 0.00060 | 0.99693 | 0.00477 | | |
| 3 | 18 | 23 | 0.99696 | 0.99645 | 0.99577 | 0.99742 | 0.00068 | 0.99705 | 0.00046 | 0.99655 | 0.00278 | | |
| 4 | 24 | 29 | 1.00150 | 1.00100 | 0.99929 | 0.99844 | 0.00113 | 0.99804 | 0.00104 | 0.99723 | 0.00208 | 0.99436 | 0.00478 |
| 5 | 30 | 35 | 1.01237 | 1.01252 | 1.00624 | 1.00123 | 0.00292 | 1.00093 | 0.00301 | 0.99903 | 0.00242 | 0.99234 | 0.01212 |

average keff results summed over 10 cycles each to form 3 batch values of keff

| batch number | start cycle | end cycle | keff estimators by batch | | | average keff estimators and deviations | | | | | |
|--------------|-------------|-----------|--------------------------|---------|----------|--|---------|---------|---------|----------|---------|
| number | cycle | cycle | k(coll) | k(abs) | k(track) | k(coll) | st dev | k(abs) | st dev | k(track) | st dev |
| 1 | 6 | 15 | 0.99727 | 0.99710 | 0.99356 | | | | | | |
| 2 | 16 | 25 | 0.99535 | 0.99468 | 0.99713 | 0.99631 | 0.00096 | 0.99589 | 0.00121 | 0.99534 | 0.00178 |
| 3 | 26 | 35 | 1.01106 | 1.01102 | 1.00642 | 1.00123 | 0.00495 | 1.00093 | 0.00509 | 0.99903 | 0.00383 |

average keff results summed over 15 cycles each to form 2 batch values of keff

| batch number | start cycle | end cycle | keff estimators by batch | | | average keff estimators and deviations | | | | | |
|--------------|-------------|-----------|--------------------------|---------|----------|--|---------|---------|---------|----------|---------|
| number | cycle | cycle | k(coll) | k(abs) | k(track) | k(coll) | st dev | k(abs) | st dev | k(track) | st dev |
| 1 | 6 | 20 | 0.99683 | 0.99635 | 0.99663 | | | | | | |
| 2 | 21 | 35 | 1.00562 | 1.00552 | 1.00144 | 1.00123 | 0.00439 | 1.00093 | 0.00458 | 0.99903 | 0.00241 |

N21 1average individual and combined collision/absorption/track-length keff results for 5 different batch sizes

CHAPTER 5
KCODE

| cycles per keff batch | number of k batches | average keff estimators and deviations | | | | | | normality | average k(c/a/t) | | k(c/a/t) confidence intervals | |
|-----------------------|---------------------|--|--------|--------|--------|--------|--------|-----------|------------------|---------|-------------------------------|-----------------|
| | | k(coll) | st dev | k(abs) | st dev | k(trk) | st dev | co/ab/trk | k(c/a/t) | st dev | 95 | |
| 1 | 30 | 1.0012 | 0.0023 | 1.0009 | 0.0023 | 0.9990 | 0.0026 | 95/95/95 | 1.00061 | 0.00242 | 0.99565-1.00558 | 0.99391-1.00732 |
| 2 | 15 | 1.0012 | 0.0026 | 1.0009 | 0.0027 | 0.9990 | 0.0025 | 95/95/95 | 0.99881 | 0.00301 | 0.99227-1.00536 | 0.98963-1.00799 |
| 3 | 10 | 1.0012 | 0.0021 | 1.0009 | 0.0022 | 0.9990 | 0.0024 | 95/95/99 | 1.00057 | 0.00323 | 0.99294-1.00821 | 0.98927-1.01188 |
| 5 | 6 | 1.0012 | 0.0032 | 1.0009 | 0.0033 | 0.9990 | 0.0029 | 95/95/95 | 0.99931 | 0.00503 | 0.98331-1.01531 | 0.96994-1.02868 |
| 6 | 5 | 1.0012 | 0.0029 | 1.0009 | 0.0030 | 0.9990 | 0.0024 | 95/99/95 | 0.99234 | 0.01212 | 0.94021-1.04447 | 0.87210-1.11258 |

N22 individual and average keff estimator results by cycle

| keff cycle | neutron histories | keff estimators by cycle | | | average keff estimators and deviations | | | | | | average k(c/a/t) | | |
|--------------------------------------|-------------------|--------------------------|---------|----------|--|---------|---------|---------|----------|---------|------------------|---------|-------|
| | | k(coll) | k(abs) | k(track) | k(coll) | st dev | k(abs) | st dev | k(track) | st dev | k(c/a/t) | st dev | fom |
| 1 | 3000 | 1.36885 | 1.36935 | 1.34679 | | | | | | | | | |
| 2 | 4120 | 1.14900 | 1.14870 | 1.14479 | | | | | | | | | |
| 3 | 2514 | 1.06439 | 1.06444 | 1.06103 | | | | | | | | | |
| 4 | 2715 | 1.02798 | 1.02879 | 1.02058 | | | | | | | | | |
| 5 | 2895 | 0.99842 | 0.99852 | 0.99175 | | | | | | | | | |
| ----- begin active keff cycles ----- | | | | | | | | | | | | | |
| 6 | 2928 | 1.00487 | 1.00555 | 1.00412 | | | | | | | | | |
| 7 | 3043 | 0.99636 | 0.99589 | 0.98626 | 1.00061 | 0.00426 | 1.00072 | 0.00483 | 0.99519 | 0.00893 | | | |
| 8 | 2995 | 0.98661 | 0.98514 | 0.99311 | 0.99595 | 0.00528 | 0.99553 | 0.00589 | 0.99450 | 0.00520 | | | |
| 9 | 2970 | 0.97235 | 0.97379 | 0.97019 | 0.99005 | 0.00698 | 0.99009 | 0.00685 | 0.98842 | 0.00710 | 0.98916 | 0.01156 | 11041 |
| 10 | 2982 | 1.01469 | 1.01665 | 1.00558 | 0.99497 | 0.00732 | 0.99540 | 0.00751 | 0.99185 | 0.00648 | 0.99142 | 0.01032 | 11093 |
| ----- | | | | | | | | | | | | | |
| 11 | 3221 | 1.00434 | 1.00347 | 0.99369 | 0.99654 | 0.00617 | 0.99675 | 0.00628 | 0.99216 | 0.00530 | 0.99151 | 0.00835 | 13913 |
| 12 | 2972 | 0.99305 | 0.99315 | 0.99671 | 0.99604 | 0.00524 | 0.99623 | 0.00533 | 0.99281 | 0.00453 | 0.99276 | 0.00622 | 21639 |
| 13 | 2944 | 1.01656 | 1.01446 | 0.99998 | 0.99860 | 0.00521 | 0.99851 | 0.00515 | 0.99371 | 0.00402 | 0.99279 | 0.00563 | 23084 |
| 14 | 3019 | 0.99026 | 0.98823 | 0.99905 | 0.99768 | 0.00469 | 0.99737 | 0.00468 | 0.99430 | 0.00360 | 0.99373 | 0.00455 | 31595 |
| 15 | 2956 | 0.99358 | 0.99469 | 0.98689 | 0.99727 | 0.00422 | 0.99710 | 0.00419 | 0.99356 | 0.00330 | 0.99316 | 0.00408 | 35288 |
| 16 | 2932 | 1.00180 | 0.99913 | 0.99736 | 0.99768 | 0.00384 | 0.99729 | 0.00380 | 0.99390 | 0.00301 | 0.99315 | 0.00378 | 37525 |
| 17 | 2958 | 0.99733 | 0.99801 | 1.03023 | 0.99765 | 0.00350 | 0.99735 | 0.00347 | 0.99693 | 0.00409 | 0.99718 | 0.00366 | 36962 |
| 18 | 2899 | 0.99821 | 0.99850 | 1.00623 | 0.99769 | 0.00322 | 0.99744 | 0.00319 | 0.99765 | 0.00383 | 0.99750 | 0.00334 | 41148 |
| 19 | 2943 | 0.99098 | 0.98925 | 0.99333 | 0.99721 | 0.00302 | 0.99685 | 0.00301 | 0.99734 | 0.00356 | 0.99713 | 0.00316 | 42559 |
| 20 | 3028 | 0.99151 | 0.98937 | 0.98665 | 0.99683 | 0.00284 | 0.99635 | 0.00285 | 0.99663 | 0.00339 | 0.99680 | 0.00304 | 42903 |
| ----- | | | | | | | | | | | | | |
| 21 | 2923 | 0.99828 | 0.99984 | 0.99518 | 0.99692 | 0.00266 | 0.99657 | 0.00267 | 0.99654 | 0.00317 | 0.99683 | 0.00276 | 48999 |
| 22 | 3073 | 0.98951 | 0.98852 | 0.98109 | 0.99649 | 0.00253 | 0.99610 | 0.00256 | 0.99563 | 0.00311 | 0.99633 | 0.00268 | 48852 |
| 23 | 2933 | 1.01326 | 1.01325 | 1.01217 | 0.99742 | 0.00256 | 0.99705 | 0.00259 | 0.99655 | 0.00307 | 0.99731 | 0.00271 | 45206 |

CHAPTER 5
KCODE

| | | | | | | | | | | | | | |
|-------|------|---------|---------|---------|---------|---------|---------|---------|---------|---------|---------|---------|-------|
| 24 | 3151 | 0.97913 | 0.97848 | 0.97516 | 0.99646 | 0.00261 | 0.99607 | 0.00264 | 0.99542 | 0.00312 | 0.99638 | 0.00279 | 40094 |
| 25 | 2844 | 0.99353 | 0.99248 | 0.99387 | 0.99631 | 0.00248 | 0.99589 | 0.00251 | 0.99534 | 0.00296 | 0.99628 | 0.00266 | 41951 |
| 26 | 3069 | 1.02011 | 1.01769 | 1.01818 | 0.99744 | 0.00262 | 0.99693 | 0.00260 | 0.99643 | 0.00302 | 0.99686 | 0.00286 | 34499 |
| 27 | 3047 | 1.00201 | 1.00464 | 0.99098 | 0.99765 | 0.00250 | 0.99728 | 0.00251 | 0.99618 | 0.00289 | 0.99711 | 0.00266 | 38252 |
| 28 | 2981 | 0.99365 | 0.99189 | 0.99478 | 0.99748 | 0.00240 | 0.99705 | 0.00241 | 0.99612 | 0.00276 | 0.99698 | 0.00256 | 39336 |
| 29 | 3071 | 1.02056 | 1.02082 | 1.02276 | 0.99844 | 0.00249 | 0.99804 | 0.00251 | 0.99723 | 0.00287 | 0.99816 | 0.00267 | 34745 |
| 30 | 3035 | 1.01294 | 1.00872 | 1.00432 | 0.99902 | 0.00246 | 0.99846 | 0.00244 | 0.99752 | 0.00276 | 0.99824 | 0.00266 | 33705 |
| ----- | | | | | | | | | | | | | |
| 31 | 2965 | 1.01898 | 1.01646 | 1.03042 | 0.99979 | 0.00248 | 0.99916 | 0.00245 | 0.99878 | 0.00294 | 0.99882 | 0.00272 | 30817 |
| 32 | 2930 | 1.01383 | 1.01663 | 1.01715 | 1.00031 | 0.00244 | 0.99980 | 0.00244 | 0.99946 | 0.00291 | 0.99994 | 0.00264 | 31742 |
| 33 | 2912 | 1.00775 | 1.00938 | 0.98841 | 1.00057 | 0.00237 | 1.00015 | 0.00238 | 0.99907 | 0.00283 | 1.00016 | 0.00254 | 32993 |
| 34 | 2954 | 1.01930 | 1.02036 | 0.99924 | 1.00122 | 0.00238 | 1.00084 | 0.00240 | 0.99907 | 0.00273 | 1.00060 | 0.00253 | 32226 |
| 35 | 3102 | 1.00143 | 1.00359 | 0.99793 | 1.00123 | 0.00230 | 1.00093 | 0.00232 | 0.99903 | 0.00264 | 1.00061 | 0.00242 | 33974 |

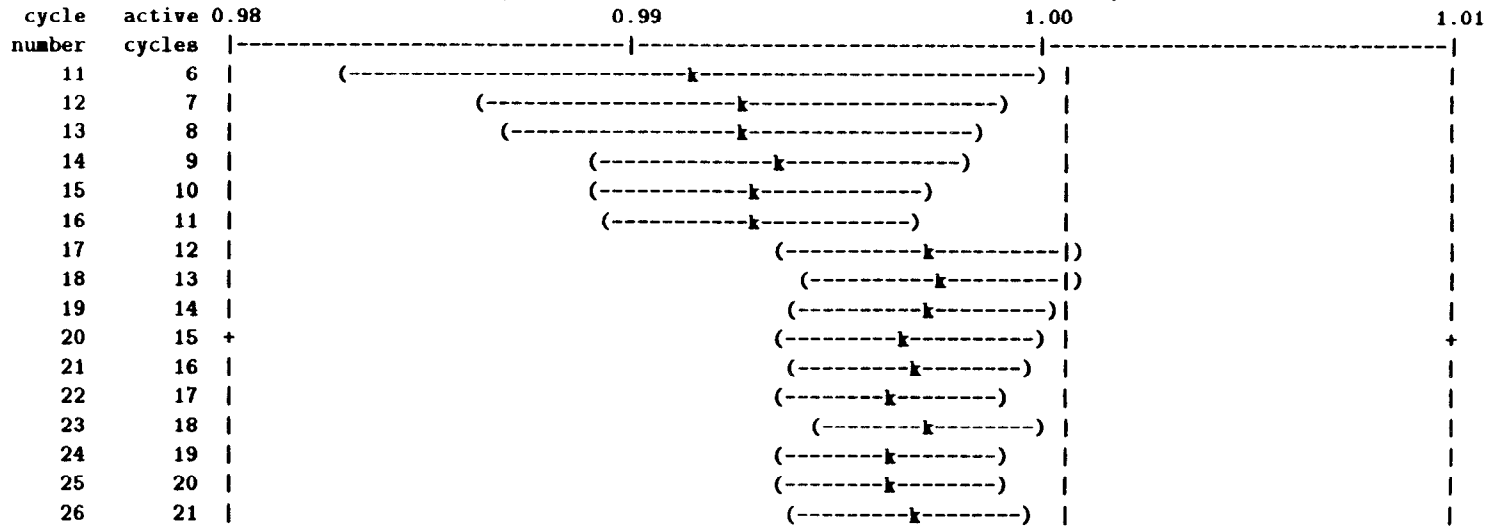
N23 the largest active cycle keffs by estimator are:

collision 1.02056 on cycle 29
 absorption 1.02082 on cycle 29
 track length 1.03042 on cycle 31

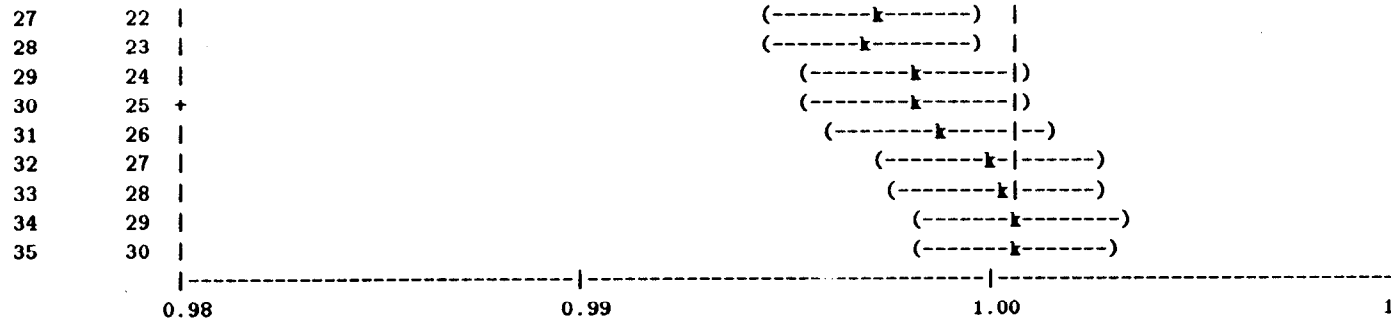
the smallest active cycle keffs by estimator are:

collision 0.97235 on cycle 9
 absorption 0.97379 on cycle 9
 track length 0.97019 on cycle 9

N24 iplot of the estimated col/abs/track-length keff one standard deviation interval versus cycle number (| = final keff = 1.00061)



CHAPTER 5
KCODE



| N25 Individual and collision/absorption/track-length keffs for different numbers of inactive cycles skipped for fission source settling | | | | | | | | | | | | | |
|---|--------|----------|--|--------|--------|--------|-----------|--------|------------------|----------|-------------------------------|-----------------|-----------------|
| skip | active | active | average keff estimators and deviations | | | | normality | | average k(c/a/t) | | k(c/a/t) confidence intervals | | |
| cycles | cycles | neutrons | k(col) | st dev | k(abs) | st dev | k(trk) | st dev | co/ab/tl | k(c/a/t) | st dev | 95 | |
| 0 | 35 | 105024 | 1.0184 | 0.0114 | 1.0182 | 0.0115 | 1.0153 | 0.0110 | no/no/no | 1.01159 | 0.01175 | 0.98766-1.03552 | 0.97941-1.04377 |
| 1 | 34 | 102024 | 1.0081 | 0.0051 | 1.0079 | 0.0051 | 1.0056 | 0.0052 | no/no/no | 1.00718 | 0.00551 | 0.99594-1.01842 | 0.99206-1.02231 |
| 2 | 33 | 97904 | 1.0039 | 0.0029 | 1.0036 | 0.0030 | 1.0013 | 0.0031 | 99/99/99 | 1.00317 | 0.00311 | 0.99680-1.00953 | 0.99460-1.01173 |
| 3 | 32 | 95390 | 1.0020 | 0.0023 | 1.0017 | 0.0023 | 0.9995 | 0.0026 | 95/95/95 | 1.00128 | 0.00243 | 0.99630-1.00626 | 0.99457-1.00799 |
| 4 | 31 | 92675 | 1.0011 | 0.0022 | 1.0009 | 0.0022 | 0.9988 | 0.0026 | 95/95/95 | 1.00050 | 0.00235 | 0.99568-1.00531 | 0.99401-1.00699 |
| 5 | 30* | 89780 | 1.0012 | 0.0023 | 1.0009 | 0.0023 | 0.9990 | 0.0026 | 95/95/95 | 1.00061 | 0.00242 | 0.99565-1.00558 | 0.99391-1.00732 |
| 6 | 29 | 86852 | 1.0011 | 0.0024 | 1.0008 | 0.0024 | 0.9989 | 0.0027 | 95/95/95 | 1.00045 | 0.00251 | 0.99529-1.00561 | 0.99347-1.00743 |
| 7 | 28 | 83809 | 1.0013 | 0.0025 | 1.0009 | 0.0025 | 0.9993 | 0.0028 | 95/95/95 | 1.00065 | 0.00257 | 0.99535-1.00595 | 0.99347-1.00783 |
| 8 | 27 | 80814 | 1.0018 | 0.0025 | 1.0015 | 0.0025 | 0.9995 | 0.0029 | 95/95/95 | 1.00115 | 0.00262 | 0.99574-1.00657 | 0.99381-1.00850 |
| 9 | 26 | 77844 | 1.0029 | 0.0023 | 1.0026 | 0.0023 | 1.0007 | 0.0028 | 95/95/95 | 1.00248 | 0.00243 | 0.99745-1.00752 | 0.99565-1.00932 |
| 10 | 25 | 74862 | 1.0025 | 0.0023 | 1.0020 | 0.0024 | 1.0005 | 0.0029 | 95/95/95 | 1.00202 | 0.00251 | 0.99682-1.00723 | 0.99496-1.00909 |
| ----- | | | | | | | | | | | | | |
| 11 | 24 | 71641 | 1.0024 | 0.0024 | 1.0020 | 0.0025 | 1.0008 | 0.0030 | 95/95/95 | 1.00202 | 0.00260 | 0.99662-1.00743 | 0.99467-1.00938 |
| 12 | 23 | 68669 | 1.0028 | 0.0025 | 1.0024 | 0.0025 | 1.0009 | 0.0031 | 95/95/95 | 1.00244 | 0.00270 | 0.99681-1.00807 | 0.99475-1.01013 |
| 13 | 22 | 65725 | 1.0022 | 0.0025 | 1.0018 | 0.0026 | 1.0010 | 0.0032 | 95/95/95 | 1.00214 | 0.00273 | 0.99643-1.00784 | 0.99434-1.00993 |
| 14 | 21 | 62706 | 1.0027 | 0.0026 | 1.0025 | 0.0026 | 1.0011 | 0.0034 | 95/95/95 | 1.00263 | 0.00280 | 0.99674-1.00852 | 0.99456-1.01070 |
| 15 | 20 | 59750 | 1.0032 | 0.0027 | 1.0029 | 0.0027 | 1.0018 | 0.0035 | 95/95/95 | 1.00315 | 0.00291 | 0.99702-1.00929 | 0.99473-1.01158 |
| 16 | 19 | 56818 | 1.0033 | 0.0028 | 1.0030 | 0.0029 | 1.0020 | 0.0037 | 95/95/95 | 1.00320 | 0.00304 | 0.99676-1.00964 | 0.99433-1.01207 |
| 17 | 18 | 53860 | 1.0036 | 0.0030 | 1.0033 | 0.0030 | 1.0004 | 0.0035 | 95/95/95 | 1.00367 | 0.00350 | 0.99620-1.01113 | 0.99335-1.01399 |
| 18 | 17 | 50961 | 1.0039 | 0.0031 | 1.0036 | 0.0032 | 1.0001 | 0.0037 | 95/95/95 | 1.00432 | 0.00389 | 0.99597-1.01266 | 0.99274-1.01590 |
| 19 | 16 | 48018 | 1.0047 | 0.0032 | 1.0045 | 0.0033 | 1.0005 | 0.0039 | 95/95/95 | 1.00535 | 0.00404 | 0.99661-1.01408 | 0.99317-1.01753 |
| 20 | 15 | 44990 | 1.0056 | 0.0033 | 1.0055 | 0.0033 | 1.0014 | 0.0041 | 95/95/95 | 1.00596 | 0.00410 | 0.99703-1.01489 | 0.99344-1.01849 |

CHAPTER 5
KCODE

| | | | | | | | | | | | | | |
|----|----|-------|--------|--------|--------|--------|--------|--------|----------|---------|---------|-----------------|-----------------|
| 21 | 14 | 42067 | 1.0061 | 0.0035 | 1.0059 | 0.0036 | 1.0019 | 0.0044 | 95/95/95 | 1.00664 | 0.00442 | 0.99692-1.01636 | 0.99292-1.02036 |
| 22 | 13 | 38994 | 1.0074 | 0.0035 | 1.0073 | 0.0036 | 1.0035 | 0.0044 | 95/95/95 | 1.00741 | 0.00437 | 0.99767-1.01714 | 0.99357-1.02125 |
| 23 | 12 | 36061 | 1.0069 | 0.0038 | 1.0068 | 0.0038 | 1.0028 | 0.0047 | 95/95/95 | 1.00681 | 0.00477 | 0.99602-1.01761 | 0.99131-1.02232 |
| 24 | 11 | 32910 | 1.0095 | 0.0031 | 1.0093 | 0.0031 | 1.0053 | 0.0043 | 95/95/95 | 1.00926 | 0.00388 | 1.00030-1.01821 | 0.99623-1.02229 |
| 25 | 10 | 30066 | 1.0111 | 0.0030 | 1.0110 | 0.0029 | 1.0064 | 0.0046 | 95/95/95 | 1.01123 | 0.00370 | 1.00249-1.01997 | 0.99829-1.02416 |
| 26 | 9 | 26997 | 1.0101 | 0.0031 | 1.0103 | 0.0031 | 1.0051 | 0.0050 | 95/95/95 | 1.01039 | 0.00400 | 1.00059-1.02018 | 0.99554-1.02523 |
| 27 | 8 | 23950 | 1.0111 | 0.0034 | 1.0110 | 0.0035 | 1.0069 | 0.0053 | 95/95/95 | 1.01111 | 0.00434 | 0.99996-1.02226 | 0.99362-1.02860 |
| 28 | 7 | 20969 | 1.0135 | 0.0026 | 1.0137 | 0.0025 | 1.0086 | 0.0057 | 95/95/95 | 1.01422 | 0.00326 | 1.00516-1.02327 | 0.99920-1.02924 |
| 29 | 6 | 17898 | 1.0124 | 0.0028 | 1.0125 | 0.0026 | 1.0062 | 0.0062 | 95/95/95 | 1.01274 | 0.00376 | 1.00077-1.02470 | 0.99078-1.03470 |
| 30 | 5 | 14863 | 1.0123 | 0.0034 | 1.0133 | 0.0030 | 1.0066 | 0.0075 | 95/95/95 | 1.01421 | 0.00463 | 0.99428-1.03414 | 0.96823-1.06019 |

| | | | | | | | | | | | | | |
|----|---|-------|--------|--------|--------|--------|--------|--------|----------|---------|---------|-----------------|-----------------|
| 31 | 4 | 11898 | 1.0106 | 0.0039 | 1.0125 | 0.0037 | 1.0007 | 0.0060 | 95/95/95 | 1.03037 | 0.07546 | 0.07133-1.98942 | 0.00000-5.83389 |
| 32 | 3 | 8968 | 1.0095 | 0.0052 | 1.0111 | 0.0049 | 0.9952 | 0.0034 | | | | | |
| 33 | 2 | 6056 | 1.0104 | 0.0089 | 1.0120 | 0.0084 | 0.9986 | 0.0007 | | | | | |

N26 the minimum estimated standard deviation for the col/abs/tl keff estimator occurs with 4 inactive cycles and 31 active cycles.

N27 the first active half of the problem skips 5 cycles and uses 15 active cycles; the second half skips 20 and uses 15 cycles.

the col/abs/trk-len keff, one standard deviation, and 68, 95, and 99 percent intervals for each active half of the problem are:

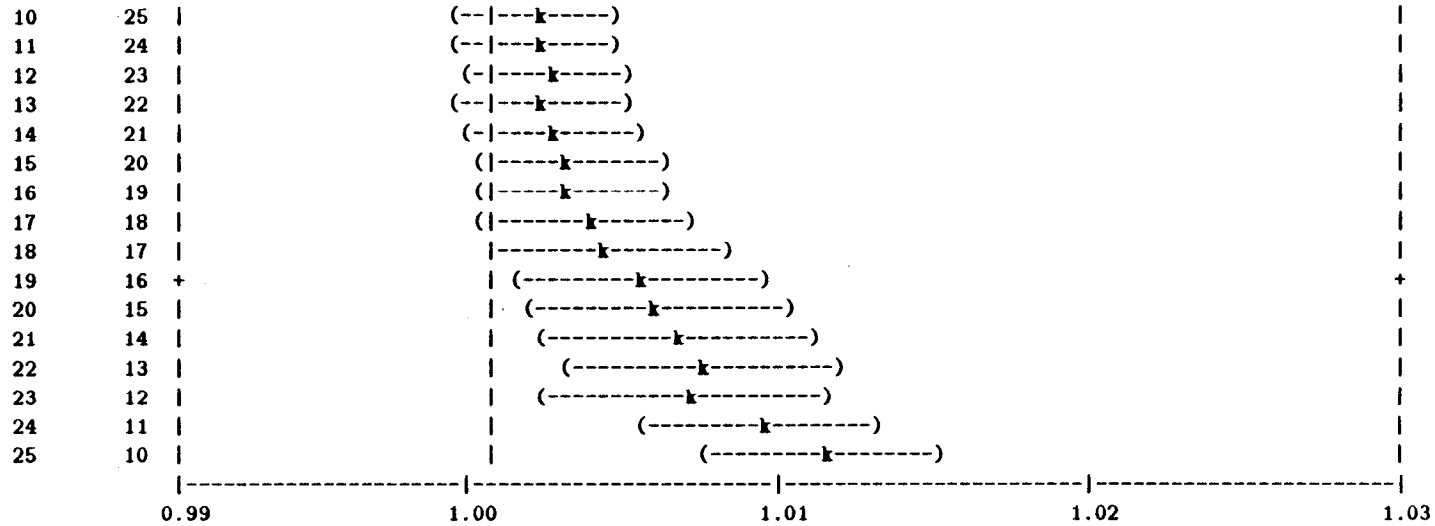
| problem | keff | standard deviation | 68 | 95 | 99 |
|--------------|---------|--------------------|--------------------|--------------------|--------------------|
| first half | 0.99680 | 0.00304 | 0.99364 to 0.99995 | 0.99017 to 1.00342 | 0.98751 to 1.00608 |
| second half | 1.00596 | 0.00410 | 1.00171 to 1.01022 | 0.99703 to 1.01489 | 0.99344 to 1.01849 |
| final result | 1.00061 | 0.00242 | 0.99816 to 1.00307 | 0.99565 to 1.00558 | 0.99391 to 1.00732 |

the first and second half values of k(collision/absorption/track length) appear to be the same at the 95 percent confidence level.

N28 plot of the estimated col/abs/track-length keff one standard deviation interval by active cycle number (| = final keff = 1.00061)

| inactive cycles | active cycles | 0.99 | 1.00 | 1.01 | 1.02 | 1.03 |
|-----------------|---------------|------|------------------------------|------|------|------|
| 0 | 35 | | (- ----- ----- ----- -----) | | | |
| 1 | 34 | | (-----k-----) | | | |
| 2 | 33 | | (-----k-----) | | | |
| 3 | 32 | | (--- k-----) | | | |
| 4 | 31 | | (-----k-----) | | | |
| 5 | 30 | * | (-----k-----) | | | * |
| 6 | 29 | | (-----k-----) | | | |
| 7 | 28 | | (-----k-----) | | | |
| 8 | 27 | | (--- k-----) | | | |
| 9 | 26 | + | (-----k-----) | | | + |

CHAPTER 5
KCODE



N29 tally 1 nps = 105024
 tally type 1 number of particles crossing a surface.
 tally for neutrons
 number of histories used for normalizing tallies = 90000.00
 surface 1

| energy | | |
|------------|-------------|--------|
| 1.0000E-07 | 0.00000E+00 | 0.0000 |
| 4.0000E-07 | 0.00000E+00 | 0.0000 |
| 1.0000E-06 | 0.00000E+00 | 0.0000 |
| 3.0000E-06 | 0.00000E+00 | 0.0000 |
| 1.0000E-05 | 0.00000E+00 | 0.0000 |
| 3.0000E-05 | 0.00000E+00 | 0.0000 |
| 1.0000E-04 | 0.00000E+00 | 0.0000 |
| 5.5000E-04 | 0.00000E+00 | 0.0000 |
| 3.0000E-03 | 9.84211E-06 | 0.7130 |
| 1.7000E-02 | 2.85292E-04 | 0.1550 |
| 1.0000E-01 | 9.64254E-03 | 0.0255 |
| 4.0000E-01 | 8.16418E-02 | 0.0086 |

CHAPTER 5
KCODE

```

9.0000E-01  1.34615E-01  0.0068
1.4000E+00  9.57863E-02  0.0088
3.0000E+00  1.62481E-01  0.0067
2.0000E+01  9.10982E-02  0.0095
total       5.75560E-01  0.0018

```

```

analysis of the results in the tally fluctuation chart bin (tfc) for tally  1 with nps = 105024  print table 160
normed average tally per history = 5.75560E-01      unnormed average tally per history = 5.75560E-01
estimated tally relative error   = 0.0018           estimated variance of the variance = 0.0000
relative error from zero tallies = 0.0013         relative error from nonzero scores = 0.0013
number of nonzero history tallies = 77627          efficiency for the nonzero tallies = 0.8625
history number of largest tally  = 61063           largest unnormalized history tally = 1.61792E+00
(largest tally)/(average tally) = 2.81103E+00      (largest tally)/(avg nonzero tally)= 2.42458E+00
(confidence interval shift)/mean = 0.0000         shifted confidence interval center = 5.75560E-01

```

if the largest history score sampled so far were to occur on the very next history, the tfc bin quantities would change as follows:
nps = 89780 for this table because 5 keff cycles and 15244 histories were skipped before tally accumulation.

| estimated quantities | value at nps | value at nps+1 | value(nps+1)/value(nps)-1. |
|--------------------------|--------------|----------------|----------------------------|
| mean | 5.75560E-01 | 5.75572E-01 | 0.000020 |
| relative error | 1.84913E-03 | 1.84181E-03 | -0.003961 |
| variance of the variance | 1.31221E-05 | 1.32743E-05 | 0.011595 |
| shifted center | 5.75560E-01 | 5.75560E-01 | 0.000000 |
| figure of merit | 5.80985E+04 | 5.85615E+04 | 0.007970 |

the estimated slope of the 43 largest tallies starting at 1.05911E+00 appears to be decreasing at least exponentially.
the empirical history score probability density function appears to be increasing at the largest history scores: please examine.
the large score tail of the empirical history score probability density function appears to have no unsampled regions.

=====

results of 10 statistical checks for the estimated answer for the tally fluctuation chart (tfc) bin of tally 1

| tfc bin | --mean-- | -----relative error----- | | | ----variance of the variance---- | | | --figure of merit-- | | -pdf- |
|----------|----------|--------------------------|----------|---------------|----------------------------------|----------|---------------|---------------------|----------|-------|
| behavior | behavior | value | decrease | decrease rate | value | decrease | decrease rate | value | behavior | slope |
| desired | random | <0.10 | yes | 1/sqrt(nps) | <0.10 | yes | 1/nps | constant | random | >3.00 |
| observed | random | 0.00 | yes | yes | 0.00 | yes | yes | constant | random | 10.00 |
| passed? | yes | yes | yes | yes | yes | yes | yes | yes | yes | yes |

=====

this tally meets the statistical criteria used to form confidence intervals: check the tally fluctuation chart to verify.

the results in other bins associated with this tally may not meet these statistical criteria.

estimated asymmetric confidence intervals(1,2,3 sigma): 5.7450E-01 to 5.7662E-01; 5.7343E-01 to 5.7769E-01; 5.7237E-01 to 5.7875E-01

estimated symmetric confidence intervals(1,2,3 sigma): 5.7450E-01 to 5.7662E-01; 5.7343E-01 to 5.7769E-01; 5.7237E-01 to 5.7875E-01

SKIP TABLES 161 AND 162 IN OUTPUT
SKIP 400 LINES IN OUTPUT

N30 tally 6 nps = 105024
tally type 6 track length estimate of heating. units mev/gram
tally for neutrons
number of histories used for normalizing tallies = 90000.00
masses
cell: 1
5.19311E+04

cell 1
energy
1.0000E-07 0.00000E+00 0.0000
4.0000E-07 0.00000E+00 0.0000
1.0000E-06 0.00000E+00 0.0000
3.0000E-06 0.00000E+00 0.0000
1.0000E-05 0.00000E+00 0.0000
3.0000E-05 0.00000E+00 0.0000
1.0000E-04 0.00000E+00 0.0000
5.5000E-04 2.49585E-08 1.0000
3.0000E-03 1.90383E-07 0.3362
1.7000E-02 2.36430E-06 0.0958
1.0000E-01 4.28619E-05 0.0209
4.0000E-01 2.18850E-04 0.0080
9.0000E-01 2.78896E-04 0.0063
1.4000E+00 1.94200E-04 0.0075
3.0000E+00 3.42771E-04 0.0057
2.0000E+01 1.76356E-04 0.0081
total 1.25651E-03 0.0019

| | |
|--|---|
| analysis of the results in the tally fluctuation chart bin (tfc) for tally 6 with nps = 105024 | print table 160 |
| normed average tally per history = 1.25651E-03 | unnormed average tally per history = 6.52522E+01 |
| estimated tally relative error = 0.0019 | estimated variance of the variance = 0.0000 |
| relative error from zero tallies = 0.0002 | relative error from nonzero scores = 0.0019 |
| number of nonzero history tallies = 89780 | efficiency for the nonzero tallies = 0.9976 |
| history number of largest tally = 19010 | largest unnormalized history tally = 3.82156E+02 |
| (largest tally)/(average tally) = 5.85660E+00 | (largest tally)/(avg nonzero tally) = 5.84228E+00 |
| (confidence interval shift)/mean = 0.0000 | shifted confidence interval center = 1.25652E-03 |

CHAPTER 5
KCODE

if the largest history score sampled so far were to occur on the very next history, the tfc bin quantities would change as follows:
nps = 89780 for this table because 5 keff cycles and 15244 histories were skipped before tally accumulation.

| estimated quantities | value at nps | value at nps+1 | value(nps+1)/value(nps)-1. |
|--------------------------|--------------|----------------|----------------------------|
| mean | 1.25651E-03 | 1.25658E-03 | 0.000054 |
| relative error | 1.94554E-03 | 1.93916E-03 | -0.003282 |
| variance of the variance | 3.45061E-05 | 3.52800E-05 | 0.022428 |
| shifted center | 1.25652E-03 | 1.25652E-03 | 0.000000 |
| figure of merit | 5.24831E+04 | 5.28294E+04 | 0.006597 |

the estimated slope of the 200 largest tallies starting at 2.12477E+02 appears to be decreasing at least exponentially.
the large score tail of the empirical history score probability density function appears to have no unsampled regions.

=====

results of 10 statistical checks for the estimated answer for the tally fluctuation chart (tfc) bin of tally 6

| tfc bin | --mean-- | -----relative error----- | | | ----variance of the variance---- | | | --figure of merit-- | | -pdf- |
|----------|----------|--------------------------|----------|---------------|----------------------------------|----------|---------------|---------------------|----------|-------|
| behavior | behavior | value | decrease | decrease rate | value | decrease | decrease rate | value | behavior | slope |
| desired | random | <0.10 | yes | 1/sqrt(nps) | <0.10 | yes | 1/nps | constant | random | >3.00 |
| observed | random | 0.00 | yes | yes | 0.00 | yes | yes | constant | random | 10.00 |
| passed? | yes | yes | yes | yes | yes | yes | yes | yes | yes | yes |

=====

this tally meets the statistical criteria used to form confidence intervals: check the tally fluctuation chart to verify.
the results in other bins associated with this tally may not meet these statistical criteria.

estimated asymmetric confidence intervals(1,2,3 sigma): 1.2541E-03 to 1.2590E-03; 1.2516E-03 to 1.2614E-03; 1.2492E-03 to 1.2639E-03
estimated symmetric confidence intervals(1,2,3 sigma): 1.2541E-03 to 1.2590E-03; 1.2516E-03 to 1.2614E-03; 1.2492E-03 to 1.2638E-03

SKIP TABLES 161 AND 162 IN OUTPUT

N31 tally 7 nps = 105024
tally type 7 track length estimate of fission heating. units mev/gram
tally for neutrons

number of histories used for normalizing tallies = 90000.00

masses

cell 1
5.19311E+04

cell 1

| energy | | | |
|------------|-------------|--------|--|
| 1.0000E-07 | 0.00000E+00 | 0.0000 | |
| 4.0000E-07 | 0.00000E+00 | 0.0000 | |
| 1.0000E-06 | 0.00000E+00 | 0.0000 | |
| 3.0000E-06 | 0.00000E+00 | 0.0000 | |

CHAPTER 5
KCODE

```

1.0000E-05  0.00000E+00  0.0000
3.0000E-05  0.00000E+00  0.0000
1.0000E-04  0.00000E+00  0.0000
5.5000E-04  2.65316E-08  1.0000
3.0000E-03  2.02845E-07  0.3362
1.7000E-02  2.51941E-06  0.0958
1.0000E-01  4.56578E-05  0.0209
4.0000E-01  2.32917E-04  0.0080
9.0000E-01  2.96302E-04  0.0063
1.4000E+00  2.06675E-04  0.0075
3.0000E+00  3.64862E-04  0.0057
2.0000E+01  1.86021E-04  0.0081
total      1.33518E-03  0.0019

```

lanalysis of the results in the tally fluctuation chart bin (tfc) for tally 7 with nps = 105024 print table 160

```

normed average tally per history = 1.33518E-03      unnormed average tally per history = 6.93376E+01
estimated tally relative error   = 0.0019          estimated variance of the variance = 0.0000
relative error from zero tallies = 0.0002         relative error from nonzero scores = 0.0019
number of nonzero history tallies = 89780         efficiency for the nonzero tallies = 0.9976
history number of largest tally  = 19010          largest unnormalized history tally = 4.07020E+02
(largest tally)/(average tally) = 5.87012E+00     (largest tally)/(avg nonzero tally)= 5.85577E+00
(confidence interval shift)/mean = 0.0000         shifted confidence interval center = 1.33519E-03

```

if the largest history score sampled so far were to occur on the very next history, the tfc bin quantities would change as follows:
nps = 89780 for this table because 5 keff cycles and 15244 histories were skipped before tally accumulation.

| estimated quantities | value at nps | value at nps+1 | value(nps+1)/value(nps)-1. |
|--------------------------|--------------|----------------|----------------------------|
| mean | 1.33518E-03 | 1.33526E-03 | 0.000054 |
| relative error | 1.94640E-03 | 1.94002E-03 | -0.003278 |
| variance of the variance | 3.45788E-05 | 3.53585E-05 | 0.022549 |
| shifted center | 1.33519E-03 | 1.33519E-03 | 0.000000 |
| figure of merit | 5.24369E+04 | 5.27823E+04 | 0.006587 |

the estimated slope of the 200 largest tallies starting at 2.25966E+02 appears to be decreasing at least exponentially.
the large score tail of the empirical history score probability density function appears to have no unsampled regions.

```

=====
results of 10 statistical checks for the estimated answer for the tally fluctuation chart (tfc) bin of tally 7
tfc bin  --mean--  -----relative error-----  ----variance of the variance----  --figure of merit--  -pdf-
behavior  behavior  value decrease decrease rate  value decrease decrease rate  value behavior slope
desired  random  <0.10  yes  1/sqrt(nps)  <0.10  yes  1/nps  constant random >3.00

```

CHAPTER 5
KCODE

```

observed    random    0.00    yes     yes     0.00    yes     yes     constant  random    10.00
passed?     yes     yes     yes     yes     yes     yes     yes     yes     yes     yes

```

```

-----
this tally meets the statistical criteria used to form confidence intervals: check the tally fluctuation chart to verify.
the results in other bins associated with this tally may not meet these statistical criteria.
estimated asymmetric confidence intervals(1,2,3 sigma): 1.3326E-03 to 1.3378E-03; 1.3300E-03 to 1.3404E-03; 1.3274E-03 to 1.3430E-03
estimated symmetric confidence intervals(1,2,3 sigma): 1.3326E-03 to 1.3378E-03; 1.3300E-03 to 1.3404E-03; 1.3274E-03 to 1.3430E-03

```

SKIP TABLES 161 AND 162 IN OUTPUT

N32 tally 14 nps = 105024

+ total neutron fluence, total fissions, total fission neutrons,
total neutron absorptions, and neutron heating (mev/gram)

tally type 4 track length estimate of particle flux.
tally for neutrons

number of histories used for normalizing tallies = 90000.00

```

multiplier bin 1: 2.76185E+03
multiplier bin 2: -2.76185E+03 10 -6
multiplier bin 3: -2.76185E+03 10 -6 -7
multiplier bin 4: -2.76185E+03 10 -2
multiplier bin 5: -5.31830E-02 10 1 -4

```

volumes

```

cell: 1
      2.76185E+03

```

cell 1

| mult bin: | 1 | 2 | 3 | 4 | 5 |
|------------|--------------------|--------------------|--------------------|--------------------|--------------------|
| energy | | | | | |
| 1.0000E-07 | 0.00000E+00 0.0000 | 0.00000E+00 0.0000 | 0.00000E+00 0.0000 | 0.00000E+00 0.0000 | 0.00000E+00 0.0000 |
| 4.0000E-07 | 0.00000E+00 0.0000 | 0.00000E+00 0.0000 | 0.00000E+00 0.0000 | 0.00000E+00 0.0000 | 0.00000E+00 0.0000 |
| 1.0000E-06 | 0.00000E+00 0.0000 | 0.00000E+00 0.0000 | 0.00000E+00 0.0000 | 0.00000E+00 0.0000 | 0.00000E+00 0.0000 |
| 3.0000E-06 | 0.00000E+00 0.0000 | 0.00000E+00 0.0000 | 0.00000E+00 0.0000 | 0.00000E+00 0.0000 | 0.00000E+00 0.0000 |
| 1.0000E-05 | 0.00000E+00 0.0000 | 0.00000E+00 0.0000 | 0.00000E+00 0.0000 | 0.00000E+00 0.0000 | 0.00000E+00 0.0000 |
| 3.0000E-05 | 0.00000E+00 0.0000 | 0.00000E+00 0.0000 | 0.00000E+00 0.0000 | 0.00000E+00 0.0000 | 0.00000E+00 0.0000 |
| 1.0000E-04 | 0.00000E+00 0.0000 | 0.00000E+00 0.0000 | 0.00000E+00 0.0000 | 0.00000E+00 0.0000 | 0.00000E+00 0.0000 |
| 5.5000E-04 | 8.28426E-06 1.0000 | 7.61728E-06 1.0000 | 1.85610E-05 1.0000 | 5.73198E-06 1.0000 | 2.49585E-08 1.0000 |
| 3.0000E-03 | 1.89333E-04 0.3453 | 5.82373E-05 0.3362 | 1.41906E-04 0.3362 | 2.74430E-05 0.3304 | 1.90383E-07 0.3362 |
| 1.7000E-02 | 5.61884E-03 0.0968 | 7.23330E-04 0.0958 | 1.76253E-03 0.0958 | 3.07280E-04 0.0962 | 2.36430E-06 0.0958 |
| 1.0000E-01 | 1.66146E-01 0.0209 | 1.31085E-02 0.0209 | 3.19916E-02 0.0209 | 4.25862E-03 0.0212 | 4.28619E-05 0.0209 |

CHAPTER 5
KCODE

```

4.0000E-01  1.11409E+00  0.0079  6.68716E-02  0.0080  1.64411E-01  0.0080  1.44496E-02  0.0082  2.18850E-04  0.0080
9.0000E-01  1.61458E+00  0.0063  8.50745E-02  0.0063  2.12250E-01  0.0063  1.20335E-02  0.0063  2.78896E-04  0.0063
1.4000E+00  1.06482E+00  0.0075  5.93417E-02  0.0075  1.50976E-01  0.0075  5.36691E-03  0.0076  1.94200E-04  0.0075
3.0000E+00  1.76402E+00  0.0057  1.04758E-01  0.0057  2.76979E-01  0.0057  4.68168E-03  0.0058  3.42771E-04  0.0057
2.0000E+01  9.53815E-01  0.0080  5.34094E-02  0.0081  1.60503E-01  0.0082  1.08038E-03  0.0084  1.76356E-04  0.0081
total        6.68329E+00  0.0019  3.83353E-01  0.0019  9.99034E-01  0.0019  4.22111E-02  0.0036  1.25651E-03  0.0019

```

analysis of the results in the tally fluctuation chart bin (tfc) for tally 14 with nps = 105024 print table 160

```

normed average tally per history = 6.68329E+00      unnormed average tally per history = 1.84583E+04
estimated tally relative error   = 0.0019           estimated variance of the variance = 0.0000
relative error from zero tallies = 0.0002         relative error from nonzero scores = 0.0019
number of nonzero history tallies =      89780      efficiency for the nonzero tallies = 0.9976
history number of largest tally  =      49932      largest unnormalized history tally = 9.05235E+04
(largest tally)/(average tally) = 4.90422E+00      (largest tally)/(avg nonzero tally)= 4.89224E+00
(confidence interval shift)/mean = 0.0000         shifted confidence interval center = 6.68331E+00

```

if the largest history score sampled so far were to occur on the very next history, the tfc bin quantities would change as follows:
nps = 89780 for this table because 5 keff cycles and 15244 histories were skipped before tally accumulation.

| estimated quantities | value at nps | value at nps+1 | value(nps+1)/value(nps)-1. |
|--------------------------|--------------|----------------|----------------------------|
| mean | 6.68329E+00 | 6.68358E+00 | 0.000043 |
| relative error | 1.92199E-03 | 1.91528E-03 | -0.003491 |
| variance of the variance | 3.05523E-05 | 3.09778E-05 | 0.013930 |
| shifted center | 6.68331E+00 | 6.68331E+00 | 0.000000 |
| figure of merit | 5.37777E+04 | 5.41551E+04 | 0.007019 |

the estimated slope of the 200 largest tallies starting at 5.83117E+04 appears to be decreasing at least exponentially.
the large score tail of the empirical history score probability density function appears to have no unsampled regions.

```

=====
results of 10 statistical checks for the estimated answer for the tally fluctuation chart (tfc) bin of tally 14
tfc bin  --mean--  -----relative error-----  ----variance of the variance----  --figure of merit--  -pdf-
behavior  behavior  value  decrease  decrease rate  value  decrease  decrease rate  value  behavior  slope
desired   random   <0.10  yes      1/sqrt(nps)    <0.10  yes      1/nps         constant  random    >3.00
observed  random   0.00   yes      yes            0.00   yes      yes           constant  random    10.00
passed?   yes      yes     yes      yes            yes     yes      yes           yes      yes      yes
=====

```

this tally meets the statistical criteria used to form confidence intervals: check the tally fluctuation chart to verify.
the results in other bins associated with this tally may not meet these statistical criteria.
estimated asymmetric confidence intervals(1,2,3 sigma): 6.6705E+00 to 6.6962E+00; 6.6576E+00 to 6.7090E+00; 6.6448E+00 to 6.7218E+00
estimated symmetric confidence intervals(1,2,3 sigma): 6.6704E+00 to 6.6961E+00; 6.6576E+00 to 6.7090E+00; 6.6448E+00 to 6.7218E+00

CHAPTER 5
KCODE

SKIP TABLES 161 AND 162 IN OUTPUT

N33 tally 24 nps = 105024

+ total neutron fluence, total fissions, total fission neutrons,
total neutron absorptions, and neutron heating (mev/gram)

tally type 4 track length estimate of particle flux.

tally for neutrons

number of histories used for normalizing tallies = 90000.00

multiplier bin 1: 2.76185E+03

multiplier bin 2: -2.76185E+03 10 -6

multiplier bin 3: -2.76185E+03 10 -6 -7

multiplier bin 4: -2.76185E+03 10 -2

multiplier bin 5: -5.31830E-02 10 1 -4

volumes

cell: 1

2.76185E+03

cell 1

mult bin:

1

2

3

4

5

energy

| | | | | | | | | | | |
|------------|-------------|--------|-------------|--------|-------------|--------|-------------|--------|-------------|--------|
| 1.6700E-04 | 8.28426E-06 | 1.0000 | 7.61728E-06 | 1.0000 | 1.85610E-05 | 1.0000 | 5.73198E-06 | 1.0000 | 2.49585E-08 | 1.0000 |
| 4.5400E-04 | 0.00000E+00 | 0.0000 | 0.00000E+00 | 0.0000 | 0.00000E+00 | 0.0000 | 0.00000E+00 | 0.0000 | 0.00000E+00 | 0.0000 |
| 1.2350E-03 | 7.06185E-05 | 0.4607 | 2.83773E-05 | 0.4821 | 6.91465E-05 | 0.4821 | 1.50679E-05 | 0.4583 | 9.27910E-08 | 0.4822 |
| 3.3500E-03 | 1.78212E-04 | 0.3771 | 4.32739E-05 | 0.3750 | 1.05446E-04 | 0.3750 | 1.73262E-05 | 0.3808 | 1.41432E-07 | 0.3750 |
| 9.1200E-03 | 1.48487E-03 | 0.1754 | 2.36775E-04 | 0.1719 | 5.76949E-04 | 0.1719 | 1.02095E-04 | 0.1739 | 7.73816E-07 | 0.1719 |
| 2.4800E-02 | 1.05798E-02 | 0.0747 | 1.12856E-03 | 0.0749 | 2.74997E-03 | 0.0749 | 4.70586E-04 | 0.0748 | 3.68937E-06 | 0.0749 |
| 6.7600E-02 | 7.40875E-02 | 0.0306 | 6.16949E-03 | 0.0306 | 1.50475E-02 | 0.0306 | 2.11415E-03 | 0.0308 | 2.01716E-05 | 0.0306 |
| 1.8400E-01 | 3.56185E-01 | 0.0143 | 2.43482E-02 | 0.0144 | 5.95710E-02 | 0.0144 | 6.52291E-03 | 0.0145 | 7.96352E-05 | 0.0144 |
| 3.0300E-01 | 4.53511E-01 | 0.0123 | 2.70026E-02 | 0.0123 | 6.63693E-02 | 0.0123 | 5.85650E-03 | 0.0123 | 8.83682E-05 | 0.0123 |
| 5.0000E-01 | 7.72843E-01 | 0.0094 | 4.24223E-02 | 0.0094 | 1.04900E-01 | 0.0094 | 7.33517E-03 | 0.0094 | 1.38933E-04 | 0.0094 |
| 8.2300E-01 | 1.03035E+00 | 0.0080 | 5.38314E-02 | 0.0080 | 1.34422E-01 | 0.0080 | 7.40464E-03 | 0.0081 | 1.76485E-04 | 0.0080 |
| 1.3530E+00 | 1.18163E+00 | 0.0071 | 6.51549E-02 | 0.0071 | 1.65368E-01 | 0.0071 | 6.26574E-03 | 0.0072 | 2.13358E-04 | 0.0071 |
| 1.7380E+00 | 6.24329E-01 | 0.0100 | 3.64327E-02 | 0.0100 | 9.41229E-02 | 0.0100 | 2.19528E-03 | 0.0100 | 1.19051E-04 | 0.0100 |
| 2.2320E+00 | 6.03935E-01 | 0.0100 | 3.65399E-02 | 0.0100 | 9.60086E-02 | 0.0100 | 1.60798E-03 | 0.0101 | 1.19597E-04 | 0.0100 |
| 2.8650E+00 | 5.33765E-01 | 0.0108 | 3.16250E-02 | 0.0108 | 8.54763E-02 | 0.0108 | 1.07163E-03 | 0.0108 | 1.03546E-04 | 0.0108 |
| 3.6800E+00 | 4.34445E-01 | 0.0123 | 2.44189E-02 | 0.0123 | 6.84404E-02 | 0.0123 | 6.59923E-04 | 0.0124 | 8.01073E-05 | 0.0123 |
| 6.0700E+00 | 4.87417E-01 | 0.0116 | 2.53571E-02 | 0.0116 | 7.58489E-02 | 0.0116 | 5.01712E-04 | 0.0117 | 8.38087E-05 | 0.0116 |
| 7.7900E+00 | 8.52832E-02 | 0.0285 | 5.83438E-03 | 0.0288 | 1.97059E-02 | 0.0288 | 5.36575E-05 | 0.0287 | 1.94623E-05 | 0.0288 |

CHAPTER 5
KCODE

| | | | | | | | | | | |
|------------|-------------|--------|-------------|--------|-------------|--------|-------------|--------|-------------|--------|
| 1.0000E+01 | 2.71914E-02 | 0.0499 | 2.27624E-03 | 0.0499 | 8.26245E-03 | 0.0499 | 9.94109E-06 | 0.0509 | 7.60786E-06 | 0.0499 |
| 1.2000E+01 | 5.41664E-03 | 0.1109 | 4.43948E-04 | 0.1109 | 1.74852E-03 | 0.1109 | 1.00878E-06 | 0.1121 | 1.48693E-06 | 0.1109 |
| 1.3500E+01 | 4.46070E-04 | 0.3665 | 3.85331E-05 | 0.3678 | 1.61584E-04 | 0.3683 | 5.95062E-08 | 0.3653 | 1.30061E-07 | 0.3679 |
| 1.5000E+01 | 7.24387E-05 | 0.6013 | 7.04338E-06 | 0.6026 | 3.10521E-05 | 0.6033 | 8.16829E-09 | 0.5996 | 2.39943E-08 | 0.6027 |
| 2.0000E+01 | 6.48325E-05 | 0.7140 | 6.01033E-06 | 0.7138 | 2.94613E-05 | 0.7141 | 4.29948E-09 | 0.7130 | 2.04417E-08 | 0.7138 |
| total | 6.68329E+00 | 0.0019 | 3.83353E-01 | 0.0019 | 9.99034E-01 | 0.0019 | 4.22111E-02 | 0.0036 | 1.25651E-03 | 0.0019 |

analysis of the results in the tally fluctuation chart bin (tfc) for tally 24 with nps = 105024 print table 160

| | |
|--|---|
| normed average tally per history = 6.68329E+00 | unnormed average tally per history = 1.84583E+04 |
| estimated tally relative error = 0.0019 | estimated variance of the variance = 0.0000 |
| relative error from zero tallies = 0.0002 | relative error from nonzero scores = 0.0019 |
| number of nonzero history tallies = 89780 | efficiency for the nonzero tallies = 0.9976 |
| history number of largest tally = 49932 | largest unnormalized history tally = 9.05235E+04 |
| (largest tally)/(average tally) = 4.90422E+00 | (largest tally)/(avg nonzero tally) = 4.89224E+00 |
| (confidence interval shift)/mean = 0.0000 | shifted confidence interval center = 6.68331E+00 |

if the largest history score sampled so far were to occur on the very next history, the tfc bin quantities would change as follows:
nps = 89780 for this table because 5 keff cycles and 15244 histories were skipped before tally accumulation.

| | | | |
|--------------------------|--------------|----------------|----------------------------|
| estimated quantities | value at nps | value at nps+1 | value(nps+1)/value(nps)-1. |
| mean | 6.68329E+00 | 6.68358E+00 | 0.000043 |
| relative error | 1.92199E-03 | 1.91528E-03 | -0.003491 |
| variance of the variance | 3.05523E-05 | 3.09778E-05 | 0.013930 |
| shifted center | 6.68331E+00 | 6.68331E+00 | 0.000000 |
| figure of merit | 5.37777E+04 | 5.41551E+04 | 0.007019 |

the estimated slope of the 200 largest tallies starting at 5.83117E+04 appears to be decreasing at least exponentially.
the large score tail of the empirical history score probability density function appears to have no unsampled regions.

=====

results of 10 statistical checks for the estimated answer for the tally fluctuation chart (tfc) bin of tally 24

| tfc bin | --mean-- | -----relative error----- | | | ----variance of the variance---- | | | --figure of merit-- | | -pdf- |
|----------|----------|--------------------------|----------|---------------|----------------------------------|----------|---------------|---------------------|----------|-------|
| behavior | behavior | value | decrease | decrease rate | value | decrease | decrease rate | value | behavior | slope |
| desired | random | <0.10 | yes | 1/sqrt(nps) | <0.10 | yes | 1/nps | constant | random | >3.00 |
| observed | random | 0.00 | yes | yes | 0.00 | yes | yes | constant | random | 10.00 |
| passed? | yes | yes | yes | yes | yes | yes | yes | yes | yes | yes |

=====

this tally meets the statistical criteria used to form confidence intervals: check the tally fluctuation chart to verify.
the results in other bins associated with this tally may not meet these statistical criteria.
estimated asymmetric confidence intervals(1,2,3 sigma): 6.6705E+00 to 6.6962E+00; 6.6576E+00 to 6.7090E+00; 6.6448E+00 to 6.7218E+00
estimated symmetric confidence intervals(1,2,3 sigma): 6.6704E+00 to 6.6961E+00; 6.6576E+00 to 6.7090E+00; 6.6448E+00 to 6.7218E+00

CHAPTER 5
KCODE

SKIP TABLES 161 AND 162 IN OUTPUT

1 status of the statistical checks used to form confidence intervals for the mean for each tally bin
 tally result of statistical checks for the tfc bin (the first check not passed is listed) and error magnitude check for all bins
 1 passed the 10 statistical checks for the tally fluctuation chart bin result
 missed all bin error check: 17 tally bins had 8 bins with zeros and 2 bins with relative errors exceeding 0.10
 2 passed the 10 statistical checks for the tally fluctuation chart bin result
 missed all bin error check: 17 tally bins had 8 bins with zeros and 2 bins with relative errors exceeding 0.10
 4 passed the 10 statistical checks for the tally fluctuation chart bin result
 missed all bin error check: 17 tally bins had 7 bins with zeros and 2 bins with relative errors exceeding 0.10
 6 passed the 10 statistical checks for the tally fluctuation chart bin result
 missed all bin error check: 17 tally bins had 7 bins with zeros and 2 bins with relative errors exceeding 0.10
 7 passed the 10 statistical checks for the tally fluctuation chart bin result
 missed all bin error check: 17 tally bins had 7 bins with zeros and 2 bins with relative errors exceeding 0.10
 14 passed the 10 statistical checks for the tally fluctuation chart bin result
 missed all bin error check: 85 tally bins had 35 bins with zeros and 10 bins with relative errors exceeding 0.10
 24 passed the 10 statistical checks for the tally fluctuation chart bin result
 missed all bin error check: 120 tally bins had 5 bins with zeros and 40 bins with relative errors exceeding 0.10
 the 10 statistical checks are only for the tally fluctuation chart bin and do not apply to other tally bins.
 the tally bins with zeros may or may not be correct: compare the source, cutoffs, multipliers, et cetera with the tally bins.
 warning. 7 of the 7 tallies had bins with relative errors greater than recommended.

N34 tally fluctuation charts

| nps | tally 1 | | | | | tally 2 | | | | | tally 4 | | | | |
|--------|------------|--------|--------|-------|---------|------------|--------|--------|-------|---------|------------|--------|--------|-------|---------|
| | mean | error | vov | slope | fom | mean | error | vov | slope | fom | mean | error | vov | slope | fom |
| 8000 | 0.0000E+00 | 0.0000 | 0.0000 | 0.0 | 0.0E+00 | 0.0000E+00 | 0.0000 | 0.0000 | 0.0 | 0.0E+00 | 0.0000E+00 | 0.0000 | 0.0000 | 0.0 | 0.0E+00 |
| 16000 | 5.7372E-01 | 0.0199 | 0.0016 | 10.0 | 59018 | 9.3436E-04 | 0.0286 | 0.0136 | 10.0 | 28735 | 2.4442E-03 | 0.0211 | 0.0025 | 10.0 | 52575 |
| 24000 | 5.7938E-01 | 0.0058 | 0.0001 | 10.0 | 60040 | 9.2937E-04 | 0.0101 | 0.0163 | 3.1 | 20138 | 2.4128E-03 | 0.0062 | 0.0003 | 10.0 | 53679 |
| 32000 | 5.7815E-01 | 0.0042 | 0.0001 | 10.0 | 60643 | 9.2348E-04 | 0.0070 | 0.0065 | 3.6 | 21640 | 2.4070E-03 | 0.0044 | 0.0002 | 10.0 | 54935 |
| 40000 | 5.7697E-01 | 0.0035 | 0.0000 | 10.0 | 59820 | 9.1828E-04 | 0.0059 | 0.0054 | 3.1 | 20925 | 2.4103E-03 | 0.0036 | 0.0001 | 10.0 | 54602 |
| 48000 | 5.7759E-01 | 0.0030 | 0.0000 | 10.0 | 59274 | 9.2043E-04 | 0.0052 | 0.0042 | 3.0 | 20454 | 2.4080E-03 | 0.0032 | 0.0001 | 10.0 | 54270 |
| 56000 | 5.7762E-01 | 0.0027 | 0.0000 | 10.0 | 58082 | 9.2148E-04 | 0.0046 | 0.0033 | 2.9 | 20353 | 2.4156E-03 | 0.0029 | 0.0001 | 10.0 | 53537 |
| 64000 | 5.7782E-01 | 0.0025 | 0.0000 | 10.0 | 58287 | 9.2432E-04 | 0.0043 | 0.0027 | 3.2 | 20065 | 2.4121E-03 | 0.0026 | 0.0001 | 10.0 | 53425 |
| 72000 | 5.7783E-01 | 0.0023 | 0.0000 | 10.0 | 58859 | 9.2387E-04 | 0.0040 | 0.0023 | 3.7 | 20211 | 2.4104E-03 | 0.0024 | 0.0000 | 10.0 | 53909 |
| 80000 | 5.7745E-01 | 0.0022 | 0.0000 | 10.0 | 58546 | 9.2274E-04 | 0.0037 | 0.0020 | 4.0 | 20154 | 2.4135E-03 | 0.0023 | 0.0000 | 10.0 | 53832 |
| 88000 | 5.7700E-01 | 0.0020 | 0.0000 | 10.0 | 58634 | 9.2238E-04 | 0.0035 | 0.0018 | 4.5 | 20075 | 2.4151E-03 | 0.0021 | 0.0000 | 10.0 | 53902 |
| 96000 | 5.7637E-01 | 0.0019 | 0.0000 | 10.0 | 58320 | 9.2221E-04 | 0.0033 | 0.0016 | 6.7 | 19920 | 2.4202E-03 | 0.0020 | 0.0000 | 10.0 | 53726 |
| 104000 | 5.7555E-01 | 0.0019 | 0.0000 | 10.0 | 58030 | 9.2137E-04 | 0.0032 | 0.0015 | 7.3 | 19867 | 2.4199E-03 | 0.0019 | 0.0000 | 10.0 | 53733 |

CHAPTER 5
KCODE

| tally 6 | | | | | | tally 7 | | | | | | tally 14 | | | | | |
|---------|------------|--------|--------|-------|---------|------------|--------|--------|-------|---------|------------|----------|--------|-------|---------|--|--|
| nps | mean | error | vov | slope | fom | mean | error | vov | slope | fom | mean | error | vov | slope | fom | | |
| 105024 | 5.7556E-01 | 0.0018 | 0.0000 | 10.0 | 58099 | 9.2151E-04 | 0.0032 | 0.0014 | 8.0 | 19883 | 2.4199E-03 | 0.0019 | 0.0000 | 10.0 | 53778 | | |
| 8000 | 0.0000E+00 | 0.0000 | 0.0000 | 0.0 | 0.0E+00 | 0.0000E+00 | 0.0000 | 0.0000 | 0.0 | 0.0E+00 | 0.0000E+00 | 0.0000 | 0.0000 | 0.0 | 0.0E+00 | | |
| 16000 | 1.2689E-03 | 0.0214 | 0.0038 | 8.1 | 51281 | 1.3485E-03 | 0.0214 | 0.0038 | 7.6 | 51243 | 6.7504E+00 | 0.0211 | 0.0025 | 10.0 | 52575 | | |
| 24000 | 1.2505E-03 | 0.0063 | 0.0004 | 10.0 | 52330 | 1.3288E-03 | 0.0063 | 0.0004 | 9.7 | 52273 | 6.6639E+00 | 0.0062 | 0.0003 | 10.0 | 53679 | | |
| 32000 | 1.2488E-03 | 0.0045 | 0.0002 | 10.0 | 53359 | 1.3270E-03 | 0.0045 | 0.0002 | 10.0 | 53305 | 6.6477E+00 | 0.0044 | 0.0002 | 10.0 | 54935 | | |
| 40000 | 1.2514E-03 | 0.0037 | 0.0001 | 10.0 | 53219 | 1.3298E-03 | 0.0037 | 0.0001 | 10.0 | 53167 | 6.6570E+00 | 0.0036 | 0.0001 | 10.0 | 54602 | | |
| 48000 | 1.2504E-03 | 0.0032 | 0.0001 | 10.0 | 52932 | 1.3287E-03 | 0.0032 | 0.0001 | 10.0 | 52883 | 6.6506E+00 | 0.0032 | 0.0001 | 10.0 | 54270 | | |
| 56000 | 1.2543E-03 | 0.0029 | 0.0001 | 10.0 | 52237 | 1.3328E-03 | 0.0029 | 0.0001 | 10.0 | 52192 | 6.6715E+00 | 0.0029 | 0.0001 | 10.0 | 53537 | | |
| 64000 | 1.2527E-03 | 0.0027 | 0.0001 | 10.0 | 52137 | 1.3311E-03 | 0.0027 | 0.0001 | 10.0 | 52092 | 6.6620E+00 | 0.0026 | 0.0001 | 10.0 | 53425 | | |
| 72000 | 1.2518E-03 | 0.0024 | 0.0001 | 10.0 | 52613 | 1.3301E-03 | 0.0024 | 0.0001 | 10.0 | 52567 | 6.6572E+00 | 0.0024 | 0.0000 | 10.0 | 53909 | | |
| 80000 | 1.2532E-03 | 0.0023 | 0.0000 | 10.0 | 52539 | 1.3316E-03 | 0.0023 | 0.0000 | 10.0 | 52492 | 6.6659E+00 | 0.0023 | 0.0000 | 10.0 | 53832 | | |
| 88000 | 1.2542E-03 | 0.0022 | 0.0000 | 10.0 | 52571 | 1.3327E-03 | 0.0022 | 0.0000 | 10.0 | 52524 | 6.6701E+00 | 0.0021 | 0.0000 | 10.0 | 53902 | | |
| 96000 | 1.2568E-03 | 0.0021 | 0.0000 | 10.0 | 52425 | 1.3355E-03 | 0.0021 | 0.0000 | 10.0 | 52379 | 6.6843E+00 | 0.0020 | 0.0000 | 10.0 | 53726 | | |
| 104000 | 1.2565E-03 | 0.0020 | 0.0000 | 10.0 | 52445 | 1.3352E-03 | 0.0020 | 0.0000 | 10.0 | 52399 | 6.6834E+00 | 0.0019 | 0.0000 | 10.0 | 53733 | | |
| 105024 | 1.2565E-03 | 0.0019 | 0.0000 | 10.0 | 52483 | 1.3352E-03 | 0.0019 | 0.0000 | 10.0 | 52437 | 6.6833E+00 | 0.0019 | 0.0000 | 10.0 | 53778 | | |

 dump no. 2 on file runtime nps = 105024 coll = 416304 ctm = 5.23 nrn = 5016855
 4 warning messages so far.

CHAPTER 5
KCODE

run terminated when 35 kcode cycles were done.
computer time = 5.25 minutes
mcnp version 4a 10/01/93

10/01/93 11:10:32

probid = 10/01/93 11:04:27

Notes:

- N1: This representation of a one-dimensional Godiva was suggested by the Nuclear Criticality Safety Group HS-6 and is from LA-4208.
- N2: The KCODE card indicates this is a criticality calculation with a nominal source size of 3000 particles, an estimate of k_{eff} of 1.0, skip 5 cycles before averaging k_{eff} or tallying, and run a total of 35 cycles if computer time permits. A tally batch size of 30 is large enough to ensure that the standard normal distribution confidence interval statements at the 1σ and 2σ levels should apply. A total of 3000 particles were selected to run the problem in less than 10 minutes. Tally normalization will be by the starting source weight by default.

To normalize a criticality calculation by the steady-state power level of a reactor, use the following conversion:

$$\left(\frac{1\text{joule/sec}}{\text{watt}}\right)\left(\frac{1\text{MeV}}{1.602E-13\text{joules}}\right)\left(\frac{\text{fission}}{180\text{MeV}}\right) \\ = 3.467E10\text{fission/watt} - \text{sec}$$

If $k_{eff} = 1$ there is one source neutron per fission (the remaining fission neutrons are absorbed or escape). For an F4 tally of 1 neutron/cm², the flux in a 10 MW reactor would be

$$(10\text{MW})\left(\frac{1\text{n/cm}^2}{\text{source}}\right)\left(\frac{1\text{source}}{\text{fission}}\right)\left(\frac{10^6\text{watts}}{1\text{MW}}\right)\left(\frac{3.467E10\text{fission}}{\text{watt} - \text{sec}}\right) \\ = 3.467E17\text{n/cm}^2 - \text{sec}$$

The normalization should be in the tally on the FM card and NOT in the source on an SDEF card.

- N3: This warning is a reminder. The tallies must be scaled by the steady state power level of the critical system in units of fission neutrons per unit time. For example, if Godiva is operating at a power level of 100 watts, the tally scaling factor would be $(3.45 \times 10^{12} \text{ fission/s}) (2.61 \text{ neutrons/fission}) = 9.0 \times 10^{12} \text{ neutrons/s}$. The tallies will then have the same time units. Tallies for subcritical systems do not include any multiplication effects because fission is treated as an absorption. Tallies can be estimated for subcritical systems by multiplying the results by the system multiplication $1/(1 - k_{eff})$. See Chapter 2 Sec. VIII for further discussion of this topic.
- N4: One source location at the center of the 94% enriched uranium sphere is used to begin the first cycle. When an SRCTP file is used, the KSRC card should be removed.

The sources for each generation are the fission locations and neutron energies from fission found in the previous generation. Therefore, in a k_{eff} calculation the fission distribution converges to a stable

CHAPTER 5

KCODE

distribution as a function of space. For complicated problem geometries, the fission distribution must converge for the calculated k_{eff} to converge. This effect is minimized by sampling a larger number of particles per generation. Usually the first generation source is not too important because subsequent later sources will have converged. If the user source selects good source points on the KSRC card, the problem will converge to a stable k_{eff} in fewer generations. It is critical that the source points have converged before k_{eff} s and tallies are calculated to ensure proper mean k_{eff} s and confidence intervals.

- N5:** This note shows the use of the FM card to calculate the quantities described by the FC14 comment card. The volume of the sphere is 2761.85 cc and is used as a multiplier to obtain total tallies. The negative sign in front of the multiplier causes the atom density to be included in the calculation. The number 0.053183 is the reciprocal of the uranium density of 18.8030 g/cc and converts the flux tally to MeV/g.
- N6:** The Hansen-Roach energy structure is used as the energy bins for all tallies except tally 24 because an E24 card exists. The energy structure on the E24 card is one commonly used at Los Alamos for a wide variety of calculations.
- N7:** This table gives detailed information about the criticality source from the KSRC card, including points accepted and rejected. Entries from the KCODE card are echoed. Table 90 shows that total (as opposed to prompt) fission $\bar{\nu}$ data are being used by default to account for the effect of delayed neutrons. Delayed neutron generation is combined with prompt neutron generation and the prompt fission neutron energy spectrum is used. Delayed neutrons typically have a softer spectrum than prompt neutrons; therefore, MCNP will predict a slightly harder fission energy spectrum. This is usually a small effect and is not significant.
- N8:** No warning of unnormalized fractions was issued because the sum of the material fractions from the M10 card is the same as the atom density in cell 1.
- N9:** The density and volume were used in determining the multipliers for the FM card.
- N10:** The cross-section tables show that ^{235}U and ^{238}U use the total $\bar{\nu}$ and ^{234}U may use prompt or total. Checking XSLIST or Table G.2 shows the ^{234}U evaluation uses the total value for $\bar{\nu}$. The neutron energy cutoff warning message is explained in N19 in the TEST1 problem output.
- N11:** If cross-section space required is too large, thinned or discrete reaction cross-section sets can be used for isotopes with small atom fractions (see Print Table 40).

- N12: An SRCTP file has been generated for possible use in future versions of the problem.
- N13: Print Table 110, showing the first 50 histories, indicates that all source points are at the origin as specified on the KSRC card. The directions are isotropic and the energy is sampled from a fission spectrum.
- N14: Five cycles are skipped before averaging of k_{eff} and tallying start. Cycle 7 begins the average tally results printout. Cycle 8 contains the first results of the simple and combined averages, which require a minimum of three values for each estimator of k_{eff} .
- N15: There are three k_{eff} estimators, and they use the collision, absorption, and track length methods discussed in Chapter 2.VIII.B. All combinations of these estimators are included. The positive correlations of the various k_{eff} estimators result in almost no reduction in the relative errors for the combined estimators. The estimator with the smallest relative error is generally selected. After 35 total cycles and 30 averaging cycles, all of the k_{eff} values agree well at unity and have an estimated relative error at the 1σ level of 0.0022. File SRCTP contains the 2814 source points that were generated during cycle 35.
- N16: The problem summary gives the results of the problem and includes the five cycles that were not used for averaging k_{eff} or tallying. The gain side on the left of the table shows that the starting source weight is slightly less than unity, which will increase the tallies slightly because of the normalization by weight. The neutrons created from fission are zero because the actual fission neutrons produced are written to the source for the next cycle. In a noncriticality problem with a point source, this value would be nonzero. The loss side of the table gives general guidelines about what happened in the problem. The values will not agree exactly with separate tallies in the problem because the point source used in the first cycle required several cycles to approach the correct spatial distribution of fission neutron sources. The loss to fission category is for the weight lost to fission, which is treated as a terminal event for the criticality calculation. Parasitic capture is listed separately. No tracks are lost to either the capture or loss to fission categories because implicit capture is being used (the default for EMCNF with no PHYS:N card present is 0).
- N17: Hundreds, often thousands, of values of k_{eff} are printed in a single KCODE problem. This page is the summary page which features the single best estimate of k_{eff} clearly outlined: "the final estimated combined collision/absorption/track-length keff = 1.00061". This summary page also includes a check to determine if each cell with fissionable material had tracks entering, collisions, and fission source points to assess problem sampling. Fissionable cells that have no

CHAPTER 5 KCODE

entering tracks may indicate geometry errors on the part of the user, excessive detail in the user's problem setup, or undersampling that can lead to an underestimate of k_{eff} . Normality tests are made of the active k_{eff} values for each estimator. If the k_{eff} estimates are not normally distributed, then all the Monte Carlo assumptions based upon the Central Limit Theorem may be suspect. In particular, the estimated relative errors and confidence intervals may not be believable. See the discussion in Chapter 2.

- N18: The summary page also gives a table of k_{eff} and confidence intervals if the largest value of k_{eff} for each estimator were to occur on the next cycle. This information provides an indication of the "upper bound" of k_{eff} in a worst-case sampling scenario.
- N19: The summary page concludes with the removal, capture, fission and escape lifetimes. These values are from the combined covariance weighted collision/absorption estimator. There is no track length estimator of lifetime.
- N20: This table show alternate batch size values. It shows k_{eff} and its variance as it would have been calculated with a different number of k_{eff} cycles per batch to assess k_{eff} correlation effects. This table saves making dozens of independent MCNP calculations to get the same information. For this problem there are seven different batch combinations: 30 batches of 1 cycle, 15 batches of 2 cycles, 10 batches of 3 cycles, 6 batches of 5 cycles, 5 batches of 6 cycles, 3 batches of 10 cycles, and 2 batches of 15 cycles. The batch size table is not the same as running 15 active cycles with 6000 histories each or 10 active cycles with 9000 histories each. Rather it is intended to see if the variance (and confidence interval) changes much by averaging over cycles to reduce the cycle-to-cycle correlation. If there is a significant change in the variance (over 30%) then there may be too much correlation between cycles. In that case the more conservative variance and confidence interval may be the larger values of the variance and confidence interval from the batch size table summary (N21).
- N21: The above alternate batch size results are summarized with confidence intervals and a normality check. The confidence intervals can be compared to assess if there appears to be a substantial cycle-to-cycle correlation effect. Because the estimated standard deviation itself has a statistical uncertainty, it is recommended to use collapses that produce at least 30 batches.
- N22: This is the k_{eff} -by-cycle table. The individual and average k_{eff} estimator results by cycle repeats the information printed while the run was in progress (see notes N14 and N15) in a more readable format. A k_{eff} figure of merit is also included.
- N23: The largest and smallest values for each of the three k_{eff} estimators and the cycle at which they occurred is provided.

- N24: The k_{eff} -by-cycle table results for the combined col/abs/track-length estimator are plotted. The final k_{eff} value (1.00061) is marked with the vertical line. This plot should be examined for any trends in the average k_{eff} . The plot shown appears to have such a trend, indicating the problem should be run farther.
- N25: This is the k_{eff} -by-number-of-active-cycles table. It provides a summary of what the results for each estimator and the combined col/abs/track-length would be had there been a different number of settle or skip cycles and active cycles. The combination actually used in this problem, 5 settle cycles and 30 active cycles, is marked with an asterisk (*).
- N26: The skip/active cycle resulting in the minimum k_{eff} error is identified. In this problem it would have been better to have 4 settle cycles and 31 active cycles rather than 5 and 30. If the best combination is significantly greater than the number of cycles actually skipped the normal spatial mode may not have been achieved in the skipped cycles and the problem should be rerun.
- N27: The k_{eff} and its estimated relative error for the first and second active halves of the problem are checked to see if they appear to be statistically the same value.
- N28: The active cycle table (N25) is plotted. The final k_{eff} value (1.00061) is marked with the vertical line.
- N29: The total leakage in tally 1 is higher than the escapes in the ledger table for two reasons. For tallying purposes the first five cycles were skipped. These five cycles had a smaller leakage because the point source in cycle one was in the center of the sphere, making leakage less likely. These smaller leakage numbers in cycles one through five are included in the ledger table escapes. Secondly, a small increase in tally 1 (0.7%) is caused by the weight normalization to 0.99271.
- N30: The heating in the uranium sphere does not include any estimate from photons. To account for photons, a coupled neutron/photon criticality problem must be run using a MODE N P card. An F7 fission heating tally may give a good approximation, see note N19.
- N31: The fission heating estimate assumes that all photons are deposited locally. The difference between the F6 and F7 tally is discussed on page 2-70. Because Godiva is an optically thick system to photons, the F7 tally should be a good approximation to the total heating. A MODE N P calculation of this problem produced a neutron heating (F6) of 1.252×10^{-3} (0.0021) MeV/g and a photon heating of 6.502×10^{-5} (0.0042), which adds to about the estimate of the F7 tally, 1.333×10^{-3} (the estimated relative errors are listed in parentheses). If the 100 watt power level normalization in note 3 is used to scale tally 7, (1.333×10^{-3} MeV/g) (51931 g) (9.0×10^{12} neutrons/s) (1.602

CHAPTER 5 KCODE

$\times 10^{-13}$ W/MeV/s) = 99.81 watts. Thus, the source normalization and tally are consistent with the 100 watt assumed power level.

- N32: Tally 14 includes several quantities based on the track length estimator. The first five cycles were not included in these estimates. Mult bin 1 is the total volume integrated fluence, which is small below 0.1 MeV because there is no moderator. Mult bin 2 is the total fissions. This is lower than the loss to fission entry in the summary because of the reduced leaking and more interactions of the point source in cycle 1. Note that the mult bin 2 result is obtained by a track length estimator and the problem summary loss to fission result is from a collision estimator. Mult bin 3 is the total fission neutrons produced, which agrees exactly with the track length k_{eff} estimator described in note 15. The estimated relative error is different for mult bin 3 because the error estimation procedures are handled differently. Dividing the total of mult bin 3 by the total of mult bin 2 gives an average value of $\bar{\nu}$ of 2.606 neutrons per fission. Mult bin 4 gives the track length estimation of absorptions, which is slightly less than the collision estimator for captures in the ledger table as expected. The neutron heating in MeV/g, mult bin 5, is the same as the F6 tally.
- N33: Tally 24 is the same as tally 14 except for the energy group structure.
- N34: The tally fluctuation charts confirm stable, efficient tallies in the bins monitored. The charts confirm that the first five cycles (15243 histories) were skipped because of the zeros after 8000 particles were run and the large reduction in the estimated relative error between 16000 and 24000 histories.

A few final points should be made about KCODE calculations. To make a KCODE calculation using the SRCTP source points file produced by a previous run, remove the KSRC card from the input file. To do a continue-run, the standard MCNP rules apply. Having an input file beginning with CONTINUE is optional. If the previous run terminated because all the cycles requested by the KCODE card were completed, another KCODE card in a continue-run input file with a new total (not how many more) number of cycles to run is needed. Otherwise, only one more cycle will be run and the code will stop again. The SRCTP file is not required for a KCODE continue-run because the source points information is contained on the RUNTPE file.

Appendix G

NEUTRON CROSS-SECTION LIBRARIES

This appendix is divided into four sections. Section I lists some of the more frequently used ENDF/B reaction types that can be used with the FMn input card. Table G.1 in Section II lists the currently available $S(\alpha, \beta)$ identifiers for the MTm card. Section III provides a brief description of the available libraries and gives a complete list of the evaluations in these libraries. Table G.2 in Section IV is a list of the cross sections maintained by X-6.

I. ENDF/B REACTION TYPES

The following list includes some of the more useful reactions for use with the FMn input card, but it is not the complete ENDF/B list. The complete list can be found in the ENDF/B manual.

| <u>R</u> | <u>Microscopic Cross-Section Description</u> |
|----------|--|
| 1 | Total |
| 2 | Elastic |
| 16 | (n,2n) |
| 17 | (n,3n) |
| 18 | Total fission (n,fx) if and only if MT=18 is used to specify fission in the original evaluation. |
| 19 | (n,f) |
| 20 | (n,n'f) |
| 21 | (n,2nf) |
| 22 | (n,n') α |
| 38 | (n,3nf) |
| 51 | (n,n') to 1 st excited state |
| 52 | (n,n') to 2 nd excited state |
| . | . |
| . | . |
| 90 | (n,n') to 40 th excited state |
| 91 | (n,n') to continuum |
| 102 | (n, γ) |
| 103 | (n,p) |
| 104 | (n,d) |
| 105 | (n,t) |
| 106 | (n, ³ He) |
| 107 | (n, α) |

In addition, for files based on ENDF/B-V *only*, the following special reactions are available:

| | |
|-----|----------------------------|
| 203 | total proton production |
| 204 | total deuterium production |

APPENDIX G

- 205 total tritium production
- 206 total ^3He production
- 207 total alpha production

Notes:

- (1) The R number for tritium production varies from nuclide to nuclide and evaluation to evaluation. For ^6Li and ^7Li

| | | |
|-----------------------------|---------|--|
| $^6\text{Li}(n,\alpha)t$ | R = 107 | AWRE, ENDF/B-IV, and Los Alamos Sublibrary evaluations |
| $^6\text{Li}(n,t)\alpha$ | R = 105 | All ENDL evaluations and ENDF/B-V |
| $^7\text{Li}(n,n')t,\alpha$ | R = 33 | ENDL evaluations |
| $^7\text{Li}(n,n')\alpha,t$ | R = 22 | AWRE evaluation |
| $^7\text{Li}(n,n')\alpha,t$ | R = 91 | ENDF/B-IV, and ENDF/B-V evaluations |
| $^7\text{Li}(n,n')\alpha,t$ | R = 205 | T-2 evaluation (3007.55) |
- (2) The nomenclature between MCNP and ENDF/B is inconsistent in that MCNP refers to the number of the reaction type as R whereas ENDF/B uses MT. They are one and the same, however. The problem arises since MCNP has an MT input card used for the $S(\alpha,\beta)$ thermal treatment.
- (3) The user looking for total production of p, d, t, ^3He , and ^4He should be warned that in some evaluations, such processes are represented using reactions with R (or MT) numbers other than the standard ones given in the above list. This is of particular importance with the so-called "pseudolevel" representation of certain reactions which take place in light isotopes. For example, the ENDF/B-V evaluation of carbon includes cross sections for the $(n,n'3\alpha)$ reaction in R = 52 to 58. The user interested in particle production from light isotopes should contact X-6 to check for the existence of pseudolevels and thus possible deviations from the above standard reaction list.

II. $S(\alpha,\beta)$ IDENTIFIERS FOR THE MTm CARD

Table G.1
Thermal $S(\alpha,\beta)$ Cross-Section Tables

| <u>ZAID</u> | <u>Description</u> | <u>*Isotopes</u> | <u>Temperature ($^{\circ}\text{K}$)</u> |
|-------------|--------------------|------------------|--|
| LWTR.01T | Light water | 1001 | 300 |
| LWTR.02T | Light water | 1001 | 400 |
| LWTR.03T | Light water | 1001 | 500 |
| LWTR.04T | Light water | 1001 | 600 |
| LWTR.05T | Light water | 1001 | 800 |
| LWTR.07T | Light water | 1001 | Don't know temp |
| POLY.01T | Polyethylene | 1001 | 300 |
| POLY.03T | Polyethylene | 1001 | Don't know temp |

APPENDIX G

| | | | |
|----------|------------------------|----------------|------|
| H/ZR.01T | ¹ H in ZrHx | 1001 | 300 |
| H/ZR.02T | ¹ H in ZrHx | 1001 | 400 |
| H/ZR.04T | ¹ H in ZrHx | 1001 | 600 |
| H/ZR.05T | ¹ H in ZrHx | 1001 | 800 |
| H/ZR.06T | ¹ H in ZrHx | 1001 | 1200 |
| | | | |
| BENZ.01T | Benzene | 1001,6000,6012 | 300 |
| BENZ.02T | Benzene | 1001,6000,6012 | 400 |
| BENZ.03T | Benzene | 1001,6000,6012 | 500 |
| BENZ.04T | Benzene | 1001,6000,6012 | 600 |
| BENZ.05T | Benzene | 1001,6000,6012 | 800 |
| | | | |
| HWTR.01T | Heavy water | 1002 | 300 |
| HWTR.02T | Heavy water | 1002 | 400 |
| HWTR.03T | Heavy water | 1002 | 500 |
| HWTR.04T | Heavy water | 1002 | 600 |
| HWTR.05T | Heavy water | 1002 | 800 |
| | | | |
| BE.01T | Beryllium metal | 4009 | 300 |
| BE.04T | Beryllium metal | 4009 | 600 |
| BE.05T | Beryllium metal | 4009 | 800 |
| BE.06T | Beryllium metal | 4009 | 1200 |
| | | | |
| BEO.01T | Beryllium oxide | 4009,8016 | 300 |
| BEO.04T | Beryllium oxide | 4009,8016 | 600 |
| BEO.05T | Beryllium oxide | 4009,8016 | 800 |
| BEO.06T | Beryllium oxide | 4009,8016 | 1200 |
| | | | |
| GRPH.01T | Graphite | 6000,6012 | 300 |
| GRPH.04T | Graphite | 6000,6012 | 600 |
| GRPH.05T | Graphite | 6000,6012 | 800 |
| GRPH.06T | Graphite | 6000,6012 | 1200 |
| GRPH.07T | Graphite | 6000,6012 | 1600 |
| GRPH.08T | Graphite | 6000,6012 | 2000 |
| | | | |
| ZR/H.01T | Zr in ZrHx | 40000 | 300 |
| ZR/H.02T | Zr in ZrHx | 40000 | 400 |
| ZR/H.04T | Zr in ZrHx | 40000 | 600 |
| ZR/H.05T | Zr in ZrHx | 40000 | 800 |
| ZR/H.06T | Zr in ZrHx | 40000 | 1200 |

*Isotopes for which the $S(\alpha, \beta)$ data are valid.

APPENDIX G

III. MCNP NEUTRON CROSS-SECTION LIBRARIES

Continuous-energy (or pointwise) neutron cross-section data for use in Monte Carlo calculations are available to MCNP from several libraries. The physics of the interactions is contained in these neutron cross-section sets. For each element or nuclide there is a set of numbers detailing (a) through which processes the inter-actions take place, (b) at which angles scattered neutrons are likely to emerge, and (c) with how much energy the scattered neutrons are likely to emerge. There is also information about photon production data, the spectra of photons produced, and the amount of energy deposited in heating. These numbers are arranged in ACE format described in Appendix F.

The cross-section data depend on incident neutron energy and are tabulated at a number of energy points sufficiently dense that linear-linear interpolation at intermediate energies represents the desired quantity to within certain specified tolerances.

Each cross-section set is generated from an evaluated data set and is then stored with a unique identifier (the ZAID number) on one of the several libraries. The evaluated data come from many sources: ENDF/B-IV, -V,¹ ENDL-79, -80, -85,² AWRE,³ as well as special Los Alamos evaluations.

Because of the linear-linear interpolation requirement as well as the detail with which the data are given in some evaluations, many of the ACE-formatted cross-section sets can be quite lengthy. For this reason, many (but not all) of the cross-section sets are also available in pseudomultigroup form. The individual cross sections have been averaged over 262 groups (263 energy boundaries) using a flat weight function. For $E_i \leq E < E_{i+1}$, MCNP uses $\sigma(E) = \sigma_i$. In the vernacular we refer to these cross sections as "discrete-reaction cross sections." One great advantage of using the discrete cross sections is that the computer storage required for cross sections is markedly reduced. Reducing storage is particularly important when running in a timesharing environment and obviously when the fully continuous sets are too large for the computer. It should be emphasized that the 262-group treatment applies only to the neutron cross sections; the secondary energy and angular distributions are identical to those on the original pointwise data file from which the discrete-reaction set was generated.

The discrete cross sections are accessed whenever a DRXS input card is used (see page 3-93). If a ZAID number is listed on the DRXS card, the cross sections are read off the corresponding discrete cross-section library rather than off the continuous-energy library. From the list in Table G.2 of this Appendix, you can determine which continuous-energy cross-section sets have discrete-reaction counterparts.

In general, cross sections (whether continuous or discrete) based on ENDF/B-V evaluations are believed to be the best available to MCNP users at this time. Therefore, the default cross sections for MCNP are based upon the ENDF/B-V evaluations, although in some cases the ENDF/B-V sets are supplemented by more recent evaluations from T-2 (the Applied Nuclear Science Group). The ENDF cross sections are denoted by the alphanumeric suf-

fixes .50C, .51C, and .50D, which represent the pointwise, thinned-pointwise, and discrete-reaction cross sections, respectively. T-2 cross-section evaluations are denoted by the .55 suffix. The cross-section file denoted by the .50D suffix is a discrete version of the ENDF continuous-energy cross-section file (.50C). The file identified by the .51C suffix is a thinned version of .50C. It is a continuous-energy cross-section file containing the same set of nuclides as the .50C file but with cross sections and angular distributions specified at far fewer energies. If there are several cross-section sets available for the same nuclide and you are uncertain which one to choose, we advise you initially to select one of the three mentioned above.

Files ENDL79 and DRL79 are continuous-energy and discrete sets based on Howerton's 1979 evaluations from Livermore. Howerton has updated some of these files (ENDL85, suffixes .35C and .35D).

Several libraries are available that contain older cross-section evaluations. BMCCS is the library that previously was RMCCS when Version 2C was current. Correspondingly, D9 is the previous version of DRMCCS. The files AMCCS, XMCCS, and UMCCS contain miscellaneous evaluations from various sources. Nuclides in these libraries should be used cautiously.

Table G.2 at the end of this Appendix lists all the cross-section sets maintained by X-6 on the standard Monte Carlo neutron libraries. The entries in each of the columns of Table G.2 are described as follows:

ZAID - the ZAID is the nuclide identification number with the form ZZZAAA.nnX

where ZZZ is the atomic number,

AAA is the mass number (000 for naturally occurring elements),

nn is the neutron cross-section identifier

X=C for continuous-energy neutron tables

X=D for discrete-reaction tables

FILE - name of one of the nuclear-data libraries. The number in parentheses following a file name refers to one of the special notes at the end of Table G.2.

SOURCE - indicates where the particular evaluation originated:

ENDF/B (Versions IV and V) is the Evaluated Nuclear Data File,¹ an American effort coordinated by the National Nuclear Data Center at Brookhaven National Laboratory. The evaluations are updated periodically by evaluators from all over the country.

ENDL (79, 80, and 85) is the Evaluated Nuclear Data Library² compiled by R. J. Howerton and his nuclear data group at the Lawrence Livermore National Laboratory. The number indicates from which year's library a particular evaluation was taken.

LASL-SUB - The Los Alamos Sublibrary is a collection of special evaluations prepared by the Nuclear Data Group (T-2) at Los Alamos.

FOSTER - special evaluations representative of the average fission

APPENDIX G

products for ^{235}U and ^{239}Pu . This work was carried out in Group T-2 and is described in Reference 4.

GROUP T-2 - recently completed evaluations of selected isotopes prepared in Group T-2 at Los Alamos. Sometimes abbreviated GP. T-2.

MAT - for ENDF/B, MAT is the material identifier for a particular evaluation. For the ENDL-85 library, a MAT was assigned for each nuclide to be compatible with ENDF/B procedures. ENDL-79 and 80 contain no MAT identifiers.

TYPE - CONT indicates a continuous-energy cross-section set;
- DISC indicates a discrete-reaction cross-section set;
- MULT indicates a multigroup cross-section set.

TEMP - the temperature (in degrees Kelvin) at which the data were processed. The temperature enters into the processing only through the Doppler broadening of cross sections. Doppler broadening, in the current context, refers to a change in cross section resulting from thermal motion (translation, rotation, and vibration) of nuclei in a target material. Doppler broadening is done on all cross sections for incident neutron (nonrelativistic energies) on a target at some temperature (TEMP) in which the free-atom approximation is valid.

In general an increase in the temperature of the material containing neutron-absorbing nuclei in a homogeneous system results in Doppler broadening of resonances and an increase in resonance absorption. Furthermore, a constant cross section at zero K goes to $1/v$ behavior as the temperature increases. You should not only use the best evaluations but also use evaluations that are at temperatures approximating temperatures in your application. Contact X-6 for guidance or generation of specific temperature libraries. All ENDF/B-V evaluations on the standard libraries (that is, pointwise, thinned-pointwise, and discrete) were processed at room temperature (300 K).

GPD "Yes" means that gamma-production data exist; "No" means that such data do not exist. Between sets with gamma-production data, there is a further distinction represented as follows: "P" indicates sets with a pointwise representation of the energy dependence of the gamma-production cross section; "H" indicates that the energy dependence of the gamma-production cross section is represented as a histogram over 30 energy groups. The "H" type of representation is found on cross-section sets processed before 1977, approximately. Before then, gamma-production information was incorporated into MCNP calculations using gamma-production matrices calculated in a 30-neutron group and 12-gamma group structure. When the ACE format was changed, the total cross section was calculated from the matrices and used in histogram form so old problems could track. In the case of discrete cross-section sets in Table G.2, the "P" or "H" refers to the type of data in the original file before processing into discrete form. Those materials that have photon-

production information given in expanded ACE format are indicated by the notation (E).

LENGTH - the total length of a particular cross-section file in decimal. It is understood that the actual storage requirement in an MCNP problem will often be less because certain data unneeded for a problem will be deleted.

NUBAR - for fissionable material, NUBAR indicates the type of fission nu data available. PROMPT means that only prompt nu data are given; TOTAL means that only total nu data are given; BOTH means that prompt and total nu are given.

ARROW - the arrow that precedes certain nuclides listed in the table indicates what we believe to be the best available evaluation. You should note that because of various size limitations, the evaluation designated by the arrow may not be the default evaluation.

Finally, you may introduce a cross-section library of your own by using the XS input card.

REFERENCES

1. D. Garber (editor), "ENDF/B-V," Report BNL-17541 (ENDF-201), National Nuclear Data Center, Brookhaven National Laboratory, Upton, N. Y. (October 1975).
2. R. J. Howerton, D. E. Cullen, R. C. Haight, M. H. MacGregor, S. T. Perkins, and E. F. Plechaty, "The LLL Evaluated Nuclear Data Library (ENDL): Evaluation Techniques, Reaction Index, and Descriptions of Individual Reactions," Lawrence Livermore National Laboratory report UCRL-50400, Vol. 15, Part A (September 1975).
3. K. Parker, "The Format and Conventions of the U.K.A.E.A. Nuclear Data Library," Atomic Weapons Research Establishment report AWRE O-70/63, Aldermasten, England (1963).
4. D. G. Foster, Jr. and E. D. Arthur, "Average Neutronic Properties of "Prompt" Fission Products," Los Alamos National Laboratory report LA-9168-MS (February 1982).

APPENDIX G

IV. CROSS SECTIONS MAINTAINED BY X-6

Table G.2
Cross Sections Maintained by X-6

| ZAID | FILE | SOURCE | MAT | TYPE | TEMP(°K) | GPD | LENGTH | NUBAR |
|----------------------------|------------|-----------|------|------|----------|----------|--------|-------|
| z = 0 ***** neutron ***** | | | | | | | | |
| ** neutron ** | | | | | | | | |
| 1.32c | neutxs(1) | endl-80 | | cont | 0 | no | 738 | |
| 1.32d | neutxsd(1) | endl-80 | | disc | 0 | no | 1603 | |
| z = 1 ***** hydrogen ***** | | | | | | | | |
| ** h-1 ** | | | | | | | | |
| 1001.04c | bmccs | endf/b-iv | 1269 | cont | 0 | yes p | 2459 | |
| 1001.04d | d9 | endf/b-iv | 1269 | disc | 0 | yes p | 2914 | |
| 1001.31c | endl79 | endl-79 | | cont | 0 | no | 2496 | |
| 1001.31d | drl79 | endl-79 | | disc | 0 | no | 2082 | |
| 1001.35c | endl85 | endl-85 | 2 | cont | 0 | yes p(e) | 3567 | |
| → 1001.50c | rmccs | endf/b-v | 1301 | cont | 300 | yes p(e) | 2827 | |
| 1001.50d | drmccs | endf/b-v | 1301 | disc | 300 | yes p(e) | 3236 | |
| 1001.50m | mgxsnp | endf/b-v | 1301 | mult | 300 | yes | 3249 | |
| 1001.51c | endf5t | endf/b-v | 1301 | cont | 300 | yes p(e) | 2827 | |
| 1001.53c | eprixs | endf/b-v | 1301 | cont | 600 | yes p(e) | 4001 | |
| ** h-2 ** | | | | | | | | |
| 1002.04c | amccs | endf/b-iv | 1120 | cont | 0 | yes p | 2144 | |
| 1002.31c | endl79 | endl-79 | | cont | 0 | no | 1926 | |
| 1002.31d | drl79 | endl-79 | | disc | 0 | no | 2630 | |
| 1002.35c | endl85 | endl-85 | 3 | cont | 0 | yes p(e) | 2568 | |
| 1002.50c | endf5p | endf/b-v | 1302 | cont | 300 | yes p(e) | 4048 | |
| 1002.50d | dre5 | endf/b-v | 1302 | disc | 300 | yes p(e) | 4747 | |
| 1002.51c | endf5t | endf/b-v | 1302 | cont | 300 | yes p(e) | 3978 | |
| → 1002.55c | rmccs | group t-2 | 120 | cont | 300 | yes p(e) | 6042 | |
| 1002.55d | drmccs | group t-2 | 120 | disc | 300 | yes p(e) | 5404 | |
| 1002.55m | mgxsnp | group t-2 | 120 | mult | 300 | yes | 3542 | |
| ** h-3 ** | | | | | | | | |
| 1003.03c | bmccs | endf/b-iv | 1169 | cont | 300 | no | 2114 | |
| 1003.03d | d9 | endf/b-iv | 1169 | disc | 300 | no | 2702 | |
| 1003.31c | endl79 | endl-79 | | cont | 0 | no | 1361 | |
| 1003.31d | drl79 | endl-79 | | disc | 0 | no | 2259 | |
| 1003.35c | endl85 | endl-85 | 4 | cont | 0 | no | 1310 | |
| → 1003.50c | rmccs | endf/b-v | 1169 | cont | 300 | no | 2469 | |
| 1003.50d | drmccs | endf/b-v | 1169 | disc | 300 | no | 2848 | |
| 1003.50m | mgxsnp | endf/b-v | 1169 | mult | 300 | no | 1927 | |
| 1003.51c | endf5t | endf/b-v | 1169 | cont | 300 | no | 2434 | |
| z = 2 ***** helium ***** | | | | | | | | |
| ** he-3 ** | | | | | | | | |
| 2003.31c | endl79 | endl-79 | | cont | 0 | no | 1743 | |
| 2003.31d | drl79 | endl-79 | | disc | 0 | no | 2313 | |
| 2003.35c | endl85 | endl-85 | 5 | cont | 0 | yes p(e) | 2542 | |
| → 2003.50c | rmccs | endf/b-v | 1146 | cont | 300 | no | 2361 | |
| 2003.50d | drmccs | endf/b-v | 1146 | disc | 300 | no | 2653 | |
| 2003.50m | mgxsnp | endf/b-v | 1146 | mult | 300 | no | 1843 | |
| 2003.51c | endf5t | endf/b-v | 1146 | cont | 300 | no | 2361 | |

APPENDIX G

| ZAID | FILE | SOURCE | MAT | TYPE | TEMP(°K) | GPD | LENGTH | NUBAR |
|------------------------------------|--------|-----------|------|------|----------|----------|--------|-------|
| ** he-4 ** | | | | | | | | |
| 2004.03c | bmccs | endf/b-iv | 1270 | cont | 300 | no | 2407 | |
| 2004.03d | d9 | endf/b-iv | 1270 | disc | 300 | no | 2202 | |
| 2004.31c | endl79 | endl-79 | | cont | 0 | no | 1548 | |
| 2004.31d | drl79 | endl-79 | | disc | 0 | no | 2408 | |
| 2004.35c | endl85 | endl-85 | 6 | cont | 0 | no | 1483 | |
| → 2004.50c | rmccs | endf/b-v | 1270 | cont | 300 | no | 3102 | |
| 2004.50d | drmccs | endf/b-v | 1270 | disc | 300 | no | 2692 | |
| 2004.50m | mgxsnp | endf/b-v | 1270 | mult | 300 | no | 1629 | |
| 2004.51c | endf5t | endf/b-v | 1270 | cont | 300 | no | 2682 | |
| z = 3 ***** lithium ***** | | | | | | | | |
| ** li-6 ** | | | | | | | | |
| 3006.04c | xmccs | endf/b-iv | 1271 | cont | 0 | yes p | 4615 | |
| 3006.10c | bmccs | lasl-sub | 101 | cont | 0 | yes p | 8294 | |
| 3006.10d | d9 | lasl-sub | 101 | disc | 0 | yes p | 6742 | |
| 3006.31c | endl79 | endl-79 | | cont | 0 | no | 5928 | |
| 3006.31d | drl79 | endl-79 | | disc | 0 | no | 5012 | |
| → 3006.50c | rmccs | endf/b-v | 1303 | cont | 300 | yes p(e) | 9993 | |
| 3006.50d | drmccs | endf/b-v | 1303 | disc | 300 | yes p(e) | 8777 | |
| 3006.50m | mgxsnp | endf/b-v | 1303 | mult | 300 | yes | 3566 | |
| 3006.51c | endf5t | endf/b-v | 1303 | cont | 300 | yes p(e) | 9196 | |
| ** li-7 ** | | | | | | | | |
| 3007.05c | bmccs | endf/b-iv | 1272 | cont | 0 | yes p | 3751 | |
| 3007.05d | d9 | endf/b-iv | 1272 | disc | 0 | yes p | 3801 | |
| 3007.31c | endl79 | endl-79 | | cont | 0 | no | 2721 | |
| 3007.31d | drl79 | endl-79 | | disc | 0 | no | 3215 | |
| 3007.50c | endf5p | endf/b-v | 1272 | cont | 300 | yes p(e) | 4925 | |
| 3007.50d | dre5 | endf/b-v | 1272 | disc | 300 | yes p(e) | 4996 | |
| 3007.51c | endf5t | endf/b-v | 1272 | cont | 300 | yes p(e) | 4925 | |
| → 3007.55c | rmccs | group t-2 | 3007 | cont | 300 | yes p(e) | 13232 | |
| 3007.55d | drmccs | group t-2 | 3007 | disc | 300 | yes p(e) | 12708 | |
| 3007.55m | mgxsnp | group t-2 | 3007 | mult | 300 | yes | 3555 | |
| z = 4 ***** beryllium ***** | | | | | | | | |
| ** be-7 ** | | | | | | | | |
| 4007.35c | endl85 | endl-85 | 9 | cont | 0 | no | 1875 | |
| 4007.35m | mgxsnp | endl-85 | 9 | mult | 0 | no | 1598 | |
| ** be-9 ** | | | | | | | | |
| 4009.03c | bmccs | lasl-sub | 104 | cont | 300 | yes p | 7885 | |
| 4009.03d | d9 | lasl-sub | 104 | disc | 300 | yes p | 6622 | |
| 4009.31c | endl79 | endl-79 | | cont | 0 | no | 7737 | |
| 4009.31d | drl79 | endl-79 | | disc | 0 | no | 7329 | |
| → 4009.50c | rmccs | endf/b-v | 1304 | cont | 300 | yes p(e) | 8947 | |
| 4009.50d | drmccs | endf/b-v | 1304 | disc | 300 | yes p(e) | 8817 | |
| 4009.50m | mgxsnp | endf/b-v | 1304 | mult | 300 | yes | 3014 | |
| 4009.51c | endf5t | endf/b-v | 1304 | cont | 300 | yes p(e) | 8073 | |
| z = 5 ***** boron ***** | | | | | | | | |
| ** b-10 ** | | | | | | | | |
| 5010.03c | bmccs | endf/b-iv | 1273 | cont | 0 | yes p | 9241 | |
| 5010.03d | d9 | endf/b-iv | 1273 | disc | 0 | yes p | 5720 | |
| 5010.31c | endl79 | endl-79 | | cont | 0 | no | 5180 | |

APPENDIX G

| ZAID | FILE | SOURCE | MAT | TYPE | TEMP(°K) | GPD | LENGTH | NUBAR |
|----------------------------|--------|-----------|------|------|----------|----------|--------|-------|
| 5010.31d | drl79 | endl-79 | | disc | 0 | no | 3902 | |
| 5010.35c | endl85 | endl-85 | 11 | cont | 0 | yes p(e) | 7204 | |
| → 5010.50c | rmccs | endf/b-v | 1305 | cont | 300 | yes p(e) | 20261 | |
| 5010.50d | drmccs | endf/b-v | 1305 | disc | 300 | yes p(e) | 12383 | |
| 5010.50m | mgxsnp | endf/b-v | 1305 | mult | 300 | yes | 3557 | |
| 5010.51c | endf5t | endf/b-v | 1305 | cont | 300 | yes p(e) | 18886 | |
| 5010.53c | eprixs | endf/b-v | 1305 | cont | 600 | yes p(e) | 23676 | |
| ** b-11 ** | | | | | | | | |
| 5011.31c | endl79 | endl-79 | | cont | 0 | no | 3024 | |
| 5011.31d | drl79 | endl-79 | | disc | 0 | no | 3946 | |
| 5011.35c | endl85 | endl-85 | 12 | cont | 0 | yes p(e) | 4350 | |
| 5011.50c | endf5p | endf/b-v | 1160 | cont | 300 | no | 4385 | |
| 5011.50d | dre5 | endf/b-v | 1160 | disc | 300 | no | 2853 | |
| 5011.51c | endf5t | endf/b-v | 1160 | cont | 300 | no | 4193 | |
| 5011.55c | rmccsa | group t-2 | 5011 | cont | 300 | yes p(e) | 12315 | |
| 5011.55d | drmccs | group t-2 | 5011 | disc | 300 | yes p(e) | 7167 | |
| → 5011.56c | newxs | group t-2 | 5011 | cont | 300 | yes p(e) | 56990 | |
| 5011.56d | newxsd | group t-2 | 5011 | disc | 300 | yes p(e) | 17409 | |
| 5011.56m | mgxsnp | group t-2 | 5011 | mult | 300 | yes | 2795 | |
| z = 6 ***** carbon ***** | | | | | | | | |
| ** c-nat ** | | | | | | | | |
| → 6000.50c | rmccs | endf/b-v | 1306 | cont | 300 | yes p(e) | 23387 | |
| 6000.50d | drmccs | endf/b-v | 1306 | disc | 300 | yes p(e) | 16905 | |
| 6000.50m | mgxsnp | endf/b-v | 1306 | mult | 300 | yes | 2933 | |
| 6000.51c | endf5t | endf/b-v | 1306 | cont | 300 | yes p(e) | 23067 | |
| ** c-12 ** | | | | | | | | |
| 6012.03c | xmccs | endf/b-iv | 1274 | cont | 0 | yes p | 7567 | |
| 6012.10c | bmccs | lasl-sub | 102 | cont | 0 | yes p(e) | 12102 | |
| 6012.10d | d9 | lasl-sub | 102 | disc | 0 | yes p(e) | 9832 | |
| 6012.31c | endl79 | endl-79 | | cont | 0 | no | 3610 | |
| 6012.31d | drl79 | endl-79 | | disc | 0 | no | 3583 | |
| 6012.35c | endl85 | endl-85 | 13 | cont | 0 | yes p(e) | 5215 | |
| → 6012.50c | rmccs | endf/b-v | 1306 | cont | 300 | yes p(e) | 23387 | |
| 6012.50d | drmccs | endf/b-v | 1306 | disc | 300 | yes p(e) | 16905 | |
| 6012.50m | mgxsnp | endf/b-v | 1306 | mult | 300 | yes | 2933 | |
| ** c-13 ** | | | | | | | | |
| 6013.35c | endl85 | endl-85 | 14 | cont | 0 | yes p(e) | 4947 | |
| z = 7 ***** nitrogen ***** | | | | | | | | |
| ** n-14 ** | | | | | | | | |
| 7014.04c | bmccs | endf/b-iv | 1275 | cont | 0 | yes p | 21553 | |
| 7014.04d | d9 | endf/b-iv | 1275 | disc | 0 | yes p | 9874 | |
| → 7014.50c | rmccs | endf/b-v | 1275 | cont | 300 | yes p(e) | 45518 | |
| 7014.50d | drmccs | endf/b-v | 1275 | disc | 300 | yes p(e) | 26854 | |
| 7014.50m | mgxsnp | endf/b-v | 1275 | mult | 300 | yes | 3501 | |
| 7014.51c | endf5t | endf/b-v | 1275 | cont | 300 | yes p(e) | 45397 | |
| ** n-15 ** | | | | | | | | |
| → 7015.55c | rmccsa | group t-2 | 9993 | cont | 300 | yes p(e) | 20981 | |
| 7015.55d | drmccs | group t-2 | 9993 | disc | 300 | yes p(e) | 15334 | |
| 7015.55m | mgxsnp | group t-2 | 9993 | mult | 300 | yes | 2743 | |

APPENDIX G

| ZAID | FILE | SOURCE | MAT | TYPE | TEMP(*K) | GPD | LENGTH | NUBAR |
|------------------------------|-----------|---------|-----------|------|----------|-----|----------|-------|
| z = 8 ***** oxygen ***** | | | | | | | | |
| ** o-16 ** | | | | | | | | |
| | 8016.04c | bmccs | endf/b-iv | 1276 | cont | 0 | yes p | 21823 |
| | 8016.04d | d9 | endf/b-iv | 1276 | disc | 0 | yes p | 10486 |
| | 8016.35c | endl85 | endl-85 | 16 | cont | 0 | yes p(e) | 10418 |
| → | 8016.50c | rmccs | endf/b-v | 1276 | cont | 300 | yes p(e) | 38003 |
| | 8016.50d | drmccs | endf/b-v | 1276 | disc | 300 | yes p(e) | 20516 |
| | 8016.50m | mgxsnp | endf/b-v | 1276 | mult | 300 | yes | 3346 |
| | 8016.51c | endf5t | endf/b-v | 1276 | cont | 300 | yes p(e) | 37996 |
| | 8016.53c | eprixs | endf/b-v | 1276 | cont | 600 | yes p(e) | 37989 |
| | 8016.54c | eprixs | endf/b-v | 1276 | cont | 900 | yes p(e) | 38017 |
| z = 9 ***** fluorine ***** | | | | | | | | |
| ** f-19 ** | | | | | | | | |
| | 9019.02c | xmccs | endf/b-iv | 1277 | cont | 0 | yes h | 26334 |
| | 9019.03c | bmccs | endf/b-iv | 1277 | cont | 0 | yes p | 24464 |
| | 9019.03d | d9 | endf/b-iv | 1277 | disc | 0 | yes p | 8926 |
| | 9019.31c | endl79 | endl-79 | | cont | 0 | no | 23368 |
| | 9019.31d | drl79 | endl-79 | | disc | 0 | no | 9764 |
| | 9019.35c | endl85 | endl-85 | 17 | cont | 0 | yes p(e) | 31608 |
| → | 9019.50c | endf5p | endf/b-v | 1309 | cont | 300 | yes p(e) | 44191 |
| | 9019.50d | dre5 | endf/b-v | 1309 | disc | 300 | yes p(e) | 23217 |
| | 9019.50m | mgxsnp | endf/b-v | 1309 | mult | 300 | yes | 3261 |
| | 9019.51c | rmccs | endf/b-v | 1309 | cont | 300 | yes p(e) | 41503 |
| | 9019.51d | drmccs | endf/b-v | 1309 | disc | 300 | yes p(e) | 23217 |
| z = 11 ***** sodium ***** | | | | | | | | |
| ** na-23 ** | | | | | | | | |
| | 11023.31c | endl79 | endl-79 | | cont | 0 | no | 14656 |
| | 11023.31d | drl79 | endl-79 | | disc | 0 | no | 4299 |
| | 11023.35c | endl85 | endl-85 | 18 | cont | 0 | yes p(e) | 22838 |
| | 11023.40c | e4xs(2) | endf/b-iv | 1156 | cont | 300 | yes p(e) | 35211 |
| → | 11023.50c | endf5p | endf/b-v | 1311 | cont | 300 | yes p(e) | 52313 |
| | 11023.50d | dre5 | endf/b-v | 1311 | disc | 300 | yes p(e) | 41726 |
| | 11023.50m | mgxsnp | endf/b-v | 1311 | mult | 300 | yes | 2982 |
| | 11023.51c | rmccs | endf/b-v | 1311 | cont | 300 | yes p(e) | 48924 |
| | 11023.51d | drmccs | endf/b-v | 1311 | disc | 300 | yes p(e) | 41726 |
| z = 12 ***** magnesium ***** | | | | | | | | |
| ** mg-nat ** | | | | | | | | |
| | 12000.31c | endl79 | endl-79 | | cont | 0 | no | 6199 |
| | 12000.31d | drl79 | endl-79 | | disc | 0 | no | 3626 |
| | 12000.35c | endl85 | endl-85 | 19 | cont | 0 | yes p(e) | 9747 |
| | 12000.40c | e4xs(2) | endf/b-iv | 1280 | cont | 300 | yes p(e) | 29763 |
| → | 12000.50c | endf5u | endf/b-v | 1312 | cont | 300 | yes p(e) | 56395 |
| | 12000.50d | dre5 | endf/b-v | 1312 | disc | 300 | yes p(e) | 14131 |
| | 12000.50m | mgxsnp | endf/b-v | 1312 | mult | 300 | yes | 3802 |
| | 12000.51c | rmccs | endf/b-v | 1312 | cont | 300 | yes p(e) | 48978 |
| | 12000.51d | drmccs | endf/b-v | 1312 | disc | 300 | yes p(e) | 14131 |

APPENDIX G

| ZAID | FILE | SOURCE | MAT | TYPE | TEMP(°K) | GPD | LENGTH | NUBAR |
|-------------------------------|---------|-----------|------|------|----------|----------|--------|-------|
| z = 13 ***** aluminum ***** | | | | | | | | |
| ** al-27 ** | | | | | | | | |
| 13027.04c | bmccs | endf/b-iv | 1193 | cont | 0 | yes p | 32517 | |
| 13027.04d | d9 | endf/b-iv | 1193 | disc | 0 | yes p | 9700 | |
| 13027.31c | endl79 | endl-79 | | cont | 0 | no | 27295 | |
| 13027.31d | drl79 | endl-79 | | disc | 0 | no | 9871 | |
| 13027.35c | endl85 | endl-85 | 20 | cont | 0 | yes p(e) | 36956 | |
| → 13027.50c | rmccs | endf/b-v | 1313 | cont | 300 | yes p(e) | 54223 | |
| 13027.50d | drmccs | endf/b-v | 1313 | disc | 300 | yes p(e) | 42008 | |
| 13027.50m | mgxsnp | endf/b-v | 1313 | mult | 300 | yes | 3853 | |
| 13027.51c | endf5t | endf/b-v | 1313 | cont | 300 | yes p(e) | 53438 | |
| z = 14 ***** silicon ***** | | | | | | | | |
| ** si-nat ** | | | | | | | | |
| 14000.31c | endl79 | endl-79 | | cont | 0 | no | 11924 | |
| 14000.31d | drl79 | endl-79 | | disc | 0 | no | 3955 | |
| 14000.35c | endl85 | endl-85 | 21 | cont | 0 | yes p(e) | 19077 | |
| 14000.40c | e4xs(2) | endf/b-iv | 1194 | cont | 300 | yes p(e) | 76132 | |
| → 14000.50c | endf5p | endf/b-v | 1314 | cont | 300 | yes p(e) | 98670 | |
| 14000.50d | dre5 | endf/b-v | 1314 | disc | 300 | yes p(e) | 69559 | |
| 14000.50m | mgxsnp | endf/b-v | 1314 | mult | 300 | yes | 3266 | |
| 14000.51c | rmccs | endf/b-v | 1314 | cont | 300 | yes p(e) | 88190 | |
| 14000.51d | drmccs | endf/b-v | 1314 | disc | 300 | yes p(e) | 69559 | |
| z = 15 ***** phosphorus ***** | | | | | | | | |
| ** p-31 ** | | | | | | | | |
| 15031.31c | endl79 | endl-79 | | cont | 0 | no | 3637 | |
| 15031.31d | drl79 | endl-79 | | disc | 0 | no | 3423 | |
| 15031.35c | endl85 | endl-85 | 22 | cont | 0 | yes p(e) | 5936 | |
| → 15031.50c | endf5u | endf/b-v | 1315 | cont | 300 | yes p(e) | 5794 | |
| 15031.50d | dre5 | endf/b-v | 1315 | disc | 300 | yes p(e) | 5822 | |
| 15031.50m | mgxsnp | endf/b-v | 1315 | mult | 300 | yes | 2123 | |
| 15031.51c | rmccs | endf/b-v | 1315 | cont | 300 | yes p(e) | 5793 | |
| 15031.51d | drmccs | endf/b-v | 1315 | disc | 300 | yes p(e) | 5822 | |
| z = 16 ***** sulfur ***** | | | | | | | | |
| ** s-32 ** | | | | | | | | |
| 16032.31c | endl79 | endl-79 | | cont | 0 | no | 4071 | |
| 16032.31d | drl79 | endl-79 | | disc | 0 | no | 3341 | |
| 16032.35c | endl85 | endl-85 | 23 | cont | 0 | yes p(e) | 7115 | |
| → 16032.50c | endf5u | endf/b-v | 1316 | cont | 300 | yes p(e) | 6850 | |
| 16032.50d | dre5 | endf/b-v | 1316 | disc | 300 | yes p(e) | 6363 | |
| 16032.50m | mgxsnp | endf/b-v | 1316 | mult | 300 | yes | 2185 | |
| 16032.51c | rmccs | endf/b-v | 1316 | cont | 300 | yes p(e) | 6841 | |
| 16032.51d | drmccs | endf/b-v | 1316 | disc | 300 | yes p(e) | 6363 | |
| z = 17 ***** chlorine ***** | | | | | | | | |
| ** cl-nat ** | | | | | | | | |
| 17000.31c | endl79 | endl-79 | | cont | 0 | no | 8664 | |
| 17000.31d | drl79 | endl-79 | | disc | 0 | no | 3430 | |

APPENDIX G

| ZAID | FILE | SOURCE | MAT | TYPE | TEMP(°K) | GPD | LENGTH | NUBAR |
|------------------------------|----------|-----------|------|------|----------|------------|--------|-------|
| 17000.35c | endl85 | endl-85 | 24 | cont | | 0 yes p(e) | 12964 | |
| → 17000.50c | endf5p | endf/b-v | 1149 | cont | 300 | yes p(e) | 23374 | |
| 17000.50d | dre5 | endf/b-v | 1149 | disc | 300 | yes p(e) | 18270 | |
| 17000.50m | mgxsnp | endf/b-v | 1149 | mult | 300 | yes | 2737 | |
| 17000.51c | rmccs | endf/b-v | 1149 | cont | 300 | yes p(e) | 21145 | |
| 17000.51d | drmccs | endf/b-v | 1149 | disc | 300 | yes p(e) | 18270 | |
| z = 18 ***** argon ***** | | | | | | | | |
| ** ar-nat ** | | | | | | | | |
| 18000.31c | endl79 | endl-79 | | cont | 0 | no | 2857 | |
| 18000.31d | drl79 | endl-79 | | disc | 0 | no | 2939 | |
| → 18000.35c | rmccsa | endl-85 | 25 | cont | 0 | yes p(e) | 5646 | |
| 18000.35d | drmccs | endl-85 | 25 | disc | 0 | yes p(e) | 14764 | |
| 18000.35m | mgxsnp | endl-85 | 25 | mult | 0 | yes | 2022 | |
| 18000.59c | arkrc(3) | gp. t-2 | 1800 | cont | 300 | yes p(e) | 3514 | |
| z = 19 ***** potassium ***** | | | | | | | | |
| ** k-nat ** | | | | | | | | |
| 19000.31c | endl79 | endl-79 | | cont | 0 | no | 6645 | |
| 19000.31d | drl79 | endl-79 | | disc | 0 | no | 3293 | |
| 19000.35c | endl85 | endl-85 | 26 | cont | 0 | yes p(e) | 11191 | |
| → 19000.50c | endf5u | endf/b-v | 1150 | cont | 300 | yes p(e) | 22112 | |
| 19000.50d | dre5 | endf/b-v | 1150 | disc | 300 | yes p(e) | 23198 | |
| 19000.50m | mgxsnp | endf/b-v | 1150 | mult | 300 | yes | 2833 | |
| 19000.51c | rmccs | endf/b-v | 1150 | cont | 300 | yes p(e) | 18859 | |
| 19000.51d | drmccs | endf/b-v | 1150 | disc | 300 | yes p(e) | 23198 | |
| z = 20 ***** calcium ***** | | | | | | | | |
| ** ca-nat ** | | | | | | | | |
| 20000.10c | bmccs | endf/b-iv | 1195 | cont | 0 | yes p | 24085 | |
| 20000.10d | d9 | endf/b-iv | 1195 | disc | 0 | yes p | 9198 | |
| 20000.31c | endl79 | endl-79 | | cont | 0 | no | 8959 | |
| 20000.31d | drl79 | endl-79 | | disc | 0 | no | 3637 | |
| 20000.35c | endl85 | endl-85 | 27 | cont | 0 | yes p(e) | 12994 | |
| → 20000.50c | endf5u | endf/b-v | 1320 | cont | 300 | yes p(e) | 62685 | |
| 20000.50d | dre5 | endf/b-v | 1320 | disc | 300 | yes p(e) | 29094 | |
| 20000.50m | mgxsnp | endf/b-v | 1320 | mult | 300 | yes | 3450 | |
| 20000.51c | rmccs | endf/b-v | 1320 | cont | 300 | yes p(e) | 53433 | |
| 20000.51d | drmccs | endf/b-v | 1320 | disc | 300 | yes p(e) | 29094 | |
| z = 21 ***** scandium ***** | | | | | | | | |
| ** sc-21 ** | | | | | | | | |
| 21045.55c | sc45(4) | group t-2 | 2145 | cont | 300 | no | 6111 | |
| z = 22 ***** titanium ***** | | | | | | | | |
| ** ti-nat ** | | | | | | | | |
| 22000.11c | bmccs | endf/b-iv | 1286 | cont | 300 | yes p | 10644 | |
| 22000.11d | d9 | endf/b-iv | 1286 | disc | 300 | yes p | 3897 | |
| 22000.31c | endl79 | endl-79 | | cont | 0 | no | 9626 | |
| 22000.31d | drl79 | endl-79 | | disc | 0 | no | 3205 | |

APPENDIX G

| ZAID | FILE | SOURCE | MAT | TYPE | TEMP(°K) | GPD | LENGTH | NUBAR |
|-------------|--------|----------|------|------|----------|----------|--------|-------|
| 22000.35c | endl85 | endl-85 | 28 | cont | 0 | yes p(e) | 13482 | |
| → 22000.50c | endf5u | endf/b-v | 1322 | cont | 300 | yes p(e) | 54862 | |
| 22000.50d | dre5 | endf/b-v | 1322 | disc | 300 | yes p(e) | 10514 | |
| 22000.50m | mgxsnp | endf/b-v | 1322 | mult | 300 | yes | 3015 | |
| 22000.51c | rmccs | endf/b-v | 1322 | cont | 300 | yes p(e) | 31893 | |
| 22000.51d | drmccs | endf/b-v | 1322 | disc | 300 | yes p(e) | 10514 | |

z = 23 ***** vanadium *****

** v-nat **

| | | | | | | | | |
|-------------|--------|-----------|------|------|-----|----------|-------|--|
| 23000.30c | bmccs | endf/b-iv | 1196 | cont | 0 | yes p | 6456 | |
| 23000.30d | d9 | endf/b-iv | 1196 | disc | 0 | yes p | 4603 | |
| → 23000.50c | endf5u | endf/b-v | 1323 | cont | 300 | yes p(e) | 38373 | |
| 23000.50d | dre5 | endf/b-v | 1323 | disc | 300 | yes p(e) | 8929 | |
| 23000.50m | mgxsnp | endf/b-v | 1323 | mult | 300 | yes | 2775 | |
| 23000.51c | rmccs | endf/b-v | 1323 | cont | 300 | yes p(e) | 34171 | |
| 23000.51d | drmccs | endf/b-v | 1323 | disc | 300 | yes p(e) | 8929 | |

** v-51 **

| | | | | | | | | |
|-----------|--------|---------|--|------|---|----|-------|--|
| 23051.31c | endl79 | endl-79 | | cont | 0 | no | 21394 | |
| 23051.31d | drl79 | endl-79 | | disc | 0 | no | 5505 | |

z = 24 ***** chromium *****

** cr-nat **

| | | | | | | | | |
|-------------|--------|-----------|------|------|-----|----------|--------|--|
| 24000.11c | bmccs | endf/b-iv | 1191 | cont | 300 | yes p | 38240 | |
| 24000.11d | d9 | endf/b-iv | 1191 | disc | 300 | yes p | 11767 | |
| 24000.12c | xmccs | endf/b-iv | 1191 | cont | 900 | yes p | 51663 | |
| 24000.31c | endl79 | endl-79 | | cont | 0 | no | 5827 | |
| 24000.31d | drl79 | endl-79 | | disc | 0 | no | 5260 | |
| 24000.35c | endl85 | endl-85 | 30 | cont | 0 | yes p(e) | 9279 | |
| → 24000.50c | rmccs | endf/b-v | 1324 | cont | 300 | yes p(e) | 134515 | |
| 24000.50d | drmccs | endf/b-v | 1324 | disc | 300 | yes p(e) | 30775 | |
| 24000.50m | mgxsnp | endf/b-v | 1324 | mult | 300 | yes | 3924 | |
| 24000.51c | endf5t | endf/b-v | 1324 | cont | 300 | yes p(e) | 55677 | |

z = 25 ***** manganese *****

** mn-55 **

| | | | | | | | | |
|-------------|--------|----------|------|------|-----|----------|--------|--|
| 25055.31c | endl79 | endl-79 | | cont | 0 | no | 4149 | |
| 25055.31d | drl79 | endl-79 | | disc | 0 | no | 3186 | |
| 25055.35c | endl85 | endl-85 | 31 | cont | 0 | yes p(e) | 7554 | |
| → 25055.50c | endf5u | endf/b-v | 1325 | cont | 300 | yes p(e) | 105154 | |
| 25055.50d | dre5 | endf/b-v | 1325 | disc | 300 | yes p(e) | 9742 | |
| 25055.50m | mgxsnp | endf/b-v | 1325 | mult | 300 | yes | 2890 | |
| 25055.51c | rmccs | endf/b-v | 1325 | cont | 300 | yes p(e) | 25788 | |
| 25055.51d | drmccs | endf/b-v | 1325 | disc | 300 | yes p(e) | 9742 | |

z = 26 ***** iron *****

** fe-nat **

| | | | | | | | | |
|-----------|--------|-----------|------|------|-----|-------|-------|--|
| 26000.11c | bmccs | endf/b-iv | 1192 | cont | 300 | yes p | 54104 | |
| 26000.11d | d9 | endf/b-iv | 1192 | disc | 300 | yes p | 8852 | |
| 26000.12c | xmccs | endf/b-iv | 1192 | cont | 900 | yes p | 57638 | |
| 26000.31c | endl79 | endl-79 | | cont | 0 | no | 23960 | |
| 26000.31d | drl79 | endl-79 | | disc | 0 | no | 3339 | |

APPENDIX G

| ZAID | FILE | SOURCE | MAT | TYPE | TEMP(*K) | GPD | LENGTH | NUBAR |
|-------------|---------|-----------|--------|------|----------|----------|--------|-------|
| 26000.35c | endl85 | endl-85 | 32 | cont | 0 | yes p(e) | 31044 | |
| 26000.50c | endf5p | endf/b-v | 1326 | cont | 300 | yes p(e) | 115508 | |
| 26000.50d | dre5 | endf/b-v | 1326 | disc | 300 | yes p(e) | 33957 | |
| 26000.51c | endf5t | endf/b-v | 1326 | cont | 300 | yes p(e) | 78377 | |
| 26000.54c | fe54(5) | endf/b-v | 1326m4 | cont | 300 | yes p(e) | 155635 | |
| → 26000.55c | rmccs | group t-2 | 260 | cont | 300 | yes p(e) | 178453 | |
| 26000.55d | drmccs | group t-2 | 260 | disc | 300 | yes p(e) | 72693 | |
| 26000.55m | mgxsnp | group t-2 | 260 | mult | 300 | yes | 4304 | |

z = 27 ***** cobalt *****

** co-59 **

| | | | | | | | | |
|-------------|--------|----------|------|------|-----|----------|--------|--|
| 27059.31c | endl79 | endl-79 | | cont | 0 | no | 31707 | |
| 27059.31d | drl79 | endl-79 | | disc | 0 | no | 6391 | |
| 27059.35c | endl85 | endl-85 | 33 | cont | 0 | yes p(e) | 39019 | |
| → 27059.50c | endf5u | endf/b-v | 1327 | cont | 300 | yes p(e) | 117136 | |
| 27059.50d | dre5 | endf/b-v | 1327 | disc | 300 | yes p(e) | 11830 | |
| 27059.50m | mgxsnp | endf/b-v | 1327 | mult | 300 | yes | 2889 | |
| 27059.51c | rmccs | endf/b-v | 1327 | cont | 300 | yes p(e) | 28416 | |
| 27059.51d | drmccs | endf/b-v | 1327 | disc | 300 | yes p(e) | 11830 | |

z = 28 ***** nickel *****

** ni-nat **

| | | | | | | | | |
|-------------|--------|-----------|------|------|-----|----------|--------|--|
| 28000.11c | bmccs | endf/b-iv | 1190 | cont | 300 | yes p | 35192 | |
| 28000.11d | d9 | endf/b-iv | 1190 | disc | 300 | yes p | 5658 | |
| 28000.12c | xmccs | endf/b-iv | 1190 | cont | 900 | yes p | 40842 | |
| 28000.31c | endl79 | endl-79 | | cont | 0 | no | 32964 | |
| 28000.31d | drl79 | endl-79 | | disc | 0 | no | 8096 | |
| → 28000.50c | rmccs | endf/b-v | 1328 | cont | 300 | yes p(e) | 139974 | |
| 28000.50d | drmccs | endf/b-v | 1328 | disc | 300 | yes p(e) | 22059 | |
| 28000.50m | mgxsnp | endf/b-v | 1328 | mult | 300 | yes | 3373 | |
| 28000.51c | endf5t | endf/b-v | 1328 | cont | 300 | yes p(e) | 93636 | |

** ni-58 **

| | | | | | | | | |
|-----------|--------|---------|----|------|---|----------|-------|--|
| 28058.35c | endl85 | endl-85 | 35 | cont | 0 | yes p(e) | 42805 | |
|-----------|--------|---------|----|------|---|----------|-------|--|

z = 29 ***** copper *****

** cu-nat **

| | | | | | | | | |
|-------------|--------|-----------|------|------|-----|----------|-------|--|
| 29000.10c | bmccs | endf/b-iv | 1295 | cont | 0 | yes p | 14703 | |
| 29000.10d | d9 | endf/b-iv | 1295 | disc | 0 | yes p | 8610 | |
| 29000.31c | endl79 | endl-79 | | cont | 0 | no | 4157 | |
| 29000.31d | drl79 | endl-79 | | disc | 0 | no | 4066 | |
| 29000.35c | endl85 | endl-85 | 36 | cont | 0 | yes p(e) | 7100 | |
| → 29000.50c | rmccs | endf/b-v | 1329 | cont | 300 | yes p(e) | 51911 | |
| 29000.50d | drmccs | endf/b-v | 1329 | disc | 300 | yes p(e) | 12838 | |
| 29000.50m | mgxsnp | endf/b-v | 1329 | mult | 300 | yes | 2803 | |
| 29000.51c | endf5t | endf/b-v | 1329 | cont | 300 | yes p(e) | 51375 | |

z = 31 ***** gallium *****

** ga-nat **

| | | | | | | | | |
|-----------|--------|---------|----|------|---|----------|------|--|
| 31000.31c | endl79 | endl-79 | | cont | 0 | no | 4225 | |
| 31000.31d | drl79 | endl-79 | | disc | 0 | no | 3027 | |
| 31000.35c | endl85 | endl-85 | 37 | cont | 0 | yes p(e) | 7570 | |

APPENDIX G

| ZAID | FILE | SOURCE | MAT | TYPE | TEMP(°K) | GPD | LENGTH | NUBAR |
|----------------------------|----------|-----------|------|------|----------|----------|--------|-------|
| → 31000.50c | rmccs | endf/b-v | 1358 | cont | 300 | yes p(e) | 7989 | |
| 31000.50d | drmccs | endf/b-v | 1358 | disc | 300 | yes p(e) | 6272 | |
| 31000.50m | mgxsnp | endf/b-v | 1358 | mult | 300 | yes | 2084 | |
| 31000.51c | endf5t | endf/b-v | 1358 | cont | 300 | yes p(e) | 7989 | |
| z = 33 ***** arsenic ***** | | | | | | | | |
| ** as-74 ** | | | | | | | | |
| 33074.35c | endl85 | endl-85 | 38 | cont | 0 | yes p(e) | 50942 | |
| ** as-75 ** | | | | | | | | |
| → 33075.35c | rmccsa | endl-85 | 39 | cont | 0 | yes p(e) | 50992 | |
| 33075.35d | drmccs | endl-85 | 39 | disc | 0 | yes p(e) | 8541 | |
| 33075.35m | mgxsnp | endl-85 | 39 | mult | 0 | yes | 2022 | |
| z = 35 ***** bromine ***** | | | | | | | | |
| ** br-79 ** | | | | | | | | |
| 35079.55c | t2ddc(6) | group t-2 | 9113 | cont | 300 | no | 10472 | |
| ** br-81 ** | | | | | | | | |
| 35081.55c | t2ddc(6) | group t-2 | 9117 | cont | 300 | no | 5383 | |
| z = 36 ***** krypton ***** | | | | | | | | |
| ** kr-78 ** | | | | | | | | |
| → 36078.50c | rmccsa | endf/b-v | 1330 | cont | 300 | no | 9098 | |
| 36078.50d | drmccs | endf/b-v | 1330 | disc | 300 | no | 4399 | |
| 36078.50m | mgxsnp | endf/b-v | 1330 | mult | 300 | no | 2108 | |
| ** kr-80 ** | | | | | | | | |
| → 36080.50c | rmccsa | endf/b-v | 1331 | cont | 300 | no | 10206 | |
| 36080.50d | drmccs | endf/b-v | 1331 | disc | 300 | no | 4317 | |
| 36080.50m | mgxsnp | endf/b-v | 1331 | mult | 300 | no | 2257 | |
| ** kr-82 ** | | | | | | | | |
| 36082.50c | rmccsa | endf/b-v | 1332 | cont | 300 | no | 7261 | |
| 36082.50d | drmccs | endf/b-v | 1332 | disc | 300 | no | 4307 | |
| 36082.50m | mgxsnp | endf/b-v | 1332 | mult | 300 | no | 2312 | |
| → 36082.59c | arkrc(3) | group t-2 | 1332 | cont | 300 | yes p | 7051 | |
| ** kr-83 ** | | | | | | | | |
| 36083.50c | rmccsa | endf/b-v | 1333 | cont | 300 | no | 8119 | |
| 36083.50d | drmccs | endf/b-v | 1333 | disc | 300 | no | 4400 | |
| 36083.50m | mgxsnp | endf/b-v | 1333 | mult | 300 | no | 2141 | |
| → 36083.59c | arkrc(3) | group t-2 | 1333 | cont | 300 | yes p | 8110 | |
| ** kr-84 ** | | | | | | | | |
| 36084.50c | rmccsa | endf/b-v | 1334 | cont | 300 | no | 9405 | |
| 36084.50d | drmccs | endf/b-v | 1334 | disc | 300 | no | 4504 | |
| 36084.50m | mgxsnp | endf/b-v | 1334 | mult | 300 | no | 2460 | |
| → 36084.59c | arkrc(3) | group t-2 | 1334 | cont | 300 | yes p | 10411 | |
| ** kr-86 ** | | | | | | | | |
| 36086.50c | rmccsa | endf/b-v | 1336 | cont | 300 | no | 10457 | |
| 36086.50d | drmccs | endf/b-v | 1336 | disc | 300 | no | 4342 | |
| 36086.50m | mgxsnp | endf/b-v | 1336 | mult | 300 | no | 2413 | |
| → 36086.59c | arkrc(3) | group t-2 | 1336 | cont | 300 | yes p | 8781 | |

APPENDIX G

| ZAID | FILE | SOURCE | MAT | TYPE | TEMP(°K) | GPD | LENGTH | NUBAR |
|-------------------------------|-----------|-----------|------|------|----------|----------|--------|-------|
| z = 37 ***** rubidium ***** | | | | | | | | |
| ** rb-85 ** | | | | | | | | |
| 37085.55c | t2ddc(6) | group t-2 | 9160 | cont | 300 | no | 27345 | |
| ** rb-87 ** | | | | | | | | |
| 37087.55c | t2ddc(6) | group t-2 | 9163 | cont | 300 | no | 8450 | |
| z = 39 ***** yttrium ***** | | | | | | | | |
| ** y-88 ** | | | | | | | | |
| 39088.35c | endl85 | endl-85 | 40 | cont | 0 | yes p(e) | 11360 | |
| ** y-89 ** | | | | | | | | |
| → 39089.35c | miscxs | endl-85 | 41 | cont | 0 | yes p(e) | 49946 | |
| 39089.50c | endf5u(7) | endf/b-v | 9202 | cont | 300 | no | 18672 | |
| 39089.50d | dre5 | endf/b-v | 9202 | disc | 300 | no | 2352 | |
| z = 40 ***** zirconium ***** | | | | | | | | |
| ** zr-nat ** | | | | | | | | |
| 40000.31c | endl79 | endl-79 | | cont | 0 | no | 10585 | |
| 40000.31d | drl79 | endl-79 | | disc | 0 | no | 4749 | |
| 40000.35c | endl85 | endl-85 | 42 | cont | 0 | yes p(e) | 14799 | |
| → 40000.50c | endf5p | endf/b-v | 1340 | cont | 300 | no | 52105 | |
| 40000.50d | dre5 | endf/b-v | 1340 | disc | 300 | no | 5441 | |
| 40000.50m | mgxsnp | endf/b-v | 1340 | mult | 300 | no | 2466 | |
| 40000.51c | rmccs | endf/b-v | 1340 | cont | 300 | no | 16857 | |
| 40000.51d | drmccs | endf/b-v | 1340 | disc | 300 | no | 5441 | |
| 40000.53c | eprixs | endf/b-v | 1340 | cont | 600 | no | 57528 | |
| ** zr-93 ** | | | | | | | | |
| 40093.50c | kidman | endf/b-v | 9232 | cont | 300 | no | 2620 | |
| z = 41 ***** niobium ***** | | | | | | | | |
| ** nb-93 ** | | | | | | | | |
| 41093.31c | endl79 | endl-79 | | cont | 0 | no | 41316 | |
| 41093.31d | drl79 | endl-79 | | disc | 0 | no | 6609 | |
| 41093.35c | endl85 | endl-85 | 43 | cont | 0 | yes p(e) | 50502 | |
| → 41093.50c | endf5p | endf/b-v | 1189 | cont | 300 | yes p(e) | 129021 | |
| 41093.50d | dre5 | endf/b-v | 1189 | disc | 300 | yes p(e) | 10393 | |
| 41093.50m | mgxsnp | endf/b-v | 1189 | mult | 300 | yes | 2746 | |
| 41093.51c | rmccs | endf/b-v | 1189 | cont | 300 | yes p(e) | 14736 | |
| 41093.51d | drmccs | endf/b-v | 1189 | disc | 300 | yes p(e) | 10393 | |
| z = 42 ***** molybdenum ***** | | | | | | | | |
| ** mo-nat ** | | | | | | | | |
| 42000.31c | endl79 | endl-79 | | cont | 0 | no | 4949 | |
| 42000.31d | drl79 | endl-79 | | disc | 0 | no | 3112 | |
| 42000.35c | endl85 | endl-85 | 44 | cont | 0 | yes p(e) | 8689 | |
| → 42000.50c | endf5u | endf/b-v | 1321 | cont | 300 | yes p(e) | 35695 | |
| 42000.50d | dre5 | endf/b-v | 1321 | disc | 300 | yes p(e) | 7815 | |
| 42000.50m | mgxsnp | endf/b-v | 1321 | mult | 300 | yes | 1991 | |
| 42000.51c | rmccs | endf/b-v | 1321 | cont | 300 | yes p(e) | 10200 | |
| 42000.51d | drmccs | endf/b-v | 1321 | disc | 300 | yes p(e) | 7815 | |

APPENDIX G

| ZAID | FILE | SOURCE | MAT | TYPE | TEMP(°K) | GPD | LENGTH | NUBAR |
|---|--------|-----------|------|------|----------|----------|--------|-------|
| ** mo-95 ** | | | | | | | | |
| 42095.50c | kidman | endf/b-v | 9282 | cont | 300 | no | 15452 | |
| z = 43 ***** technetium ***** | | | | | | | | |
| ** tc-99 ** | | | | | | | | |
| 43099.50c | kidman | endf/b-v | 1308 | cont | 300 | no | 12193 | |
| z = 44 ***** ruthenium ***** | | | | | | | | |
| ** ru-101 ** | | | | | | | | |
| 44101.50c | kidman | endf/b-v | 9330 | cont | 300 | no | 5340 | |
| ** ru-103 ** | | | | | | | | |
| 44103.50c | kidman | endf/b-v | 9332 | cont | 300 | no | 3093 | |
| z = 45 ***** rhodium ***** | | | | | | | | |
| ** rh-103 ** | | | | | | | | |
| → 45103.50c | rmccsa | endf/b-v | 1310 | cont | 300 | no | 18911 | |
| 45103.50d | drmccs | endf/b-v | 1310 | disc | 300 | no | 4704 | |
| 45103.50m | mgxsnp | endf/b-v | 1310 | mult | 300 | no | 2147 | |
| ** rh-105 ** | | | | | | | | |
| 45105.50c | kidman | endf/b-v | 9355 | cont | 300 | no | 1632 | |
| z = 45 ***** average fission product from uranium-235 ***** | | | | | | | | |
| ** u-235 fp ** | | | | | | | | |
| → 45117.90c | rmccs | foster | 998 | cont | 300 | yes p(e) | 10375 | |
| 45117.90d | drmccs | foster | 998 | disc | 300 | yes p(e) | 9568 | |
| 45117.90m | mgxsnp | foster | 998 | mult | 300 | yes | 2709 | |
| z = 46 ***** palladium ***** | | | | | | | | |
| ** pd-105 ** | | | | | | | | |
| 46105.50c | kidman | endf/b-v | 9382 | cont | 300 | no | 4688 | |
| ** pd-108 ** | | | | | | | | |
| 46108.50c | kidman | endf/b-v | 9386 | cont | 300 | no | 4590 | |
| z = 46 ***** average fission product from plutonium-239 ***** | | | | | | | | |
| ** pu-239 fp ** | | | | | | | | |
| → 46119.90c | rmccs | foster | 999 | cont | 300 | yes p(e) | 10505 | |
| 46119.90d | drmccs | foster | 999 | disc | 300 | yes p(e) | 9603 | |
| 46119.90m | mgxsnp | foster | 999 | mult | 300 | yes | 2629 | |
| z = 47 ***** silver ***** | | | | | | | | |
| ** ag-nat ** | | | | | | | | |
| → 47000.55c | rmccsa | group t-2 | 47 | cont | 300 | yes p(e) | 29153 | |
| 47000.55d | drmccs | group t-2 | 47 | disc | 300 | yes p(e) | 12470 | |
| 47000.55m | mgxsnp | group t-2 | 47 | mult | 300 | yes | 2693 | |
| ** ag-107 ** | | | | | | | | |
| 47107.35c | endl85 | endl-85 | 45 | cont | 0 | yes p(e) | 13195 | |
| → 47107.50c | rmccsa | endf/b-v | 1371 | cont | 300 | no | 12152 | |
| 47107.50d | drmccs | endf/b-v | 1371 | disc | 300 | no | 4124 | |
| 47107.50m | mgxsnp | endf/b-v | 1371 | mult | 300 | no | 2107 | |

APPENDIX G

| ZAID | FILE | SOURCE | MAT | TYPE | TEMP(°K) | GPD | LENGTH | NUBAR |
|-------------------------------------|----------|-----------|------|------|----------|-----|----------|-------|
| ** ag-109 ** | | | | | | | | |
| 47109.35c | endl85 | endl-85 | 46 | cont | | 0 | yes p(e) | 13513 |
| → 47109.50c | rmccsa | endf/b-v | 1373 | cont | | 300 | no | 14626 |
| 47109.50d | drmccs | endf/b-v | 1373 | disc | | 300 | no | 3864 |
| 47109.50m | mgxsnp | endf/b-v | 1373 | mult | | 300 | no | 1924 |
| z = 48 ***** cadmium ***** | | | | | | | | |
| ** cd-nat ** | | | | | | | | |
| 48000.31c | endl79 | endl-79 | | cont | | 0 | no | 8131 |
| 48000.31d | drl79 | endl-79 | | disc | | 0 | no | 3031 |
| 48000.35c | endl85 | endl-85 | 47 | cont | | 0 | yes p(e) | 12344 |
| → 48000.50c | endf5u | endf/b-v | 1281 | cont | | 300 | no | 19755 |
| 48000.50d | dre5 | endf/b-v | 1281 | disc | | 300 | no | 3067 |
| 48000.50m | mgxsnp | endf/b-v | 1281 | mult | | 300 | no | 1841 |
| 48000.51c | rmccs | endf/b-v | 1281 | cont | | 300 | no | 6775 |
| 48000.51d | drmccs | endf/b-v | 1281 | disc | | 300 | no | 3067 |
| z = 50 ***** tin ***** | | | | | | | | |
| ** sn-nat ** | | | | | | | | |
| 50000.31c | endl79 | endl-79 | | cont | | 0 | no | 2876 |
| 50000.31d | drl79 | endl-79 | | disc | | 0 | no | 3256 |
| → 50000.35c | endl85 | endl-85 | 48 | cont | | 0 | yes p(e) | 6031 |
| z = 50 ***** fission products ***** | | | | | | | | |
| ** ave fp ** | | | | | | | | |
| → 50120.35c | rmccs | endl-85 | 102 | cont | | 0 | yes p(e) | 8427 |
| 50120.35d | drmccs | endl-85 | 102 | disc | | 0 | yes p(e) | 9024 |
| 50120.35m | mgxsnp | endl-85 | 102 | mult | | 0 | yes | 1929 |
| 50998.99m | mgxsnp | permfile | | mult | | 0 | no | 1382 |
| 50999.99m | mgxsnp | permfile | | mult | | 0 | no | 1413 |
| z = 53 ***** iodine ***** | | | | | | | | |
| ** i-127 ** | | | | | | | | |
| 53127.55c | t2ddc(6) | group t-2 | 9606 | cont | | 300 | no | 59766 |
| ** i-135 ** | | | | | | | | |
| 53135.50c | kidman | endf/b-v | 9618 | cont | | 300 | no | 1273 |
| z = 54 ***** xenon ***** | | | | | | | | |
| ** xe-nat ** | | | | | | | | |
| → 54000.35c | endl85 | endl-85 | 49 | cont | | 0 | yes p(e) | 41493 |
| 54000.35m | mgxsnp | endl-85 | 49 | mult | | 0 | yes | 1929 |
| ** xe-131 ** | | | | | | | | |
| 54131.50c | kidman | endf/b-v | 1351 | cont | | 300 | no | 22613 |
| ** xe-134 ** | | | | | | | | |
| 54134.35c | endl85 | endl-85 | 50 | cont | | 0 | yes p(e) | 7524 |
| ** xe-135 ** | | | | | | | | |
| 54135.50c | eprixs | endf/b-v | 1294 | cont | | 300 | no | 5529 |
| 54135.53c | eprixs | endf/b-v | 1294 | cont | | 600 | no | 5541 |
| 54135.54c | eprixs | endf/b-v | 1294 | cont | | 900 | no | 5577 |

APPENDIX G

| ZAID | FILE | SOURCE | MAT | TYPE | TEMP(°K) | GPD | LENGTH | NUBAR |
|---------------------------------|----------|-----------|------|------|----------|----------|--------|-------|
| z = 55 ***** cesium ***** | | | | | | | | |
| ** cs-133 ** | | | | | | | | |
| → 55133.50c | kidman | endf/b-v | 1355 | cont | 300 | no | 26754 | |
| 55133.55c | t2ddc(6) | group t-2 | 1355 | cont | 300 | no | 67934 | |
| ** cs-135 ** | | | | | | | | |
| 55135.50c | kidman | endf/b-v | 9665 | cont | 300 | no | 1944 | |
| z = 56 ***** barium ***** | | | | | | | | |
| ** ba-138 ** | | | | | | | | |
| 56138.31c | endl79 | endl-79 | | cont | 0 | no | 3059 | |
| 56138.31d | drl79 | endl-79 | | disc | 0 | no | 3218 | |
| 56138.35c | endl85 | endl-85 | 51 | cont | 0 | yes p(e) | 6046 | |
| → 56138.50c | rmccs | endf/b-v | 1353 | cont | 300 | yes p(e) | 6079 | |
| 56138.50d | drmccs | endf/b-v | 1353 | disc | 300 | yes p(e) | 6381 | |
| 56138.50m | mgxsnp | endf/b-v | 1353 | mult | 300 | yes | 2115 | |
| 56138.51c | endf5t | endf/b-v | 1353 | cont | 300 | yes p(e) | 6064 | |
| z = 59 ***** praseodymium ***** | | | | | | | | |
| ** pr-141 ** | | | | | | | | |
| 59141.50c | kidman | endf/b-v | 9742 | cont | 300 | no | 15661 | |
| z = 60 ***** neodymium ***** | | | | | | | | |
| ** nd-143 ** | | | | | | | | |
| 60143.50c | kidman | endf/b-v | 9764 | cont | 300 | no | 17257 | |
| ** nd-145 ** | | | | | | | | |
| 60145.50c | kidman | endf/b-v | 9766 | cont | 300 | no | 38514 | |
| ** nd-147 ** | | | | | | | | |
| 60147.50c | kidman | endf/b-v | 9768 | cont | 300 | no | 1857 | |
| ** nd-148 ** | | | | | | | | |
| 60148.50c | kidman | endf/b-v | 9769 | cont | 300 | no | 10908 | |
| z = 61 ***** promethium ***** | | | | | | | | |
| ** pm-147 ** | | | | | | | | |
| 61147.50c | kidman | endf/b-v | 9783 | cont | 300 | no | 9193 | |
| ** pm-148 ** | | | | | | | | |
| 61148.50c | kidman | endf/b-v | 9784 | cont | 300 | no | 1684 | |
| ** pm-149 ** | | | | | | | | |
| 61149.50c | kidman | endf/b-v | 9786 | cont | 300 | no | 2110 | |
| z = 62 ***** samarium ***** | | | | | | | | |
| ** sm-147 ** | | | | | | | | |
| 62147.50c | kidman | endf/b-v | 9806 | cont | 300 | no | 33814 | |
| ** sm-149 ** | | | | | | | | |
| → 62149.50c | endf5u | endf/b-v | 1319 | cont | 300 | no | 15703 | |
| 62149.50d | dre5 | endf/b-v | 1319 | disc | 300 | no | 4470 | |
| ** sm-150 ** | | | | | | | | |
| 62150.50c | kidman | endf/b-v | 9809 | cont | 300 | no | 9386 | |

APPENDIX G

| ZAID | FILE | SOURCE | MAT | TYPE | TEMP(°K) | GPD | LENGTH | NUBAR |
|-------------------------------|------------|-----------|------|------|----------|----------|--------|-------|
| ** sm-151 ** | | | | | | | | |
| 62151.50c | kidman | endf/b-v | 9810 | cont | 300 | no | 7344 | |
| ** sm-152 ** | | | | | | | | |
| 62152.50c | kidman | endf/b-v | 9811 | cont | 300 | no | 41293 | |
| z = 63 ***** europium ***** | | | | | | | | |
| ** eu-nat ** | | | | | | | | |
| 63000.31c | endl79 | endl-79 | | cont | 0 | no | 3532 | |
| 63000.31d | drl79 | endl-79 | | disc | 0 | no | 3039 | |
| → 63000.35c | rmccsa | endl-85 | 52 | cont | 0 | yes p(e) | 6987 | |
| 63000.35d | drmccs | endl-85 | 52 | disc | 0 | yes p(e) | 6715 | |
| 63000.35m | mgxsnp | endl-85 | 52 | mult | 0 | yes | 1933 | |
| ** eu-151 ** | | | | | | | | |
| 63151.50c | rmccs | endf/b-v | 1357 | cont | 300 | yes p(e) | 68118 | |
| 63151.50d | drmccs | endf/b-v | 1357 | disc | 300 | yes p(e) | 10074 | |
| 63151.51c | endf5t | endf/b-v | 1357 | cont | 300 | yes p(e) | 16796 | |
| → 63151.55c | newxs | group t-2 | 151 | cont | 300 | yes p(e) | 86636 | |
| 63151.55d | newxsd | group t-2 | 151 | disc | 300 | yes p(e) | 35260 | |
| 63151.55m | mgxsnp | group t-2 | 151 | mult | 300 | yes | 2976 | |
| ** eu-152 ** | | | | | | | | |
| → 63152.50c | endf5u | endf/b-v | 1292 | cont | 300 | no | 49354 | |
| 63152.50d | dre5 | endf/b-v | 1292 | disc | 300 | no | 5696 | |
| 63152.51c | endf5t | endf/b-v | 1292 | cont | 300 | no | 10893 | |
| ** eu-153 ** | | | | | | | | |
| 63153.50c | rmccs | endf/b-v | 1359 | cont | 300 | yes p(e) | 55292 | |
| 63153.50d | drmccs | endf/b-v | 1359 | disc | 300 | yes p(e) | 11305 | |
| 63153.51c | endf5t | endf/b-v | 1359 | cont | 300 | yes p(e) | 15463 | |
| → 63153.55c | newxs | group t-2 | 153 | cont | 300 | yes p(e) | 73032 | |
| 63153.55d | newxsd | group t-2 | 153 | disc | 300 | yes p(e) | 36433 | |
| 63153.55m | mgxsnp | group t-2 | 153 | mult | 300 | yes | 2976 | |
| ** eu-154 ** | | | | | | | | |
| → 63154.50c | endf5u | endf/b-v | 1293 | cont | 300 | no | 37049 | |
| 63154.50d | dre5 | endf/b-v | 1293 | disc | 300 | no | 5499 | |
| 63154.51c | endf5t | endf/b-v | 1293 | cont | 300 | no | 10407 | |
| ** eu-155 ** | | | | | | | | |
| 63155.50c | kidman | endf/b-v | 9832 | cont | 300 | no | 4573 | |
| z = 64 ***** gadolinium ***** | | | | | | | | |
| ** gd-nat ** | | | | | | | | |
| 64000.31c | endl79 | endl-79 | | cont | 0 | no | 4192 | |
| 64000.31d | drl79 | endl-79 | | disc | 0 | no | 3092 | |
| → 64000.35c | rmccsa | endl-85 | 53 | cont | 0 | yes p(e) | 7939 | |
| 64000.35d | drmccs | endl-85 | 53 | disc | 0 | yes p(e) | 6894 | |
| 64000.35m | mgxsnp | endl-85 | 53 | mult | 0 | yes | 1929 | |
| ** gd-152 ** | | | | | | | | |
| 64152.50c | endf5u | endf/b-v | 1362 | cont | 300 | no | 26292 | |
| 64152.50d | dre5 | endf/b-v | 1362 | disc | 300 | no | 5940 | |
| 64152.51c | endf5t | endf/b-v | 1362 | cont | 300 | no | 10970 | |
| → 64152.52c | gd2hedl(8) | hedl | 1362 | cont | 300 | no | 15879 | |
| 64152.53c | gd2hedl(8) | hedl | 1362 | cont | 800 | no | 15237 | |
| 64152.55c | gdt2gp(9) | gp. t-2 | 1362 | cont | 300 | yes p(e) | 32651 | |

APPENDIX G

| ZAID | FILE | SOURCE | MAT | TYPE | TEMP(°K) | GPD | LENGTH | NUBAR |
|----------------------------|-----------|-----------|------|------|----------|----------|--------|-------|
| ** gd-154 ** | | | | | | | | |
| → 64154.50c | endf5u | endf/b-v | 1364 | cont | 300 | no | 49613 | |
| 64154.50d | dre5 | endf/b-v | 1364 | disc | 300 | no | 5971 | |
| 64154.51c | endf5t | endf/b-v | 1364 | cont | 300 | no | 11520 | |
| 64154.55c | gdt2gp(9) | gp. t-2 | 1364 | cont | 300 | yes p(e) | 59875 | |
| ** gd-155 ** | | | | | | | | |
| → 64155.50c | endf5u | endf/b-v | 1365 | cont | 300 | no | 45006 | |
| 64155.50d | dre5 | endf/b-v | 1365 | disc | 300 | no | 6569 | |
| 64155.51c | endf5t | endf/b-v | 1365 | cont | 300 | no | 11919 | |
| 64155.55c | gdt2gp(9) | gp. t-2 | 1365 | cont | 300 | yes p(e) | 54407 | |
| ** gd-156 ** | | | | | | | | |
| → 64156.50c | endf5u | endf/b-v | 1366 | cont | 300 | no | 37412 | |
| 64156.50d | dre5 | endf/b-v | 1366 | disc | 300 | no | 6216 | |
| 64156.51c | endf5t | endf/b-v | 1366 | cont | 300 | no | 11443 | |
| 64156.55c | gdt2gp(9) | gp. t-2 | 1366 | cont | 300 | yes p(e) | 44452 | |
| ** gd-157 ** | | | | | | | | |
| → 64157.50c | endf5u | endf/b-v | 1367 | cont | 300 | no | 39016 | |
| 64157.50d | dre5 | endf/b-v | 1367 | disc | 300 | no | 6387 | |
| 64157.51c | endf5t | endf/b-v | 1367 | cont | 300 | no | 11365 | |
| 64157.55c | gdt2gp(9) | gp. t-2 | 1367 | cont | 300 | yes p(e) | 47332 | |
| ** gd-158 ** | | | | | | | | |
| → 64158.50c | endf5u | endf/b-v | 1368 | cont | 300 | no | 95917 | |
| 64158.50d | dre5 | endf/b-v | 1368 | disc | 300 | no | 5852 | |
| 64158.51c | endf5t | endf/b-v | 1368 | cont | 300 | no | 11975 | |
| 64158.55c | gdt2gp(9) | gp. t-2 | 1368 | cont | 300 | yes p(e) | 113977 | |
| ** gd-160 ** | | | | | | | | |
| → 64160.50c | endf5u | endf/b-v | 1370 | cont | 300 | no | 54029 | |
| 64160.50d | dre5 | endf/b-v | 1370 | disc | 300 | no | 5071 | |
| 64160.51c | endf5t | endf/b-v | 1370 | cont | 300 | no | 10021 | |
| 64160.55c | gdt2gp(9) | gp. t-2 | 1370 | cont | 300 | yes p(e) | 65322 | |
| z = 67 ***** holmium ***** | | | | | | | | |
| ** ho-165 ** | | | | | | | | |
| 67165.31c | endl79 | endl-79 | | cont | 0 | no | 44092 | |
| 67165.31d | drl79 | endl-79 | | disc | 0 | no | 3311 | |
| 67165.35c | rmccsa | endl-85 | 54 | cont | 0 | yes p(e) | 54340 | |
| 67165.35d | drmccs | endl-85 | 54 | disc | 0 | yes p(e) | 7080 | |
| → 67165.55c | newxs | group t-2 | 165 | cont | 300 | yes p(e) | 56666 | |
| 67165.55d | newxsd | group t-2 | 165 | disc | 300 | yes p(e) | 42327 | |
| 67165.55m | mgxsnp | group t-2 | 165 | mult | 300 | yes | 2526 | |
| z = 69 ***** thulium ***** | | | | | | | | |
| ** th-169 ** | | | | | | | | |
| 69169.55c | tm169(10) | gp. t-2 | 169 | cont | 300 | no | 47982 | |
| z = 72 ***** hafnium ***** | | | | | | | | |
| ** hf-nat ** | | | | | | | | |
| 72000.35c | endl85 | endl-85 | 55 | cont | 0 | yes p(e) | 75923 | |
| → 72000.50c | newxs | endf/b-v | 1372 | cont | 300 | no | 52272 | |
| 72000.50d | newxsd | endf/b-v | 1372 | disc | 300 | no | 4792 | |

APPENDIX G

| ZAID | FILE | SOURCE | MAT | TYPE | TEMP(°K) | GPD | LENGTH | NUBAR |
|-----------------------------|-----------|--------|-----------|------|----------|-----|----------|--------|
| z = 73 ***** tantalum ***** | | | | | | | | |
| ** ta-181 ** | | | | | | | | |
| | 73181.31c | endl79 | endl-79 | | cont | 0 | no | 20876 |
| | 73181.31d | drl79 | endl-79 | | disc | 0 | no | 5871 |
| | 73181.35c | endl85 | endl-85 | 56 | cont | 0 | yes p(e) | 33608 |
| → | 73181.50c | endf5u | endf/b-v | 1285 | cont | 300 | yes p(e) | 60801 |
| | 73181.50d | dre5 | endf/b-v | 1285 | disc | 300 | yes p(e) | 16422 |
| | 73181.50m | mgxsnp | endf/b-v | 1285 | mult | 300 | yes | 2787 |
| | 73181.51c | rmccs | endf/b-v | 1285 | cont | 300 | yes p(e) | 21588 |
| | 73181.51d | drmccs | endf/b-v | 1285 | disc | 300 | yes p(e) | 16422 |
| z = 74 ***** tungsten ***** | | | | | | | | |
| ** w-nat ** | | | | | | | | |
| | 74000.31c | endl79 | endl-79 | | cont | 0 | no | 20541 |
| | 74000.31d | drl79 | endl-79 | | disc | 0 | no | 3212 |
| | 74000.35c | endl85 | endl-85 | 57 | cont | 0 | yes p(e) | 27091 |
| → | 74000.55c | rmccs | group t-2 | 7400 | cont | 300 | yes p(e) | 50700 |
| | 74000.55d | drmccs | group t-2 | 7400 | disc | 300 | yes p(e) | 34333 |
| | 74000.55m | mgxsnp | group t-2 | 7400 | mult | 300 | yes | 4360 |
| ** w-182 ** | | | | | | | | |
| | 74182.10c | bmccs | endf/b-iv | 1128 | cont | 0 | yes p | 33247 |
| | 74182.10d | d9 | endf/b-iv | 1128 | disc | 0 | yes p | 5920 |
| | 74182.50c | endf5p | endf/b-v | 1128 | cont | 300 | yes p(e) | 94428 |
| | 74182.50d | dre5 | endf/b-v | 1128 | disc | 300 | yes p(e) | 17790 |
| | 74182.51c | endf5t | endf/b-v | 1128 | cont | 300 | yes p(e) | 23259 |
| → | 74182.55c | rmccsa | group t-2 | 182 | cont | 300 | yes p(e) | 122351 |
| | 74182.55d | drmccs | group t-2 | 182 | disc | 300 | yes p(e) | 26448 |
| | 74182.55m | mgxsnp | group t-2 | 182 | mult | 300 | yes | 3687 |
| ** w-183 ** | | | | | | | | |
| | 74183.10c | bmccs | endf/b-iv | 1129 | cont | 0 | yes p | 27816 |
| | 74183.10d | d9 | endf/b-iv | 1129 | disc | 0 | yes p | 7125 |
| | 74183.50c | endf5p | endf/b-v | 1129 | cont | 300 | yes p(e) | 58860 |
| | 74183.50d | dre5 | endf/b-v | 1129 | disc | 300 | yes p(e) | 19504 |
| | 74183.51c | endf5t | endf/b-v | 1129 | cont | 300 | yes p(e) | 22707 |
| → | 74183.55c | rmccsa | group t-2 | 183 | cont | 300 | yes p(e) | 79595 |
| | 74183.55d | drmccs | group t-2 | 183 | disc | 300 | yes p(e) | 26381 |
| | 74183.55m | mgxsnp | group t-2 | 183 | mult | 300 | yes | 3628 |
| ** w-184 ** | | | | | | | | |
| | 74184.10c | bmccs | endf/b-iv | 1130 | cont | 0 | yes p | 27996 |
| | 74184.10d | d9 | endf/b-iv | 1130 | disc | 0 | yes p | 6139 |
| | 74184.50c | endf5p | endf/b-v | 1130 | cont | 300 | yes p(e) | 58931 |
| | 74184.50d | dre5 | endf/b-v | 1130 | disc | 300 | yes p(e) | 17093 |
| | 74184.51c | endf5t | endf/b-v | 1130 | cont | 300 | yes p(e) | 20631 |
| → | 74184.55c | rmccsa | group t-2 | 184 | cont | 300 | yes p(e) | 80067 |
| | 74184.55d | drmccs | group t-2 | 184 | disc | 300 | yes p(e) | 26171 |
| | 74184.55m | mgxsnp | group t-2 | 184 | mult | 300 | yes | 3664 |
| ** w-186 ** | | | | | | | | |
| | 74186.10c | bmccs | endf/b-iv | 1131 | cont | 0 | yes p | 30916 |
| | 74186.10d | d9 | endf/b-iv | 1131 | disc | 0 | yes p | 6208 |
| | 74186.50c | endf5p | endf/b-v | 1131 | cont | 300 | yes p(e) | 63762 |
| | 74186.50d | dre5 | endf/b-v | 1131 | disc | 300 | yes p(e) | 17079 |

APPENDIX G

| ZAID | FILE | SOURCE | MAT | TYPE | TEMP(°K) | GPD | LENGTH | NUBAR |
|-----------------------------|-----------|-----------|------|------|----------|----------|--------|-------|
| 74186.51c | endf5t | endf/b-v | 1131 | cont | 300 | yes p(e) | 21487 | |
| → 74186.55c | rmccsa | group t-2 | 186 | cont | 300 | yes p(e) | 83679 | |
| 74186.55d | drmccs | group t-2 | 186 | disc | 300 | yes p(e) | 26342 | |
| 74186.55m | mgxsnp | group t-2 | 186 | mult | 300 | yes | 3672 | |
| z = 75 ***** rhenium ***** | | | | | | | | |
| ** re-185 ** | | | | | | | | |
| 75185.32c | miscxs | endl-80 | | cont | 0 | yes p | 13691 | |
| → 75185.35c | endl85 | endl-85 | 58 | cont | 0 | yes p(e) | 16099 | |
| 75185.50c | rmccsa | endf/b-v | 1083 | cont | 300 | no | 9231 | |
| 75185.50d | drmccs | endf/b-v | 1083 | disc | 300 | no | 4293 | |
| 75185.50m | mgxsnp | endf/b-v | 1083 | mult | 300 | no | 1968 | |
| ** re-187 ** | | | | | | | | |
| 75187.32c | miscxs | endl-80 | | cont | 0 | yes p | 12359 | |
| → 75187.35c | endl85 | endl-85 | 59 | cont | 0 | yes p(e) | 14830 | |
| 75187.50c | rmccsa | endf/b-v | 1084 | cont | 300 | no | 8303 | |
| 75187.50d | drmccs | endf/b-v | 1084 | disc | 300 | no | 4716 | |
| 75187.50m | mgxsnp | endf/b-v | 1084 | mult | 300 | no | 2061 | |
| z = 77 ***** iridium ***** | | | | | | | | |
| ** ir-nat ** | | | | | | | | |
| 77000.55c | irnat(11) | gp. t-2 | 2002 | cont | 300 | no | 43112 | |
| z = 78 ***** platinum ***** | | | | | | | | |
| ** pt-nat ** | | | | | | | | |
| 78000.31c | endl79 | endl-79 | | cont | 0 | no | 10657 | |
| 78000.31d | dri79 | endl-79 | | disc | 0 | no | 3209 | |
| → 78000.35c | rmccsa | endl-85 | 60 | cont | 0 | yes p(e) | 15432 | |
| 78000.35d | drmccs | endl-85 | 60 | disc | 0 | yes p(e) | 6994 | |
| 78000.35m | mgxsnp | endl-85 | 60 | mult | 0 | yes | 1929 | |
| z = 79 ***** gold ***** | | | | | | | | |
| ** au-197 ** | | | | | | | | |
| 79197.31c | endl79 | endl-79 | | cont | 0 | no | 25040 | |
| 79197.31d | dri79 | endl-79 | | disc | 0 | no | 3965 | |
| 79197.35c | endl85 | endl-85 | 61 | cont | 0 | yes p(e) | 31932 | |
| 79197.50c | endf5p | endf/b-v | 1379 | cont | 300 | no | 139466 | |
| 79197.50d | dre5 | endf/b-v | 1379 | disc | 300 | no | 4923 | |
| 79197.51c | endf5t | endf/b-v | 1379 | cont | 300 | no | 12283 | |
| 79197.55c | rmccsa | group t-2 | 1379 | cont | 300 | yes p(e) | 134386 | |
| 79197.55d | drmccs | group t-2 | 1379 | disc | 300 | yes p(e) | 7944 | |
| → 79197.56c | newxs | group t-2 | 197 | cont | 300 | yes p(e) | 122543 | |
| 79197.56d | newxsd | group t-2 | 197 | disc | 300 | yes p(e) | 38862 | |
| 79197.56m | mgxsnp | group t-2 | 197 | mult | 300 | yes | 3490 | |
| z = 82 ***** lead ***** | | | | | | | | |
| ** pb-nat ** | | | | | | | | |
| 82000.10c | bmccs | endf/b-iv | 1288 | cont | 0 | yes p | 21052 | |
| 82000.10d | d9 | endf/b-iv | 1288 | disc | 0 | yes p | 11526 | |

APPENDIX G

| ZAID | FILE | SOURCE | MAT | TYPE | TEMP(°K) | GPD | LENGTH | NUBAR |
|---------------------------------|-----------|----------|------|------|----------|----------|--------|--------|
| 82000.31c | endl79 | endl-79 | | cont | 0 | no | 3964 | |
| 82000.31d | drl79 | endl-79 | | disc | 0 | no | 3383 | |
| 82000.35c | endl85 | endl-85 | 62 | cont | 0 | yes p(e) | 6700 | |
| → 82000.50c | rmccs | endf/b-v | 1382 | cont | 300 | yes p(e) | 37694 | |
| 82000.50d | drmccs | endf/b-v | 1382 | disc | 300 | yes p(e) | 20710 | |
| 82000.50m | mgxsnp | endf/b-v | 1382 | mult | 300 | yes | 3384 | |
| 82000.51c | endf5t | endf/b-v | 1382 | cont | 300 | yes p(e) | 37694 | |
| z = 83 ***** bismuth ***** | | | | | | | | |
| ** bi-209 ** | | | | | | | | |
| 83209.35c | endl85 | endl-85 | 63 | cont | 0 | yes p(e) | 18377 | |
| → 83209.50c | endf5u | endf/b-v | 1375 | cont | 300 | yes p(e) | 15000 | |
| 83209.50d | dre5 | endf/b-v | 1375 | disc | 300 | yes p(e) | 7577 | |
| 83209.50m | mgxsnp | endf/b-v | 1375 | mult | 300 | yes | 2524 | |
| 83209.51c | rmccs | endf/b-v | 1375 | cont | 300 | yes p(e) | 13782 | |
| 83209.51d | drmccs | endf/b-v | 1375 | disc | 300 | yes p(e) | 7577 | |
| z = 90 ***** thorium ***** | | | | | | | | |
| ** th-231 ** | | | | | | | | |
| 90231.35c | endl85 | endl-85 | 64 | cont | 0 | yes p(e) | 9218 | prompt |
| ** th-232 ** | | | | | | | | |
| 90232.31c | endl79 | endl-79 | | cont | 0 | no | 40220 | prompt |
| 90232.31d | drl79 | endl-79 | | disc | 0 | no | 4045 | prompt |
| 90232.35c | endl85 | endl-85 | 65 | cont | 0 | yes p(e) | 56152 | prompt |
| → 90232.50c | endf5u | endf/b-v | 1390 | cont | 300 | yes p(e) | 152843 | both |
| 90232.50d | dre5 | endf/b-v | 1390 | disc | 300 | yes p(e) | 11998 | both |
| 90232.50m | mgxsnp | endf/b-v | 1390 | mult | 300 | yes | 2896 | both |
| 90232.51c | rmccs | endf/b-v | 1390 | cont | 300 | yes p(e) | 17986 | both |
| 90232.51d | drmccs | endf/b-v | 1390 | disc | 300 | yes p(e) | 11998 | both |
| ** th-233 ** | | | | | | | | |
| 90233.35c | endl85 | endl-85 | 66 | cont | 0 | yes p(e) | 9413 | prompt |
| z = 91 ***** protactinium ***** | | | | | | | | |
| ** pa-231 ** | | | | | | | | |
| 91231.50c | pa231(12) | endf/b-v | 8131 | cont | 300 | no | 7066 | total |
| ** pa-233 ** | | | | | | | | |
| 91233.35c | endl85 | endl-85 | 67 | cont | 0 | yes p(e) | 19231 | prompt |
| → 91233.50c | endf5u | endf/b-v | 1391 | cont | 300 | no | 19560 | total |
| 91233.50d | dre5 | endf/b-v | 1391 | disc | 300 | no | 3741 | total |
| 91233.50m | mgxsnp | endf/b-v | 1391 | mult | 300 | no | 1970 | total |
| 91233.51c | rmccs | endf/b-v | 1391 | cont | 300 | no | 5682 | total |
| 91233.51d | drmccs | endf/b-v | 1391 | disc | 300 | no | 3741 | total |
| z = 92 ***** uranium ***** | | | | | | | | |
| ** u-233 ** | | | | | | | | |
| 92233.31c | endl79 | endl-79 | | cont | 0 | no | 22575 | prompt |
| 92233.31d | drl79 | endl-79 | | disc | 0 | no | 4029 | prompt |
| 92233.35c | endl85 | endl-85 | 68 | cont | 0 | yes p(e) | 29735 | prompt |
| → 92233.50c | rmccs | endf/b-v | 1393 | cont | 300 | no | 18856 | both |

APPENDIX G

| | ZAID | FILE | SOURCE | MAT | TYPE | TEMP(°K) | GPD | LENGTH | NUBAR |
|---|-------------|---------|-----------|------|------|----------|----------|--------|--------|
| | 92233.50d | drmccs | endf/b-v | 1393 | disc | 300 | no | 4213 | both |
| | 92233.50m | mgxsnp | endf/b-v | 1393 | mult | 300 | no | 1988 | both |
| | 92233.51c | endf5t | endf/b-v | 1393 | cont | 300 | no | 7754 | both |
| | ** u-234 ** | | | | | | | | |
| | 92234.31c | endl79 | endl-79 | | cont | 0 | no | 4033 | prompt |
| | 92234.31d | drl79 | endl-79 | | disc | 0 | no | 4311 | prompt |
| | 92234.35c | endl85 | endl-85 | 69 | cont | 0 | yes p(e) | 9618 | prompt |
| — | 92234.50c | endf5p | endf/b-v | 1394 | cont | 300 | no | 89474 | total |
| | 92234.50d | dre5 | endf/b-v | 1394 | disc | 300 | no | 4874 | total |
| | 92234.50m | mgxsnp | endf/b-v | 1394 | mult | 300 | no | 2150 | total |
| | 92234.51c | rmccs | endf/b-v | 1394 | cont | 300 | no | 6467 | total |
| | 92234.51d | drmccs | endf/b-v | 1394 | disc | 300 | no | 4874 | total |
| | ** u-235 ** | | | | | | | | |
| | 92235.04c | xmccs | endf/b-iv | 1261 | cont | 3000 | yes h | 29516 | both |
| | 92235.05c | xmccs | endf/b-iv | 1261 | cont | 30000 | yes h | 18573 | both |
| | 92235.06c | xmccs | endf/b-iv | 1261 | cont | 6.e+05 | yes h | 12560 | both |
| | 92235.07c | xmccs | endf/b-iv | 1261 | cont | 1.2e+07 | yes h | 11268 | both |
| | 92235.08c | xmccs | endf/b-iv | 1261 | cont | 0 | yes h | 42923 | both |
| | 92235.09c | xmccs | endf/b-iv | 1261 | cont | 300 | yes h | 41638 | both |
| | 92235.10c | amccs | endf/b-iv | 1261 | cont | 0 | yes p | 42716 | both |
| | 92235.10d | d9 | endf/b-iv | 1261 | disc | 0 | yes p | 7412 | both |
| | 92235.11c | amccs | endf/b-iv | 1261 | cont | 300 | yes p | 41332 | both |
| | 92235.11d | d9 | endf/b-iv | 1261 | disc | 300 | yes p | 7412 | both |
| | 92235.15c | rmccsb | endf/b-iv | 1261 | cont | 1.2e+07 | yes p(e) | 15173 | both |
| | 92235.15d | d9 | endf/b-iv | 1261 | disc | 1.2e+07 | yes p(e) | 11406 | both |
| | 92235.18c | amccs | endf/b-iv | 1261 | cont | 3000 | yes p | 29254 | both |
| | 92235.18d | d9 | endf/b-iv | 1261 | disc | 3000 | yes p | 7412 | both |
| | 92235.19c | rmccsb | endf/b-iv | 1261 | cont | 30000 | yes p(e) | 22298 | both |
| | 92235.19d | d9 | endf/b-iv | 1261 | disc | 30000 | yes p(e) | 11406 | both |
| | 92235.20c | amccs | endf/b-iv | 1261 | cont | 6.e+05 | yes p | 12497 | both |
| | 92235.20d | d9 | endf/b-iv | 1261 | disc | 6.e+05 | yes p | 7412 | both |
| | 92235.31c | endl79 | endl-79 | | cont | 0 | no | 19132 | prompt |
| | 92235.31d | drl79 | endl-79 | | disc | 0 | no | 4638 | prompt |
| — | 92235.50c | rmccs | endf/b-v | 1395 | cont | 300 | yes p(e) | 60550 | both |
| | 92235.50d | drmccs | endf/b-v | 1395 | disc | 300 | yes p(e) | 11849 | both |
| | 92235.50m | mgxsnp | endf/b-v | 1395 | mult | 300 | yes | 3164 | both |
| | 92235.51c | endf5t | endf/b-v | 1395 | cont | 300 | yes p(e) | 25862 | both |
| | 92235.52c | u600k | endf/b-v | 1395 | cont | 600 | yes p(e) | 65347 | both |
| | 92235.53c | eprixs | endf/b-v | 1395 | cont | 600 | yes p(e) | 36120 | both |
| | 92235.54c | eprixs | endf/b-v | 1395 | cont | 900 | yes p(e) | 36008 | both |
| | 92235.56c | endf5ht | endf/b-v | 1395 | cont | 1.2e+04 | yes p(e) | 28555 | both |
| | 92235.57c | endf5ht | endf/b-v | 1395 | cont | 1.2e+05 | yes p(e) | 25275 | both |
| | 92235.58c | endf5ht | endf/b-v | 1395 | cont | 1.2e+06 | yes p(e) | 23027 | both |
| | 92235.59c | endf5ht | endf/b-v | 1395 | cont | 1.2e+07 | yes p(e) | 22467 | both |
| | ** u-236 ** | | | | | | | | |
| | 92236.31c | endl79 | endl-79 | | cont | 0 | no | 4023 | prompt |
| | 92236.31d | drl79 | endl-79 | | disc | 0 | no | 4350 | prompt |
| | 92236.35c | endl85 | endl-85 | 71 | cont | 0 | yes p(e) | 9760 | prompt |
| — | 92236.50c | endf5p | endf/b-v | 1396 | cont | 300 | no | 138756 | total |
| | 92236.50d | dre5 | endf/b-v | 1396 | disc | 300 | no | 4879 | total |
| | 92236.50m | mgxsnp | endf/b-v | 1396 | mult | 300 | no | 2166 | total |
| | 92236.51c | rmccs | endf/b-v | 1396 | cont | 300 | no | 7343 | total |
| | 92236.51d | drmccs | endf/b-v | 1396 | disc | 300 | no | 4879 | total |

APPENDIX G

| ZAID | FILE | SOURCE | MAT | TYPE | TEMP(°K) | GPD | LENGTH | NUBAR | |
|-------------|-----------|---------|-----------|------|----------|---------|----------|--------|--------|
| ** u-237 ** | | | | | | | | | |
| | 92237.31c | endl79 | endl-79 | | cont | 0 | no | 4549 | prompt |
| | 92237.31d | drl79 | endl-79 | | disc | 0 | no | 3986 | prompt |
| | 92237.35c | endl85 | endl-85 | 72 | cont | 0 | yes p(e) | 9425 | prompt |
| → | 92237.50c | endf5p | endf/b-v | 8237 | cont | 300 | yes p(e) | 32506 | total |
| | 92237.50d | dre5 | endf/b-v | 8237 | disc | 300 | yes p(e) | 8912 | total |
| | 92237.50m | mgxsnp | endf/b-v | 8237 | mult | 300 | yes | 2174 | total |
| | 92237.51c | rmccs | endf/b-v | 8237 | cont | 300 | yes p(e) | 10378 | total |
| | 92237.51d | drmccs | endf/b-v | 8237 | disc | 300 | yes p(e) | 8912 | total |
| ** u-238 ** | | | | | | | | | |
| | 92238.04c | xmccs | endf/b-iv | 1262 | cont | 30000 | yes h | 32918 | both |
| | 92238.05c | xmccs | endf/b-iv | 1262 | cont | 6.e+05 | yes h | 18803 | both |
| | 92238.06c | xmccs | endf/b-iv | 1262 | cont | 1.2e+07 | yes h | 10399 | both |
| | 92238.12c | umccs | endf/b-iv | 1262 | cont | 300 | yes p | 50412 | both |
| | 92238.13c | rmccsb | endf/b-iv | 1262 | cont | 30000 | yes p(e) | 38686 | both |
| | 92238.13d | d9 | endf/b-iv | 1262 | disc | 30000 | yes p(e) | 12905 | both |
| | 92238.15c | rmccsb | endf/b-iv | 1262 | cont | 1.2e+07 | yes p(e) | 16230 | both |
| | 92238.15d | d9 | endf/b-iv | 1262 | disc | 1.2e+07 | yes p(e) | 13045 | both |
| | 92238.20c | amccs | endf/b-iv | 1262 | cont | 6.e+05 | yes p | 18721 | both |
| | 92238.20d | d9 | endf/b-iv | 1262 | disc | 6.e+05 | yes p | 7034 | both |
| | 92238.31c | endl79 | endl-79 | | cont | 0 | no | 18324 | prompt |
| | 92238.31d | drl79 | endl-79 | | disc | 0 | no | 8985 | prompt |
| | 92238.35c | endl85 | endl-85 | 73 | cont | 0 | yes p(e) | 27229 | prompt |
| → | 92238.50c | rmccs | endf/b-v | 1398 | cont | 300 | yes p(e) | 89059 | both |
| | 92238.50d | drmccs | endf/b-v | 1398 | disc | 300 | yes p(e) | 16876 | both |
| | 92238.50m | mgxsnp | endf/b-v | 1398 | mult | 300 | yes | 3553 | both |
| | 92238.51c | endf5t | endf/b-v | 1398 | cont | 300 | yes p(e) | 23921 | both |
| | 92238.52c | u600k | endf/b-v | 1398 | cont | 600 | yes p(e) | 123260 | both |
| | 92238.53c | eprixs | endf/b-v | 1398 | cont | 600 | yes p(e) | 160107 | both |
| | 92238.54c | eprixs | endf/b-v | 1398 | cont | 900 | yes p(e) | 160971 | both |
| | 92238.56c | endf5ht | endf/b-v | 1398 | cont | 1.2e+04 | yes p(e) | 82531 | both |
| | 92238.57c | endf5ht | endf/b-v | 1398 | cont | 1.2e+05 | yes p(e) | 47267 | both |
| | 92238.58c | endf5ht | endf/b-v | 1398 | cont | 1.2e+06 | yes p(e) | 27875 | both |
| | 92238.59c | endf5ht | endf/b-v | 1398 | cont | 1.2e+07 | yes p(e) | 22139 | both |
| ** u-239 ** | | | | | | | | | |
| → | 92239.35c | rmccsa | endl-85 | 74 | cont | 0 | yes p(e) | 9870 | prompt |
| | 92239.35d | drmccs | endl-85 | 74 | disc | 0 | yes p(e) | 9347 | prompt |
| | 92239.35m | mgxsnp | endl-85 | 74 | mult | 0 | yes | 2147 | prompt |
| ** u-240 ** | | | | | | | | | |
| | 92240.31c | endl79 | endl-79 | | cont | 0 | no | 3804 | prompt |
| | 92240.31d | drl79 | endl-79 | | disc | 0 | no | 4238 | prompt |
| → | 92240.35c | endl85 | endl-85 | 75 | cont | 0 | yes p(e) | 9556 | prompt |

z = 93 ***** neptunium *****

| | | | | | | | | | |
|--------------|-----------|--------|----------|------|------|-----|----------|-------|--------|
| ** np-235 ** | | | | | | | | | |
| | 93235.35c | endl85 | endl-85 | 76 | cont | 0 | yes p(e) | 9551 | prompt |
| ** np-236 ** | | | | | | | | | |
| | 93236.35c | endl85 | endl-85 | 77 | cont | 0 | yes p(e) | 9882 | prompt |
| ** np-237 ** | | | | | | | | | |
| | 93237.31c | endl79 | endl-79 | | cont | 0 | no | 14149 | total |
| | 93237.31d | drl79 | endl-79 | | disc | 0 | no | 4032 | total |
| | 93237.35c | endl85 | endl-85 | 78 | cont | 0 | yes p(e) | 20286 | prompt |
| | 93237.50c | endf5p | endf/b-v | 1337 | cont | 300 | no | 63264 | total |
| | 93237.50d | dre5 | endf/b-v | 1337 | disc | 300 | no | 5308 | total |

APPENDIX G

| | ZAID | FILE | SOURCE | MAT | TYPE | TEMP(°K) | GPD | LENGTH | NUBAR |
|------------------------------|-----------|---------|-----------|------|------|----------|----------|--------|--------|
| | 93237.51c | endf5t | endf/b-v | 1337 | cont | 300 | no | 9787 | total |
| — | 93237.55c | rmccsa | group t-2 | 1337 | cont | 300 | no | 32599 | both |
| | 93237.55d | drmccs | group t-2 | 1337 | disc | 300 | no | 20525 | both |
| | 93237.55m | mgxsnp | group t-2 | 1337 | mult | 300 | no | 2812 | both |
| ** np-238 ** | 93238.35c | endl85 | endl-85 | 79 | cont | 0 | yes p(e) | 9939 | prompt |
| z = 94 ***** plutonium ***** | | | | | | | | | |
| ** pu-237 ** | 94237.35c | endl85 | endl-85 | 80 | cont | 0 | yes p(e) | 11361 | prompt |
| ** pu-238 ** | 94238.31c | endl79 | endl-79 | | cont | 0 | no | 8624 | prompt |
| | 94238.31d | drl79 | endl-79 | | disc | 0 | no | 3901 | prompt |
| | 94238.35c | endl85 | endl-85 | 81 | cont | 0 | yes p(e) | 15680 | prompt |
| — | 94238.50c | endf5p | endf/b-v | 1338 | cont | 300 | no | 18804 | total |
| | 94238.50d | dre5 | endf/b-v | 1338 | disc | 300 | no | 5445 | total |
| | 94238.50m | mgxsnp | endf/b-v | 1338 | mult | 300 | no | 2442 | total |
| | 94238.51c | rmccs | endf/b-v | 1338 | cont | 300 | no | 6108 | total |
| | 94238.51d | drmccs | endf/b-v | 1338 | disc | 300 | no | 5445 | total |
| ** pu-239 ** | 94239.02c | xmccs | endf/b-iv | 1264 | cont | 3000 | yes h | 40464 | both |
| | 94239.03c | xmccs | endf/b-iv | 1264 | cont | 30000 | yes h | 25460 | both |
| | 94239.04c | xmccs | endf/b-iv | 1264 | cont | 6.e+05 | yes h | 13633 | both |
| | 94239.05c | xmccs | endf/b-iv | 1264 | cont | 1.2e+07 | yes h | 11349 | both |
| | 94239.06c | xmccs | endf/b-iv | 1264 | cont | 0 | yes h | 41167 | both |
| | 94239.07c | xmccs | endf/b-iv | 1264 | cont | 300 | yes h | 34659 | both |
| | 94239.15c | rmccsb | endf/b-iv | 1264 | cont | 1.2e+07 | yes p(e) | 14205 | both |
| | 94239.15d | d9 | endf/b-iv | 1264 | disc | 1.2e+07 | yes p(e) | 11541 | both |
| | 94239.16c | amccs | endf/b-iv | 1264 | cont | 0 | yes p | 41153 | both |
| | 94239.16d | d9 | endf/b-iv | 1264 | disc | 0 | yes p | 8056 | both |
| | 94239.17c | amccs | endf/b-iv | 1264 | cont | 300 | yes p | 34631 | both |
| | 94239.17d | d9 | endf/b-iv | 1264 | disc | 300 | yes p | 8056 | both |
| | 94239.18c | amccs | endf/b-iv | 1264 | cont | 3000 | yes p | 40421 | both |
| | 94239.18d | d9 | endf/b-iv | 1264 | disc | 3000 | yes p | 8056 | both |
| | 94239.19c | rmccsb | endf/b-iv | 1264 | cont | 30000 | yes p(e) | 28311 | both |
| | 94239.19d | d9 | endf/b-iv | 1264 | disc | 30000 | yes p(e) | 11541 | both |
| | 94239.20c | amccs | endf/b-iv | 1264 | cont | 6.e+05 | yes p | 13590 | both |
| | 94239.20d | d9 | endf/b-iv | 1264 | disc | 6.e+05 | yes p | 8056 | both |
| | 94239.31c | endl79 | endl-79 | | cont | 0 | no | 20976 | prompt |
| | 94239.31d | drl79 | endl-79 | | disc | 0 | no | 5926 | prompt |
| | 94239.50c | endf5p | endf/b-v | 1399 | cont | 300 | yes p(e) | 74110 | both |
| | 94239.50d | dre5 | endf/b-v | 1399 | disc | 300 | yes p(e) | 12692 | both |
| | 94239.51c | endf5t | endf/b-v | 1399 | cont | 300 | yes p(e) | 18898 | both |
| — | 94239.55c | rmccs | group t-2 | 1399 | cont | 300 | yes p(e) | 102160 | both |
| | 94239.55d | drmccs | group t-2 | 1399 | disc | 300 | yes p(e) | 20788 | both |
| | 94239.55m | mgxsnp | group t-2 | 1399 | mult | 300 | yes | 3038 | both |
| | 94239.56c | endf5ht | group t-2 | 1399 | cont | 1.2e+04 | yes p(e) | 45590 | both |
| | 94239.57c | endf5ht | group t-2 | 1399 | cont | 1.2e+05 | yes p(e) | 36262 | both |
| | 94239.58c | endf5ht | group t-2 | 1399 | cont | 1.2e+06 | yes p(e) | 31110 | both |
| | 94239.59c | endf5ht | group t-2 | 1399 | cont | 1.2e+07 | yes p(e) | 29822 | both |
| ** pu-240 ** | 94240.12c | bmccs | endf/b-iv | 1265 | cont | 900 | yes p | 41821 | both |
| | 94240.12d | d9 | endf/b-iv | 1265 | disc | 900 | yes p | 6087 | both |

APPENDIX G

| ZAID | FILE | SOURCE | MAT | TYPE | TEMP(°K) | GPD | LENGTH | NUBAR |
|------------------------------|--------|----------|------|------|----------|----------|--------|--------|
| 94240.31c | endl79 | endl-79 | | cont | 0 | no | 33109 | prompt |
| 94240.31d | drl79 | endl-79 | | disc | 0 | no | 5339 | prompt |
| → 94240.50c | rmccs | endf/b-v | 1380 | cont | 300 | yes p(e) | 58978 | both |
| 94240.50d | drmccs | endf/b-v | 1380 | disc | 300 | yes p(e) | 9630 | both |
| 94240.50m | mgxsnp | endf/b-v | 1380 | mult | 300 | yes | 3044 | both |
| 94240.51c | endf5t | endf/b-v | 1380 | cont | 300 | yes p(e) | 15195 | both |
| ** pu-241 ** | | | | | | | | |
| 94241.31c | endl79 | endl-79 | | cont | 0 | no | 4139 | prompt |
| 94241.31d | drl79 | endl-79 | | disc | 0 | no | 4303 | prompt |
| 94241.35c | endl85 | endl-85 | 84 | cont | 0 | yes p(e) | 9905 | prompt |
| → 94241.50c | endf5p | endf/b-v | 1381 | cont | 300 | yes p(e) | 38662 | both |
| 94241.50d | dre5 | endf/b-v | 1381 | disc | 300 | yes p(e) | 11636 | both |
| 94241.50m | mgxsnp | endf/b-v | 1381 | mult | 300 | yes | 2856 | both |
| 94241.51c | rmccs | endf/b-v | 1381 | cont | | yes p(e) | 13464 | both |
| 94241.51d | drmccs | endf/b-v | 1381 | disc | 300 | yes p(e) | 11636 | both |
| ** pu-242 ** | | | | | | | | |
| 94242.35c | endl85 | endl-85 | 85 | cont | 0 | yes p(e) | 21220 | prompt |
| → 94242.50c | endf5p | endf/b-v | 1342 | cont | 300 | yes p(e) | 71490 | both |
| 94242.50d | dre5 | endf/b-v | 1342 | disc | 300 | yes p(e) | 12524 | both |
| 94242.50m | mgxsnp | endf/b-v | 1342 | mult | 300 | yes | 2956 | both |
| 94242.51c | rmccs | endf/b-v | 1342 | cont | 300 | yes p(e) | 15763 | both |
| 94242.51d | drmccs | endf/b-v | 1342 | disc | 300 | yes p(e) | 12524 | both |
| ** pu-243 ** | | | | | | | | |
| 94243.31c | bmccs | endl-79 | | cont | 0 | no | 7087 | prompt |
| 94243.31d | d9 | endl-79 | | disc | 0 | no | 5547 | prompt |
| → 94243.35c | endl85 | endl-85 | 86 | cont | 0 | yes p(e) | 10824 | prompt |
| z = 95 ***** americium ***** | | | | | | | | |
| ** am-241 ** | | | | | | | | |
| 95241.31c | endl79 | endl-79 | | cont | 0 | no | 19896 | prompt |
| 95241.31d | drl79 | endl-79 | | disc | 0 | no | 4378 | prompt |
| 95241.35c | endl85 | endl-85 | 87 | cont | 0 | yes p(e) | 25351 | prompt |
| → 95241.50c | endf5u | endf/b-v | 1361 | cont | 300 | yes p(e) | 42145 | total |
| 95241.50d | dre5 | endf/b-v | 1361 | disc | 300 | yes p(e) | 10032 | total |
| 95241.50m | mgxsnp | endf/b-v | 1361 | mult | 300 | no | 2535 | total |
| 95241.51c | rmccs | endf/b-v | 1361 | cont | 300 | yes p(e) | 12435 | total |
| 95241.51d | drmccs | endf/b-v | 1361 | disc | 300 | yes p(e) | 10032 | total |
| ** am-242m ** | | | | | | | | |
| 95242.31c | endl79 | endl-79 | | cont | 0 | no | 6575 | prompt |
| 95242.31d | drl79 | endl-79 | | disc | 0 | no | 4005 | prompt |
| 95242.35c | endl85 | endl-85 | 88 | cont | 0 | yes p(e) | 20969 | prompt |
| → 95242.50c | endf5u | endf/b-v | 1369 | cont | 300 | yes p(e) | 8654 | total |
| 95242.50d | dre5 | endf/b-v | 1369 | disc | 300 | yes p(e) | 9109 | total |
| 95242.50m | mgxsnp | endf/b-v | 1369 | mult | 300 | no | 2284 | total |
| 95242.51c | rmccs | endf/b-v | 1369 | cont | 300 | yes p(e) | 8563 | total |
| 95242.51d | drmccs | endf/b-v | 1369 | disc | 300 | yes p(e) | 9109 | total |
| ** am-243 ** | | | | | | | | |
| 95243.31c | endl79 | endl-79 | | cont | 0 | no | 31050 | total |
| 95243.31d | drl79 | endl-79 | | disc | 0 | no | 4255 | total |
| 95243.35c | endl85 | endl-85 | 89 | cont | 0 | yes p(e) | 39461 | prompt |
| → 95243.50c | endf5u | endf/b-v | 1363 | cont | 300 | yes p(e) | 92076 | total |
| 95243.50d | dre5 | endf/b-v | 1363 | disc | 300 | yes p(e) | 11803 | total |
| 95243.50m | mgxsnp | endf/b-v | 1363 | mult | 300 | no | 2480 | total |

APPENDIX G

| ZAID | FILE | SOURCE | MAT | TYPE | TEMP(°K) | GPD | LENGTH | NUBAR |
|--------------------------------|-----------|----------|------|------|----------|----------|--------|--------|
| 95243.51c | rmccs | endf/b-v | 1363 | cont | 300 | yes p(e) | 13745 | total |
| 95243.51d | drmcchs | endf/b-v | 1363 | disc | 300 | yes p(e) | 11803 | total |
| z = 96 ***** curium ***** | | | | | | | | |
| ** cm-242 ** | | | | | | | | |
| 96242.31c | endl79 | endl-79 | | cont | 0 | no | 15537 | total |
| 96242.31d | drl79 | endl-79 | | disc | 0 | no | 4197 | total |
| 96242.35c | endl85 | endl-85 | 90 | cont | 0 | yes p(e) | 21714 | prompt |
| → 96242.50c | endf5u | endf/b-v | 8642 | cont | 300 | yes p(e) | 30958 | total |
| 96242.50d | dre5 | endf/b-v | 8642 | disc | 300 | yes p(e) | 8964 | total |
| 96242.50m | mgxsnp | endf/b-v | 8642 | mult | 300 | no | 1970 | total |
| 96242.51c | rmccs | endf/b-v | 8642 | cont | 300 | yes p(e) | 9828 | total |
| 96242.51d | drmcchs | endf/b-v | 8642 | disc | 300 | yes p(e) | 8964 | total |
| ** cm-243 ** | | | | | | | | |
| 96243.35c | endl85 | endl-85 | 91 | cont | 0 | yes p(e) | 21638 | prompt |
| ** cm-244 ** | | | | | | | | |
| 96244.31c | endl79 | endl-79 | | cont | 0 | no | 15126 | total |
| 96244.31d | drl79 | endl-79 | | disc | 0 | no | 4290 | total |
| 96244.35c | endl85 | endl-85 | 92 | cont | 0 | yes p(e) | 21257 | prompt |
| → 96244.50c | endf5u | endf/b-v | 1344 | cont | 300 | yes p(e) | 46052 | total |
| 96244.50d | dre5 | endf/b-v | 1344 | disc | 300 | yes p(e) | 9570 | total |
| 96244.50m | mgxsnp | endf/b-v | 1344 | mult | 300 | no | 1950 | total |
| 96244.51c | rmccs | endf/b-v | 1344 | cont | 300 | yes p(e) | 10908 | total |
| 96244.51d | drmcchs | endf/b-v | 1344 | disc | 300 | yes p(e) | 9570 | total |
| ** cm-245 ** | | | | | | | | |
| 96245.35c | endl85 | endl-85 | 93 | cont | 0 | yes p(e) | 24189 | prompt |
| 96245.50c | cm245(13) | endf/b-v | 1345 | cont | 300 | yes p(e) | 11664 | total |
| → 96245.52c | cm245(13) | ndfb-v.2 | 1345 | cont | 300 | yes p(e) | 21314 | both |
| ** cm-246 ** | | | | | | | | |
| 96246.35c | endl85 | endl-85 | 94 | cont | 0 | yes p(e) | 12550 | prompt |
| ** cm-247 ** | | | | | | | | |
| 96247.35c | endl85 | endl-85 | 95 | cont | 0 | yes p(e) | 20326 | prompt |
| ** cm-248 ** | | | | | | | | |
| 96248.35c | endl85 | endl-85 | 96 | cont | 0 | yes p(e) | 18239 | prompt |
| z = 97 ***** berkelium ***** | | | | | | | | |
| ** bk-249 ** | | | | | | | | |
| 97249.35c | endl85 | endl-85 | 97 | cont | 0 | yes p(e) | 11844 | prompt |
| z = 98 ***** californium ***** | | | | | | | | |
| ** cf-249 ** | | | | | | | | |
| 98249.35c | endl85 | endl-85 | 98 | cont | 0 | yes p(e) | 28116 | prompt |
| ** cf-250 ** | | | | | | | | |
| 98250.35c | endl85 | endl-85 | 99 | cont | 0 | yes p(e) | 10548 | prompt |
| ** cf-251 ** | | | | | | | | |
| 98251.35c | endl85 | endl-85 | 100 | cont | 0 | yes p(e) | 11030 | prompt |
| ** cf-252 ** | | | | | | | | |
| 98252.35c | endl85 | endl-85 | 101 | cont | 0 | yes p(e) | 17969 | prompt |

SPECIAL NOTES

- note 1. When performing calculations utilizing neutron-neutron cross sections, it is essential to incorporate the effects of motion of the target neutron. This capability does not exist today in MCNP. This limitation makes the use of the neutron-neutron cross sections unadvisable for most applications. Reference: R.C.Little and R.E.Seamon, "Additional Neutron Cross-Section Tables for MCNP," Los Alamos National Laboratory internal memorandum X-6:RCL/RES-85-288 to distribution (June 3, 1985).
- note 2. These ENDF/B-IV sets are recommended without reservation. They include photon-production data in expanded ACE format. Reference: R.C.Little, "ENDF/B-IV Cross Sections for MCNP," Los Alamos National Laboratory internal memorandum X-6:RCL-84-251 to T.E.Booth (November 21, 1984).
- note 3. Photon production added to ENDF/B-V neutron files by R.E.Macfarlane, T-2, with intent to estimate photon heating roughly. Reference: R.C.Little, "Argon and Krypton Cross-Section Files," Los Alamos National Laboratory internal memorandum to P.D.Soran (June 30, 1982).
- note 4. These data are valid to 5 MeV; they were extended to 20 MeV for completeness only. Reference: R.C.Little, "Sc-45 Cross Sections for MCNP," Los Alamos National Laboratory internal memorandum X-6:RCL-85-430 to C.D.Bowman (August 27, 1985).
- note 5. The evaluation was performed by C.Y.Fu and D.M.Hetrick at Oak Ridge, who refer to it as mat 1326, mod 4. Reference: R.C.Little, "Monte Carlo Cross Sections for Fe Based on ORNL Evaluation," Los Alamos National Laboratory internal memorandum X-6:RCL-86-436 to P.P.Whalen (October 3, 1986).
- note 6. These data were taken from incomplete fission-product evaluations. Reference: R.C.Little, "Cross Sections in ACE Format for Various IP Target Materials," Los Alamos National Laboratory internal memorandum to D.Davidson (August 19, 1982).
- note 7. This is ENDF/B-V after modification by evaluator to get better agreement with ENDL85. References: R.C.Little, "Y-89 Cross Sections for MCNP," Los Alamos National Laboratory internal memorandum X-6:RCL-85-419 to distribution (August 16, 1985); R.C.Little, "Modified ENDF/B-V Y-89 Cross Sections for MCNP," Los Alamos National Laboratory internal memorandum X-6:RCL-85-443 to distribution (September 6, 1985).
- note 8. This is ENDF/B-V after modification by evaluator to get better agreement with Japanese measurements. Reference: R.C.Little, "Revised Gd-152 Evaluation from HEDL," Los Alamos National Laboratory internal memorandum X-6:RCL-87-132 to distribution (March 24, 1987).
- note 9. Photon-production data were added to ENDF/B-V neutron cross sections by P.G.Young, T-2. These data are valid to 1 MeV only. Reference: R.C.Little and R.E.Seamon, "ENDF/B-V Gd Cross Sections with Photon Production," Los Alamos National Laboratory internal memorandum X-6:RCL/RES-86-30 to A.R.Larson (January 22, 1986).

APPENDIX G

- note 10. This has to do with file tm169. We have no reference for this file. The file itself was first written on 86/09/29.
- note 11. This has to do with file irnat. We have no reference for this file. The file itself was first written on 86/09/19.
- note 12. This has to do with file pa231. We have no reference for this file. The file itself was first written on 88/01/25.
- note 13. Very little detail was given in the original ENDF/B-V evaluation for cm-245. The updated evaluation available under ENDF/B-V Revision 2 is very complete. The two sets are compared in Little's memo X-6:RCL-86-220. Reference: R.C.Little, "Monte Carlo Cross Sections for Cm-245," Los Alamos National Laboratory internal memorandum X-6:RCL-86-220 to J.T.West (June 3, 1986).

15. J. F. Briesmeister, Ed., "MCNP-A General Monte Carlo Code for Neutron and Photon Transport, Version 3A," Los Alamos National Laboratory report LA-7396-M, Rev. 2, Manual (September 1986).

In some cases, calculated results are desirable to fill in experimental data or to extend them. Where they appear in this report, they are identified as calculations because of the uncertainty associated with them. In general, the 16-group Hansen-Roach cross-section set¹⁰ is used with the one-dimensional transport code, DSN,¹¹ or its modern version, ONEDANT¹² in one dimension and TWODANT¹³ in two dimensions. The reason for this choice is Stratton's extensive comparison of results of such calculations with experimental data.¹⁴ Where this comparison is unfavorable, particularly for solution or hydrogeneous mixtures of few-percent ²³⁵U-enriched uranium, the ~~Los Alamos MCNP Monte Carlo code¹⁵~~ and cross-sections based on ENDF-B/V* are used instead. This combination is also applied in the few cases where finite-cylinder calculations are desired.

Calculated extensions of experimental data are included to show the nature of trends, not to substitute for results of experiments. They should be used with caution.

A fundamental aim of this document is to illustrate relationships among critical data. The compilation and correlation of data for this purpose, from many measurements in a number of laboratories, require a certain amount of normalization or reduction to common terms. Frequently, for example, the effects of variations in geometry or density must be removed to show trends in data. The manner in which these alterations may be made is discussed in the early section RELATIONS FOR CONVERSION TO STANDARD CONDITIONS.

Reactor mockups and related critical assemblies are generally outside the scope of this document. Many of those that are appropriate to serve as computational models are fast-neutron systems that are of secondary interest in criticality safety matters.¹⁶ Nevertheless, fast-reactor mockups which are used as benchmark assemblies (for comparison with calculations) are instructive, for they illustrate the value of data other than criticality specifications, namely, spectral information, neutron flux distributions, prompt-neutron lifetime, and reactivity coefficients. Unfortunately, data for critical assemblies suitable as safety benchmarks are usually limited to critical compositions, dimensions and masses without useful supplementary information.

* Robert C. Little, Los Alamos National Laboratory, Los Alamos, NM 87545, 1986.

URANIUM OF VARIOUS ENRICHMENTS

Tables 9 and 10 give critical data for homogeneous hydrogen-moderated units of uranium enriched in ^{235}U to various degrees. In addition to UO_2F_2 solutions, there are solid uranium-bearing mixtures in which the hydrogenous material is polyethylene, paraffin, or Sterotex (glycerol tristearate, $[(\text{C}_{17}\text{H}_{35}\text{COO})_3\text{C}_3\text{H}_5]$). In the tables there has been no attempt to convert to a common composition. In Table 9, critical values of one-dimensional forms (spheres, infinite cylinders and infinite slabs) are obtained from Oak Ridge reports of critical experiments. They are derived from quoted values of buckling, extrapolation distance and reflector savings. Results of other experiments at various enrichments appear in Table 10.

Reports of U(4.89), U(3.00) and U(2.00) systems give values of buckling, extrapolation distance, and reflector saving, from which spherical equivalents are derived (as well as equivalent infinite cylinders and slabs). Otherwise, listed spherical equivalents are as reported with the original data or as they appear in Ref. 14. The entries for U(95.3) and U(29.8) are from the only heterogeneous systems for which there is sufficient experimental information to permit correction to homogeneous compositions.

15
14
Critical masses and critical volumes of hydrogen-moderated spheres of U(93), U(30.3), U(4.89), U(3.00), and U(2.00) are displayed in Figs. 14 and 15. Values for U(3.00) and U(2.00) include those listed in Table 9 for $\text{U}(3.00)\text{F}_4$ -paraffin and $\text{U}(2.00)\text{F}_4$ -paraffin compacts. Dashed curves that extend beyond experimental ranges follow points computed by the MCNP Monte Carlo code¹⁵ and the associated cross section set.* Critical data for uranyl fluoride-water mixtures at the four smaller enrichments are reproduced by this means within 0.01 k_{eff} and the method is used for conversion to U(2.00) and U(3.00) solutions.** It may be noted that the use of Hansen-Roach cross sections leads to 3% to 4% overestimates of $\text{U}(2.00)\text{F}_4$ -paraffin critical sphere radii.¹⁴

Figures 16 and 17 give estimated infinite cylinder diameters and infinite slab thicknesses for U(93), U(30.3), U(4.89), U(3.00), and U(2.00). Values for the latter four ^{235}U enrichments were obtained from sphere radii by means of extrapolation distances consistent with the sphere radii, infinite cylinder diameters, and infinite slab thicknesses tabulated in Ref. 14.

* Robert C. Little, Los Alamos National Laboratory, Los Alamos, NM 87545, 1986.

** N. L. Pruvost, Los Alamos National Laboratory, Los Alamos, NM 87545 (1986).

NORM PRUVOST
HSE-6 7-4789

RCVD OCT. 15, 1986

LA-7396-M, Rev. 2
Manual

UC-32
Issued: September 1986

MCNP—A General Monte Carlo Code for Neutron and Photon Transport

Version 3A

Judith F. Briesmeister, Editor

*Copy of this report
(orig 3 ring binder
legit blue) on
Norm's book shelf.*

CONTRIBUTORS

| | | |
|--------------------|------------------|----------------|
| T. E. Booth | R. A. Forster | R. G. Schrandt |
| J. F. Briesmeister | T. N. K. Godfrey | R. E. Seamon |
| D. G. Collins | J. S. Hendricks | E. C. Snow |
| J. J. Devaney | H. G. Hughes | W. L. Thompson |
| G. P. Estes | R. C. Little | W. T. Urban |
| H. M. Fisher | R. E. Prael | J. T. West |